Function of STAT3 and SMG1 in maintaining Glioblastoma stem cells

A Dissertation submitted by

Sejuti Sengupta

In partial fulfillment of the requirements for the degree of

Doctor of Philosophy

in

Cellular & Molecular Physiology

TUFTS UNIVERSITY
Sackler School of Graduate Biomedical Sciences

May, 2016

Advisor: Dr. Brent Cochran

Thursday March 24, 2016

Thesis Chair: Dr. Dan Jay
Committee Member: Dr. Peter Juo
Outside Examiner: Dr Keith Ligon

Abstract

Glioblastoma multiforme (GBM) is the most common and most aggressive tumor of the central nervous system, with a mean survival of only 14 months post diagnosis. Due to the highly lethal nature of glioblastoma, new therapies are urgently needed. It is thought that the major reason for poor prognosis of GBM is that a small population of GBM stem cells (GSC) selectively survives therapy and leads to tumor re-growth. Therefore, in this thesis I have identified new potential therapeutic targets for GBM stem cells and investigated the underlying mechanisms by which these targets regulate the growth of GBM stem cells.

The transcription factor STAT3 is required for the self-renewal of several stem cell types including GSC. Interestingly, STAT3 inhibition leads to an irreversible decrease in proliferation and neurosphere formation, as well as loss of stem cell markers. The work presented in this thesis reports a novel epigenetic mechanism for inhibiting self-renewal of GSC. by STAT3. Here, we show that STAT3 inhibition upregulates histone H3K27me2/3 demethylase JMJD3 (KDM6B), which can reverse polycomb complex mediated repression of neural differentiation genes. To identify the set of STAT3 regulated differentiation-specific genes, genome wide ChIP-sequencing and microarray analysis were performed to determine changes in histone H3K27 methylation as well as gene expression following STAT3 inhibition. STAT3 inhibition leads to reduced promoter histone H3K27 trimethylation of neural differentiation genes, such as MYT1, FGF21 and GDF15. While MYT1 gene expression requires the presence of an additional growth factor in addition to STAT3 inhibition, FGF21 and GDF15 genes are expressed upon STAT3 inhibition alone.

In addition to genetic and epigenetic alterations, microenvironment factors like tumor hypoxia play an important role in GSC tumorigenicity. GSC preferentially reside in hypoxic niches in the tumor, which is believed to be a major factor in maintaining GSC survival and tumor progression following therapy. There have been no systematic attempts to identify and target molecular mechanisms responsible for GSC survival under hypoxia. Since kinases are druggable targets that play an important role in maintaining GSC growth and survival, we conducted a functional RNAi kinome-wide screen across three GSC lines under normoxia (21% oxygen) as well as hypoxia (1% oxygen). We found that only 25% of the kinase hits in the screen were common to the three GSC lines screened, demonstrating a high level of heterogeneity between these lines. Some of the common targets were previously known to be involved in gliomagenesis, while some are novel targets in GBM. There were hits unique to both hypoxia as well as normoxia, thereby emphasizing differential GBM stem cell sensitivity to kinase inhibition in different microenvironments.

The SMG1 (suppressor with morphological effects on genitalia) kinase was identified and validated as a gene that can preferentially inhibit the growth of selected GBM stem cell lines under hypoxia (1% oxygen). Strikingly, knockdown of SMG1 sensitized all the GBM stem cell lines tested to temozolomide (TMZ), the frontline chemotherapeutic used to treat GBM patients. Importantly, we found significant reduction in intracranial tumor growth and prolonged survival in mice when SMG1 is knocked down in combination with TMZ treatment, as compared to TMZ alone. We have used the Cell Collective modeling software platform to simulate the mechanism of action of the SMG1 kinase network in GSC by integrating our data with results in the literature.

Based on the prediction of our model, we found that SMG1 inhibits GSC growth through its well-characterized role in the classical mRNA surveillance mechanism, nonsense mediated mRNA decay (NMD) pathway. Thus, the kinase targets and the mechanisms identified here are therapeutically important for developing inhibitors for treating GBM.

Acknowledgements

I would like to thank my mentor Brent Cochran who spearheaded this work and made us plough through it when we got stuck. His great mentorship is reflected in his support and guidance to motivate us, direct us and give us the freedom to make mistakes and learn to overcome them. He led us by example, with his incredible love and passion for science and mentoring his students to push boundaries and excel in every way. I have thoroughly enjoyed my time and grown as a scientist with the other members of the Cochran lab, especially Shreya Kulkarni, Surbhi Goel-Bhattacharya and Simon Khagi. I am grateful to have the privilege of a lab family away from home. I would like to thank the very cordial and stimulating environment of Cell and Molecular Physiology program, during my time at Tufts. I would like to thank the members of my thesis committee, Dan Jay, Peter Juo and Keith Ligon. I am grateful to have had their insight and guidance on my thesis and career development through the years. I would like to thank the Physiology and now the DMCB department, especially Ira Herman, Brent Cochran and Phil Hinds who served as program and department heads during my time at Tufts, and Laura Liscum and Jerry Faust for being inspiring teachers and role models. I also would like to thank the office staff for their support, help, and interest in all students and organizing holiday gatherings that we would look forward to. I would like to thank the ISP program and the labs I rotated in for laying the foundation for being successful in graduate school. I consider myself lucky to truly enjoy what I do and am indebted to Tufts, as a double jumbo, to give me this opportunity. I am grateful to have made many good friends here at Tufts, especially our ISP class, CMP students and graduate student council members, that made me want to come to work and stay for tea and other events after work. Lastly, I would

like to thank my parents, Sumit Kumar Sengupta and Jharna Sengupta, for inspiring me to do this in the first place and keep me going. Their dreams and aspirations have let me dream and nurture the passion for science and making a difference. The wonderful friends I made in Boston, especially Christina McWilliams and my now husband, have stuck with me through thick and thin and made me love the city. I couldn't have done it without my husband, Chitrang Patel, who was always there for me with his love and support and never failed to make me breathe and laugh when I needed it. Our 5-month-old son, Kabir Sengupta Patel, and our pet, Gracie, always got us re-energized for a productive day at work.

Table of Contents

List of Tables:

List of Figures:

Abbreviations:

bFGF	Basic fibroblast growth factor
BMP4	Bone morphogenic factor 4
ChIP	Chromatin immunoprecipitation
DDR	DNA damage response
EGF	Epidermal growth factor
FGF	Fibroblast growth factor
GBM	Glioblastoma multiforme
GDF15	Growth differentiation derived factor
GSC	Glioblastoma multiforme stem cells
H3K27me3	Histone 3 lysine 27 trimethylation
HIF	Hypoxia inducible factor
JMJD3	Jumanji domain containing 3
MAD	Median absolute deviation
MAPK	Mitogen activatated protein kinase
MYT1	Myelin transcription fcator 1
NMD	Nonsense mediated mRNA decay
PI3K	Phosphoinositide 3 kinase
RNAi	RNA interference
SMG1	Suppressor of morphogenesis in genitalia 1
STAT3	Signal transducer and activator of transcription 3
TCGA	The cancer genome atlas
TMZ	Temozolomide
VEGF	Vascular endothelial growth factor

Chapter 1

Introduction

Glioblastoma multiforme (GBM) is the most common and most aggressive tumor of the central nervous system (CNS). In the United States, GBM has the highest incidence rate among malignant brain and CNS tumors, i.e. 3 new cases per 100,000 (Dolecek et al. 2012). The incidence rate of GBM increases with increasing age, with highest rates between ages 75 to 84 (Dolecek et al. 2012). Gliomas include tumors from astrocytic, ependymal, oligodendroglial and mixed lineage (Rich and Bigner 2004). World Health Organization classifies astrocytoma into 4 histopathologic grades based on their malignant features. Low grade gliomas include relatively benign grade I pilocytic and well-differentiated grade II diffuse astrocytoma. High grade gliomas comprise of grade III anaplastic astrocytoma and finally the most aggressive grade IV GBM (Rich and Bigner 2004; Maher et al. 2001). GBM is characterized by nuclear atypia, high cellular density, high mitotic activity and even necrosis and microvascular proliferation (Rich and Bigner 2004; Maher et al. 2001). Glioblastoma tumor cells are highly invasive and infiltrate surrounding brain parenchyma. The symptoms of GBM include headaches, progressive neurologic deficits and seizures, eventually leading to death. 90% of clinical cases consist of primary GBM, which arise de novo without pre-existing tumor, whereas secondary GBM progresses from low-grade gliomas (Cancer Genome Atlas Research Network et al. 2015; Wiencke et al. 2007). Current standard therapy for newly diagnosed GBM patients is gross total surgical resection of the tumor, chemotherapy with temozolomide (TMZ) and radiation (Stupp et al. 2005). Despite the current aggressive multimodal treatment, the overall median survival of patients is only about 14-15 months (Stupp et al. 2005; Prados et al. 2009).

Response to GBM therapeutic approaches

Alkylating agents, like chloroethylnitrosoureas (CNUs) and TMZ have been commonly used to treat malignant brain tumors (Reithmeier et al. 2010). The combination of TMZ and radiation showed significant improvement over radiation alone, with respect to median progression-free survival (PFS) (6.9 versus 5 months), overall survival (OS) (14.6 versus 12.1 months) and 2-year survival rate (26% versus 10%) (Stupp et al. 2005). The cytotoxicity of TMZ is mediated by the addition of methyl groups to adenine and guanine bases of genomic DNA (Hegi et al. 2008). The most common modifications, N7-methylguanine and N3-methyladenine adducts, are efficiently repaired by the base excision repair pathway and have a low cytotoxic potential (Hegi et al. 2008). Only 5-10% of TMZ mediated methylation yields cytotoxic O-6-methylguanine (O-6-MeG), which mispairs with thymine (T) in double-stranded DNA (Hegi et al. 2008). These recurrent G-T mismatches induce futile cycles of mismatch repair resulting in either double strand breaks or apurinic/athymidinic sites, which can induce irreversible growth arrest or trigger apoptosis (Gaspar et al. 2010). DNA repair pathways normally protect against genomic instability and cancer. However, tumor cells can exploit this natural cellular defense against TMZ-induced DNA damage, leading to chemoresistance. Therefore, clinical response to alkylating agents is significantly compromised in GBM patients with increased activity of the DNA repair enzyme, O6-Methylguanine-DNA methyltransferase (MGMT). MGMT is a DNA repair protein that removes the cytotoxic methyl group from the O-6-MeG adducts generated by TMZ and restores DNA to its native form (Taylor et al. 2015; Stupp et al. 2005). This ability of tumor cells to repair the DNA damage induced by TMZ, results in

chemoresistance. Methylation of the MGMT promoter results in epigenetic silencing of the gene and decreases the tumor cell's DNA repair ability thereby increasing TMZ sensitivity. Patients with MGMT promoter methylation exhibit two-fold median survival advantage of 21.7 versus 12.7 months and improved 2-year survival rates of 46% versus 13.8% upon TMZ treatment (Hegi et al. 2005). Hence, MGMT promoter methylation status has become the most powerful prognostic marker for predicting response to alkylating agent chemotherapy in GBM and a marker for stratifying GBM patients within clinical trials (Hegi et al. 2005). Glioma tumors with unmethylated MGMT typically show minimal response to alkylating drugs (Hegi et al. 2005) and rapidly progress to more formidable recurrent GBM, necessitating effective treatment regimens targeted for this resistant patient population. Tumor recurrence occurs rapidly in a median time of 6.9 months after surgery and is associated with a median survival of only 3-6 months (Reithmeier et al. 2010). Bevacizumab is used to target angiogenesis which commonly occurs in recurrent GBM. Although trials showed alleviation of symptoms with bevacizumab, it did not lead to an increase in overall survival and only a marginal improvement in progression free survival (Niyazi et al. 2015) and also results in more aggressive GBM upon recurrence. Since EGFR amplification is the most frequent alteration in 40% of GBM cases, EGFR kinase inhibitors erlotinib and gefitinib were tested in GBM trials (Prados et al. 2009). However, such single-agent targeted therapy did not provide significant survival benefit, presumably due to PI3K/Akt pathway mediated resistance in GBM. Therefore, more recent trials have pursued combination therapy of EGFR inhibitor, erlotinib, with mTOR inhibitor, temsirolimus (Wen et al. 2014). However, there was no improvement in patient response partly due to insufficient

EGFR inhibition in the tumor. Class II EGFR inhibitors, like imatinib, that are capable of targeting the inactive conformation of the EGFR are believed to be more effective in this regard (Liu and Gray 2006). Precision oncology is being explored to take advantage of the large scale molecular profiling and subtype studies as part of the TCGA initiative and target driver gene mutations in each tumor (Martinez-Ledesma et al. 2015).

GBM genomic and pathway aberrations

Tumors evolve from benign to malignant lesions by acquiring a series of genetic or epigenetic alterations over time. GBM tumors are highly heterogeneous and exhibit high frequency of gene alterations. The first "Gatekeeper mutations" offer a small selective growth advantage to tumor cells, but the impact gets amplified over time, thereby progressing from benign lower grade glioma to higher grade malignant GBM. A variety of alterations occur at the gene and chromosome level, including single base substitutions (SBS), small insertions and deletions (INDEL), gene amplifications and homozygous deletions, affect protein-coding genes (**Fig 1.1**) (Vogelstein et al. 2013). Of these, >99.9% of the alterations are passenger changes that are a result of tumorigenesis, rather than the cause. A major goal of large-scale genome analysis and network biology is to predict functional consequence of mutations and distinguish oncogenic "driver mutations" from passively selected "passenger mutations" that do not contribute to tumorigenesis (Cerami et al. 2010).

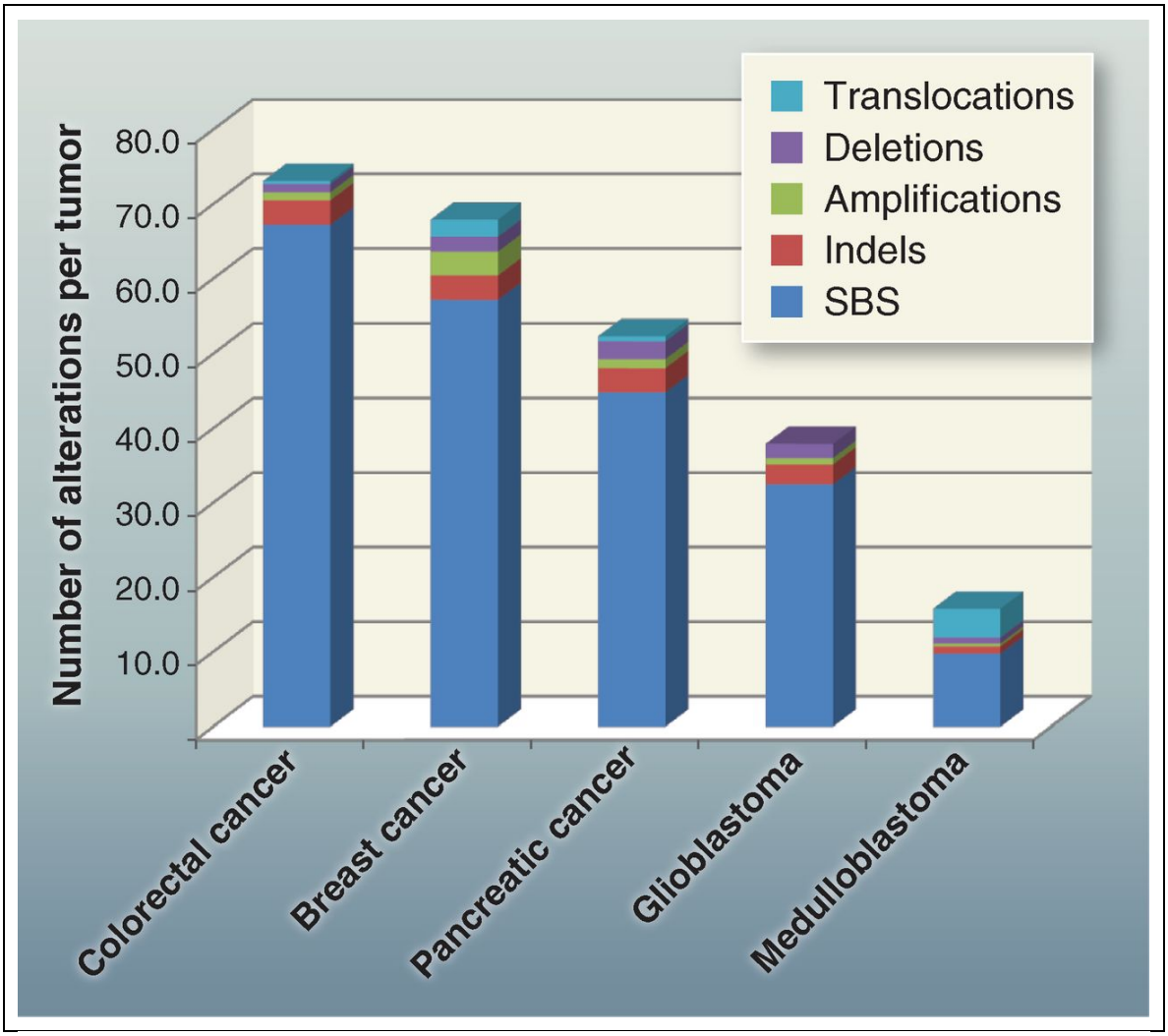

Fig 1.1: Total alterations affecting protein-coding genes in selected tumors. Average number and types of genomic alterations per tumor, including single-base substitutions (SBS), small insertions and deletions (indels), amplifications, and homozygous deletions, as determined by genome-wide sequencing studies. For colorectal, breast, and pancreatic ductal cancer, and medulloblastomas, translocations are also included (Vogelstein et al. 2013).

Consequently, GBM is the first cancer whose genomic profile has been extensively characterized by the Cancer Genome Atlas (TCGA) project as a concerted effort to identify alterations in genes and biological processes (Cerami et al. 2010). The

goal is to develop novel targets for GBM and stratify therapeutic approaches for each tumor subtype. A cohort of GBM tumors were analyzed for DNA sequence and copy number, DNA methylation, gene expression and patient clinical information. This initial TCGA study validated previously known genetic alterations in TP53, PTEN, EGFR, RB1, NF1, ERBB2, PIK3R1 and PIK3CA genes (Cancer Genome Atlas Research Network 2008). The original TCGA report identified alterations in three core pathways, namely p53 (87%), retinoblastoma (Rb) (78%), and receptor tyrosine kinase (RTK)/Ras/phosphoinositide 3-kinase (PI3K) signaling (88%) (Cancer Genome Atlas Research Network 2008) (**Fig 1.2**). Whole-exome and transcriptome sequencing data identified additional mutually exclusive alterations affecting the core pathways: either p53 pathway (MDM2, MDM4, and TP53), or Rb pathway (CDK4, CDK6, CCND2, CDKN2A/B and RB1), or members of the PI3K pathway (PIK3CA,PIK3R1, PTEN, EGFR, PDGFRA and NF1) (Ciriello et al. 2012). More comprehensive DNA sequencing and methylation analysis studies independently identified tumors with novel biomarkers, like isocitrate dehydrogenase (IDH1) gene mutation (Parsons et al. 2008) and glioma CpG island methylator (G-CIMP) phenotype (Noushmehr et al. 2010), both of which show significantly improved prognosis in the clinic (Lathia et al. 2015). It is now known that IDH1 mutations are largely responsible for the hypermethylator phenotype due to increased production of the oncometabolite, 2-hydroxyglutarate, which inhibits DNA demethylation by TET enzymes (Verhaak et al. 2010). Additionally, mutations in the TERT promoter is a major feature found in 80% of GBM that are mutually exclusive with mutations in the chromatin remodeling protein, ATRX (Ceccarelli et al. 2016). Currently, the NIH Roadmap Epigenomics Consortium is actively profiling normal cells

and tissues to generate a global reference human epigenomic map (Roadmap Epigenomics Consortium et al. 2015). This will be extremely valuable to characterize critical epigenetic changes involved in the regulation of aberrant GBM stem cells. Network based analysis shows that GBM genetic alterations cluster within specific non-random functional modules that may target multiple signaling pathways and act as key drivers of cancer (Cerami et al. 2010). Comprehensive molecular profiling of all TCGA data for newly diagnosed glioma identified gene alterations in IDH1, TP53, ATRX, EGFR, PTEN, CIC, FUBP1, SETD2, DNMT3A, ARID2 and KRAS/NRAS oncogenes as driver events in glioma. These genetic drivers converged into the Ras-RafMEK-ERK, p53/apoptosis, PI3K/AKT/mTOR, chromatin modification and cell cycle pathways (Ceccarelli et al. 2016).

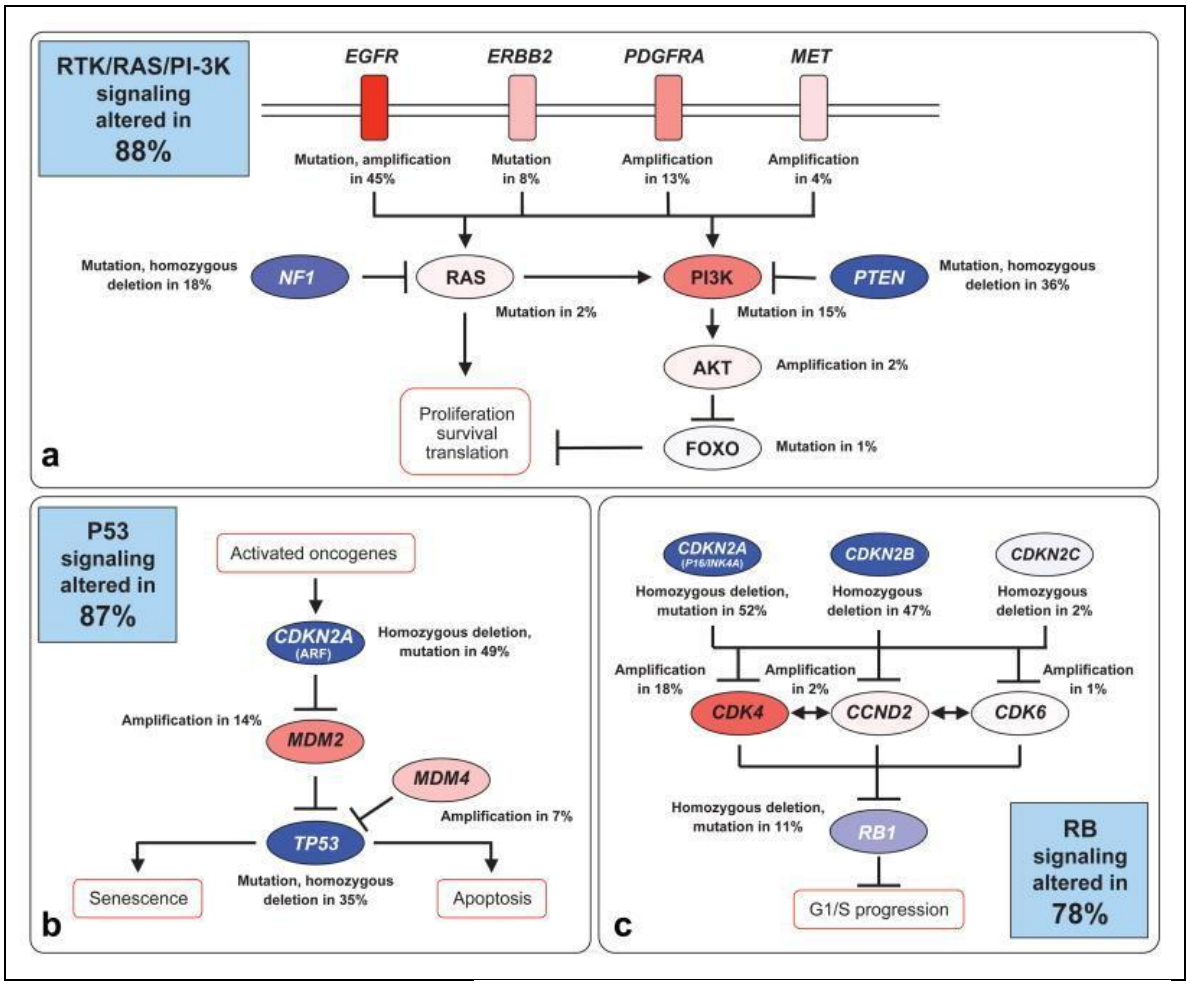

Fig 1.2: GBM Core pathways. Genetic aberrations identified in GBM TCGA data impacted three core pathways, namely receptor tyrosine kinase (RTK)/Ras/phosphoinositide 3-kinase (PI3K) signaling (88%), p53 (87%) and retinoblastoma (Rb) (78%) (Cancer Genome Atlas Research Network 2008).

On the basis of their gene expression signature, GBM has been classified into proneural, neural, classical, and mesenchymal molecular subtypes (Verhaak et al. 2010) (**Fig 1.3**). The gene expression patterns of the GBM subgroups showed correlations with either oligodendrocyte or astrocyte or neural lineage markers, suggestive of their origin. While the classical, mesenchymal, and proneural subtypes were defined by aberrations of EGFR, NF1 and PDGFRA/IDH1 respectively, the neural subtype was defined by the

expression of neuron markers such as NEFL, GABRA1, SYT1 and SLC12A5 (Verhaak et al. 2010). More recently, multi-platform analysis of adult diffuse glioma elucidated clinically relevant subclasses of IDH wild-type and IDH mutant gliomas based on genome-wide DNA methylation (**Fig 1.4**). IDH-wild-type gliomas segregated into three DNA methylation clusters; the high grade Classic-like group and Mesenchymal-like group and low grade glioma (LGG)-enriched group. On the other hand, IDH-mutant gliomas clustered into G-CIMP low subset with lower survival than G-CIMP high subset and subset with codeletions of chromosome 1p and 19q (codel) (Ceccarelli et al. 2016). In fact, the G-CIMP low group was also associated with high expression of SOX and OLIG2 family members, which are known to promote self-renewal of aggressive GBM stem cells (Ceccarelli et al. 2016). Such molecular classification overcomes the bias associated with inter-observer variation in histological grading. Although the molecular subtypes of GBM detected the dominant transcriptional program within a tumor, single cell RNA sequencing showed that each tumor contains a spectrum of multiple transcriptional subtypes and diverse cellular states (Patel et al. 2014). This clearly demonstrates intra-tumor heterogeneity in GBM. In fact, a novel single nucleus sequencing technology identified GBM tumor cell subpopulations with distinct co-existing genetic alterations that potentially give rise to EGFR targeted therapy resistance (Francis et al. 2014).

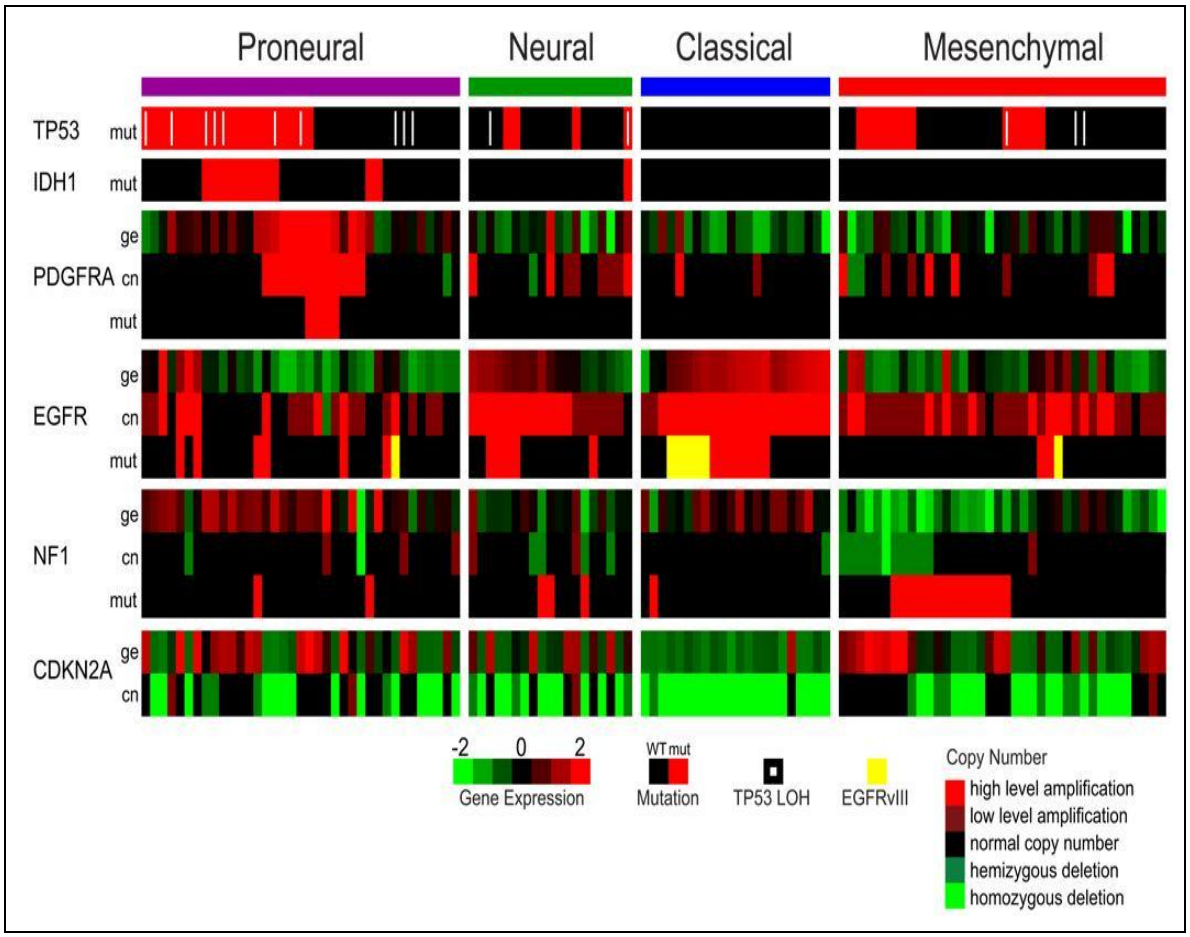

Fig 1.3: **Subtype Classification of GBM.** GBM has been classified into 4 subtypes, proneural, neural, classical and mesenchymal, based on gene expression signature (Verhaak et al. 2010).

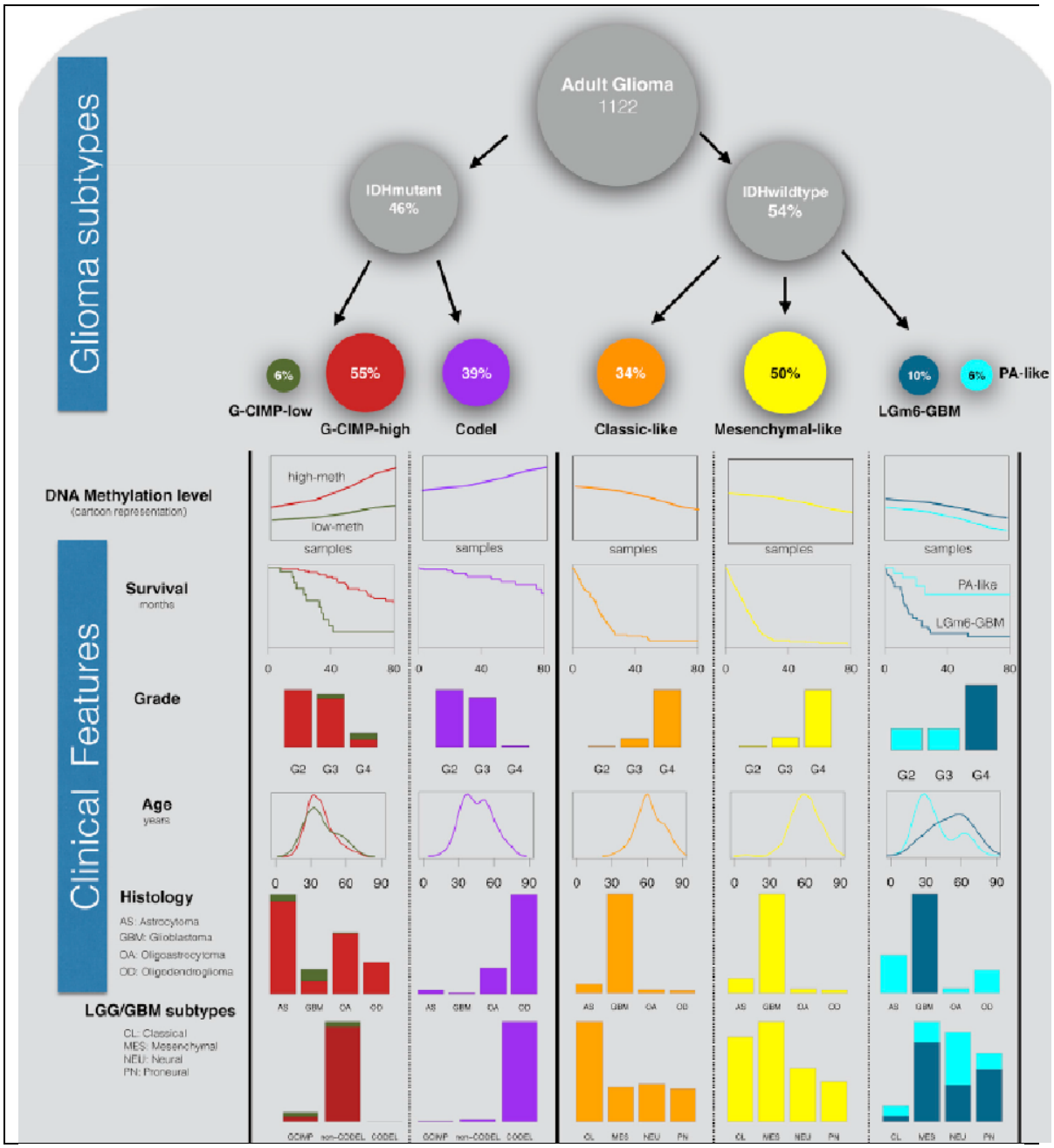

Fig 1.4: Clinically relevant glioma subtypes. Molecular profiling of all adult diffuse glioma subdivided IDH wild type and IDH mutant glioma into different subtypes based on their gene expression and DNA methylation profile, which was indicative of clinical prognosis and survival of patients (Ceccarelli et al. 2016).

In summary, both frequency based and network based analysis identified 2 major pathway aberrations in GBM involving activation of the PI3K/RTK pathway and inactivation of the p53 and Rb tumor suppressor pathways (Cancer Genome Atlas Research Network 2008; Cerami et al. 2010). The different GBM subtypes are dependent on distinct signaling pathways, likely necessitating distinct therapeutic strategies to target the driver mutations in each tumor type. However, with the exception of the IDH1 mutation and MGMT promoter methylation, none of the molecular subtypes have proven to be useful guides to therapy as yet. The major reason for the poor prognosis of GBM is believed to be tumor heterogeneity that results in recurrences attributed to a small population of refractory GBM stem cells (GSC). We will expand on both of these factors in the following sub-sections.

GBM stem cells

The advent of the cancer stem cell (CSC) hypothesis challenged the clonal evolution theory to explain the heterogeneity of tumors. The stochastic clonal evolution theory states that tumor cells are biologically equivalent but behave differently due to random genetic or epigenetic mutations or extrinsic microenvironment factors (Dick 2009). Tumor evolution follows the Darwinian model of natural selection whereby the fittest clone(s) will expand and outgrow the weaker clones during tumor expansion (Inda et al. 2014). On the other hand, the hierarchical stem cell model suggests that a distinct, rare population of the tumor cells maintains the tumor by their self-renewal, proliferation and differentiation ability, similar to tissue specific adult stem cells (Chen et al. 2012). The cancer stem cells at the apex were believed to undergo asymmetric cell division to give rise to a stem cell population and rapidly cycling progenitor cells that form the bulk

of the tumor (Houghton et al, 2008). Unlike normal stem cells, cancer stem cells harbor oncogenic mutations leading to uncontrolled cell growth and proliferation characteristic of a malignant phenotype (Pardal et al. 2003). Indeed, a genetically engineered mouse model with Nf1 and p53 deleted neural progenitor cells develops malignant astrocytoma originating from the subventricular zone (SVZ), where neural stem cells reside (Zhu et al. 2005).

Recent evidence has revised the rigid unidirectional hierarchy of CSCs to address stem cell plasticity, whereby tumor-generating CSCs could develop from mutations in normal stem cells or dedifferentiation of downstream progenitor cells or terminally differentiated somatic cells (Chen et al. 2012; Dick 2008; Pattabiraman and Weinberg 2014) (**Fig 1.5**). Malignant melanoma cells were shown to dynamically cycle between a tumor-initiating CSC state and a non-stem state, owing to reversible epigenetic regulation by the H3K4 demethylase JARID1A41 (Pattabiraman and Weinberg 2014). To put the stem cell hypothesis in perspective with intratumoral heterogeneity, it is now posited that each genetically diverse subpopulation within a tumor evolves independently from its own stem cell compartment (Pattabiraman and Weinberg 2014). Quintana et al also showed that cancer stem cell population need not be rare in melanoma, using a mice transplantation model lacking innate immunity (Quintana et al. 2008; Morrison and Spradling 2008). Thus, some tumors may have a higher stem cell-like characteristic than others.

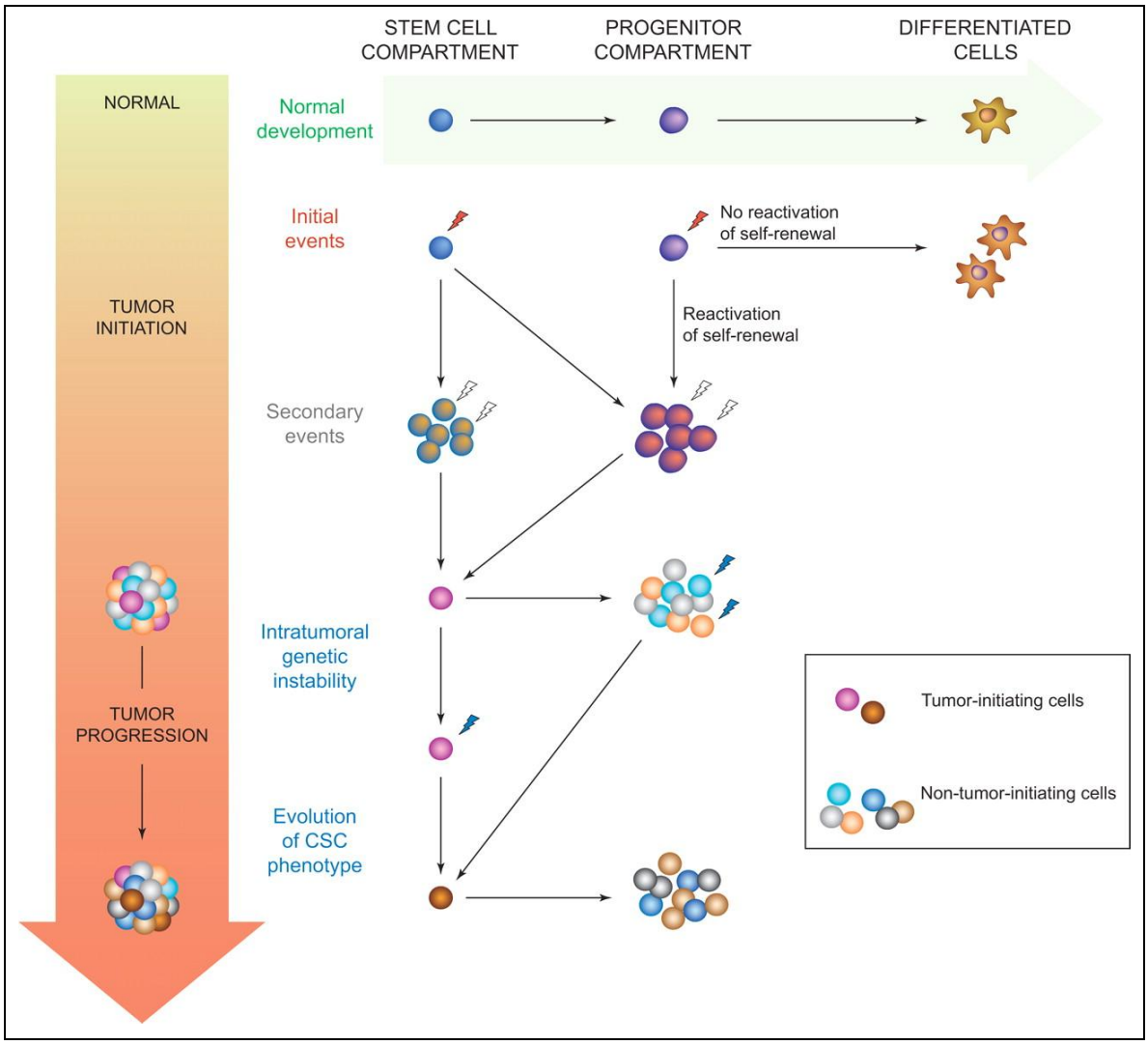

Fig 1.5: Cancer stem cell hypothesis. Aberrant tumor-generating cancer stem cells arise from stem cell or progenitor compartments and are responsible for tumor initiation and progression (Dick 2008).

Cancer stem cell populations have been identified in many cancer types, including leukemia, glioblastoma, medulloblastoma, breast, pancreatic and colon tumors (Ailles and Weissman 2007). Glioblastoma was one of the first tumors for which the cancer stem cell hypothesis was shown to be applicable. Isolation of normal neural stem cells in culture was first described by Reynolds and Weiss in the early 1990s (Reynolds and Weiss). Serum free media supplemented with the growth factors, fibroblast growth

factor-2 (FGF2) and epidermal growth factor (EGF), allowed the growth and maintenance of neural stem cells as undifferentiated neurospheres. This method of neurosphere culture was applied to isolate glioblastoma stem cells from primary patient samples by Ignatova et al in 2002 (Ignatova et al. 2002) and later by the Vescovi, Dirks, and Yu groups (Reynolds and Vescovi 2009; Dirks 2010). The probability of deriving stem-like neurospheres from patient tumors can be low and is indicative of disease severity and prognosis (Laks et al. 2009). The stem-like spheroids exhibit self-renewal and can be maintained as an undifferentiated and heterogeneous population in culture (Lathia et al., 2011). However, non adherent neurosphere culture makes it challenging to perform high throughput assays (Woolard and Fine, 2009). An alternative method is to plate adherent GBM tumor stem cells on laminin coated surface (Pollard et al., 2009). This can be a promising avenue for personalized medicine to screen adherent GSC population isolated from every patient tumor.

GBM stem cells share the properties of normal neural stem cells to self-renew, proliferate and differentiate into multiple neural lineages (Lathia et al. 2005) and even vascular lineages (Ricci-Vitiani et al., 2010) (**Fig 1.6**). Glioblastoma stem cells express similar markers to normal neural stem cells, including CD133, CD15, nestin, Bmi1, sox2, nanog, myc and olig2 (Lathia et al. 2015). Originally, the CD133 surface marker was used to define and prospectively isolate GBM stem cells. Singh et al showed that as few as 1000 CD133+ cells could form serially transplantable tumors in mice, whereas CD133- cells were not able to cause tumors (Singh et al. 2004). However, it has since been demonstrated that CD133- glioblastoma stem cells can also be isolated from some tumors and that they are highly tumorigenic (Beier et al. 2007). Additionally, work from

Fine's group suggested the normal mouse neural stem cell marker, CD15/SSEA, enriches for a tumor initiating population in GBM (Son et al. 2009). However, the molecular markers for CSCs vary depending on tumor subtype. Therefore, the challenge remains to identify ideal markers for isolating GBM stem cells.

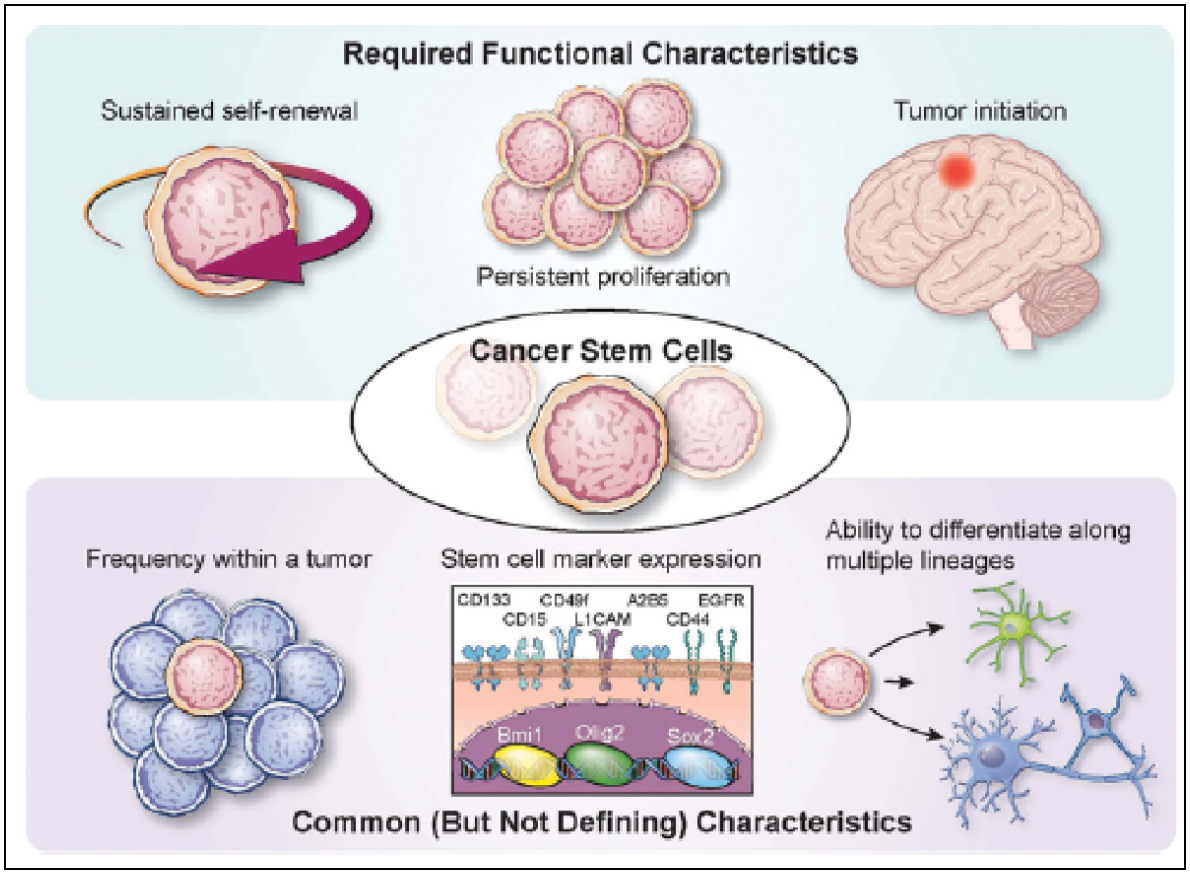

Fig 1.6: Cancer stem cell properties. Cancer stem cells are capable of self-renewal, proliferation, stem cell marker expression, multipotency and tumor-initiation (Lathia et al. 2015).

In addition to in-vitro culture and xenotransplantation studies to support the CSC hypothesis, Luis Parada's group used a Nestin-delTK-GFP; Mut7 glioma-prone genetically engineered mouse model to track nestin expressing tumor initiating population in GBM. The relative fraction of nestin expressing quiescent cell population

in the tumor was shown to increase post TMZ treatment, implying that these cancer stem cells are more chemo-resistant than the bulk tumor cells (Chen et al. 2012). Further, prolonged gancyclovir mediated elimination of this neural progenitor population led to tumor regression in mice. More recently, Peter Dirk's group performed genetic lineage tracing experiments showing that rare, quiescent stem-like cells expressing Sox2 had significantly higher self-renewal and tumor propagating ability and were enriched after chemotherapy in the sonic hedgehog subgroup of medulloblastoma (Vanner et al. 2014). However, lineage tracing of the stem-like neurospheres exhibited more symmetric than asymmetric division to propagate them in culture and maintain heterogeneity (Lathia et al, 2011).

GBM stem cells are also highly tumorigenic and have been shown to initiate and sustain tumor growth in glioma xenograft models (Lathia et al. 2015). In fact, only 100 CD133+ GSC cells were capable of forming a serially transplantable tumor in mice (Singh et al. 2004). These GSC lines form more invasive and poorly differentiated tumors in mouse brains that resemble the tumor of origin more closely than traditional serum lines (Wakimoto et al. 2012). Moreover, gene expression profiling shows GSC lines are far more similar to the tumor of origin than serum lines derived from the same tumor (Lee et al. 2006; Patel et al. 2014). Tumor-initiating stem-like population was enriched in post-chemotherapy breast tumor patient specimens, indicating higher chemoresistance of tumor stem cells in patients (Creighton et al, 2009). Importantly, neurosphere formation correlates to significantly poor clinical outcome in patients (Laks et al. 2009). Thus, GBM stem cell lines are both a genetically and clinically relevant model. Understanding

the signaling pathways necessary for their growth and self-renewal may lead to new therapeutic targets.

Targeting GBM stem cells

Given the evidence for cancer stem cells in GBM, it is important to understand the mechanisms of GSC maintenance and target these cells specifically and in addition to traditional treatment. Consistent with this, the EORTC/NCIC trial first identified a stem cell related HOX gene signature associated with chemo and radio-resistance in glioma patients (Murat et al. 2008; Bao et al. 2006)). A later study validated that the HOX gene signature mediated by PI3K axis was functionally associated with GBM stem cells and chemoresistance. Inhibiting this PI3K axis reduced GSC survival (Gaspar et al. 2010). Developmental pathways that regulate normal stem cells, like Bmi1, Oct4, Olig2 and c-Myc, are also useful to target in GBM stem cells (Lathia et al. 2011). Notch, TGF-β, NF-κB and Wnt signaling pathways are commonly activated in GSC (Lathia et al. 2015). Targeting BMP (Piccirillo et al. 2006; Lee et al. 2008), TGFβ (Ikushima et al. 2009), Leukemia inhibitory factor (LIF) (Peñuelas et al. 2009), Notch (Fan et al. 2010) and Hedgehog (Clement et al. 2007) pathways reduced self-renewal and, in some cases, tumorigenicity of GSC. Maternal embryonic leucine zipper kinase (MELK) may also be a key regulator of brain tumor stem cell activity (Joshi et al. 2013). The potential of blocking interaction of GSC with the tumor vasculature by means of anti-angiogenic agents like bevacizumab has also been pursued (Niyazi et al. 2015).

Recent genome-wide profiling data revealed two mutually exclusive GSC populations, namely the proneural subtype and the more aggressive mesenchymal subtype (Mao et al. 2013; Bhat et al. 2013). The mesenchymal subtype is driven by

elevated expression of the glycolytic enzyme, ALDH1A3, and DNA repair genes, leading to increased therapy resistance (Mao et al. 2013). Activation of NF-κB, a paracrine tumor niche factor, can induce mesenchymal transformation by activating the master regulators, STAT3, C/EBPβ and TAZ (Bhat et al. 2013). In fact, the antibiotic minocycline, inhibits the NF-κB pathway and thereby targets this mesenchymal subclass. Transcriptomic expression analysis combined with kinome wide shRNA screening of mesenchymal and proneural GSC identified the role of the receptor tyrosine kinase AXL in self-renewal and tumorigenicity of mesenchymal GSC (Cheng et al. 2015). Both chemical and RNAi screens, discussed later, can also allow us to identify other novel targets for GSC.

Another therapeutic strategy to eliminate GSC is to block self-renewal and promote differentiation of the cells. All-trans retinoic acid (ATRA) and phorbol myristate acetate (PMA) have shown benefits as differentiation therapy for leukemic stem cells (Pattabiraman and Weinberg 2014). Epigenetic drugs like the HDAC inhibitor, SAHA, and DNMT inhibitor, AzaC, have been shown to de-repress differentiation specific gene promoters and induce differentiation of cancer stem cells (Johnstone 2002). In particular, the HDAC inhibitors, Valproic acid (VPA) and Trichostatin A (TSA) reduced proliferation and stem cell marker expression and induced differentiation of GBM stem cells, and can be potentially used for combination therapy (Safa et al., 2015). An EZH2 inhibitor E7438 is currently in Phase I/II clinical trials for advanced solid tumours and B cell lymphomas (ClinicalTrials.gov identifier: NCT01897571) (Pattabiraman and Weinberg 2014). However, one of the challenges is to target GBM stem cells without affecting the normal neural stem cells.

Epigenetics in GBM

It is important to understand regulatory epigenetic mechanisms to inhibit the multipotency of GBM stem cells. Epigenetic modifications, such as changes in histone and DNA methylation marks, can be exploited to induce differentiation of stem cells to specific lineages. The histone proteins, particularly histone 3, play an important role in regulating gene expression by undergoing modifications in certain lysine (K) residues. Methylation of histone H3 can be associated with gene activation, in case of H3K4 methylation, as well as gene repression, in the case of H3K9 and H3K27 methylation. Bivalent genes are marked by both repressive H3K27me3 and the activating histone mark H3K4me3. These genes are transcriptionally repressed, and it has been postulated that these bivalent domains are poised for rapid transcriptional activation during differentiation (Christophersen and Helin 2010).

Polycomb repressive complexes (PRC) initiate repression by marking the promoter with H3K27 methylation mark. The PRC2 complex consists of Eed (ectoderm development) and Suz12 (suppressor of Zeste 12) which is responsible for forming the complex and its binding to the histone; while Ezh2 (enhancer of Zeste homolog 2) catalyzes histone H3K27 trimethylation and chromatin condensation. Subsequently, the PRC1 complex, consisting of Ring1A or Ring1B and BMI1, binds to this unit to stabilize chromatin compaction (**Fig 1.7**) (Viré et al. 2006, Mack 2010). This inhibits RNA polymerase II access to target genes and thereby transcription. Therefore, both PRC1 and PRC2 are critical for regulating transcription of differentiation-specific genes in stem cells (Di Croce and Helin 2013). In addition to regulating histone modifications, polycomb group proteins also target DNA methyltransferases (DNMTs) to specific gene promoters. The family of DNMTs includes the maintenance methyltransferase, DNMT1

and de novo methyltransferases, DNMT3A and DNMT3B. The DNMTs methylate CpG islands concentrated upstream of the promoter at the cytosine residue, leading to gene silencing (Viré et al. 2006). The resulting methylated CpG residues will recruit PRC1 histone modifiers to make the chromatin inaccessible and block transcription factor binding. It is still not clear how PRC targeting to specific genes is controlled. Noncoding RNAs play an important role in polycomb targeting. It was reported that the long noncoding RNA, HOTAIR, binds PRC2 and thereby directs H3K27me3 methylation (Tsai et al. 2010).

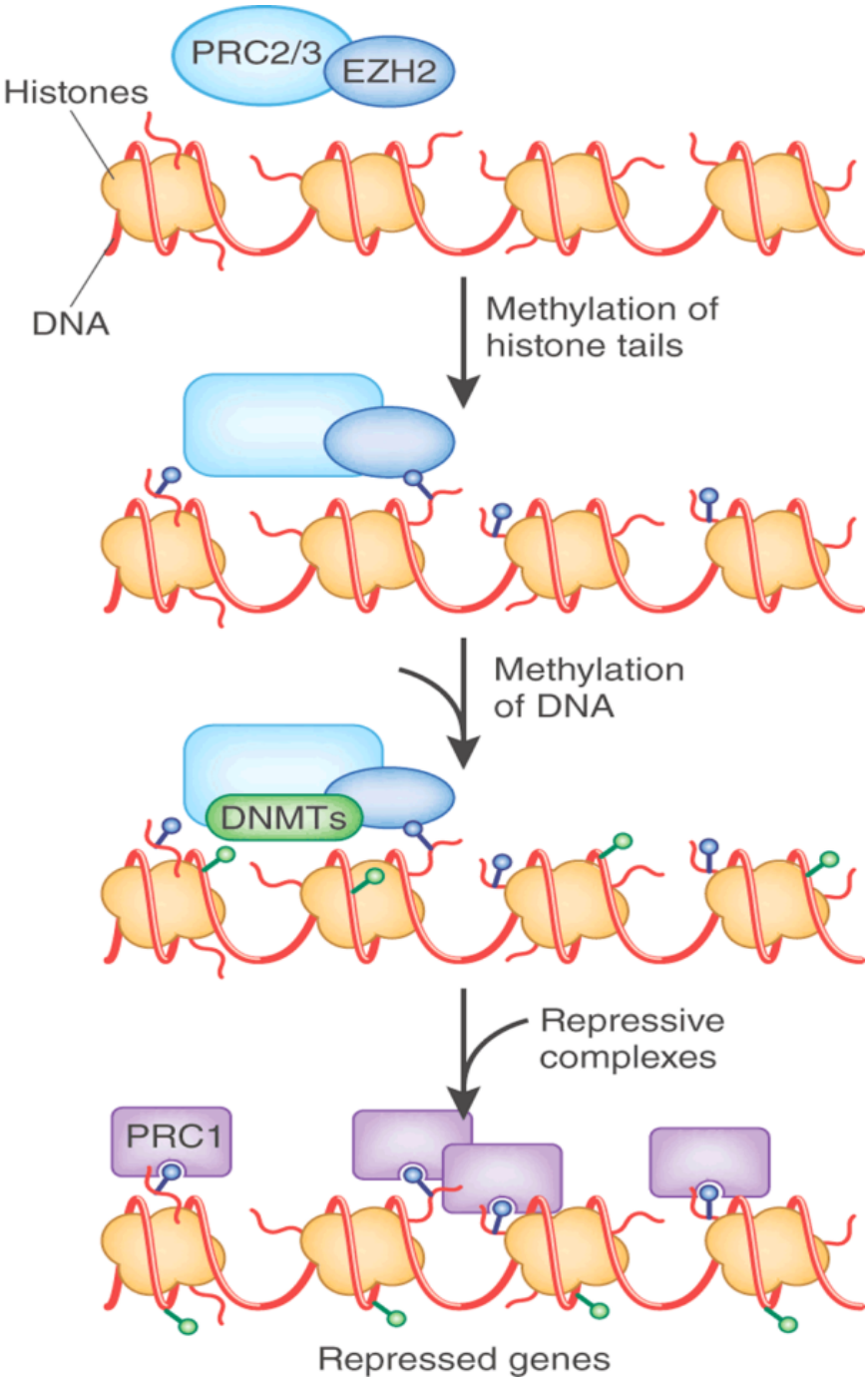

Fig 1.7: Proposed model for DNMT action in conjunction with histone modification.

Histone methylation by PRC2 might lead to DNA methylation by the DNMTs (Mack 2010).

In addition to genetic alterations, GBM stem cells also harbor critical epigenetic modifications (Cancer Genome Atlas Research Network 2008). DNA methylation analysis performed as part of the TCGA study was able to identify a CpG island methylator phenotype (CIMP) associated with IDH1 mutations in GBMs (Noushmehr et al. 2010), both of which showed favorable prognosis in patients. Importantly, MGMT promoter hypermethylation is now routinely assessed in the clinic due to its favorable response to the standard chemotherapeutic drug, TMZ treatment. On the other hand, aberrant hypomethylation at DNA repetitive sequences in GSC results in genomic instability driving glioma progression (Fanelli et al. 2008). Epigenetic dysregulation has been shown to drive gliomagenesis by silencing tumor suppressors like p16 (Costello et al. 1996) and PTEN (Wiencke et al. 2007), or aberrant activation of oncogenes. In fact, it was recently found that critical oncogenes in tumor cells contain large regions of super-enhancers where chromatin regulators and coactivators are concentrated. Super-enhancers were mapped in multiple tumor types by assessing the genome-wide occupancy of the chromatin regulator, BRD4, along with its co-activator, Mediator, and associated H3K27 acetylation mark. In GBM, super-enhancers were found in genes encoding RUNX1, FOSL2 and BHLHE40 transcription factors responsible for mesenchymal transformation of brain tumors (Lovén et al. 2013). Therefore, targeting these chromatin regulators or super-enhancer functions can be used to target specific tumor-associated genes.

Interestingly, a number of gene mutations found in GBM can directly or indirectly regulate the chromatin. These include histones HIST1H3B and H3F3A, ATRX and DAXX, DNMT1 and TET1 and EZH2 and KDM6A (Suvà et al. 2009; Schwartzentruber

et al. 2012; Wu et al. 2012; Sturm et al. 2012). Histone H3 dominant negative mutations that sequester and inhibit PRC2 activity resulting in reduced global H3K27me3 levels, were found to be directly involved in tumor initiation in pediatric GBM (Bender et al. 2013, Lewis et al, 2013, (Venneti et al. 2013). PRC2 was shown to regulate GSC plasticity by induction of H3K27me3 marks on developmental genes like Nanog, Wnt1 and BMP5 (Natsume et al. 2013). In particular, EZH2 is overexpressed in GSC, and its knockdown leads to decreased self-renewal capacity, proliferation and tumorigenicity of GSC (K. Zhang et al. 2015; Suvà et al. 2009; J. Zhang et al. 2015). EZH2 is also amplified or overexpressed in a high proportion of metastatic breast and prostate tumors (Chang and Hung 2012). Lee et al have also demonstrated that EZH2 prevents differentiation in GSC by repressing the BMP receptor 1B. Restoration of BMPR1B expression restores sensitivity to differentiation signals, specifically to CNTF-mediated activation of STAT3, thereby promoting astrocyte differentiation (Lee et al. 2008). In addition to silencing pro-differentiation genes, EZH2 phosphorylation was also shown to activate STAT3 and maintain pluripotency of GSC (Kim et al. 2013).

JMJD3 (or KDM6B) is a histone demethylase which opposes PRC2 by removing the methyl mark from H3K27me3. Together with UTX (or KDM6A) and its male homolog, UTY; JMJD3 is a member of the Jumanji (JmjC) domain containing protein family which demethylates histone H3K27 methylation marks and affects transcription of multiple genes involved in cellular growth and differentiation (Agger et al. 2007; De Santa et al. 2007; Lan et al. 2007). In particular, JMJD3 contributes to neural differentiation in different model systems. JMJD3 upregulation is important for neural commitment and spinal cord neurogenesis in murine embryonic stem (ES) cells (Burgold

et al. 2008; Akizu et al. 2010). Smads 2/3 recruit JMJD3 for histone demethylation at the promoter of the BMP inhibitor, Noggin, and thereby control interneuron differentiation in the chick neural tube (Estarás et al. 2012). Premature JMJD3 induction by deletion of SMRT corepressor, which normally represses JMJD3, was shown to impair brain development in mice. Neural stem cells isolated from SMRT-/- embryos also showed reduced neurosphere formation and an upregulation of neural markers (Jepsen et al. 2007). JMJD3 has also been shown to induce INK4A/ARF dependent senescence in human fibroblasts and mesenchymal stem cells, implying that it may be a tumor suppressor (Barradas et al. 2009; Agger et al. 2009). Recently, it has been shown that JMJD3 is induced during GBM stem cell differentiation and has a tumor suppressor function in GSC through p53 stabilization in an INK4A/ARF independent manner (Ene et al. 2012). We will show for the first time that STAT3 signaling epigenetically regulates GBM stem cells by JMJD3 induction.

Epigenetic regulation of GBM stem cells by STAT3

STAT3

The STAT (Signal transducers and activators of transcription) family of transcription factors mediate response to many cytokines and growth factors and comprise of seven members: STAT1, STAT2, STAT3, STAT4, STAT5A, STAT5B and STAT6. The STATs were initially discovered in the Cochran lab as trans-acting factors that bind to the c-fos promoter in response to PDGF stimulation (Hayes et al. 1987), and then described by the Darnell lab as interferon responsive factors (Levy et al. 1988). These factors bound DNA at specific conserved response elements upstream of the target genes and did not require protein synthesis for activation. This suggested that

they are pre-existing cellular proteins that undergo modification upon stimulation, leading to signal transduction to the nucleus. Fu et al subsequently cloned this interferon inducible complex and termed it interferon stimulated gene factor-3 (ISGF-3) complex in 1992 (Fu et al. 1992). The STATs were shown to have five domains; an amino-terminal domain, a coiled-coil domain, a DNA-binding domain, an SH2 domain and a carboxy-terminal transactivation domain (Miklossy et al. 2013). Once a ligand interacts with its receptor, STAT activation is induced by the phosphorylation of specific tyrosine residues in the STAT transactivation domain by growth factor receptors, Janus kinases (JAKs), SRC family kinases and other tyrosine kinases. This leads to STAT–STAT dimerization through a reciprocal phospho-tyrosine (pTyr)-SH2 domain interaction, leading to nuclear translocation and DNA binding and the transcription of target genes. Suppressors of cytokine signalling (SOCS) and protein tyrosine phosphatases (PTPs) negatively regulate STAT signalling under physiologic conditions. Small molecules or peptides have been designed to inhibit Stat3 by targeting pTyr-SH2 domain interaction and prevent dimerization of STAT3 (Miklossy et al. 2013).

STAT3 was originally found to be activated by IL-6 and subsequently by other cytokines like IL11, LIF, Oncostatin-M; growth factors like EGF, NGF and G-CSF; interferons; BMP4 and notch(Takeda et al. 1997). STAT3 plays an important role in proliferation, survival, epithelial to mesenchymal transition and the immune and inflammatory response (Rajan 2011). Through these varied functions, STAT3 plays an indispensable role in regulating stem cell pluripotency and neural lineage commitment. Early embryonic lethality of STAT3 deficient mice showed that it plays a unique role in early embryonic development, which cannot be compensated by other STAT family

members (Takeda et al. 1997). STAT3 is activated in the subventricular zone of the brain where neural stem cells are enriched. STAT3 is required for the maintenance of pluripotency of murine embryonic and neural stem cells and facilitates reprogramming of somatic cells to the pluripotent state (Niwa et al., 1998; Rajan and McKay, 1998; Yang et al., 2010). Either expression of dominant negative STAT3 or deletion of STAT3 impaired embryonic neural stem cell pluripotency and promoted neuronal differentiation, possibly by its effects on the expression of Notch ligand (Gu et al. 2005; Yoshimatsu et al. 2006).

Of all its family members, STAT3 attracts the most attention as a therapeutic target to control tumorigenesis. Early experiments showed that STAT3 is required for v-src-mediated transformation (Turkson et al. 1998; Bromberg et al. 1998). Also, knockout of STAT3 in the mouse epidermis prevents chemical induction of skin tumors(Chan et al. 2004). STAT3 is constitutively activated in $CD44^{+}CD24^{-}$ breast cancer stem cells (Marotta et al. 2011), prostate cancer stem cells (Kroon et al. 2013) and GBM stem cells (Sherry et al. 2009). Our lab and others have previously shown that STAT3 promotes GBM survival by directly upregulating the antiapoptotic genes Bcl-xl, Mcl-1 and survivin (Konnikova et al. 2003; Rahaman et al. 2002). Blocking the IL6/JAK/STAT3 pathway was shown to reduce tumorigenicity of solid tumor stem cell lines, including GBM stem cells (Hedvat et al. 2009; Stechishin et al. 2013; Iwamaru et al. 2007). STAT3 acts at the convergence of multiple oncogenesis pathways, including proliferation genes c-myc, p21, cyclin D; the anti-apototic genes bcl-xl and survivin; the angiogenic gene VEGF; the EMT transition genes twist and LIV1; the invasion genes MMPs and the immortalization gene h-TERT (Kim et al. 2014; Konnikova et al. 2005). STAT3 is one of the transcription

factors, along with Myc, Sox2, Nanog and Gli1, which are critical to maintain GBM stem cell identity by recruiting chromatin regulators (Lathia et al. 2015). In fact, STAT3 is part of a set of 5 master transcription factors, namely POU3F2, SOX2, SALL2, and OLIG2, which can reprogram differentiated tumor cells to GSC and are required to retain the tumorigenic ability of GSC (Rheinbay et al. 2013). STAT3 is also one of the master regulators responsible for a phenotypic shift of GSC to the more aggressive mesenchymal subtype (Carro et al. 2010). We have shown that even transient STAT3 inhibition results in long-term loss of self-renewal capacities in GBM stem cells (Sherry et al. 2009), suggesting an epigenetic mechanism for STAT3 function in GBM stem cells.

Interaction between epigenetic factors and STAT3

Analogous to our results, STAT3 plays a role in maintaining self-renewal of normal ES cells in mice by upregulating Eed expression which represses differentiation genes (Ura et al. 2008). STAT3 has also been shown to regulate the expression of the H3K9 demethylase Jmjd1a(Ko et al. 2006), which is also necessary for murine ES cell self-renewal. Jak/Stat3 activity was recently shown to promote reprogramming of induced pluripotent stem cells from differentiated mouse embryonic fibroblast cells through an epigenetic mechanism. JAK/STAT3 signaling represses DNMTs and histone deacetylases and facilitates demethylation of Oct4 and Nanog pluripotent genes (Tang et al. 2012). In *Drosophila,* mutation of the PcG complex leads to aberrant STAT activation and uncontrolled growth of imaginal discs, suggesting a delicate balance between epigenetic state of the cells and mitogenic signaling pathways (Classen et al. 2009). The epigenetic state of cells also determines how STAT activation affects neurogenesis (Rajan 2011). CpG methylation or histone methylation of the STAT3 site on glial

fibrillary acidic protein (GFAP) promoter inhibits astroglial differentiation of neural stem cells. During astrocytic differentiation, retinoic acid induces H3 acetylation near the STAT3 site on GFAP gene and increases STAT3 mediated activation of GFAP (Rajan 2011). Upon astrocytic differentiation of human neuroepithelial-like N-Tera2 cells, STAT3 binding correlated with activating H4K3me3, H3K9ac and H3K14ac chromatin marks and RNApol II recruitment, resulting in GFAP gene activation. On the other hand, binding of the Sin3A and MeCp2 corepressor complex at the STAT3 binding site could block access to STAT3 and thereby suppressed GFAP expression and astrocytic differentiation (Cheng et al. 2011). In the context of glioma, hypermethylation of SOCS1 and SOCS3, which negatively regulate STAT3, correlates with poor patient outcome (Rajan 2011).

Epigenomic analyses has shown that a high proportion of STAT3 regulated genes in glioma were associated with histone modification (Kruczyk et al. 2014). STAT3 can also epigenetically regulate tumorigenesis by targeting DNMT1 to suppress tumor suppressor genes, for instance, the PTEN gene in Epstein Barr-induced gastric carcinoma (Hino et al. 2009) and the phosphatase SHP-1 in T-cell lymphoma (Zhang et al. 2005). In MCF10A breast cells, tamoxifen treatment activates STAT3, which then regulates the expression of microRNAs, miR-21 and miR-181-B to induce stable transformation of the cells (Iliopoulos et al. 2010). Here, STAT3 target genes can impart stable change to a cell, presumably in an epigenetically mediated manner.

Tumor hypoxia

In addition to intrinsic genetic and epigenetic alterations in tumor cells, extrinsic microenvironment factors also play a role in regulating GSC. Like many solid tumors,

GBM tumors typically have a hypoxic (~1% oxygen) core, which has been associated with tumor progression, invasion and therapeutic resistance (Soeda et al, 2009). GBM stem cells have been found to be enriched in hypoxic regions (Bar et al. 2010) since they can adapt to the hypoxic microenvironment of the tumor and even form new vessels to obtain nutrients. GSC can survive in the tumor microenvironment with limited nutrients, such as glucose and oxygen. Under such conditions, they exhibit the "Warburg" effect, a metabolic shift toward anaerobic glycolysis to generate ATP and metabolites (Lathia et al. 2015, Masson and Ratcliffe 2014). In the presence of hypoxia, the cells display a reduced rate of proliferation and hence escape traditional chemotherapy that targets dividing cells. Hypoxia also activates stress-induced transcription factors like HIF, NF-KB, JNK and Myc. The HIF family of transcription factors is the most widely known master regulators of hypoxia response genes. HIF proteins, HIF-1, HIF-2 and HIF-3, are composed of a constitutively expressed beta subunit and an inducible alpha subunit. Under normoxic conditions, HIF alpha proteins are hydroxylated by prolyl hydroxylases (PHD) and subsequently get degraded by ubiquitination by a protein complex containing von Hippel-Lindau proteins (pVHL). However, the PHD proteins cannot function under hypoxia, resulting in stabilization of HIF alpha subunits. HIF-1α or HIF-2α then binds to HIF1β to form heterodimers and bind to hypoxic response elements (HREs) to activate its target genes(Chi et al. 2006). A possible mechanism by which HIF-1/HIF-2 promotes tumorigenesis is by activation of MET and AXL oncogenes. HIF-2alpha promotes aberrant tumor cell growth and cell cycle progression by activating the EGF-receptor and IGF-1 receptor tyrosine kinases and their downstream signaling (Franovic et al. 2009). In addition, HIF-2alpha activates tumor cell growth by activating a number of targets, including c-myc, cyclin D1,

TGF-alpha and importantly, stem cell regulator, Oct4 (Seidel et al. 2010; Gordan et al. 2007). In fact, GBM stem cells are enriched in tumor hypoxic niches through HIF-2 alpha activation (Seidel et al. 2010). Intriguingly, elevated HIF-1 levels also lead to efficient angiogenesis by induction of VEGF under hypoxia.

It is well established that solid tumor growth is angiogenesis-dependent. There is evidence that a microscopic tumor is entrapped in a dormant 'avascular state' requiring an 'angiogenic switch' to be transformed into a growing, clinically detectable tumor (Bergers and Benjamin 2003). The switch begins with perivascular detachment and vessel dilation, followed by angiogenic sprouting when new vessels are formed and perivascular cells are recruited. Vascular endothelial growth factor (VEGF) is a proangiogenic factor which promotes vascular permeability and thereby tumor progression. This is especially important in the hypoxic and necrotic areas of GBM tumors to provide it with essential nutrients and oxygen. These tumor cells can induce neoangiogenesis from existing blood vessels and/or recruit endothelial cells from the bone marrow. GBM tumors are, thus, characterized by excessive, disorganized and leaky vasculature resulting in impaired blood supply and drug delivery as well as hypoxia and acidosis(Jain 2005). This leads to a vicious cycle of HIF initiated poorly functioning vasculature, which perpetuates hypoxia and tumor progression.

Current evidence suggests that GSC preferentially reside in the perivascular niche and recapitulates the interaction between normal neural stem cells and the vasculature. Neural stem cells also survive in a physiologically hypoxic microenvironment in the brain, with partial oxygen pressure ranging from 2% to 5% (Moreno et al. 2015). In fact, low oxygen conditions are believed to maintain self-renewal and pluripotency of both normal and GBM stem cells by upregulating Oct4, Nanog and c-Myc genes (Heddleston et al.

2009; Soeda et al. 2009). Both normal NSCs as well as GSC, together with the hypoxic microenvironment, secrete angiogenic factors, like VEGF and angiopoetin 2, to recruit capillaries to the stem cell niche (Bao, Wu, McLendon, et al. 2006). Bao et al showed that CD133 expressing GSC formed more vascular tumors in mice and targeting the proangiogenic factor, VEGF, significantly reduced in vivo tumor burden and vascularity. GSC grow in the perivascular niche in close contact with the endothelial cells, which contribute to maintaining its stem cell properties through Notch pathway activation (Zhu et al. 2011). Thus, the cancer stem cell niche is a critical therapeutic target for GBM.

While it has been shown in other cancers that tumor cells in the proximity of blood vessels are co-opted to undergo vasculogenic mimicry and take on the properties of endothelial cells, there is now direct evidence that GSC exhibit lineage plasticity into vascular lineage. Normal NSCs and GSC can also transdifferentiate into tumor derived endothelial cells, thereby helping to create their own microvasculature to bring about angiogenic switch (Wurmser et al. 2004; Wang et al. 2010; Ricci-Vitiani et al. 2010). Experiments showed that GSC have the ability to generate progeny with phenotypic and functional features of endothelial cells in vitro and in mice (Wang et al. 2010; Ricci-Vitiani et al. 2010). Wang et al. further showed that blocking Notch signaling blocked the differentiation of GSC to endothelial progenitors, while blocking VEGF inhibited the maturation of endothelial progenitors into endothelium (Wang et al. 2010). Selective targeting of the endothelial progenitor cells generated by GSC led to tumor reduction in mouse xenografts (Ricci-Vitiani et al. 2010). Soda et al showed that hypoxia is a key factor for GBM tumor derived endothelial cell formation and that GBM-initiating cells were able to differentiate into endothelial cells by a VEGF or FGF-independent mechanism (Soda et

al. 2011). It is thus, critical to identify and target novel kinase(s) that allow GSC to survive under hypoxic conditions.

Understanding the origin of tumor microvasculature is key to understand how angiogenesis sustains tumor progression and come up with opportunities for therapeutic intervention to normalize tumor vasculature and alleviate hypoxia. Therapies combined antiangiogenic therapy, like bevacizumab, with cytotoxic chemotherapy, like irinotecan, to target tumor cells as well as the vascular niche. The anti-VEGF antibody, bevacizumab, reduced tumor size transiently but the surviving tumor has been shown to be more invasive and activate compensatory angiogenic pathways (Lathia et al. 2015). For instance, targeting DLL4-Notch signaling overcame bevacizumab resistance in DLL4-upregulated GBM xenografts growing in mice (Li et al. 2011). Therefore, small molecules targeting multiple kinases involved in angiogenesis were tested, but gave rise to significant side effects in patients. In addition to activating angiogenic factors, like VEGF, HIF also produces a coordinated response of ancillary growth factors like matrix metalloproteases (MMP), thereby bringing about robust angiogenesis. Consequently, targeting the master regulator HIF might be more beneficial than targeting VEGF alone, and needs to be assessed for side-effects. Hypoxia inducible factor 2A (HIF-2A) was also shown to be a therapeutic target specific for GSC (Li et al. 2009; Heddleston et al. 2009). The epigenetic regulator, mixed lineage leukemia-1 (MLL1) and suppressor of morphogenesis-1 (SMG1) were shown to be hypoxia responsive genes that regulate HIF expression and their downstream targets that often play a role in tumorigenesis (Heddleston et al. 2012; Chen et al. 2009). Jeremy Rich's group demonstrated that CD133+ CSCs from gliomas preferentially expressed HIF-2A (Heddleston et al., 2009; Li et al., 2009). Knockdown of HIF1A or

HIF2A led to the inhibition of self-renewal, proliferation and in vivo tumorigenesis of glioma CSCs (Li et al., 2009). In addition to being necessary for gliomagenesis, HIF-2A was also sufficient to induce cancer stem cell phenotype to non-stem cell glioma population (Heddleston et al. 2009). Although HIF inhibitors are being developed, selective therapeutic targeting of HIFs is difficult (Burroughs et al. 2013). In addition, HIF isoforms have different roles in different cells depending on the metabolic context (Franovic et al. 2009). The molecular mechanisms that allow cells to survive in low oxygen are insufficiently understood. Activation of 5'-AMP activated protein kinase (AMPK) has been shown to be important for tumor cell resistance to hypoxia in a HIF independent manner (Laderoute et al. 2006). A number of receptor tyrosine kinases, like VEGF, SRC, MET, ErbB, FGF and EGFR family members, are also activated under hypoxia in both HIF dependent as well as independent manners. On the other hand, receptor tyrosine kinases can also activate the HIF pathway and thus constitute critical molecular targets in cancer (Glück et al. 2015). Since GBM stem cells are more resistant to hypoxic stressors than other cells in the tumor population, we have performed an RNAi screen to identify specific kinases that enable the survival of GSC in hypoxic microenvironments, in order to achieve effective tumor remission.

Summary

In summary, aberrant self-renewal and proliferation of GBM stem cells and their interaction with the hypoxic tumor microenvironment is a major reason for tumor aggressiveness and therapy resistance. Through the research presented in this thesis, we elucidate how targeting the constitutively active transcription factor, STAT3, in GBM stem cells tilts the lineage fate determination towards neural differentiation by stable epigenetic

changes and thereby inhibits uncontrolled tumor stem cell proliferation. In addition to genetic and epigenetic alterations in the tumor cells, tumor microenvironment factors like oxygen and vascular supply, also affect GBM progression and response to TMZ treatment. Therefore, we, hereby, perform a RNAi screen and follow up the mechanism of action of a kinase target that is essential for the growth of GBM stem cells under low oxygen conditions.

Chapter 2

Regulation of the JMJD3 (KDM6B) histone demethylase in glioblastoma stem cells by STAT3

Relative Contributions

Maureen M. Sherry-Lynes[1] performed the experiments shown in figures 2.1A,D-G; 2.2; 2.4; S2.1A, C-G; S2.2A-D; S2.4.B,D. and Sejuti Sengupta[1] performed the experiments shown in figures 2.1B,C; 2.3; S2.1B; S2.2E-H; S2.3; S2.4A,C; Tables S2.1-2.3.

[1]co-first authors on a manuscript titled "**Regulation of the JMJD3 (KDM6B) histone demethylase in glioblastoma stem cells by STAT3".** Maureen M. Sherry-Lynes, Sejuti Sengupta, Shreya Kulkarni and Brent H. Cochran.

Glioblastoma stem cells (GSC) are highly tumorigenic, and share many properties with normal neural stem cells (Lee et al., 2006; Vescovi et al., 2006). GSC have gene expression patterns that more closely resemble their tumor of origin than do matched serum-derived cell lines (Lee et al., 2006). STAT3 is a transcription factor that is activated by many cytokines and growth factors, and has a demonstrated role in oncogenesis of many human tumors including glioblastoma (Darnell, 2005; Yu and Jove, 2004). STAT3 is required for the maintenance of pluripotency of murine embryonic and neural stem cells and facilitates reprogramming of somatic cells to the pluripotent state (Niwa et al., 1998; Rajan and McKay, 1998; Yang et al., 2010).

We and others have previously shown that the transcription factor STAT3 is essential for glioblastoma stem cell proliferation and multipotency (Carro et al., 2010; Li et al., 2010; Sherry et al., 2009; Wang et al., 2009). Inhibition or RNAi knockdown of STAT3 leads to a dramatic decrease in proliferation and neurosphere formation, as well as loss of stem cell markers (Sherry et al., 2009). Interestingly, this phenotype is irreversible. Transient treatment with STAT3 inhibitors for as little as four hours leads to a permanent loss of neurosphere formation capacity, despite the fact that STAT3 signaling is restored upon drug removal (Sherry et al., 2009). This observation suggests that STAT3 regulates the epigenetic state of the cells, thereby causing a stable change in the ability of the cells to respond to stem cell growth factors.

In stem cells, including normal neural stem cells and GSC, polycomb-mediated repression of differentiation specific genes is a major mechanism by which multipotency is maintained (Bracken and Helin, 2009). PRC2 adds methyl groups to histone H3K27, which leads to the recruitment of the PRC1 and the heritable inhibition of transcription

(Kirmizis et al., 2004; Kuzmichev et al., 2002). The H3K27me2/3 histone demethylase JMJD3 (KDM6B) antagonizes the enzymatic activity of the polycomb repressive complex 2 (PRC2) (Agger et al., 2007; De Santa et al., 2007b; Lan et al., 2007; Xiang et al., 2007). JMJD3 demethylates histone H3K27 at the promoters of neuronal-specific genes in mice (Jepsen et al., 2007), and is required for neural differentiation of murine embryonic stem cells(Burgold et al., 2008). JMJD3 expression can also be rapidly induced in macrophages in response to LPS stimulation (De Santa et al., 2007b).

It is becoming increasingly apparent that H3K27 trimethylation is aberrantly regulated in several cancers. Inactivating mutations have been identified in the H3K27 demethylase *UTX (KDM6A)*, suggesting that UTX acts as a tumor suppressor (van Haaften et al., 2009). Overexpression of EZH2 has been demonstrated in multiple cancer types as well, including medulloblastoma and glioblastoma brain tumors (Robinson et al., 2012; Suva et al., 2009; Zhang et al., 2015). EZH2 expression is necessary for the self-renewal of glioblastoma stem cells (Suva et al., 2009). Mutations in histone H3 itself have been found in pediatric glioblastoma (Bender et al., 2013; Venneti et al., 2013; Wu et al., 2012). Recently, it has been shown that JMJD3 is induced during glioblastoma stem cell differentiation and is mutated in some GSC and that constitutive JMJD3 expression in GSC inhibits their tumorigenesis (Ene et al., 2012). These findings suggest that the aberrant maintenance of H3K27 methylation contributes to oncogenesis. Based on these observations and the STAT3 inhibition phenotype, we investigated the possibility that the H3K27 demethylase JMJD3 may mediate effects of STAT3 in glioblastoma stem cells.

EXPERIMENTAL PROCEDURES

Culture of glioblastoma stem cells and normal neural stem cells

Glioblastoma stem cell lines and culture conditions were described previously (Sherry et al., 2009). Normal human neural stem cells derived from H9 embryonic stem cells were obtained from Gibco (Carlsbad, CA). Cells were grown according to instructions of the manufacturer. For neurosphere formation assays, cells were dissociated from the coated plates with accutase and plated in neural stem cell media in uncoated plates. STAT3 inhibitors S3I-201, STA-21 (NCI/DTP Open Chemical Repository) or BP1-102 (EMD Millipore, Billerica, MA) were used at the indicated concentrations. Recombinant BMP4 (Life technologies, Grand Island, NY) was added to the culture media when indicated.

Immunoblotting

Immunoblots were performed as previously described (Sherry et al., 2009) with the exception that immunoblots to be probed with anti-JMJD3 antibody were transferred in 10 mM CAPS (3-[Cyclohexylamino]-1-propanesulfonic acid, pH 10.5) buffer. Anti-β-Actin (1:2000) was obtained from Sigma (St. Louis, MO); anti-STAT3 (1:1000), anti pSer-STAT3 (1:200), anti-pTyr STAT3 (1:500) were obtained from Cell Signaling Technologies (Beverly, MA). Anti-JMJD3 was obtained from Abgent (San Diego, CA) or generously provided by the lab of Yang Shi.

RT-qPCR

RT-qPCR was performed as previously described (Sherry et al., 2009). Fold changes were calculated relative to control by the $2^{-\Delta\Delta Ct}$ method (Livak and Schmittgen, 2001). Statistical analysis was performed according to the comparative C_T method. All primer sets amplify a single product of the predicted size; primer sequences can be found in supplemental experimental procedures. b-actin was used as the housekeeping gene.

Lentiviral shRNA infection and overexpression retrovirus infection

Cells were infected with either PLKO.1 non-targeting control lentivirus (Sigma) or shSTAT3 PLKO.1 lentivirus (clones TRCN0000020843 and TRCN0000020842), shJMJD3 (V2LHS_139678, Open Biosystems, Figure 2), shJMJD3 2 (pSico-R-PGKPuro lentivirus from (Burgold et al., 2008), Supplementary Figure 2), in the presence of 8 μg/mL polybrene. 24 hours post-infection the virus containing media was removed and replaced with fresh stem cell media for 24 hours. Cells were then treated with 2.5 μg/mL puromycin. After 2-3 days of puromycin selection, cells were plated for assays as described in the figure legends.

The MSCV-JMJD3 (Addgene plasmid 21212) (Sen et al., 2008), MSCV-JMJD3 mutant (Addgene plasmid 21214) (Sen et al., 2008) and MSCV-Tap Control (Addgene plasmid 12570) (Frias et al., 2006) retroviral plasmids were obtained from Addgene (Cambridge, MA). The viruses were packaged in 293GPG cells as described by Ory et al (Ory et al., 1996). Glioma stem cells were infected at an approximate MOI of 1 overnight, and then overnight again. 96 hours after the first infection cells were treated

with 2.5 ug/mL puromycin for 4 days. After 4 days of puromycin selection cells were plated for assays as described in the figure legends.

ChIP and ChIP-Sequencing

Cells were lysed, fixed, and sonicated according to the methods of De Santa et. al (De Santa et al., 2007a). Sonicated lysates were incubated overnight with either anti-STAT3 (Santa Cruz Biotechnology, Santa Cruz, CA), anti-H3K27me3 (Millipore, Billerica, MA), or IgG control. Immunoprecipitation was carried out using StaphA cells according to the protocol of Kirmizis et al. (2004) or using Protein A-Sepharose beads according to the nano ChIP-seq protocol (Adli and Bernstein (2011). After washing and cross-link reversal, immunoprecipitated DNA was purified using the Qiagen PCR Purification kit (Qiagen, Valencia, CA) and subjected to either qPCR or PCR as indicated in figure legends. For nano ChIP sequencing and nano ChIP-qPCR, the immunoprecipitated DNA was subjected to two intermediate rounds of amplification (Adli and Bernstein (2011) with custom primers containing barcodes that allowed us to multiplex 3 replicates for each of the two treatment groups in a sequencing lane (supplemental procedure). It was then subjected to either library amplification using TruSeq ChIP Sample preparation kit (Illumina Inc, San Diego, CA) followed by next generation sequencing on HiSeq 2500 (Illumina Inc, San Diego, CA) or qPCR. Detailed chip protocol available upon request. Myt1 primers were first described in (Sarma et al., 2008). FGF21 and GDF15 primers were designed to span regions of H3K27me3 enrichment near the gene promoter from ChIP-Sequencing data analysis. Primers used

appear in supplemental experimental procedures. ChIP qPCR data was analyzed according to the percent of input method described by Haring et. al (Haring et al., 2007).

ChIP-Sequencing data analysis

ChIP Sequencing reads were aligned to the human genome (hg19) using Bowtie in GALAXY platform and visualized in the UCSC genome browser (Karolchik et al., 2009). The average read count through the 5kb upstream promoter region of each gene was computed across the genome. The normalized read counts at the promoters of STAT3 inhibited and control treatment groups was compared and a list of genes that showed reduction in H3K27me3 mark upon STAT3 inhibition was obtained (Hebenstreit et al., 2011; Maze et al., 2011).

Microarray

Microarray gene expression data was generated using GeneChip Human gene U133A 2.0 Arrays (Affymetrix, Santa Clara, CA). The CEL files were processed by Transcriptome Analysis Console (Affymetrix) software to analyze differentially expressed genes based on fold change.

List of primers

qRT-PCR primers

JMJD3 forward: CTACCCCCTTCACATGGCAG;

JMJD3 reverse: CTCTGACTCGTACAGTTGCCC;

Myt1 forward: TGCTTGCCCCAAAGATTCAGA;

Myt1 reverse: AGTGCTCCTCACATAACTACTGG;

βIII-tubulin forward: GCCTCTTCTCACAAGTACGTG;

βIII-tubulin reverse: CCCCACTCTGACCAAAGATGAA;

β-actin forward: CCTGGGCATGGAGTCCTGTGG;

β-actin reverse: CTGTGTTGGCGTACAGGTCTT;

FGF21 forward: CTGTGGGTTTCTGTGCTGG;

FGF21 reverse: CCGGCTTCAAGGCTTTCAG;

GDF15 forward: ACCTGCACCTGCGTATCTCT;

GDF15 reverse: CGGACGAAGATTCTGCCAG.

Nano-ChIP-Seq Library preparation primers

Primer 1: GACATGTATCCGGATGTA [X] NNNNNNNNN;

where [X] denotes the custom barcodes for each sample as specified below:

ATCACG; TTAGGC; ACAGTG; GATCAG; TAGCTT or GGCTAC;

Primer 2: GACATGTATCCGGATGT.

ChIP primers

JMJD3 forward: AGGAAGAGCTGGGGCTAAAG;

JMJD3 reverse: CTGGCTTTCTGGGTCTTCAA;

MYT1 forward: AGGCACCTTCTGTTGGCCGA;

MYT1 reverse: AGGCAGCTGCCTCCCGTACA;

FGF21 forward: CACAGTGCTGGGATTACCG;

FGF21 reverse: AGACGCTGGCCAACTAGAGA;

GDF15 forward: CAGGCACAGTGTCAACCAAG;

GDF15 reverse: AGGTTGCAGTGAGCCAAGA

RESULTS

STAT3 represses JMJD3 expression in glioblastoma stem cells

We first examined JMJD3 expression in response to STAT3 inhibition in two glioblastoma stem cell lines, GS6-22 and GS7-2, which we have previously characterized (Sherry et al., 2009). Upon STAT3 inhibition with the SH2-domain-targeting small molecule inhibitors STA-21 and S3I-201 (Siddiquee et al., 2007; Song et al., 2005), JMJD3 expression is upregulated at both the protein and mRNA levels by 2-15 fold (Figure 2.1A,B, Figure S2.1A, B). JMJD3 mRNA is also upregulated upon STAT3 knockdown using two different shRNAs (Figure 2.1C, Figure S2.1D). Additionally, JMJD3 mRNA is upregulated by a highly potent next-generation STAT3 inhibitor BP-1-102 (Zhang et al, 2012) and S3I-201 treatment in additional GSC lines tested (Figure S1B). Thus, multiple STAT3 specific inhibitors lead to upregulation of JMJD3 expression in different GSC lines.

By chromatin immunoprecipitation assay, STAT3 was found to bind to the JMJD3 promoter at a position containing a conserved STAT3 binding site (Figure 2.1D, Figure S2.1C), suggesting that JMJD3 is a direct STAT3 target gene. Previously it has been shown that JMJD3 is upregulated during murine neural stem cell differentiation, and that it targets several neural specific genes upon differentiation of neural stem cells (Burgold et al., 2008; Jepsen et al., 2007). Consistent with this we have found that JMJD3 is upregulated during GSC differentiation as well (Figure 2.1E, Figure S2.1E). UTX, another member of the JMJD3 family of H3K27me3 demethylases, is not consistently upregulated by the two STAT3 inhibitors, S3I-201 and STA-21, in both of our cell lines (Figure S2.1F, G)

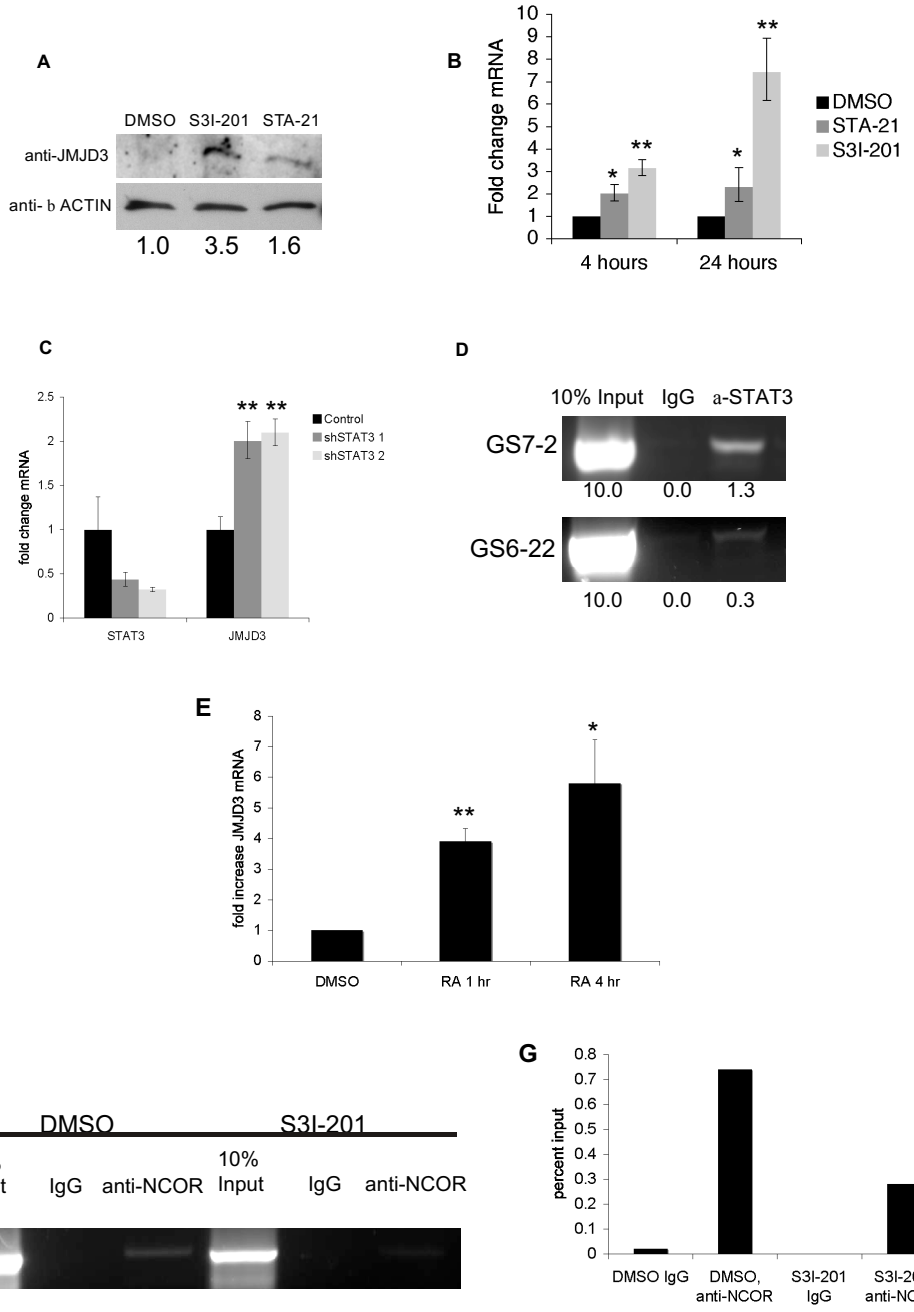
A
DMSO S3I-201 STA-21
anti-JMJD3
anti- b ACTIN
1.0 3.5 1.6
B
Fold change mRNA
DMSO
STA-21
S3I-201
4 hours
24 hours
C
fold change mRNA
Control
shSTAT3 1
shSTAT3 2
STAT3
JMJD3
D
10% Input IgG a-STAT3
GS7-2
10.0 0.0 1.3
GS6-22
10.0 0.0 0.3
E
fold increase JMJD3 mRNA
DMSO
RA 1 hr
RA 4 hr
F
DMSO
S3I-201
10% Input
IgG
anti-NCOR
10% Input
IgG
anti-NCOR
G
percent input
DMSO IgG
DMSO, anti-NCOR
S3I-201 IgG
S3I-201, anti-NCOR

Figure 2.1. STAT3 represses JMJD3 expression in glioblastoma stem cells. A. Treatment of GS6-22 and GS7-2 cells with the STAT3 inhibitor S3I-201 (50 μM) or STA-21 (50 μM) causes upregulation of JMJD3 protein levels. Cells were lysed for immunoblotting after 8 hours of drug treatment. Relative JMJD3 protein levels were quantified using ImageJ and are shown below each lane. B. RT-qPCR of GS6-22 cells treated with S3I-201 or STA-21 demonstrates that JMJD3 mRNA is upregulated at both 4 hours and 24 hours after inhibitor treatment. Values represent the fold change relative to DMSO treated cells for three experiments; bars SD (**$p<0.01$). C. Knockdown of STAT3 using an shRNA-containing lentivirus leads to the upregulation of JMJD3 mRNA in GS6-22 cells, two days after selection. Values represent the fold change relative to DMSO treated cells for three experiments; bars SD (**$p<0.01$). D. Chromatin immunoprecipitation using anti-STAT3 antibody, followed by PCR using primers to the JMJD3 promoter demonstrates STAT3 binding in GS7-2 and GS6-22 cells. Enrichment of DNA in STAT3 immunoprecipitation (relative to input) was quantified by ImageJ. E. Treatment of GS6-22 cells with retinoic acid increases JMJD3 mRNA levels. GS6-22 cells were treated for 1 and 4 hours with 1 μM RA. Values represent the fold change relative to DMSO treated cells for three experiments; bars SD (*$p<0.05$, **$p<0.01$). F. S3I-201 treatment decreases NCor binding at the JMJD3 promoter. GS6-22 cells were treated with S3I-201 (50 μM) or DMSO for 4 hours, fixed, lysed, and sonicated. Sonicated lysates were incubated overnight with anti-NCor or IgG control and subjected to chromatin immunoprecipitation. The resulting DNA was subjected to PCR using primers to the JMJD3 promoter. G. Densitometry of F was performed using ImageJ.

Interestingly, STAT3 appears to repress JMJD3 expression, rather than activate it as is typical for STAT3 target genes (Bromberg and Darnell, 2000). However, STAT3 has been shown to repress genes in other cell types, and is associated with both transcriptionally active and repressed genes in embryonic stem cells (Kidder et al., 2008). In murine neural stem cells, JMJD3 is repressed by the NCoR and SMRT nuclear co-repressors, which associate with the retinoic acid receptor to repress transcription (Jepsen et al., 2007). STAT3 has been shown to associate with the retinoic acid receptor (RAR), so we considered the possibility that NCoR repression is involved in regulating JMJD3 in glioblastoma stem cells (Asano et al., 2009; Yang et al., 2004). Retinoic acid treatment of GS6-22 cells leads to a rapid increase in JMJD3 mRNA (Figure 2.1E). Additionally, the NCoR co-repressor can be found at the JMJD3 promoter by chromatin immunoprecipitation (Figure 2.1F,G). NCoR can be immunoprecipitated using the same primers as STAT3, suggesting it binds a similar region of the JMJD3 promoter. Furthermore, treatment with the STAT3 inhibitor S3I-201 decreases NCoR binding to the JMJD3 promoter (Figure 2.1F,G). It is possible, then, that STAT3 represses JMJD3 expression by interaction with the NCoR-RAR complex, and that treatment with S3I-201 abolishes this interaction, thereby relieving the repression of JMJD3.

STAT3 regulates GSC neurosphere formation and proliferation through repression of JMJD3

Neurosphere formation is a hallmark of neural stem cells, and the ability to culture neurospheres from glioblastomas strongly correlates with poor patient prognosis (Laks et al., 2009). Because STAT3 represses JMJD3 expression in GSC, we

investigated whether knockdown of JMJD3 expression could rescue the abrogation of neurosphere formation that accompanies STAT3 inhibition. GS6-22 and GS7-2 cells were infected with lentiviruses expressing shRNA to JMJD3 or with control lentiviruses. Control infected cells exhibited decreased neurosphere formation in response to S3I-201 treatment as expected (Figure 2.2A,B,C). shJMJD3 infected cells, however, were able to form spheres in the presence of S3I-201 (Figure 2.2A,B,C). This was also true for cells infected with a second, distinct shRNA to JMJD3, indicating that this is a specific effect of JMJD3 knockdown (Figure S2.2A,B). This effect was more pronounced in the GS7-2 cells (Figure 2.2C) than the GS6-22 cells (Figure 2.2B) likely due to the enhanced degree of knockdown in the GS7-2 cells (78% knockdown in the GS7-2 cells versus 55% for GS6-22 cells) (Figure S2.2C,D). These data indicate that STAT3 repression of JMJD3 is necessary for neurosphere formation.

Consistent with this, overexpression of JMJD3 recapitulates significant aspects of the STAT3 inhibition phenotype. Both GS6-22 and GS7-2 cells that had been engineered to constitutively express JMJD3 fail to form neurospheres in stem cell media (Figure 2.2D,E). Overexpression of a catalytic dead mutant of JMJD3, however, does not inhibit sphere formation (Figure 2.2D,E). In addition, overexpression of JMJD3, but not mutant JMJD3, decreased proliferation in both GS6-22 and GS7-2 cells (Figure 2.2F,G). This effect was more pronounced in GS7-2 cells, but the degree of overexpression was also higher in these cells (Figure S2.2E,F). This indicates that the demethylase activity of JMJD3 is necessary for the inhibition of sphere formation and proliferation of GSC. STAT3 repression of JMJD3, then, is required for GSC neurosphere formation and proliferation.

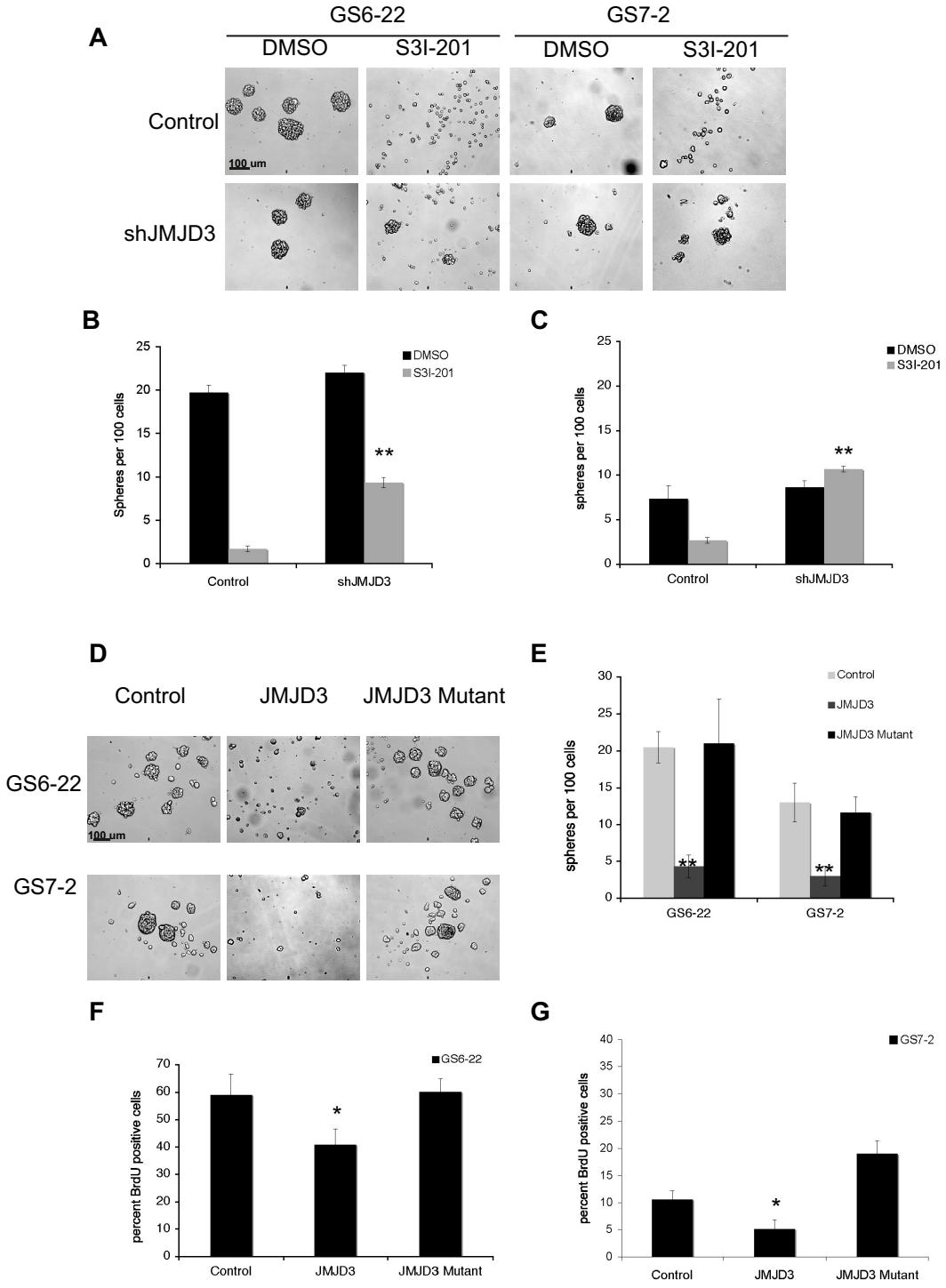
A
GS6-22
GS7-2
DMSO
S3I-201
DMSO
S3I-201
Control
shJMJD3
100 um
B
Spheres per 100 cells
DMSO
S3I-201
**
Control
shJMJD3
C
spheres per 100 cells
DMSO
S3I-201
**
Control
shJMJD3
D
Control
JMJD3
JMJD3 Mutant
GS6-22
GS7-2
100 um
E
spheres per 100 cells
Control
JMJD3
JMJD3 Mutant
**
**
GS6-22
GS7-2
F
percent BrdU positive cells
GS6-22
*
Control
JMJD3
JMJD3 Mutant
G
percent BrdU positive cells
GS7-2
*
Control
JMJD3
JMJD3 Mutant

Figure 2.2. STAT3 controls GSC neurosphere formation and proliferation through repression of JMJD3. A. Knockdown of JMJD3 rescues neurosphere formation in the presence of S3I-201. Representative images of GS6-22 and GS7-2 cells infected with either control or shJMJD3 containing lentivirus treated with DMSO or S3I-201 (50 μM). Images for GS6-22 cells were taken after 6 days and GS7-2 cells were taken after 4 days, based on differences in sphere formation rate in these lines. B. Quantification of neurosphere formation in GS6-22 cells. After 6 days of inhibitor treatment, the number of spheres per 100 cells was counted. Values represent the mean of triplicates within each treatment; bars SE (**$p<0.01$). C. After 4 days of inhibitor treatment, GS7-2 cell sphere formation was quantified as described for GS6-22 cells. Values represent the mean of triplicates within each treatment; bars SE (**$p<0.01$ relative to DMSO control, upon shJMJD3 infection). D. Representative images of GS6-22 and GS7-2 cells infected with overexpression retrovirus containing either a control (empty) plasmid, JMJD3, or a catalytic domain mutant of JMJD3. After three days of selection, cells were dissociated and replated at 100 cells per ml. Pictures were taken at 50X seven days after replating. E. Quantification of neurosphere formation capacity in GS6-22 and GS7-2 cells infected with the JMJD3 overexpression retrovirus. Limiting dilution was performed in triplicate (**$p<0.01$). F. GS6-22 and G. GS7-2 cells were infected with either control, JMJD3, or JMJD3 mutant retroviruses as previously described. Cells were pulsed with 30 μM BrdU for 16 hours. After 24 hours, cells were fixed and stained with an anti-BrdU antibody. Cells were also stained with 7-AAD at this time. The percentage of BrdU positive cells was analyzed using flow cytometry. Values represent the mean of 3 experiments; bars SD of the mean (*$p<0.05$).

Interestingly, overexpression of both wildtype JMJD3 and the mutant increased apoptosis in GS6-22 cells (Figure S2.2G). It is possible the mutant JMJD3 may interfere with some cellular functions by substrate binding and sequestration. JMJD3 has been found to have demethylase independent functions(Chen et al., 2012). This effect was not observed in GS7-2 cells (Figure S2.2H). This may be because these cells lack expression of the INK4A/ARF locus.

STAT3 regulates H3K27 trimethylation and neural gene induction in GSC

To identify putative STAT3 regulated genes that show induction of gene expression concurrent with histone H3K27 demethylation in GS6-22, we performed microarrays and genome wide CHIP-sequencing analysis using an antibody specific to H3K27me3, following STAT3 inhibition. Differential analysis of STAT3 inhibited and control GS6-22 cells yielded a ranked list of genes that were likely to show reduction in H3K27me3 mark (Table S2.1) or are induced upon STAT3 inhibition with a fold change >2 (Table S2.2). The intersected list of genes showing both reduction in repressive H3K27me3 mark as well as 2 fold or higher gene expression upon S3i treatment is tabulated in Table S2.3.

We subsequently confirmed that STAT3 inhibition by the next-generation STAT3 inhibitor BP-1-102 (Zhang et al, 2012) upregulates mRNA expression of Fibroblast Growth Factor 21 (FGF21) and Growth Differentiation Factor 15 (GDF15) in GS6-22 and GS7-2 cells (Fig 2.3A,S2.3A). These genes are known to play roles in neural development (Carrillo-Garcia et al., 2014; Huang et al., 2013). GDF15 has also been

A

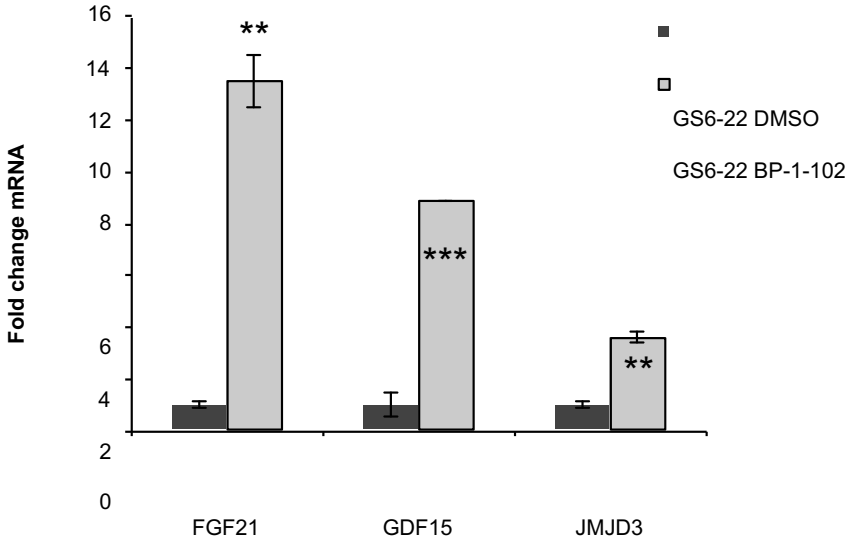
16
14
12
10
8
6
4
2
0
Fold change mRNA
**
***
**
GS6-22 DMSO
GS6-22 BP-1-102
FGF21
GDF15
JMJD3

B

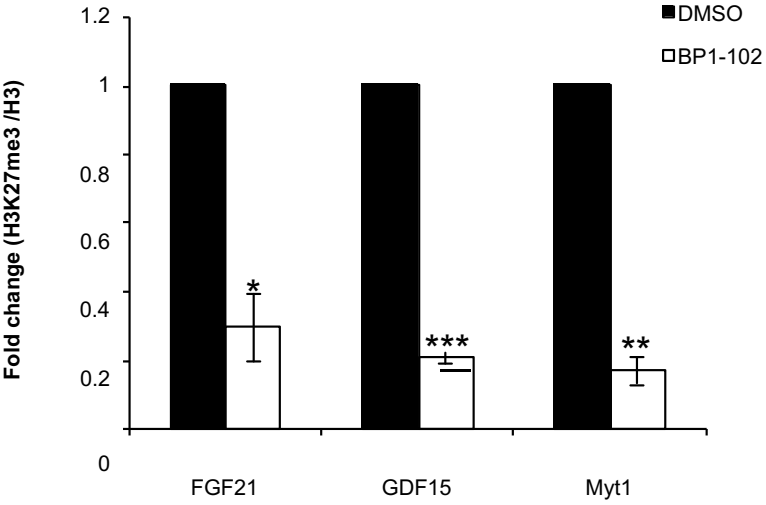
1.2
1
0.8
0.6
0.4
0.2
0
Fold change (H3K27me3 /H3)
DMSO
BP1-102
*
***
**
FGF21
GDF15
Myt1

C

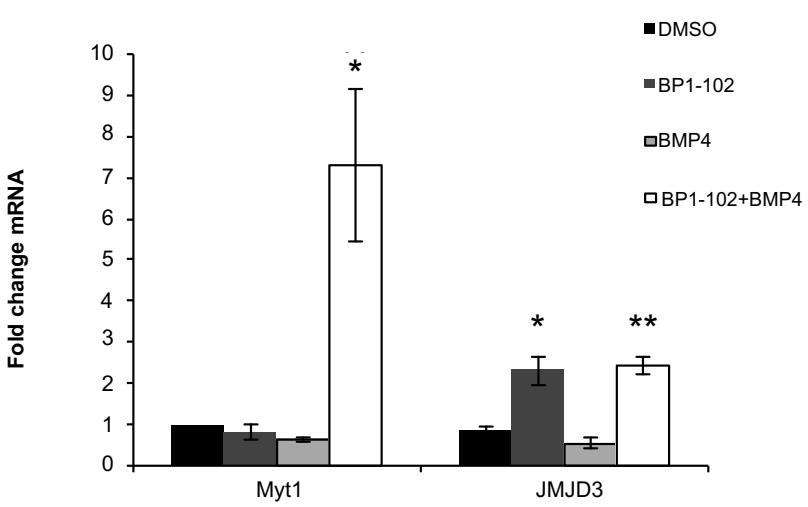
10
9
8
7
6
5
4
3
2
1
0
Fold change mRNA
DMSO
BP1-102
BMP4
BP1-102+BMP4
*
*
**
Myt1
JMJD3

Figure 2.3. STAT3 regulates H3K27 trimethylation and neural gene induction in GSC. A. RT-qPCR analysis of FGF21, GDF15 and JMJD3 expression in GS6-22 cells treated with BP-1-102 (15uM) for 6 hours. Values represent the fold change relative to control cells for three experiments; bars SD (**p<0.01, ***p<0.005). B. GS6-22 cells were treated with BP-1-102 (15 μM) or DMSO for 6 hours, fixed, lysed, and subjected to chromatin immunoprecipitation with an antibody to H3K27 trimethylation or total histone H3. Quantitative PCR using primers to FGF21 or GDF15 or Myt1 genes was performed after immunoprecipitation, amplification and DNA purification. Data is displayed as percentage of input DNA of H3K27me3/H3 ChIP, normalized relative to control cells for three experiments (*p<0.05, **p<0.01, ***p<0.005). C. Demethylation of H3K27 at the Myt1 promoter confers BMP4 inducibility of the gene. RT-qPCR analysis of Myt1 and JMJD3 expression in GS6-22 cells treated with BP-1-102 (15uM), recombinant BMP4 (10 ng/ml) or a combination of both for 6 hours. Values represent the fold change relative to DMSO treated control cells for three experiments; bars SD (*p<0.05, **p<0.01).

shown to induce apoptosis and inhibit tumorigenesis in GBM (Lee et al., 2010; Shimizu et al., 2013).

Consistent with the induction of gene expression, ChIP-sequencing data analysis suggested loss of H3K27me3 peaks at FGF21 and GDF15 promoters in STAT3 inhibited GS6-22 cells compared to control. This was confirmed using ChIP-qPCR analysis, which showed that STAT3 inhibition by BP-1-102 decreases H3K27 trimethylation at FGF21 and GDF15 promoters (Fig 2.3B), concurrent with JMJD3 upregulation in GS6-22 cells (Fig 2.3A). The amount of total histone H3 does not change upon BP-1-102 treatment indicating that there is a loss of H3K27 trimethylation at these promoters and not just a loss of histone H3 association (Fig S2.3B, C). These results indicate that inhibition of STAT3 induces H3K27 demethylation and subsequent expression of target genes involved in neural differentiation of GSC.

Demethylation of H3K27 at the Myt1 promoter confers BMP4 inducibility

Because JMJD3 inhibits sphere formation and proliferation of GSC in a demethylase-dependent manner, we examined the H3K27me3 status at the promoter of a known JMJD3 and polycomb target gene, myelin transcription factor 1, Myt1 (Kirmizis et al., 2004), which is a gene that has been implicated in neuronal differentiation (Romm et al., 2005). GS6-22 cells were treated with STAT3 inhibitor, BP-1-102, and subjected to chromatin immunoprecipitation (ChIP) using an antibody specific to H3K27me3. In GS6-22 cells, a decrease in H3K27 trimethylation was observed at the Myt1 promoter (Fig. 2.3B, S2.3D), concurrent with JMJD3 upregulation. The degree of decrease in H3K27 trimethylation is consistent with that seen at other promoters demethylated by

JMJD3 (Barradas et al., 2009; Jepsen et al., 2007) and suggests that Myt1 is a JMJD3 target gene in GSC.

However, STAT3 inhibition or expression of JMJD3 in stem cell growth conditions was not sufficient to induce Myt1 gene expression (Figure 2.3C, Fig. S2.4B), suggesting that other factors or signals are required to activate these neural specific gene expression. It has been previously shown that Bone Morphogenetic Protein 4 (BMP4) activates the Smad signaling cascade and induces differentiation of stem-like, tumor-initiating precursors of GBMs (Piccirillo et al., 2006) and that SMADs and JMJD3 co-regulate genes in NSCs (Estaras et al., 2012). Myt1 expression is strongly induced upon BMP4 treatment when STAT3 is inhibited in GS6-22 and GS7-2 cells (Figure 2.3C, S2.4A). This suggests that STAT3 inhibition and subsequent demethylation of histone H3K27 at the promoter renders the chromatin accessible to BMP4 induced transcription factors at this locus.

Interestingly, we have not found a change in H3K27me3 at the *INK4A/Arf* locus (Figure S2.4C) in GS6-22 cells. This locus is a well-characterized JMJD3 target (Agger et al., 2007; Agherbi et al., 2009; Barradas et al., 2009), and its demethylation is necessary for the induction of growth arrest and senescence in several cell types. In GS7-2 cells, we failed to see PCR amplification of INK4A/ARF in genomic DNA, which suggests that this locus is deleted in GS7-2 cells (Figure S2.4D). This is not surprising given that over half of glioblastomas exhibit homozygous deletion of this locus (Ivanchuk et al., 2001). Together, these observations suggest that JMJD3 regulation of GSC proliferation and sphere formation is independent of *INK4A/ARF*. Ene et al (2012) came to a similar conclusion.

STAT3 regulates JMJD3 expression in human neural stem cells

Finally, we examined whether STAT3 repression of JMJD3 was specific to glioblastoma stem cells, or whether the STAT3 inhibition phenotype is recapitulated in normal human neural stem cells. In neural stem cells derived from H9 embryonic stem cells (Marei et al., 2011; Yan et al., 2013), STAT3 is activated by phosphorylation on both pTyr705 and pSer727 (Figure 2.4A). S3I-201 treatment of these cells inhibited neurosphere formation (Figure 2.4B) and lead to upregulation of JMJD3 mRNA (Figure 2.4C), as well as to dose-dependent inhibition of proliferation as judged by BrdU incorporation (Figure 2.4D). STAT3, then, regulates neurosphere formation and proliferation in normal embryonic neural stem cells as well as in glioblastoma stem cells. STAT3 repression of JMJD3 is also maintained in normal neural stem cells. This indicates that STAT3 control of the epigenetic program through JMJD3 repression is a key mechanism of stem cell maintenance in both normal and tumorigenic neural stem cells.

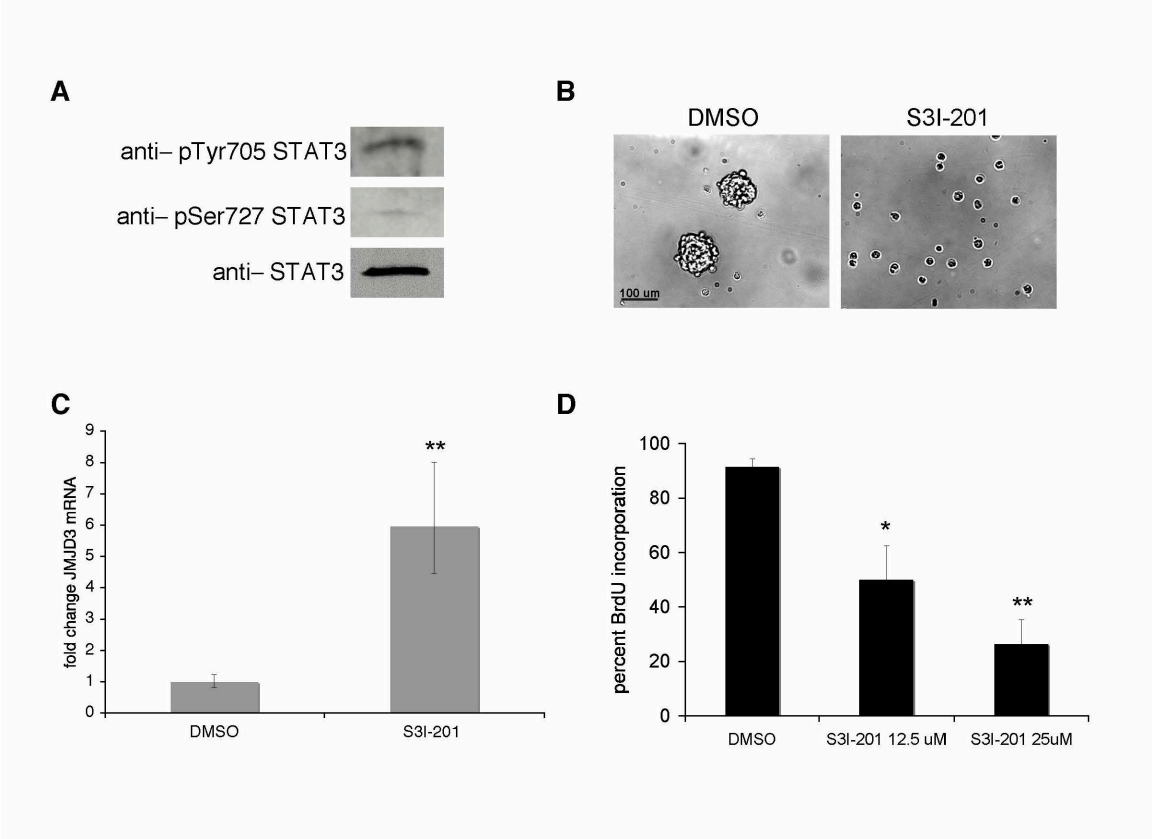

Figure 2.4. STAT3 inhibition in human neural stem cells leads to a decrease in neurosphere formation and proliferation, and an upregulation of JMJD3 expression. A. STAT3 activation in human neural stem cells was assessed by immunoblotting with phospho-specific antibodies. B. Human neural stem cells were plated in serum free media supplemented with EGF and FGF2. 24 hours after plating, cells were treated with S3I-201 (50 μM) or DMSO control. Pictures were taken 3 days after treatment. C. STAT3 regulation of JMJD3 was assessed by qRT-PCR. Human neural stem cells were treated with S3I-201 (50 μM) for 24 hours. Values represent the fold change relative to control cells for three experiments; bars SD (**$p<0.01$). D. Cells were treated with DMSO or S3I-201 for 24 hours, and then subjected to a 15 μM BrdU pulse for 20 hours. Values represent the average of three experiments; bars SE (*$p<0.05$, **$p<0.01$).

Discussion

We have shown that STAT3 maintains normal neural and glioblastoma stem cells in a proliferative, self-renewing state via the repression of the histone demethylase JMJD3. STAT3 repression of JMJD3 is consistent with our previous data that STAT3 inhibition is irreversible in GSC. We have found that STAT3 inhibition or knockdown leads to rapid upregulation of JMJD3. We have also found that STAT3 binds to the JMJD3 promoter in human GSC which is consistent with published genomic data from murine ES cells (Kidder et al., 2008) and suggests that STAT3 is a direct regulator of JMJD3.

While STAT3 is best known as a transcriptional activator, there is evidence that it can act as a repressor (Fukada et al., 1998; Rokavec et al., 2014). ChIP-ChIP and microarray studies suggest that STAT3 represses genes in multiple cell types (Dauer et al., 2005; Kidder et al., 2008). Previous studies indicated that NCoR negatively regulates JMJD3 (Jepsen et al., 2007). We have found that following STAT3 inhibition NcoR binding is reduced at the same promoter fragment that binds STAT3, suggesting that the mechanism of repression is recruitment or stabilization of the NCoR repressor complex at the promoter. While Ene et al (2012) have found evidence that DNA methylation can also contribute to JMJD3 repression, the sites of that STAT3 binds to appear to be distinct from the regions of DNA methylation (Ene et al., 2012). However, given recent evidence that STAT3 can control DNA methylation (Lee et al., 2012), this mechanism of regulation merits further investigation.

We have also found that JMJD3 overexpression inhibits neurosphere formation and cell proliferation. JMJD3 overexpression also induces apoptosis in GS6-22 cells. A

similar effect on both proliferation and apoptosis of GSC has been reported for knockdown of BMI-1, part of the PRC1 complex (Abdouh et al., 2009). Similarly, inhibition of EZH2, part of the PRC2 complex, causes a decrease in sphere formation and proliferation of GSC (Suva et al., 2009). Interestingly, EZH2 also methylates and regulates STAT3 in GSC which further suggests a tight coordination between STAT3 and H3K27 trimethylation (Kim et al., 2013).

In this regard, it is also worth noting the role of histone H3K27 trimethylation in brain tumors is complex. While induction and maintenance of this mark is pro-oncogenic in medulloblastoma and adult glioblastomas(Kim et al., 2013; Robinson et al., 2012; Suva et al., 2009; Zhang et al., 2015), global loss of H3K27 methylation is oncogenic in pediatric gliomas(Bender et al., 2013; Venneti et al., 2013). Thus, the effects of H3K27 trimethylation are are context dependent. This is consistent with findings from other cancers as well (Ntziachristos et al., 2014; Yamaguchi and Hung, 2014).

Recently, JMJD3 overexpression has been shown to decrease the tumorigenicity of GSC *in vivo* (Ene et al., 2012). This is consistent with our data that overexpression of JMJD3, which opposes PRC2 activity, decreases proliferation and sphere formation (Figures 2,3). We have also found that a catalytic mutant of JMJD3 does not affect neurosphere formation or proliferation. Thus, JMJD3 upregulation and the subsequent demethylation of histone H3K27 on target genes is likely necessary for the decrease in GSC growth. This induction of JMJD3 likely imparts widespread changes to the chromatin and sustained mRNA expression of target genes involved in neural differentiation of GSC. This would explain why either the restoration of STAT3 signaling following removal of S3I-201 STAT3 inhibitor (Sherry et al., 2009), or

sustained STAT3 signaling when JMJD3 is constitutively expressed, does not rescue neurosphere formation. This difference in epigenetic state may also explain how STAT3 can induce astrocytic differentiation of neural stem cells under some conditions and preserve neural stem cell self-renewal in others (Bonni et al., 1997; Gu et al., 2005; Lee et al., 2008; Rajan and McKay, 1998). A similar persistence of a stable STAT3 phenotype has been demonstrated in breast epithelial cells, in which a transient expression of either of two STAT3-regulated microRNAs is sufficient to induce and maintain a stably transformed state that is also polycomb mediated (Iliopoulos et al., 2009; Iliopoulos et al., 2010). Thus, there is precedence for the transient upregulation of a single STAT3 target gene imparting permanent change to the cellular state.

Interestingly, although STAT3 inhibition induces neural genes, such as FGF21 and GDF15, neither JMJD3 overexpression or STAT3 inhibition are sufficient to drive differentiation of the glioblastoma stem cells (Figure S4B, (Sherry et al., 2009)). While JMJD3 overexpression is sufficient to induce differentiation in some systems (Jepsen et al., 2007; Sen et al., 2008), it is likely that additional positive differentiation signals are required both in these cases and in the case of the GSC. Histone H3K27 demethylation may be sufficient to open the chromatin at specific genes, but positively acting transcription factors are likely needed in addition to bind to these promoters to activate transcription. Consistent with this, we have found that JMJD3 overexpression can demethylate histone H3K27 at differentiation-specific genes such as Myt1, but the gene is upregulated only in the presence of recombinant BMP4. This situation is similar to previous results for the GFAP gene where epigenetic changes must occur before factors like CNTF are able to induce the gene during astrocytic differentiation (Song and Ghosh,

2004; Takizawa et al., 2001; Urayama et al., 2013). Interestingly, STAT3 regulates GFAP as well (Song and Ghosh, 2004; Takizawa et al., 2001; Urayama et al., 2013).

In addition, JMJD3 overexpression alone does not completely recapitulate the STAT3 inhibition phenotype, at least with respect to βIII-tubulin expression (Figure 3D, S4B, and (Sherry et al., 2009)). Given that STAT3 signaling likely regulates many genes in addition to JMJD3 in GSC, this is not surprising. However, the fact that constitutive JMJD3 expression substantially inhibits neurosphere formation as well as proliferation indicates that JMJD3 repression by STAT3 is required for glioblastoma stem cell maintenance.

Strikingly, we have also found that STAT3 repression of JMJD3 is a mechanism shared by both glioma stem cells and normal neural stem cells (Figure 4). While this could complicate therapeutic targeting of STAT3 in glioblastoma, it does provide further evidence that similar signaling and epigenetic mechanisms that govern both cancer stem cells and tissue stem cells at least in this case. STAT3 is necessary for the self-renewal of a variety of stem cell types, including murine embryonic stem cells (Niwa et al., 1998), and its regulation of the epigenetic program may prove to be a widespread and developmentally critical mechanism of maintaining stem cell self-renewal.

Figure S2.1, related to Figure 2.1

A

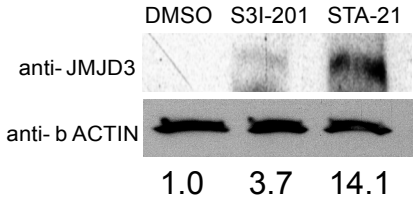

B

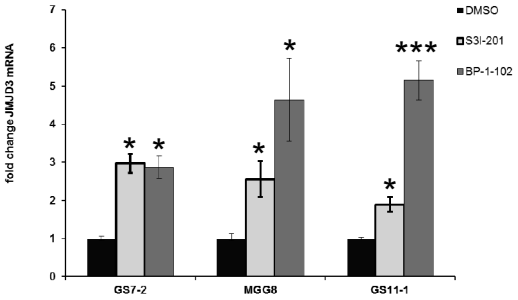

C

AAGGAAGAGCTGGGGCTAAAGGGAAGGTGCCCAAGAGAGGGGAGCGCTGTGCCAGTCGGGGGTCCAGTCGGCACCAAAGCGAAAGGGTG
GGGGGGGCGTGAAGGAGGAAGTGAAACGAGTTCTGGGTTCTTTAAGGGAGTGGGTGGTGAGAGTGGGACAAGGGTGATGTCACTGCCTG
TCGGGCCCCGCCCTCCTCCCTCCCTCAGGACCCCCCCCCCCGCAGTACATTTACACACACCGCTTCCGCTGCGCAAGTAGCCACGTCAC
GGGCAACCCCCGAAATCCCCCCTCCCTTGGGGGGCGGGGGCCACGTGGGCCGTGGGGAACCGCGTGGCCCCGGCGGGGAAGGGCAGAGA
GGATACGCGAGCCACGAGAGAGGGGCCACTCGGGACCGCGGTGCGCGAC**TTCTCGGAA**GTTGGGGGACTAAAAGGGGTCTGATTTTGGG
GGTCGGTCGGTATTGAAGACCCAGAAAGCCAG

D

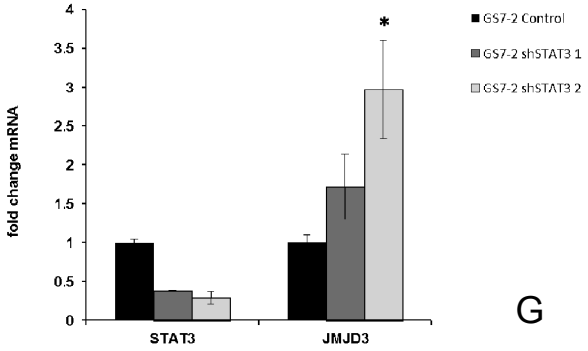

E

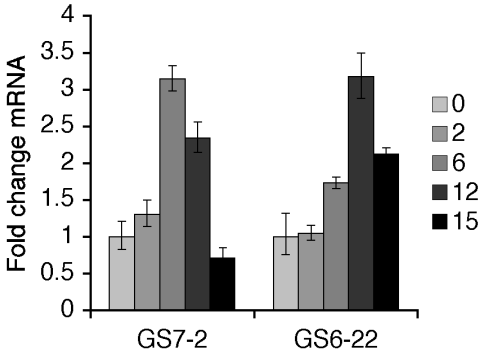

F

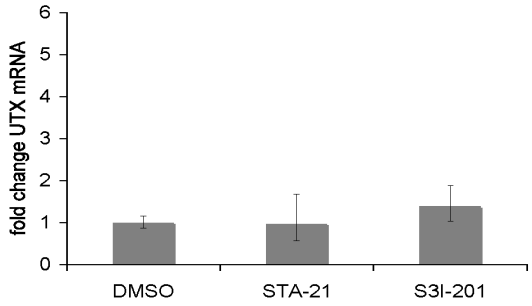

G

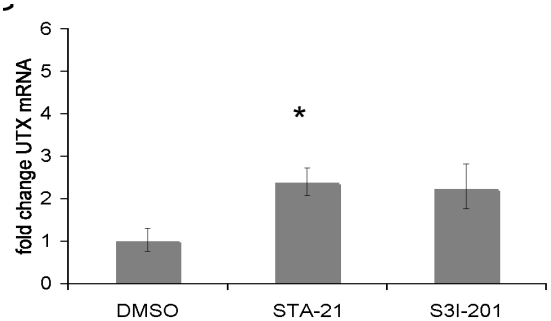

Figure S2.1. STAT3 represses JMJD3 expression in glioblastoma stem cells. A. Treatment of GS7-2 cells with the STAT3 inhibitor S3I-201 (50 uM) or STA-21 (50 uM) causes upregulation of JMJD3 protein levels. Cells were lysed for immunoblotting after 8 hours of drug treatment. JMJD3 protein levels relative to control were calculated using ImageJ and are displayed below each lane. B. RT-qPCR of GS7-2, MGG8 and GS11-1 cells treated with S3I-201 or BP-1-102 demonstrates that JMJD3 mRNA is upregulated 6 hours after inhibitor treatment. The MGG8 line was obtained from Wakimoto et. al (2012). Values represent the fold change relative to control cells for three experiments. * $p < 0.05$ and *** $p < 0.001$ compared to DMSO control (Student‘s t test, two-tailed). C. Segment of the JMJD3 first intron (shown to be an alternate promoter in De Santa et al 2007) amplified in Fig- ure 1D. Underlined letters signify the primer sequences, while bold underlined sequence represents the con- served STAT3 binding site (Chr17:7,747,573 UCSC GRCh37/hg19) which corresponds to the consensus binding site TTCNNNGAA (Horvath et al., 1995). In the murine JMJD3 promoter this sequence is TTCCCAGAA. D. Knockdown of STAT3 using an shRNA-containing lentivirus leads to the upregulation of JMJD3 mRNA in GS7-2 cells, two days after selection. Values represent the fold change relative to DMSO treated cells for three experi- ments; bars SD (*$p<0.05$). E. GS6-22 and GS7-2 cells were differentiated for 15 days, and RNA was isolated at the timepoints indicated. Values represent the fold change of JMJD3 mRNA relative to control cells for biological triplicate. Bars represent variation, calculated as described in materials and methods. ** $p <0.01$; * $p < 0.05$ com- pared to DMSO control (Student’s t test, two-tailed). Unlabeled bars are not significant. F. GS6-22 and G. GS7-2 cells were treated with S3I201 (50uM) or STA-21 (50 uM) for 24 hours, and then subjected to qPCR using primers to UTX. Values represent the fold change relative to controls for three experiments. Bars represent standard devi- ations, which were calculated as described in materials and methods. ** $p < 0.01$; * $p <0.05$ compared to DMSO control (Student‘s t test, two-tailed). Unlabeled bars are not significant.

Figure S2.2, Related to Figure 2.2

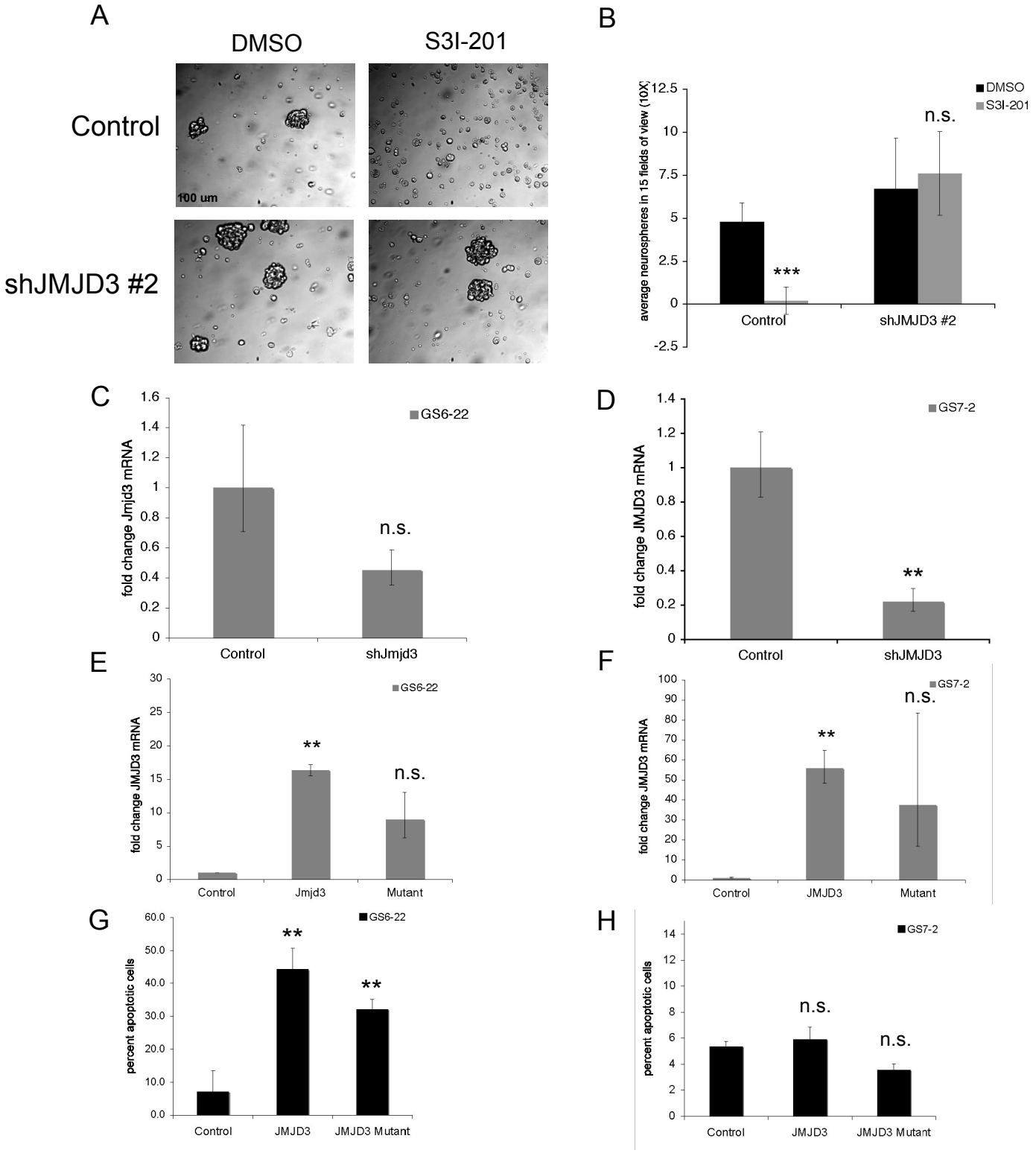

Figure S2.2. JMJD3 knockdown partially rescues neurosphere formation in S3I-201. A. GS6-22 cells were infected with a second shRNA to JMJD3, and plated in either DMSO or S3I-201 (50 uM). Representative images were taken 6 days after inhibitor treatment. B. Quantification of neurosphere formation after 6 days of drug treatment. Data represents the average number of spheres per field for one experiment (15 total fields per condition). *** $p < 0.001$; (Student's t test, two-tailed, compared to DMSO). Knockdown of JMJD3 mRNA was 45% compared to shLuc control (data not shown). C. GS6-22 cells infected with shRNA to JMJD3 (Figure 2A) had 55% knockdown of JMJD3 mRNA compared to con- trols as assessed by qRT-PCR ($p = 0.07$). D. GS7-2 cells infected with shRNA to JMJD3 had 78% knockdown compared to controls (Figure 2A). Values represent the fold change relative to control cells for triplicate experiments. Bars represent stan- dard variation, calculated as described in materials and methods. n.s.indicates not significant ($p>0.05$); ** $p < 0.01$ (Student's t test, two-tailed). E. GS6-22 and GS7-2 (F) cells were lysed, RNA extracted, and subjected to RT-qPCR. n.s. indicates $p > 0.05$ ($p = 0.07$); ** $p < 0.01$ compared to control. (Student's t test, two-tailed). JMJD3 overexpression is significantly higher in the GS7-2 cells than in the GS6-22 cells ($p < 0.01$). G. and H. Percent apoptotic cells was assessed in GS6-22 (A) and GS7-2 (B) cells with BrdU and 7-AAD staining. Values represent the average percentage of sub G0/G1 cells in 3 experiments; bars repre- sent SD of the mean. n.s. indicates not significant; $p > 0.05$. ** $p < 0.01$ (Student's t test, two-tailed; each compared to control infected cells).

Figure S2.3, related to Figure 2.3

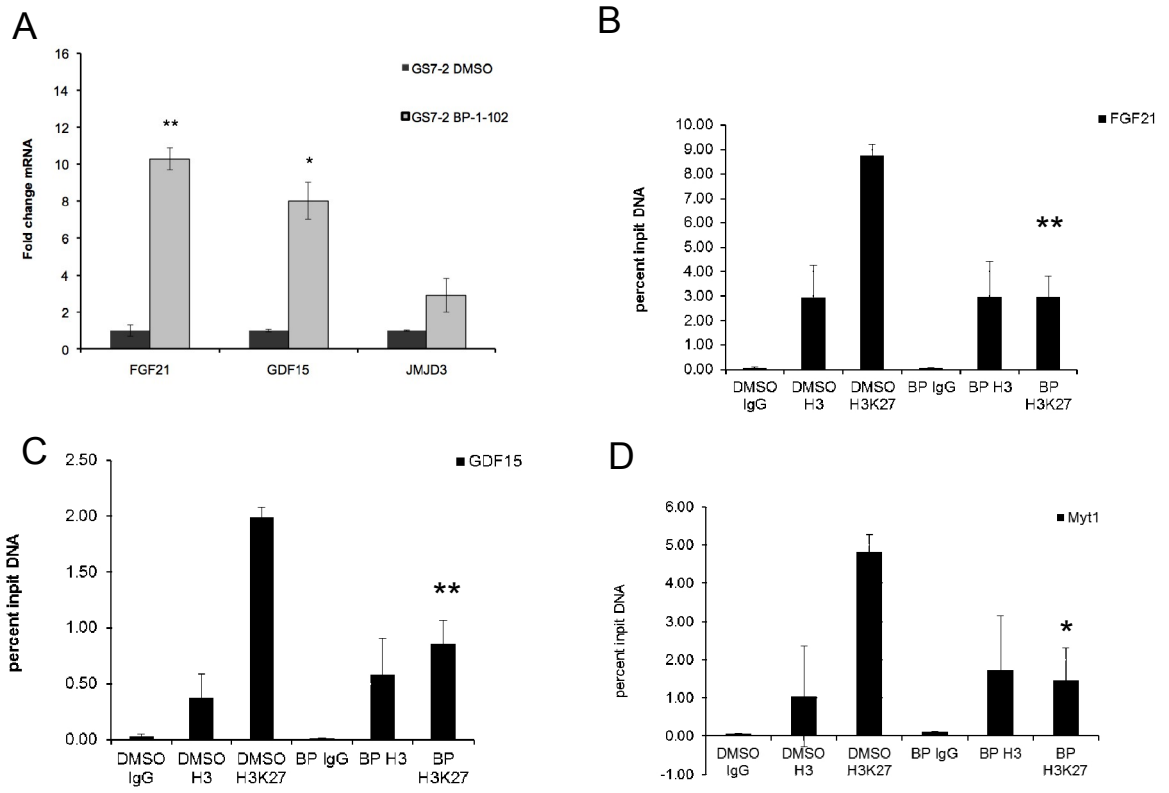

Figure S2.3. Neural gene induction and H3K27 demethylation in BP-1-102-treated GSC. A. RT-qPCR analysis of FGF21, GDF15 and JMJD3 expression in GS7-2 cells treated with BP-1-102 (15 uM) for 6 hours. Values represent the fold change relative to control cells; bars SD. B-D. GS6-22 cells were treated with BP-1-102 (15 uM) or DMSO for 6 hours, fixed, lysed, and subjected to chromatin immunoprecipitation with an antibody to H3K27 trimethylation or total histone H3. Quantitative PCR using primers to FGF21 (B) or GDF15 (C) or (D) Myt1 genes was performed after immunoprecipitation and DNA purification. Data is displayed as percentage of input DNA. * indicates p value less than or equal to 0.05, ** indicates p value less than or equal to 0.01 (Student's T test, two tailed; compared to DMSO treated cells).

Figure S2.4, related to Figure 2.3

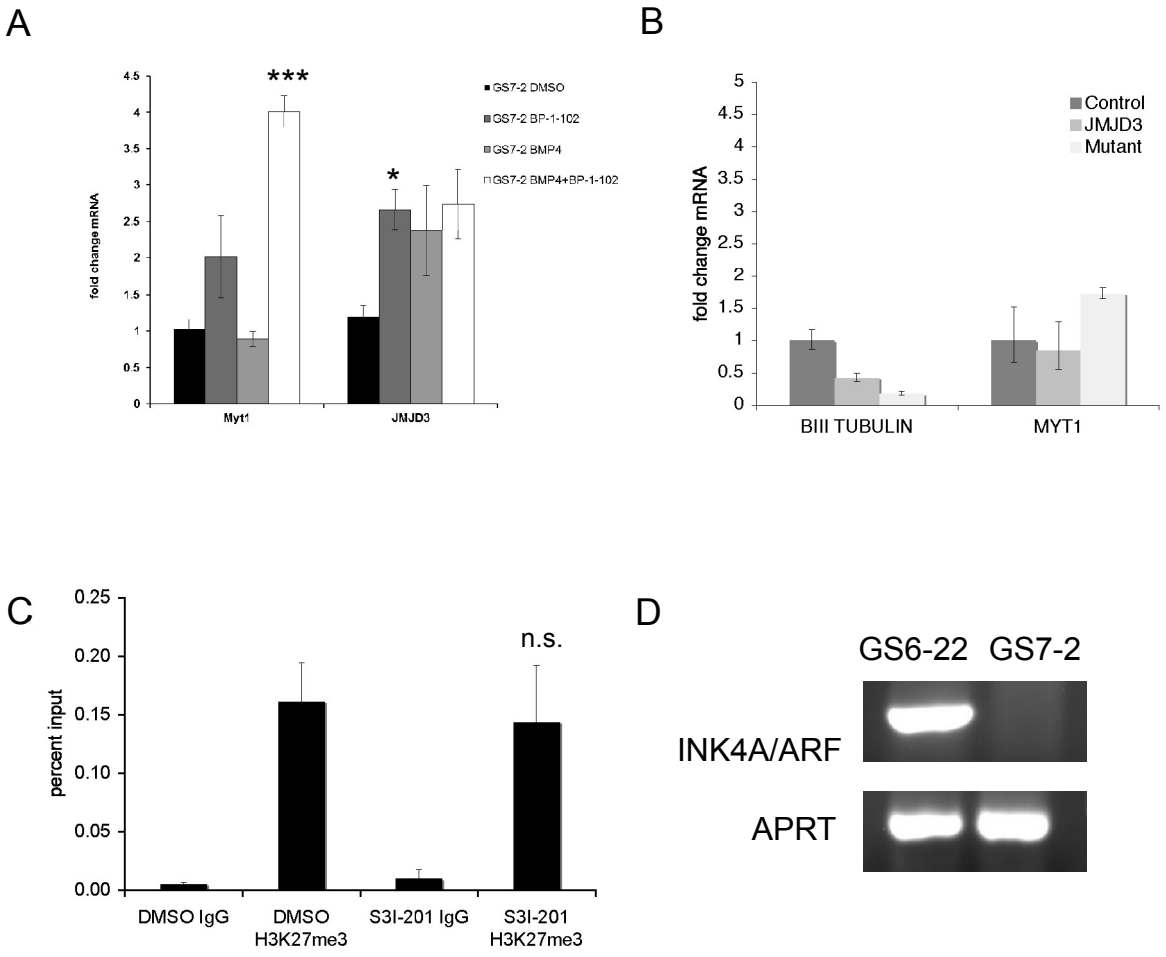

Figure S2.4. MYT1 expression and INK4A/ARF H3K27 methylation in GSC. A. RT-qPCR analy- sis of Myt1 and JMJD3 expression in GS7-2 cells treated with BP-1-102 (15uM), recombinant BMP4 (10 ng/ml) or a combination of both for 6 hours. Values represent the fold change relative to DMSO treated control cells for three experiments; bars SD (*$p<0.05$, ***$p<0.001$). B. GS7-2 cells infected with JMJD3, Mutant, or control retroviruses were subjected to qRT-PCR in order to assess marker expression. Data is analyzed as previously described. C. GS6-22 cells treated with the STAT3 inhibitor S3I-201 (100 uM) for 3 days were subjected to chromatin immunoprecipitation with an antibody to H3K27 trimethylation. Quantitative PCR using primers to a region of the Ink4A/Arf locus shown to be regulated by JMJD3 (Barradas et al., 2009) was performed after immunoprecipitation and DNA purification. Data is displayed as percentage of input DNA. Data represents 6 PCR reactions performed on two independent ChIP experiments. n.s indicates $p > 0.05$ (not signficant, Student‘s t test, two-tailed). D. GS6- 22 cells possess an intact INK4A/ARF locus, but GS7-2 cells do not. GS6-22 and GS7-2 genomic DNA was sub- jected to PCR using primers to either the INK4A/ARF locus, or to the APRT (adenine phosphoribosyltransferase) gene as a control. Primers were constructed and PCR was performed according to the methods of Iwato et al (2000).

https://www.dropbox.com/s/c416ny3znczwct9/Table%20S1.%20Annotation%20of%20gene%20promoters%20with%20reduced%20H3K27me3%20mark%20upon%20S3i%20treatment%209-11-15.xlsx?dl=0

Table S1. Histone H3K27 methylation changes upon STAT3 inhibition. GS6-22 cells were treated with S3I-201 (50uM) or DMSO control for 3 days. ChIP Sequencing analysis using H3K27me3 antibody yielded a list of gene promoters that likely show a reduction in repressive H3K27me3 mark upon S3i treatment.

https://www.dropbox.com/s/dgt3p9txinu95wr/Table%20S2.%20Annotation%20of%20genes%20with%202%20fold%20or%20higher%20gene%20expression%20upon%20S3i%20treatment%209-10-15.xlsx?dl=0

Table S2. Gene expression changes upon STAT3 inhibition. GS6-22 cells were treated with S3I-201 (50uM) or DMSO control for 3 days. Microarray analysis yielded a list of genes that likely show 2 fold or higher gene expression upon S3i treatment.

https://www.dropbox.com/s/k2qo0hovhwf857v/Table%20S3.%20Annotation%20of%20genes%20with%20reduced%20H3K27me3%20mark%20as%20well%20as%202%20fold%20or%20higher%20gene%20expression%20upon%20S3i%20treatment.xlsx?dl=0

Table S3. Intersected list of genes with H3K27me3 reduction and gene induction. GS6-22 cells that show both reduction in histone H3K27 methylation and greater than 2 fold increase in gene expression upon S3I-201 (50uM) treatment have been tabulated.

Chapter 3

RNAi kinome screen of GBM stem cells under normoxia and hypoxia

Relative author contributions
Sejuti Sengupta and Surbhi Goel Bhattacharya equally contributed to the RNAi screening and analysis.

Glioblastoma is characterized by a poor median survival of only 14 months despite aggressive multimodal therapy (Dolecek et al. 2012). Clinical trials for targeted therapy for GBM have failed to date. This is attributed to a small population of GBM stem cells (GSC) that survive therapy and initiate tumor recurrence (Lathia et al. 2015). Although the TCGA project has extensively characterized the genomic alterations in GBM, there is a need to identify new therapeutic targets for GBM, which are not necessarily synonymous with mutations. Moreover, therapeutic targets for GBM stem cells may differ from those identified from traditional serum grown gliomas cells that been used for most in vitro studies until recently. In addition, the tumor hypoxic niche is believed to be a major factor that contributes to maintaining GSC survival and tumor progression (Kaur et al. 2005) and there have been no systematic attempts to identify GBM targets under hypoxia. This calls for a systematic effort to identify molecular mechanisms responsible for GSC survival under hypoxia.

Kinases play an important role in maintaining tumor growth and survival by regulating the hallmarks of cancer, including survival/apoptosis, cell-cycle progression, stem cell maintenance, DNA damage repair, tumor cell invasion and therapeutic resistance (Cheng et al. 2015). In addition, kinases are readily amenable to drug inhibition by virtue of a druggable ATP-binding pocket, thereby making them ideal candidates for developing cancer therapeutics (Knight et al. 2010). Kinase inhibitors targeting EGFR, VEGF, PI3K or DNA repair pathway proteins, ATM and ATR, are being explored for GBM therapy (Ramirez et al. 2015; Nadkarni et al. 2012; Mellinghoff et al. 2012). While we still do not have a successful targeted therapeutic for GBM, identification of kinases whose inhibition attenuates GSC properties may pave the way

toward novel therapeutics. However, it is difficult to predict which kinases are essential for tumor cells, since the essential kinases does not always correspond to altered gene expression and mutation status. For instance, deletions in the PTEN tumor suppressor gene leads to activation of the downstream pro-tumorigenic Akt kinase family that are not themselves mutated (Vogelstein et al. 2013). Therefore, a functional kinome-wide RNAi screen was conducted to identify kinase targets essential for GBM stem cell growth and maintenance. Three different GBM stem cell lines were screened under normoxic and hypoxic conditions to identify kinases that are essential across multiple glioblastomas under different oxygen environments.

Experimental procedures

RNAi screening protocol

A shRNA library by the RNAi consortium (TRC; Broad Institute, Cambridge, MA; www.broad.mit.edu/genome_bio/trc) was used for screening the human kinome in a Sigma lentiexpress 96 well array (Moffat et al. 2006). The kinome library contains 3,200 lentivirally encoded sequence verified shRNA constructs, with 5 or more independent shRNAs targeting each of 501 human kinases (http://www.sigmaaldrich.com/life-science/functional-genomics-and-rnai/shrna/trc-shrna-products/lentiexpress-technology.html). The shRNAs were encoded in PLKO.1 lentivirus vector, which carries the puromycin-resistance gene and drives shRNA expression from a human U6 promoter. Each lentiviral plate contains media only control wells, non-targeting shRNA negative control wells and test shRNA hairpins at a low MOI in order to reduce off-target effects.

Screening parameters, including polybrene concentration, media replacement, puromycin selection condition and viability assay and timepoints were individually optimized for GS6-22, GS7-2 and GS11-1 under both normoxia and hypoxia. The best conditions were those that minimized nonspecific toxicity in the negative control wells while resulting in a discernible growth reduction with the essential kinase hairpins. Low passage GS6-22, GS7-2 or GS11-1 were seeded onto duplicate 96 well library plates at a density of 5000 cells/well in 2ug/ml polybrene. A complete media change was performed the next day in GS7-2 and GS11-1 cells. To avoid loss of GS6-22 cells, the media was diluted to twice its volume the next day after plating cells and half of the media replaced during puromycin addition. Two days after virus infection, the infected GS6-22, GS7-2 and GS11-1 cells were selected in 1, 0.25 and 0.75 ug/ml puromycin respectively. One set of cells were then transferred to 1% oxygen atmosphere in oxygen controlled incubator (Biospherix) and the other identical set left to incubate under 21% normoxic conditions. Relative GSC viability was determined when the negative control wells became saturated at 6 to 9 days after plating the cells depending on the cell line under normoxic or hypoxic growth conditions. In order to minimize effects of sphere formation on the assay, neurospheres were dissociated into single cell suspension by trypsin. GBM stem cell viability was then determined using the membrane permeant, resazurin based Prestoblue assay (ThermoFisher). The end product of the assay was quantitatively measured after 30 minutes in a fluorescent plate reader (Spectrafluor Plus) at 590 nm to determine cell viability. Prestoblue is a quantitative method to measure relative cell viability. This method generated a linear standard curve over broad range of GSC concentrations. The

correlation coefficient as measured for one set of duplicate GS6-22 plates screened was 0.94, indicating that the screening results were highly reproducible.

Screen end-point analysis/Hit selection criteria

The median ± 2 Median of Absolute Deviation (MAD) method was used for platewise analysis on normalized percentage inhibition of cell growth in each well to identify shRNA hairpins that effectively inhibit cell growth (Chung et al. 2008). Z* scores based on MAD analysis were calculated as the difference in viability between test shRNA and the median of non-targeting control shRNA wells, normalized to the median absolute deviation of the non-targeting control shRNA replicates (Zhang 2011). The platewise MAD analysis minimizes plate-to-plate variability and well position effects in defining hits. shRNA hits in each plate were defined as hairpins with a Z* score based on MAD analysis > 2 and < 50% of the growth of control wells in each plate. To account for off-target effects, genes were scored as hits only if a given gene had at least 2 unique shRNAs targeting the same gene that scored as hits. Additionally, platewise Z* score distance between normoxia and hypoxia was plotted to confirm differential growth by the hairpins which were enriched under specific conditions. Genes which were targeted by at least 2 shRNAs that scored as hits in only one condition were selected as condition sensitive hits and their Z* scores were plotted to determine differential growth inhibition between the two conditions. A stringent two-step criterion was used to select strong condition sensitive hits with at least 2 hairpins showing a minimum difference in robust Z* of 2 between normoxia and hypoxia.

Bioinformatic analysis for intersection, pathway distribution and intersection of the hits

The BioVenn web application was used to generate a venn diagram intersecting hits between the 3 GSC lines under either conditions or hits sensitive to hypoxia or normoxia (http://www.cmbi.ru.nl/cdd/biovenn/) (Hulsen et al. 2008). The Oncomine™ Platform (Thermo Fisher, Ann Arbor, MI) and cbioportal (http://www.cbioportal.org/) was used for analysis and visualization of mutation and overexpression of selected kinase hits in TCGA GBM set (Cerami et al. 2012; Gao et al. 2013). Functional information regarding the canonical pathway and disease biofunction of the hits were obtained from QIAGEN's Ingenuity Pathway Analysis (IPA® , QIAGEN Redwood City, www.qiagen.com/ingenuity) . Gene descriptions were obtained from the human gene database, Genecards (www.genecards.org) (Rebhan et al. 1998), DAVID (the Database for Annotation, Visualization and Integrated Discovery) Functional Annotation Tool (www.david.abcc.ncifcrf.gov/) (Huang et al., 2009) and literature mining.

Results

In order to identify the kinases essential for growth and survival of GBM stem cells, an arrayed shRNA screen was performed to test individual shRNAs targeting ~501 kinases in a well by well approach. GS6-22, GS7-2 and GS11-1 patient derived neurosphere lines were added to wells coated with lentiviral stock of each shRNA hairpin, under normoxic and hypoxic conditions in parallel (**Fig 3.1**). Cell number and viability was assessed about a week after transduction by prestoblue assay. Hits were identified as genes for which 2 or more shRNA hairpins that caused a significant growth

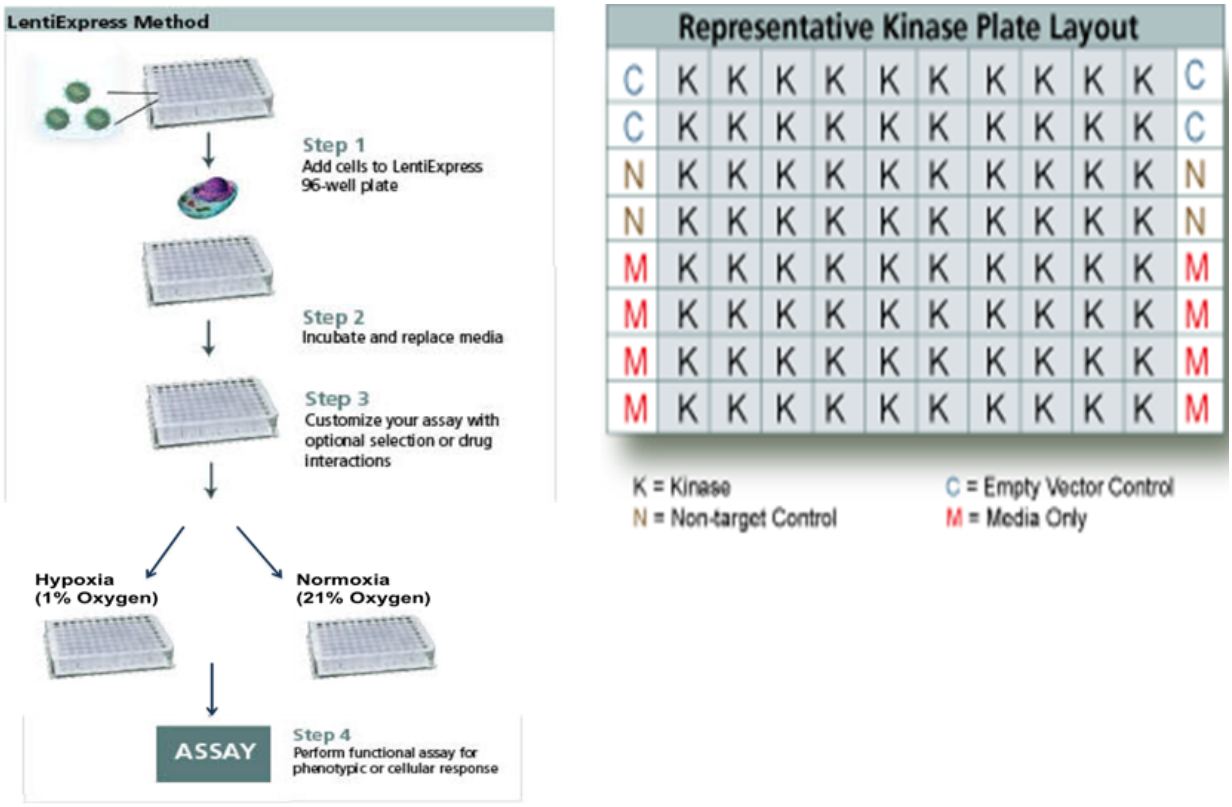

Figure 3.1. RNAi screening protocol following lentiexpress method. A. Cells were plated to shRNA coated lentiexpress plates and cultured under normoxia or hypoxia post puromycin selection. B. Representative kinase plate layout with empty vector or media only control wells on the sides.

inhibition with a statistical MAD based z score > 2 in addition to a > 50% reduction in growth compared with that of control hairpins. The 50% growth inhibition condition was imposed in addition to the 2 MAD criteria to ensure the selection of the most biologically significant as well as statistically significant gene hits. This analysis identified 38 to 56 kinase hits in each of the three GSC lines, resulting in a hit rate of about 10% of the kinases and 7% of the shRNA hairpins screened (**Fig 3.2**). Strikingly, only about 25% of the kinase hits (12 kinases) were common to all three GSC lines in at least one condition (**Fig 3.2**). Notably, 5 of the 12 common kinase hits from our screen were previously known to be involved in gliomagenesis, including ERBB3, CDK6, PLK1, KDR and CHK1. PLK1, in particular, is lethal in multiple small molecule screens in different cancer forms (Pezuk et al. 2013; Lee et al. 2012; Tiedemann et al. 2010), and was one of the very few common hits in multiple arrayed RNAi screens across tumor lines (Bhinder and Djaballah 2013). While CDK6, PLK1 and CHK1 are cell cycle and mitotic genes (J A Pezuk et al. 2013; Lee et al. 2012; Tiedemann et al. 2010), ERBB3 is an anti-apoptotic gene (Kim et al. 2010; Sithanandam and Anderson 2008; Soler et al. 2009) and KDR (VEGF receptor) is involved in inducing angiogenesis as well as stem cell proliferation (Geng et al. 2001; Yao et al. 2013; Lathia et al. 2015; Bao et al. 2006) (**Table 3.1**). Of the novel common hits, STK39 and PKN1 are involved in stress response, YES1 is involved in cell survival and differentiation, CDKL5 plays a role in neuronal plasticity by phosphorylating methyl CpG binding protein-2 (MECP2), DDR1 functions in cell-matrix adhesion and TXK plays an important role in immune function, but is expressed in the brain (See **Table 3.2** for list and references). Of the novel hits,

DDR1, YES1 and PKN1 were significantly overexpressed in GBM tumors, as compared

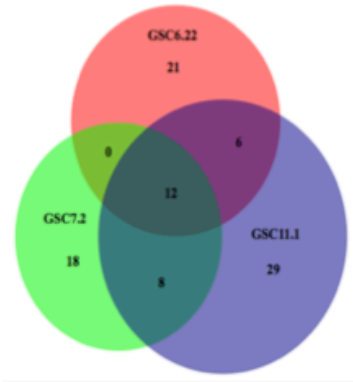

Either condition

No. of Hits	GS6.22	GS7.2	GS11.1
Both Normoxia & Hypoxia	23	30	30
Normoxia enriched	10	3	10
Hypoxia enriched	6	5	14
Total	39	38	54

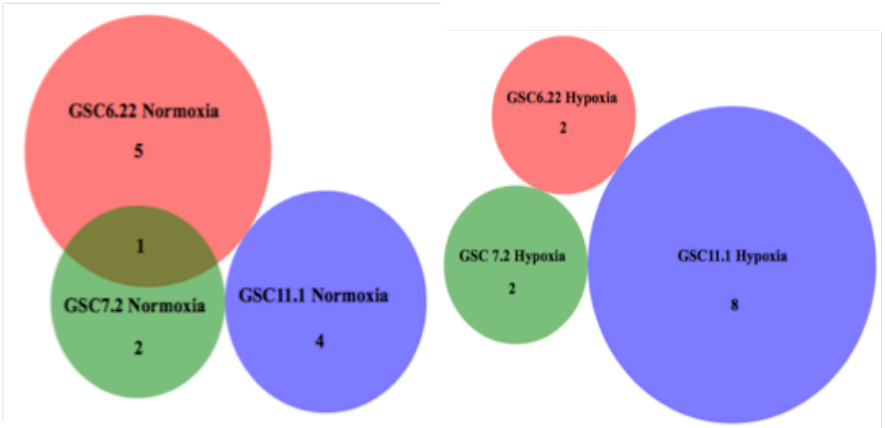

Normoxia sensitive

Hypoxia sensitive

Fig. 3.2. Screen hit distribution. A. Table depicts hit distribution under hypoxia, normoxia or both conditions in each cell line. B. Biovenn was used to represent cell-line intersection between kinase hits that were identified under either conditions or sensitive to hypoxia or normoxia.

Known hits	Signaling Pathway	Cellular function	Relevance to GBM
ERBB3	EGFR family, PI3K related	Anti-apoptosis, cell proliferation	Amplified and/or overexpressed in prostate, bladder (Sithanandam and Anderson 2008; Soler et al. 2009), and breast tumors; implicated in glioma (Clark et al. 2012)
CDK6	CDK family, PI3K/Akt related	Cell cycle progression and differentiation	Phosphorylates Rb, implicated in glioma (Wiedemeyer et al. 2010; Ruano et al. 2006)
PLK1	Regulates AURKA, APC/C activator	Cell cycle and mitosis, DNA damage response	Negative regulator of p53, overexpression correlates with cellular proliferation and poor prognosis in glioma (J A Pezuk et al. 2013; Lee et al. 2012; Julia Alejandra Pezuk et al. 2013; Tiedemann et al. 2010; Danovi et al. 2013; Bhinder and Djaballah 2013)
KDR	VEGF receptor, PI3K/Akt and RhoGDI related	Endothelial proliferation, survival, migration, tubular morphogenesis and sprouting	Promotes tumor angiogenesis in glioma (Geng et al. 2001; Lee et al. 2016; Yao et al. 2013; Lu et al. 2012)
CHEK1	p53, PI3K, GPCR related	Cell cycle arrest in response to DNA damage	Physiological stress response to hypoxia, apoptosis/cell cycle control in glioma (Geng et al. 2001; J. Lee et al. 2016; Yao et al. 2013; Lu et al. 2012)

Table 3.1. Known common hit list annotation. Common hits between the 3 GSC lines screened that play a known role in glioma are listed above. Genecards, DAVID functional annotation tool and literature was used to annotate their signaling pathways, cellular function and relevance to cancer.

Novel hits	Signaling Pathway	Cellular function	Relevance to Cancer
STK39	MAP14, WNK4	Stress response pathway, Ion transport	Mediates genotoxic stress induced apoptosis in B-cell lymphoma
YES1	Src, Fyn, CDK4, RTK	Cell growth, survival and differentiation, apoptosis, cell-cell adhesion, T cell and Akt mediated migration	Cell cycle progression and apoptosis in mesenthelioma (Sato et al. 2012), colon cancer (Rosenbluh et al. 2012) and ovarian cancer (Li et al. 2015); migration of GBM stem cells (Li et al. 2015; Han et al. 2014; Rosenbluh et al. 2012; Sato et al. 2012).
DDR1	GPCR, Nanog, Rho GTPase, AKT	Cell-matrix adhesion, cell growth, receptor for binding collagen, Phosphorylates PTPN11	Mediates EMT and invasion in breast cancer (Koh et al. 2015) and pancreatic cancer (Chow et al. 2016) respectively; K-RAS driven lung adenocarcinoma initiation and progression (Ambrogio et al. 2016; Chow et al. 2016; Koh et al. 2015).
CDKL5	STK, BDNF	Phosphorylation of MeCP2, synaptic transmission, cell spreading	Novel tumor-associated antigen in T cell leukemia (Kawahara et al. 2007); mutated in gastric cancer (Zang et al. 2011); kinase inactivation causes neurodevelopmental disorder, Rett syndrome (Leoncini et al. 2015).
PKN1	RhoA/B, p38, JNK, PKC-related kinase	Cell cycle arrest in response to DNA damage, tumor cell invasion	Identified as an essential kinase in multiple myeloma screen (Tiedemann et al. 2010)
TXK	PI3K, Src, FAK, integrin	Th1, IL2 cytokine production, actin cytoskeleton regulation	Immunomodulatory activities, regulates PI3-K binding to T cell antigen (Schneider et al. 1998)
CDC2L1	CDK family, Regulates PLK1	Cell cycle progression, mitosis and apoptotic signaling	Inhibits breast cancer growth, invasion and angiogenesis (Chi et al. 2015; Chi et al. 2014); essential kinase target identified in multiple myeloma (Tiedemann et al. 2010); possible tumor suppressor role in neuroblastoma and non-hodgkin lymphoma (Dave et al. 1999; WHITE et al. n.d.)

Table 3.2. **Novel common hit list annotation.** Common hits between the 3 GSC lines screened that play a novel role in glioma are listed above. Genecards, DAVID functional annotation tool and literature was used to annotate their signaling pathways, cellular function and relevance to cancer.

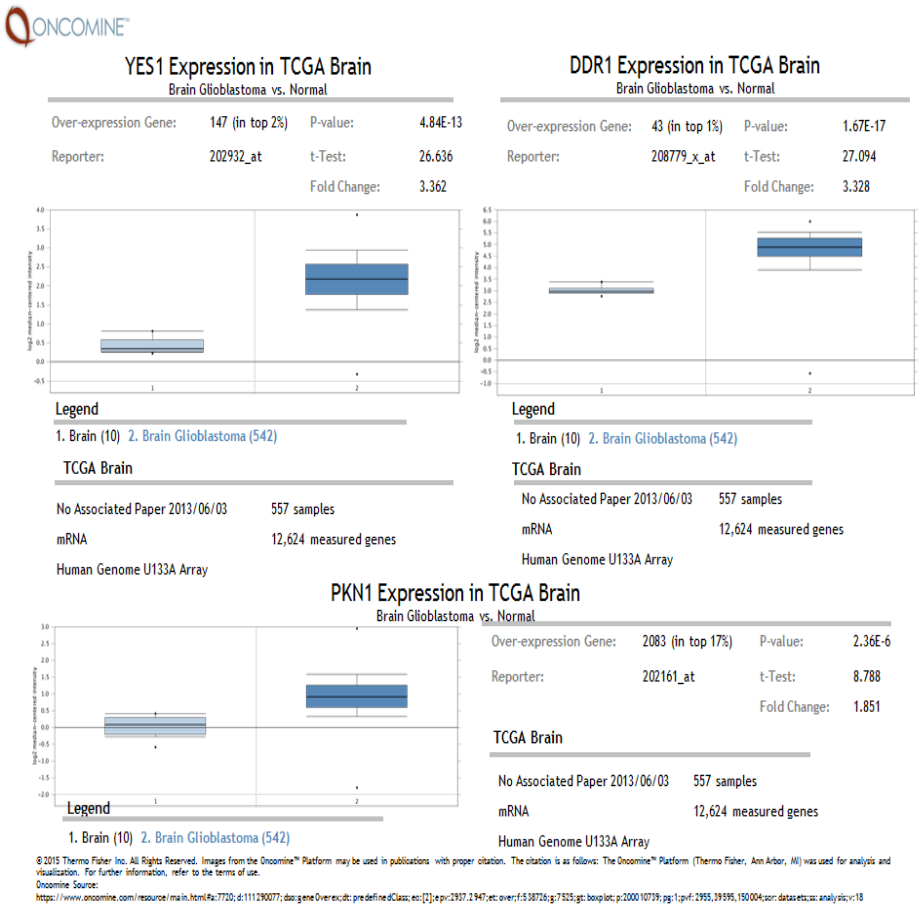

Figure 3.3. Oncomine gene expression of novel hits. YES1, DDR1 and PKN1 gene expression in GBM brain as compared to normal brain (TCGA study).

to normal brain tissue (oncomine) as determined by the TCGA data (**Fig 3.3**). This made these hits strong candidates for validation. However, none of the common kinase hits were frequently mutated in GBM tumors sequenced by the TCGA 2013 study (cbioportal). Genes which had at least 2 hairpins targeting them and which had a minimum difference in robust Z* score of 2 between normoxia and hypoxia, were selected as oxygen condition sensitive hits. See Figure 4. Only 5-15% of the hits were strongly sensitive under either condition, while majority (85-95%) of the hits were concordant between both normoxia and hypoxia. Interestingly, no two hypoxia sensitive hits were common between any of the 2 GSC lines screened, which can be due to the small number of condition sensitive hits or that GBM stem cell lines do not have a common resistance mechanism for hypoxia. The hypoxia sensitive hits, along with their physiological functions are listed in **table 3.3**, in the order of their enrichment under hypoxia. Interestingly, functional annotation of the hypoxia enriched genes, like MAP3K12, STK39, MAP4K2 and PTK2, reveal a high frequency of involvement in the MAPK mediated cellular stress response. A number of our hypoxia enriched genes were involved in the physiologically relevant angiogenic pathways, including the VEGF receptor gene (KDR) (Bao et al. 2006) and HGF receptor MET gene which is involved in stemness (Shojaei et al. 2010; Joo et al. 2012). In addition, ROCK2 and PTK2 kinases were hypoxia sensitive hits in GS6-22, while LIMK1 showed trend towards hypoxia sensitivity in GS11-1 line (**Fig 3.4**). These kinases belong to the Rho-Rac-Focal adhesion kinase pathway involved in cell motility, which have also been implicated in angiogenesis (Chung et al. 2008). In addition, PRKAA1/AMPK and SIK1 are kinases known to be involved in metabolic processes and trend towards hypoxia sensitivity. The

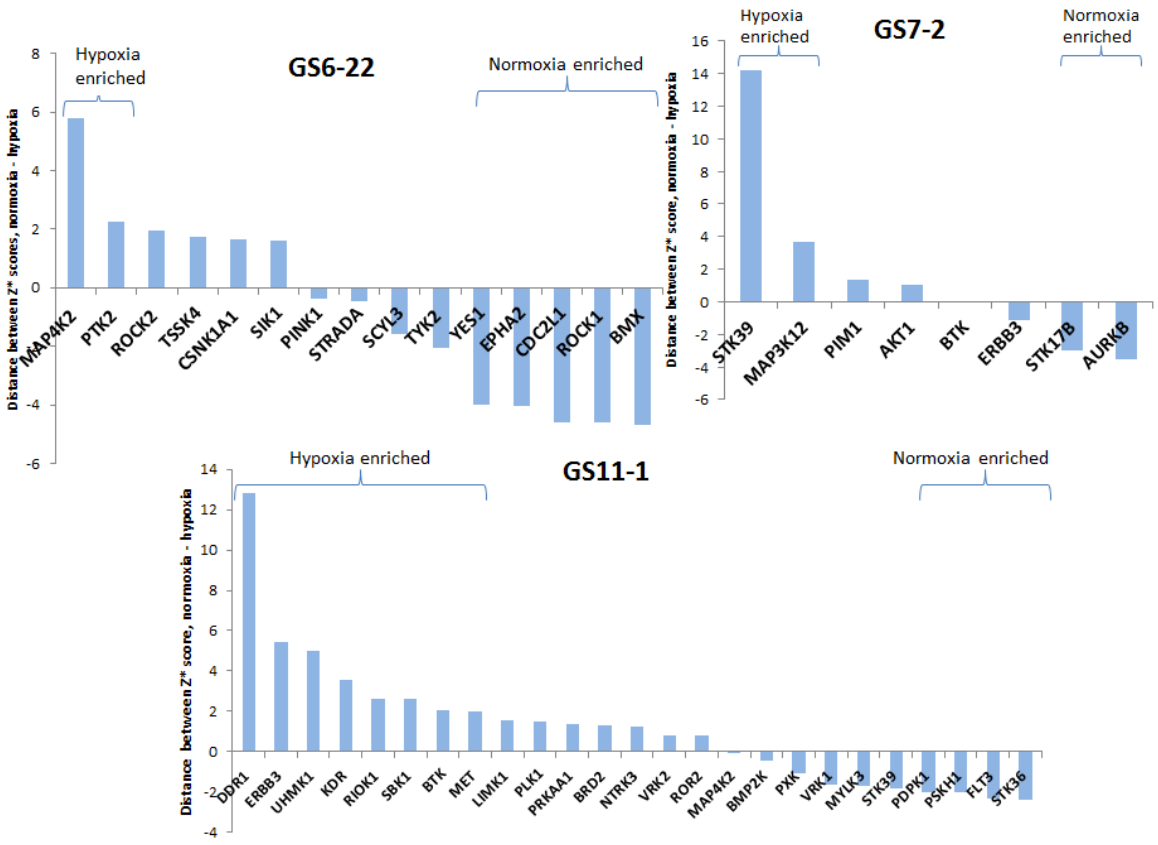

Figure 3.4. Z* score distribution of hypoxia and normoxia sensitive genes. Z* score distance between hypoxia and normoxia of the condition sensitive genes in GS6-22, GS7-2 and GS11-1 cells are shown.

Strong Hypoxia sensitive genes	Signaling pathways	Cellular function
STK39	MAPK, WNK4	Stress response pathway, Ion transport
DDR1	GPCR, Nanog, Rho GTPase, AKT	Cell-matrix adhesion, cell growth, receptor for binding collagen, Phosphorylates PTPN11
MAP4K2	MAPK	Stress response, immune response
ERBB3	EGFR, PI3K	Cell proliferation, neuron differentiation, anti-apoptosis
UHMK1	GPCR	Cell cycle progression, RNA processing and/or trafficking
MAP3K12	MAPK, JNK	Stress response, chromatin modification
KDR or VEGF-R2	VEGF	VEGF, Hypoxia and angiogenesis
RIOK1	Ribosome biogenesis	Not known
SBK1	Not known	Brain development
PTK2	FAK, MAPK, PI3K	VEGF, hypoxia, angiogenesis, neurogenesis, cell adhesion and migration
BTK	Tec, PI3-K related	B cell development, Function of immune cells, apoptosis regulation
MET	HGF	Cell migration, endocytosis, angiogenesis

Table 3.3. Annotation of strong hypoxia sensitive genes. Signaling pathway and cellular functions of strong hypoxia sensitive genes are shown.

Weak Hypoxia sensitive genes	Signaling pathways	Cellular function
ROCK2	Rho/Rac, PKC, PI3K, LIMK	Cell cycle regulation, actin cytoskeleton regulation, focal adhesion, negative regulator of angiogenesis
TSSK4	CREB, TGF-BR1	Spermatogenesis, cell differentiation
CSNK1A1	Wnt, NFAT	Hypoxia and p53 in cardiovascular system
SIK1	LKB1	Cell cycle regulation, metabolic processes, tumor suppression
LIMK1	Rho/Rac, CCR3	Regulation of cell differentiation and actin cytoskeleton, neural development
PLK1	Regulates AURKA, APC/C activator	Cell cycle and mitosis, DNA damage response
PRKAA1 or AMPK2	MAPK, cAMP, mTOR	Response to hypoxia, regulation of autophagy, metabolism
PIM1	JAK/STAT	Mitotic cell cycle, cell proliferation
BRD2	Cell cycle/checkpoint, Wnt/hedgehog/notch	Spermatogenesis, regulates transcription by chromatin remodeling
NTRK3	GPCR	Cell growth regulation, neuron differentiation, Neurotrophin receptor
AKT1	PI3K, Insulin, MAPK, ErbB	Cell survival, DNA damage response, hypoxia and p53, metabolic process, VEGF signaling
VRK2	MAPK	Stress response to hypoxia, DNA repair, tumor cell growth regulation
ROR2	GPCR	Cartilage development and osteogenesis

Table 3.3. Annotation of weak hypoxia sensitive genes. Signaling pathway and cellular functions of weak hypoxia sensitive genes are shown.

Strong Normoxia sensitive genes	Signaling pathways	Cellular function
CDC2L1	Cell cycle/Mitotic	Cell cycle progression, apoptosis
BMX	Jak/STAT	Cell migration, angiogenesis, cell proliferation and survival.
ROCK1	Rho/Rac, FAK, PI3K, LIMK	Actin cytoskeleton regulation, focal adhesion, negative regulator of angiogenesis
EPHA2	PI3K-Akt, GPCR, MAPK	Cell migration and integrin-mediated adhesion, cell proliferation and differentiation
YES1	Src, Fyn, CDK4, RTK	Cell growth, survival and differentiation, apoptosis, cell-cell adhesion, T cell and Akt mediated migration
AURKB	Cell cycle/Mitotic	Mitotic cell cycle
STK17B	Apoptosis, autophagy	Actin cytoskeleton. Induction of apoptosis
FLT3	Erythrocyte differentiation pathway	Hematopoietic lineage differentiation, immune system process
TYK2	JAK/STAT, TGF-B	Interferon signaling
PSKH1	mRNA splicing	Pre-mRNA processing
PDPK1	Akt-mTOR, Insulin signaling, focal adhesion	Glucose uptake and transport, PTEN dependent cell cycle arrest and apoptosis, cell adhesion

Table 3.5. Annotation of strong normoxia sensitive genes. Signaling pathway and cellular functions of strong normoxia sensitive genes are shown.

Weak Normoxia sensitive genes	Signaling pathways	Cellular function
STK39	MAP14, WNK4	Stress response pathway, Ion transport
MYLK3	Calcium signaling pathway, focal adhesion	Vascular smooth muscle contraction, Regulation of actin cytoskeleton
VRK1	Cell cycle/Mitotic	Golgi disassembly during cell cycle, promotes p53 stability, phosphorylates histone H3, c-JUN
SCYL3	Ion transport	Cell motility, synaptic transmission, Binds to and modulates brain Na,K-ATPase
PXK	Not known	Defense and inflammatory response, regulation of neurological processes and ion transport
BMP2K	Transcriptional misregulation in cancer	Regulation of ossification and bone mineralization
STRADA	mTORmTOR	Identified as a target in medulloblastoma screen, Neural functionChemoresistance, target in medulloblastoma
PINK1	Respiratory electron transport, ATP synthesis	Regulation of neurological processes, regulation of cell communication and transport, protect cells from stress-induced mitochondrial dysfunction
MAP4K2	MAPK	Stress response, immune response

Table 3.6. Annotation of weak normoxia sensitive genes. Signaling pathway and cellular functions of weak hypoxia sensitive genes are shown.

CDC2L1 and BMX kinases showed highest normoxia sensitivity and require careful validation, since they have been implicated as oncogenic targets (Guryanova et al. 2011; Tiedemann et al. 2010). Interestingly, some of the same genes like STK39 or family members, such as ROCK1 and ROCK2, showed differential condition sensitivity in different cell lines, indicating variable resistance mechanisms of the cells.

Protein interaction and pathway database, Ingenuity Pathway Analysis (www.ingenuity.com) was used to categorize hits into distinct pathways and biological processes (**Fig 3.5**). Not unexpectedly, the hits were enriched for fundamental cellular processes characteristic of kinases, like posttranslational modification, amino acid metabolism and small molecule biochemistry, followed by cancer, cell survival and cell cycle processes. As observed in previous kinome screen in GBM (Ding et al. 2013), we did not find specific biological processes to prioritize the hits. The hits common between the GSC lines were enriched for a broad range of pathways, with cell cycle checkpoint control and STAT3 pathway at the top, followed by other oncogenic pathways such as HER2 signaling, DNA damage response and PTEN signaling. The hypoxic hits were most enriched for angiogenic HGF and STAT3 signaling pathway, followed by the relevant angiogenic VEGF and stress activated JNK signaling. Amino acid metabolism, posttranslational modification and small molecule biochemistry were the top processes enriched, followed by cellular movement and cancer. The normoxia sensitive hits, on the other hand, were enriched for Tec kinase, Ephrin signaling, ErBb2-ErBb3 and signaling pathways in hematopoietic progenitor cells as well as posttranslational modification, cancer, hematological disease and immunological disease processes. Some of these, such

A

Common hits

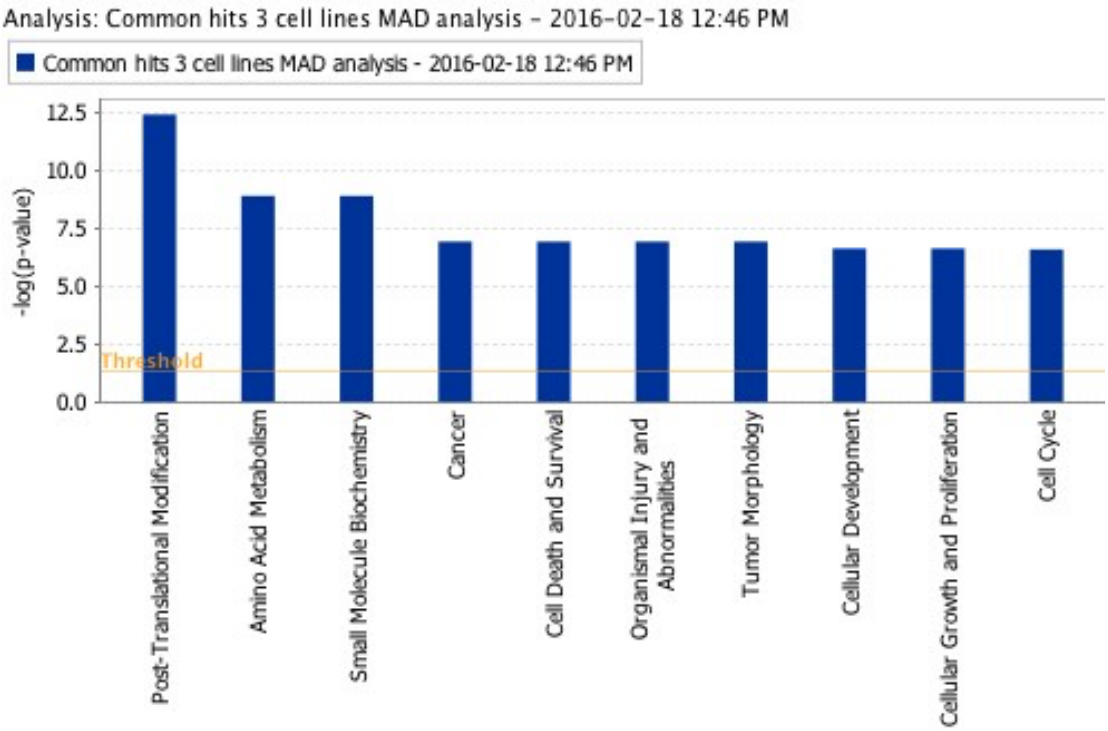

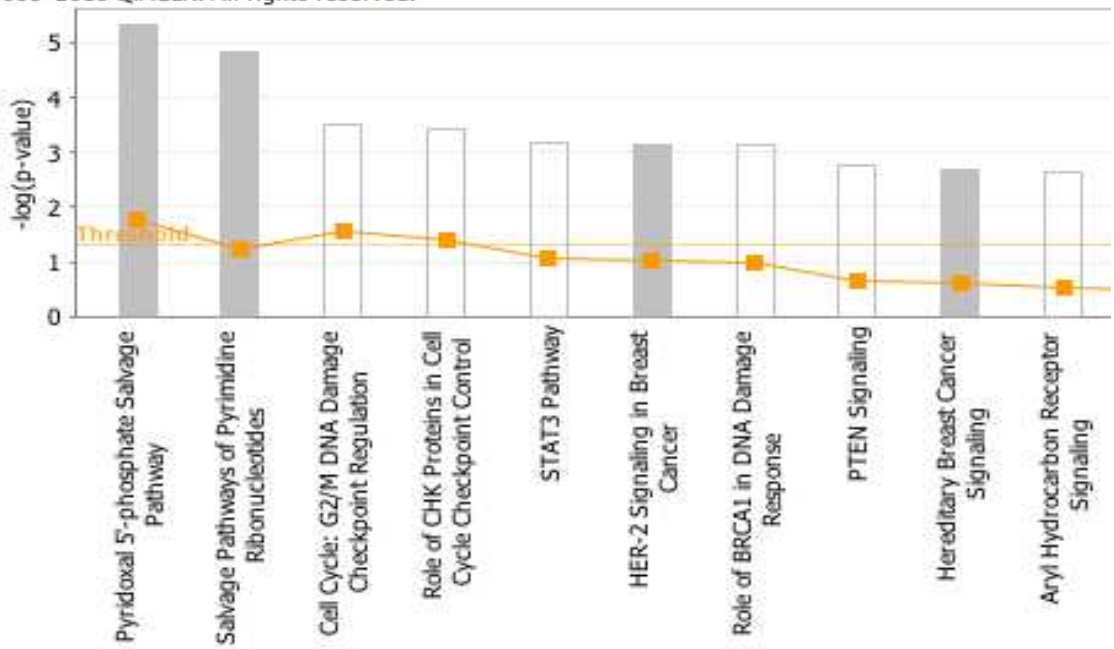

Hypoxia sensitive hits

B

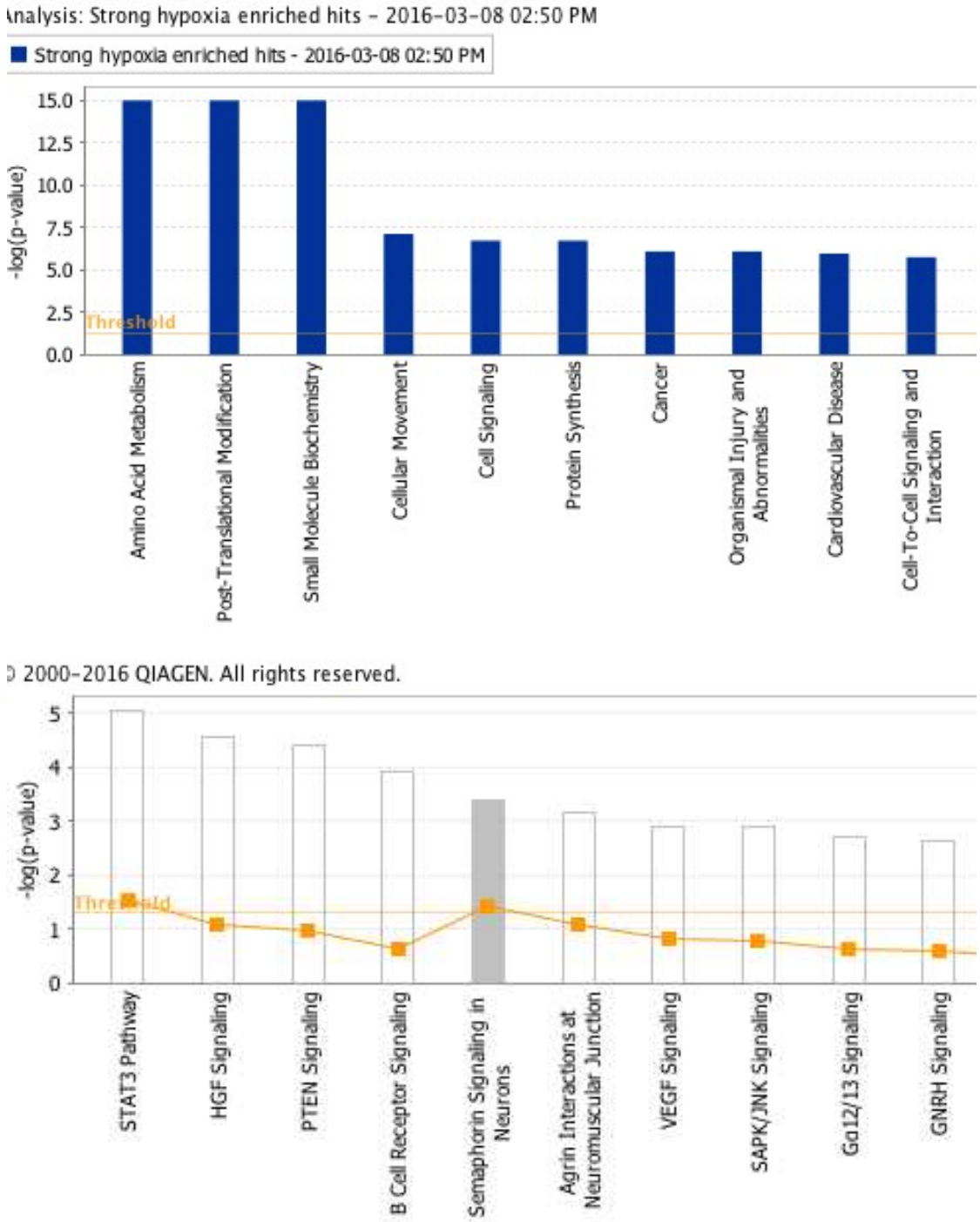

C

Normoxia sensitive hits

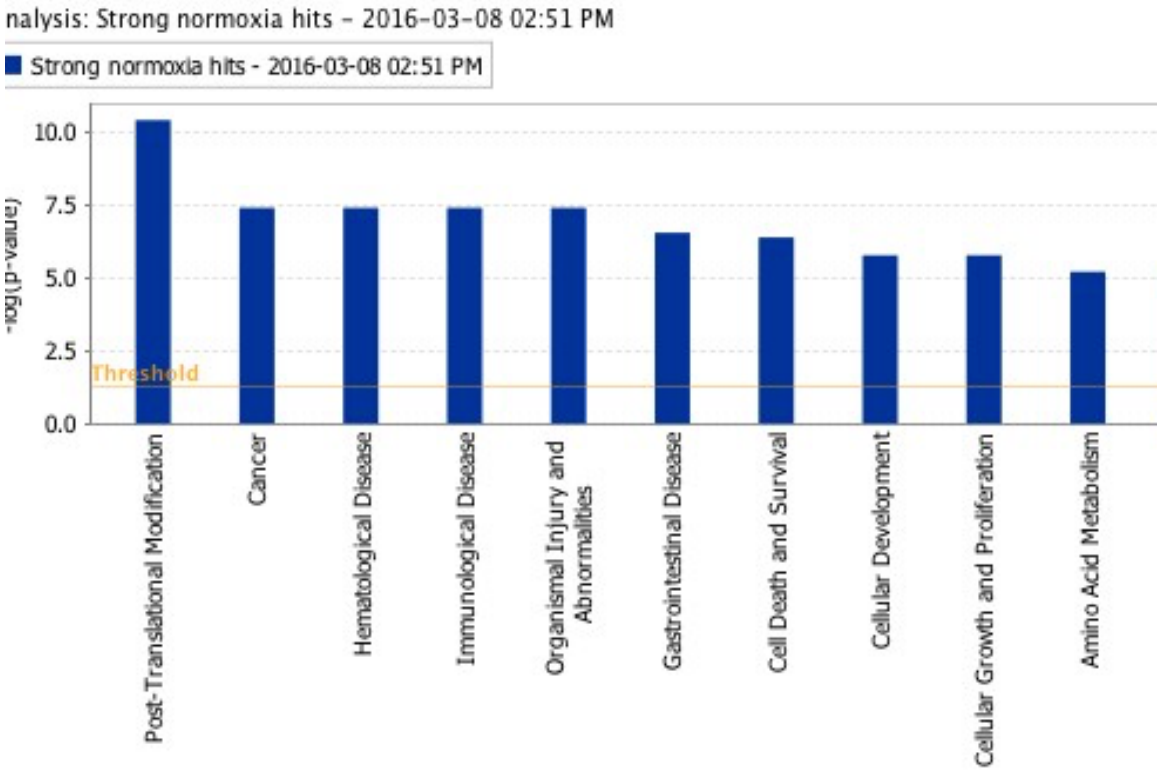

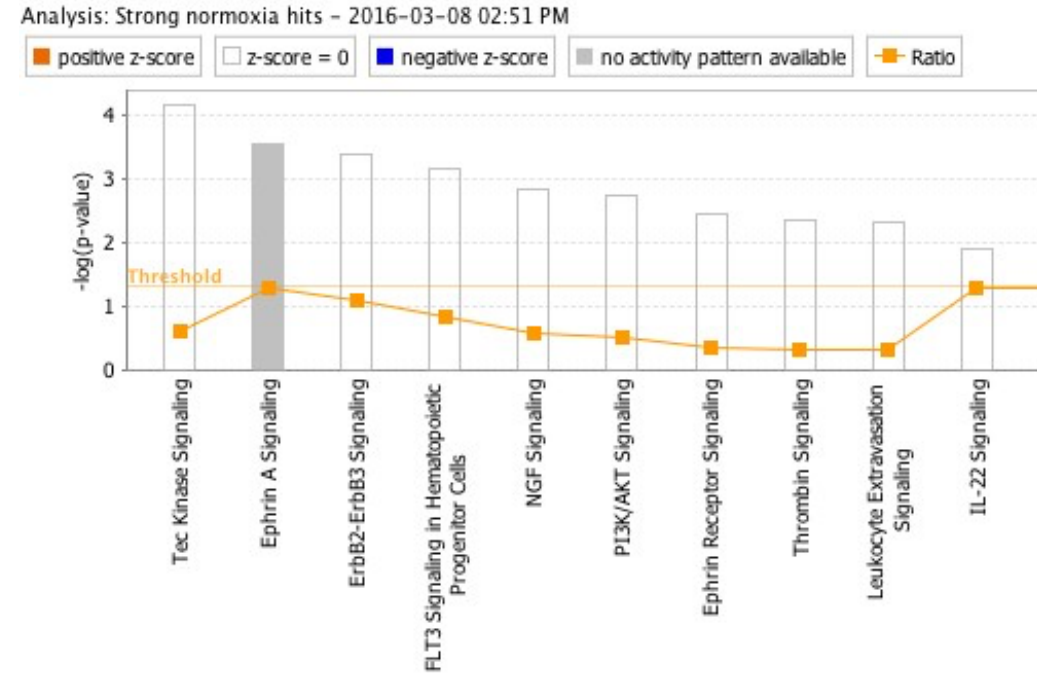

D GS6-22 hits

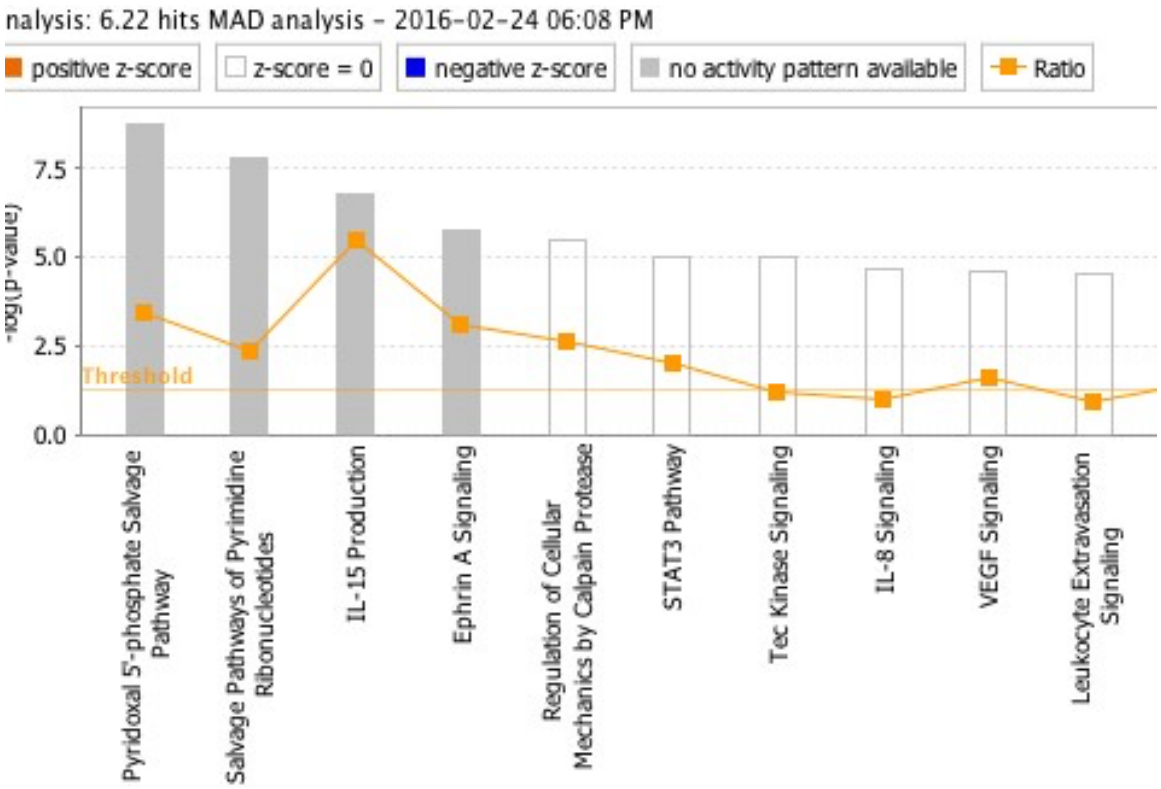

GS7-2 hits

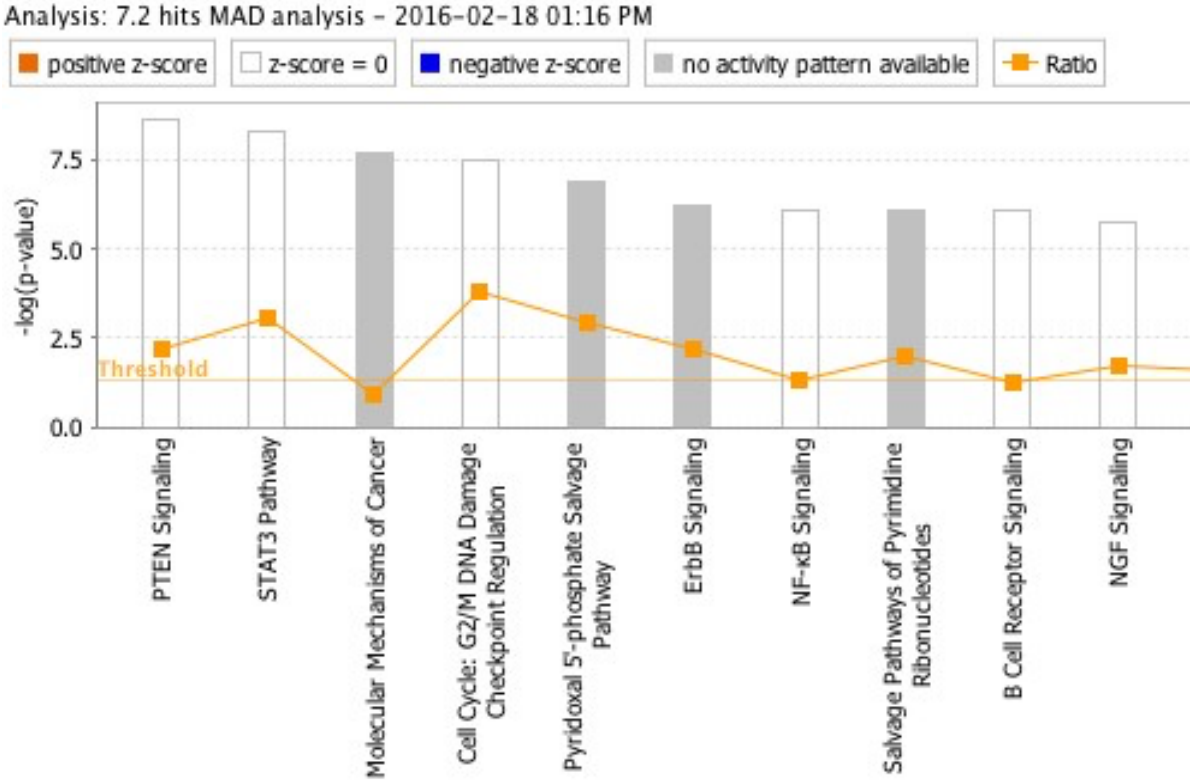

GS11-1 hits

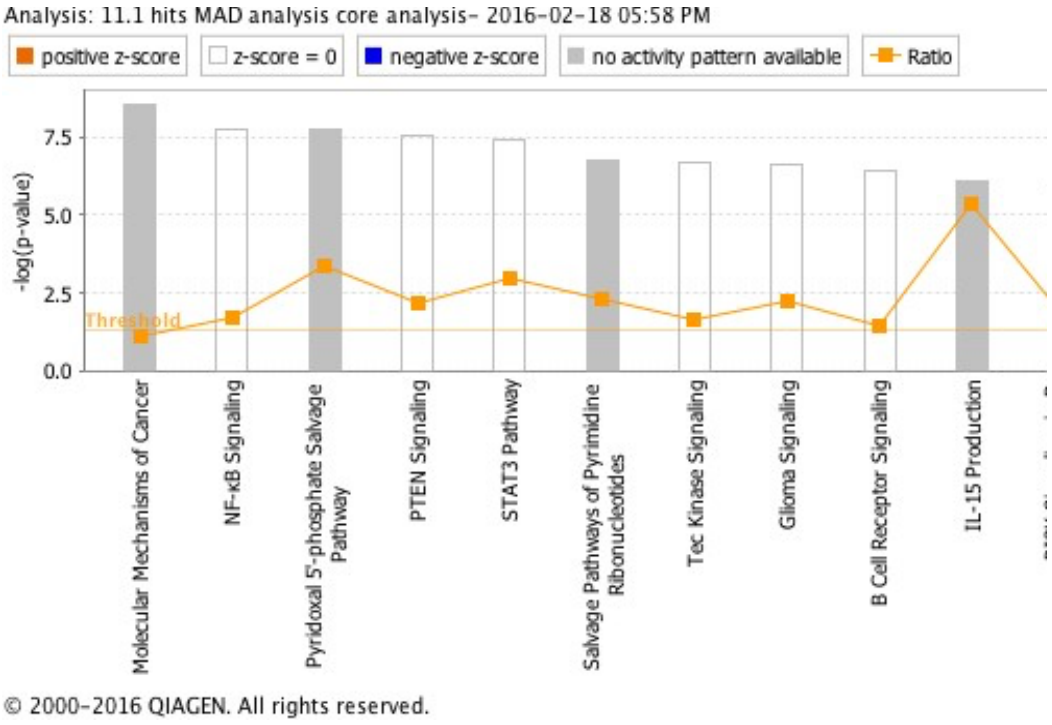

Fig 3.5: IPA analysis was used to categorize canonical pathways and disease biofunction of the hits. A. Top 10 pathway and biofunction distribution of hits under either normoxia or hypoxia common between all 3 GSC lines screened, B. hypoxia sensitive hits, C. normoxia sensitive hits and D. GS6-22 or GS7-2 or GS11-1 cell-line specific hits.

as CDC2L1, AURKB and YES1, are involved in growth control and can be attributed to faster growth rate of control cells in normoxia as compared to hypoxia (**Fig 3.5.C**).

The Yes1 kinase was an interesting common target in all the three GSC lines screened under both normoxia and hypoxia. It was selected as a hit for further investigation due to its relevance across varying glioma patient derived stem cells and under refractory hypoxic conditions. Moreover, it was significantly overexpressed in TCGA dataset of GBM tumors, as compared to normal brain tissue (oncomine). Yes1 has been confirmed by Surbhi Goel Bhattacharya in the lab to inhibit growth of GSCs both in vitro and in vivo and will be reported in a separate publication.

Discussion

Our screen generated some expected kinase hits, CDK6, CHK1, ERBB3, PLK1 and KDR/VEGF-R2, that are known to play a role in GBM as well as identified novel hits for GBM stem cells. Only 25% of our hits were common between the 3 GSC lines screened, reflecting the heterogeneity and narrow spectrum of common kinase vulnerability of the disease. One of the hits common between 3 GSC lines, YES1, and one hypoxia sensitive hit in GS6-22 cells, STK39, has been validated. Our list of hits included some of the genes identified from screens to be essential in other types of cancer, including PLK1, AURKA, AURKB, CDK6, RPS6KA4, PRKAA1 and PRKDC (Hart et al. 2015; Hart et al. 2014). Interestingly, the MAPK/ERK pathway genes, such as MAP4K2, STK39, MAP3K12, PTK2 and ROCK2, showed the strongest hypoxia sensitivity when platewise Z* score distance between normoxia and hypoxia was

calculated. These hits could contribute to GSC survival under hypoxia by activating cellular stress response pathway (Blanco et al. 2007; Laderoute et al. 1999) as well as activate cellular motility associated with angiogenic response (Burroughs et al. 2013; Lamalice et al. 2007). In fact, the cJNK and p38-MAPK pathway constitutes an alternative HIF-independent route for cell survival under hypoxic stress in both cancer cells (Kunz and Ibrahim 2003) and neurons (Park and Rongo 2016). MAPK/ERK is the most significantly enriched pathway in glioma (Ceccarelli et al. 2016; Cancer Genome Atlas Research Network 2008) and is hereby shown to be a potential target for refractory GBM stem cells under hypoxia. A few of our hypoxia enriched hits, such as KDR/VEGF-R2 and MET also affected angiogenic pathways, possibly because hypoxia has been shown to push GSCs towards endothelial lineage (Soda et al. 2011; Wang et al. 2010; Ricci-Vitiani et al. 2010). We have also shown that some kinases are required only under normoxic conditions. Thus, drugs that target these kinases unique to normoxia would fail to inhibit the stem cells in hypoxic areas of the tumor and give rise to tumor recurrence. This is an important issue that requires validation since our top normoxia enriched hits, CDC2L1 and BMX kinases have been previously identified as therapeutic targets in multiple myeloma and GBM respectively (Guryanova et al. 2011; Tiedemann et al. 2010).

Screening the GSC lines in parallel under normoxia or hypoxia enabled us to assess differences in kinase requirements by cells under different oxygen conditions. Differential growth inhibition was calculated by platewise MAD analysis to account for intrinsic differences in growth rate under each condition and the effect of outliers on true hits (Chung et al. 2008). A stringent analysis condition of Z* score > 2 as well as growth

inhibition > 50% of control wells, was applied to select statistically as well as biologically significant hits. In order to minimize false positive results, genes were scored as hits if at least two independent shRNAs targeting a gene produced growth inhibition. In addition, condition sensitive hits were selected if at least 2 hairpins targeting them produced a Z* score difference of 2 between normoxic and hypoxic conditions. Although stringent analysis of the screen results was performed to identify true hits, inefficient knockdown by some shRNA hairpins can give rise to false negatives. Therefore, our hits may not include all of the essential kinases in the GBM stem cell lines tested. Overall, our hit rate of 10% is comparable or slightly lower than other kinome screens in GBM or other cancer types (Ding et al. 2013; Tiedemann et al. 2010; Wurdak et al. 2010; Cheng et al. 2015).

Conclusion

There are many functionally essential genes involved in tumor development that are not genetically altered at the genome level. Therefore, integrating both functional and structural characterization of genes is needed to comprehensively identify therapeutic targets in cancer (Luo et al. 2008). We performed an RNAi screen of the kinome to identify specific genes that are essential for GBM stem cell growth and survival. We found that only 25% of the kinase hits were common between the 3 cell lines, thereby emphasizing the need for personalized therapeutic approach. YES1 gene, a member of the SRC family of tyrosine kinase, and a common target in all the three GSC lines under both normoxia and hypoxia, is being investigated in the lab in an effort to identify context-independent essential genes in GSC. In addition, we found hits unique to either

normoxia or hypoxia. Thus, therapeutic targeting of GBM must take into account the differential sensitivities of GBM stem cell under different microenvironments. Since GBM stem cells preferentially reside in hypoxic niches in the tumor that contribute to its maintenance and resistance, our goal is to elucidate the molecular mechanisms that allow them to survive in hypoxia and selectively target them.

Chapter 4

SMG1 kinase inhibition sensitizes GBM stem cells to hypoxia and temozolomide

The Suppressor of Morphogenesis in Genitalia 1 (SMG1) kinase was identified and validated from a pilot RNAikinome screen as a gene that can preferentially inhibit the growth of GS7-2 cells under hypoxia (1% oxygen).The SMG1 kinase is a member of the phosphoinositide-related kinase (PIKK) family of proteins that also includes the ATM, ATR and DNA-PK kinases. SMG1 is involved in multiple cellular pathways, including nonsense-mediated mRNA decay (NMD), DNA damage response (DDR) and telomere maintenance (Isken and Maquat 2008), all of which have important functions in cancer. SMG1 was discovered in *Caenorhabditis elegans* in relation to its role in nonsense-mediated mRNA decay (NMD) and is required in mammalian embryogenesis (Pulak and Anderson 1993; McIlwain et al. 2010). Nonsense-mediated mRNA decay is a RNA surveillance mechanism for degrading mRNA transcripts containing premature termination codons (PTC) within a protein encoding exon and thereby protects cells from accumulating non-functional or potentially harmful proteins encoded by such aberrant mRNAs (Isken and Maquat 2008). In mammals, newly synthesized PTC-containing mRNAs are targeted for NMD after pre-mRNA splicing and export from the nucleus to the cytoplasm. SMG-1 directly phosphorylates Upstreamframeshift protein, Upf1, a key NMD factor that associates with the terminating ribosome at the PTC and forms the SURF complex consisting of SMG1, UPF1 and eukaryotic release factors, eRF1-eRF3. Following PTC recognition, the SURF complex binds to UPF2 at the exon junction complex resulting in the formation of decay inducing complex (DECID). DECID formation leads to phosphorylation of UPF1 by SMG1, resulting in recruiting SMG5-7factors and the dissociation of the ribosome and eRF from Upf1 to advance mRNA decay.

Aberrant transcripts that escape NMD can lead to diseases. For example, β-thalassemia is caused by a PTC-containing β-globin mRNA that generate dominantly negative-acting polypeptides (Popp and Maquat 2014). Human cancers also exhibit aberrant transcription and mRNA processing, leading to PTC generation (Wang et al. 2011). In addition, NMD enables cells to adapt in varying physiological contexts through its role in stress response, cellular differentiation, development and homeostasis (Lykke-Andersen and Jensen 2015). For instance, UPF1 was shown to be required to maintain proliferation and restrict differentiation in neuronal stem cells (Lou et al. 2014).

SMG1 kinase has also been shown to induce DNA damage response pathways, in a similar manner to the other PIKK family members (Brumbaugh et al. 2004). GBM stem cells are believed to be responsible for tumor recurrence in spite of the DNA-damage induced by radiotherapy and traditional chemotherapy. One of the major reasons for therapy resistance of GSCs is a highly active DNA repair capacity (Beier et al. 2011). CD133+ GBM stem cells have been shown to exhibit radiation resistance by DNA damage checkpoint activation and an increase in DNA-repair capacity (Bao et al. 2006). Thus, strategies targeting DNA repair and anti-apoptotic mechanisms in tumor cells may sensitize tumors to chemotherapeutic drugs such as TMZ. Though MGMT is the best known DNA repair gene in GBM (Hegi et al. 2005), the SMG1 related kinases, ATM, ATR and DNA-PK also play key roles in DNA repair and sensitizing selected subsets of GBM tumors to TMZ (Ramirez et al. 2015; Quiros et al. 2011; Nadkarni et al.2012). Therefore, the role of SMG1 in the DNA damage response pathway makes it a potential target for combination therapy with TMZ.

Here I have validated that SMG1 loss leads to differential growth inhibition in different GBM stem cell lines using individual lentiviral shRNA and CRISPR constructs. I also shown that knockdown of SMG1 sensitized multiple GBM stem cell lines to the chemotherapeutic agent, temozolomide (TMZ) both in vitro and in vivo. Furthermore, we have built a computational model of the SMG1 signaling network in GBM stem cells and validated predictions of the model experimentally.

Materials and Methods

Cell Lines and Reagents

Human GBM stem cell lines, GS6-22, GS7-2 and GS11-1 were isolated in the laboratory from patient tumors from Tufts Medical Center following neurosphere culture method (Sherry et al. 2009). MGG8 and GBM12 cells were obtained from Wakimoto and Sarkaria labs (Ramirez et al. 2015; Wakimoto et al. 2012). Human GBM stem cell lines (Sherry et al. 2009) were cultured in serum-free Dulbecco's modified Eagle's medium (DMEM)/F12 supplemented with B27 (Gemini Bio-products, San Francisco, CA, www.gembio.com), epidermal growth factor (EGF) (20 ng/ml; Peprotech, Rocky Hill, NJ, http://www.peprotech.com), and fibroblast growth factor (FGF)-2 (20 ng/ml; Peprotech). Whenever indicated, the cell lines were treated with temozolomide at a concentration of 20uM, Chk1 inhibitor, PF47736 (Tocris Biosciences, Bristol, UK), Chk2 inhibitor, NSC 109555 ditosylate (Tocris Biosciences, Bristol, UK), ATM inhibitor, KU-55933 (Tocris Biosciences, Bristol, UK), ATR inhibitor IV (Cell Signaling Technology, MA, USA).

Lentiviral shRNA infection

Constitutive shRNA constructs targeting SMG1 were purchased from the RNAi consortium Mission lentiviral library available from Sigma (TRCN0000037411, TRCN0000037412 and TRCN0000037413), while doxycycline inducible shRNA constructs targeting SMG1 were purchased from Thermofisher Scientific (#RHS4740-EG23049). CRISPR (clustered regularly interspaced short palindromic repeats)-Cas9 guide RNA targeting SMG1 exon 2 (5'CACCGCCGAGATGTTGATCCGAATAGG 3'; 5' AAACCCTATTCGGATCAACATCTCGGC 3') was cloned into the lentiCRISPRv2 vector backbone, as previously described (http://www.ncbi.nlm.nih.gov/pmc/articles/ PMC4486245/pdf/nihms-702435.pdf). The lentiCRISPR v2 was a gift from Feng Zhang (Addgene plasmid # 52961). shRNA and CRISPR plasmid DNA constructs were then transfected into HEK293T cells to prepare lentivirus, following the standard Lipofectamine® LTX transfection procedure. GBM stem cell lines were infected with lentivirus in the presence of 2ug/ml polybrene. Two days after virus infection, the infected cells were selected in 0.5 to 1 ug/ml puromycin. One set of cells were then transferred to 1% hypoxic conditions in oxygen controlled incubator (Biospherix) and the other identical set left to incubate under 21% normoxic conditions. Relative changes in cell viability or gene expression of virus infected cells were compared to the kinase targeted infected cells after 7 days by prestoblue assay.

siRNA transfection

GSC neurospheres were passaged and plated overnight in antibiotic-free complete MEM medium and then transfected with 25 nM siRNA using Lipofectamine®

RNAiMAX Transfection Reagent (Thermofisher Scientific, MA, USA) according to the manufacturer's instructions. The non-targeting siRNA and the SMARTpool Accell siRNA against SMG7, UPF1 and ATG7 were purchased from Dharmacon Research Inc. (Lafayette, CO).

Cell viability assay

GSC neurospheres were dissociated to single cell suspension by trypsin and cell viability assessed using the membrane permeant, resazurin based Prestoblue assay (Sigma-Aldrich). Metabolically active cells reduce Prestoblue reagent to yield a red fluorescent resorufin product, which was quantitatively measured in a fluorescent plate reader (Spectrafluor Plus) at 590nm to determine cell viability.

RT-PCR

RNA was isolated using the RNeasy mini-kit (Qiagen, Valencia, CA) according to the manufacturer's instructions and treated with DNAse I (Invitrogen) for 30 minutes in order to digest genomic DNA. RNA was reverse-transcribed with iscript kit (Biorad). Quantitative PCR was performed using the Quantitect SYBR Green PCR Kit (Qiagen) and the MX3000 real time cycler (Stratagene, La Jolla, CA). Data presented is the average of three individual experiments; within each experiment technical triplicates were performed. Fold changes were calculated relative to control by the 2-ΔΔCt method. All primer sets amplify a single product of expected size; the following sequences were used:

SMG1 forward: GGTGGCTCGATGTTACCCTC;

SMG1 reverse: CTGCGTGAGCGAAGGTTTC;

β-Actin forward: CCTGGGCATGGAGTCCTGTGG;

β-Actin reverse: CTGTGTTGGCGTACAGGTCTT.

β-globin forward: GCACCTGACTCCTGAGG

β-globin reverse: CCGAGCACTTTCTTGCCA

MUP forward: CTGATGGGGCTCTATG

MUP reverse: TCCTGGTGAGAAGTCTCC

Computational modeling with Cell Collective platform

We used Cell Collective platform, an online open source collaborative software modeling platform (Helikar et al. 2012), to model biologic signaling pathways.. We used this platform to first construct a modified Boolean petrinet type model of SMG1 signaling in GS7-2 cell line under hypoxia and TMZ-induced stress. The Cell Collective platform (www.cellcollective.org) was then utilized to run pathway simulations and predict output after simulated inhibition of specific components of the pathway.

Western Blot

Cells were harvested in RIPA buffer (0.15 mol/l NaCl, 1% NP40, 0.01 mol/l desoxycholate, 0.1% SDS, 0.05 mol/l Tris-HCl (pH, 8.0)) and quantified by BCA assay (Invitrogen). Equal amounts of protein were subjected to SDS-PAGE and transferred to nitrocellulose membrane. The membrane was blocked in 5% non-fat skimmed milk in TBS-T for 1 hour. Primary antibodies were diluted and used according to manufacturer's

recommended protocol. Antibodies used and dilutions with sources. Horseradish peroxidase conjugated secondary antibodies were incubated for 1hr at room temperature in TBS-T. Protein bands were visualized by ECL kit.

NMD read-out assay

GBM stem cells were transiently transfected with a *pmCMV-Gl* plasmid, which expressed β-globin (*Gl*) mRNA that was either nonsense-free (Norm) or harbored a premature termination codon at position 39 within exon 2 (Ter) (Zhang et al., 1998a) and the reference *phCMV-MUP* plasmid was used as a reference plasmid (Belgrader and Maquat, 1994), which expressed mRNA for the mouse major urinary protein (MUP) and served to control for variations in the efficiencies of cell transfection (Ishigaki et al. 2001). We tested transfected β-globin by qRT-PCR using previously described primers, as listed, for β-globin (Hwang et al. 2010) and MUP.

Intracranial tumor implantation in mice and TMZ treatment

All mice studies were conducted in compliance with IACUC protocol approved by Tufts Medical Centre. Studies aimed to assess if there was an additive effect of SMG1 knockdown with TMZ treatment in MGG8 GBM stem cells in vivo. GS7-2 or MGG8 cells were tagged with luciferase (LV-Pico2-Fluc.mCherry (Bagci-Onder et al. 2011))to monitor tumor cell growth in vivo by real-time bioluminescence using Xenogen IVIS 200 imager and p-value was calculated by t-test at the termination of experiment. NCR nude mice model were intracranially injected with GS7-2 luciferase empty vector control or constitutive shSMG1 infected GS7-2 or MGG8 cells in groups of at least 5 mice

each. TMZ was administered at the standard dosing regimen of 50 mg/kg body weight for 5 consecutive days (Momota et al., 2005) after the MGG8 tumors were allowed to form for 5 weeks. The mice were imaged until death or were euthanized once tumors reached 30 mm^3 or mice showed symptoms, like weight loss, hunching and seizures. After euthanasia, brain slices were obtained and subjected to H&E and Ki67 staining. Mice survival was monitored and assessed by Kaplan-Meier analysis and statistical significance was determined with log rank score.

Results

SMG1 knockdown preferentially inhibits the GS 7-2 cell line under hypoxia

SMG1 was found to be a hypoxia sensitive hit in GS7-2 cells from a pilot RNAi screen of these GSCs under normoxia and hypoxia. We validated the SMG1 knockdown showing that either constitutive shRNA hairpins or doxycycline inducible shRNAs knocked down SMG1 up to 75% and inhibited GS7-2 growth up to 70% in hypoxia vs only 30% under normoxia (**Fig 4.1A, C; S4.1A**). SMG1 knockdown using these shRNA hairpins led to a similar trend of enhanced growth inhibition under hypoxia (up to 70% under hypoxia, as compared to 30% under normoxia) in the GBM12 cell line as well (**Fig 4.1B**). However, SMG1 knockdown did not sensitize MGG8 cells to hypoxia (**Fig S4.1B**). In addition, SMG1 knockdown only weakly affected the growth of GBM serum lines and normal human fibroblast line, HS27, and transformed human fibroblast line, HT1080, indicating a GBM stem cell sensitive requirement for this kinase (**Fig S4.1C**). CRISPR-Cas9 hairpins targeting of the SMG1 gene led to almost complete knockdown of

SMG1 kinase up to 90% (**Fig 4.1D**) (in contrast to ~70% knockdown by shRNA) and led to strong growth inhibition (up to 90%) in GS7-2 cells under both normoxia and hypoxia (**Fig 4.1C**). This result suggests that a minimal level of SMG1 kinase expression is required for tumor cell growth irrespective of oxygen levels. In order to test if the cellular requirement for SMG1 varied under physiological oxygen levels, we tested GSC growth when SMG1 was inhibited under cell culture oxygen level (21% oxygen), physiological oxygen level (5% oxygen) (Moreno et al. 2015) or tumor hypoxia levels (1% oxygen) (Soeda et al. 2009; Wilson and Hay 2011). We found that SMG1 was required for GS7-2 growth under both 1% and 5% oxygen, as opposed to 21% oxygen (**Fig S4.1D**).

SMG1 knockdown sensitizes GBM stem cells to temozolomide (TMZ) treatment

Since SMG1 regulates DNA repair and the DNA-damaging drug TMZ is the standard of care for GBM patients, we examined the combinatorial effect of SMG1 knockdown with TMZ treatment in GBM stem cells. We found an enhanced growth inhibitory effect of SMG1 knockdown of up to 90% in the presence of TMZ in GS7-2 and GS12 under hypoxia (**Fig 4.2A**). In addition, the GS6-22 and MGG8 cell lines that were less sensitive to SMG1 knockdown alone, also showed significant growth inhibitory effect when SMG1 is knocked down in the presence of TMZ (**Fig 4.2B**).

SMG1 knockdown and TMZ treatment inhibit tumor growth in mouse xenografts

To test the in vivo tumorigenic potential of SMG1 inhibition, we performed a preliminary experiment with shSMG1-infected GS7-2 cells, intracranially injected at a low density

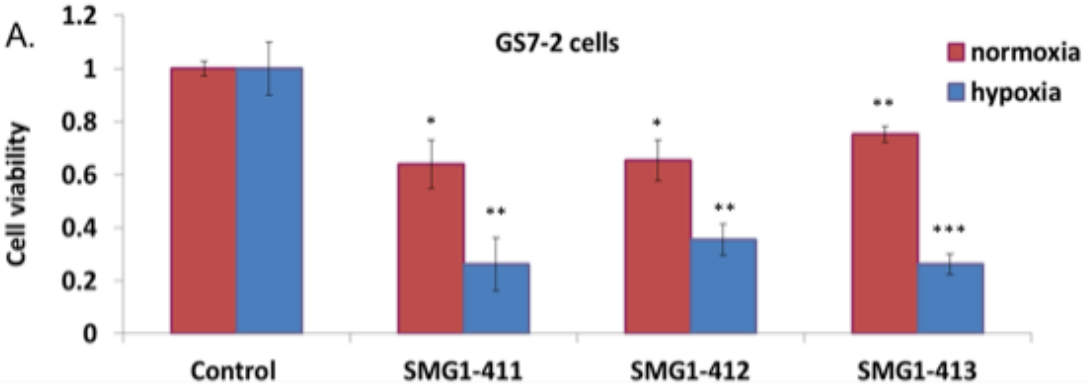
A.
GS7-2 cells
normoxia
hypoxia
Cell viability
1.2
1
0.8
0.6
0.4
0.2
0
Control
SMG1-411
SMG1-412
SMG1-413

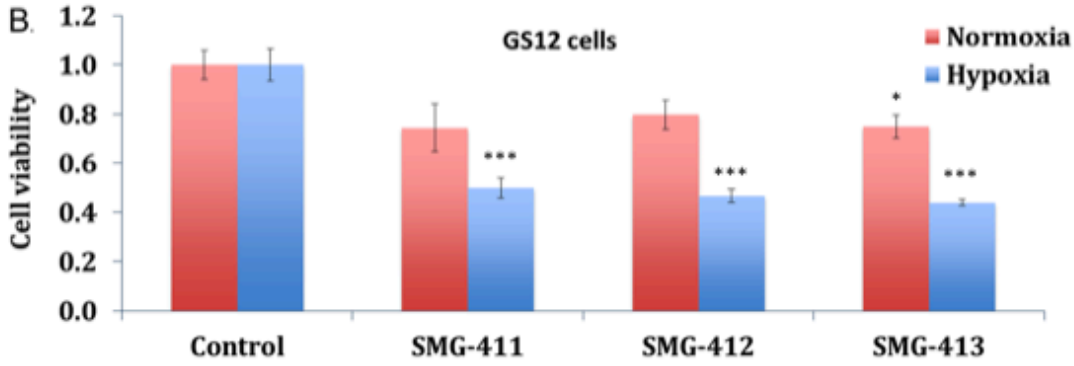
B.
GS12 cells
Normoxia
Hypoxia
Cell viability
1.2
1.0
0.8
0.6
0.4
0.2
0.0
Control
SMG-411
SMG-412
SMG-413

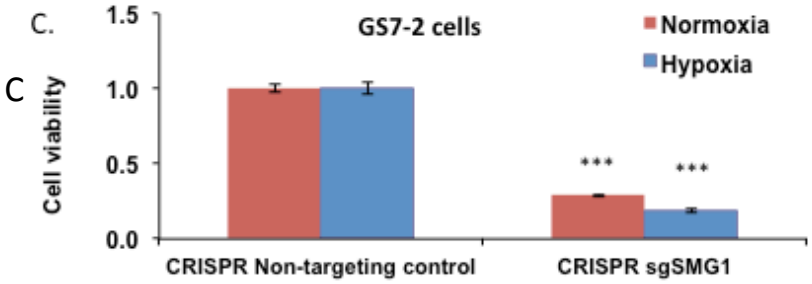
C.
C
GS7-2 cells
Normoxia
Hypoxia
Cell viability
1.5
1.0
0.5
0.0
CRISPR Non-targeting control
CRISPR sgSMG1

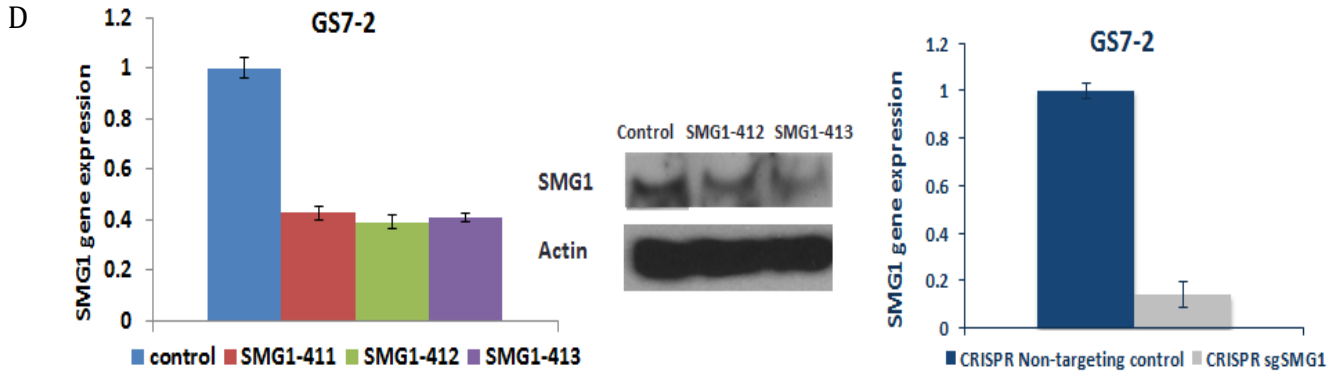
D
GS7-2
SMG1 gene expression
1.2
1
0.8
0.6
0.4
0.2
0
control
SMG1-411
SMG1-412
SMG1-413
Control
SMG1-412
SMG1-413
SMG1
Actin
GS7-2
SMG1 gene expression
CRISPR Non-targeting control
CRISPR sgSMG1

Fig 4.1. SMG1 knockdown inhibits selected GSC lines under hypoxia. A. GS7-2 or B. GS12 cells were stably infected with the indicated shRNA hairpins for SMG1 or control vector and assayed for growth in 1% oxygen or 21% oxygen, over 7 days. C. GS7-2 cells were stably infected with constitutive CRISPR-Cas lentiviral vector and assayed for growth in 1% or 21% oxygen over 7 days. *, **, and *** denote p values <0.5, 0.01 and 0.005 respectively with respect to control, student's two-tailed t-test, bars SD. D. SMG1 knockdown with multiple shRNA hairpins and CRISPR-Cas hairpin was assayed in GS7-2 cells by RT-qPCR and western blot, whenever sufficient lysate could be obtained.

to follow tumor growth in mice over time. Though the GS7-2 cells only grew to a limited extent before reaching a steady state, we found that shSMG1-infected GS7-2 tumor cells showed significantly less growth over time as compared to control tumor cells (p-value = 0.008) (**Fig S4.2B**). We then assessed the therapeutic potential of targeting SMG1 alone or in combination with TMZ in the highly tumorigenic MGG8 cells. The control and shSMG1 injected groups were allowed to form tumors for a month and observed in real time with or without TMZ treatment. Bioluminescence tracking of tumor growth in vivo showed that shSMG1-infected MGG8 cells grew at a slower rate than control cells, but multiplied over time and eventually killed the mice within 2 months (**Fig 4.3A, S4.2A**). Strikingly, shSMG1-infected MGG8luc tumors showed an almost 1000 fold greater remission when treated with TMZ after a month, as compared to control MGG8luc tumor. In addition, TMZ treatment significantly prolonged survival of mice injected with these shSMG1-infected MGG8 cells, when compared to control (**Fig 4.3B**). Representative mice brain slices with staining for H&E and Ki67, a marker for cellular proliferation, showed that shSMG1 infected mice had a lower proportion of Ki67 stained MGG8 cells than control mice (**Fig 4.3C**). Thus, SMG1 knockdown significantly reduced tumor growth and mice survival when MGG8 cells were treated with the current standard of care, TMZ.

Computational modeling of the SMG1 network

Since SMG1 regulates a large number of complex cellular processes, we used the Cell Collective platform in order to model and predict which of these mechanisms is responsible for the preferential growth inhibitory effect of SMG1 knockdown under

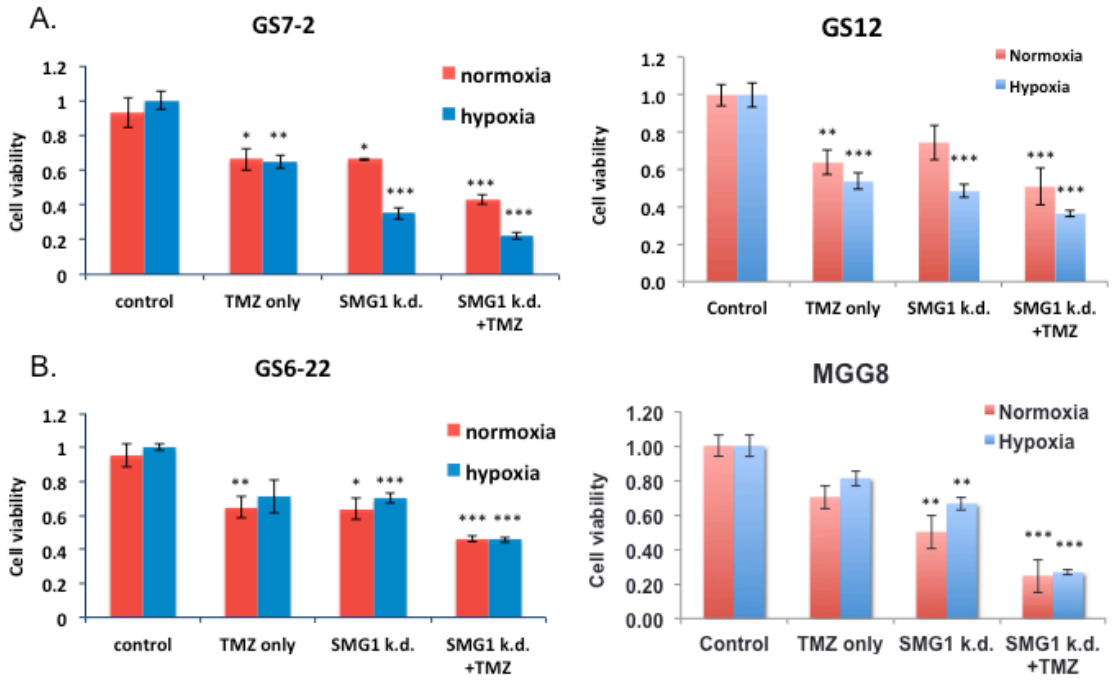

Fig 4.2. SMG1 knockdown leads to enhanced growth inhibition of GBM stem cells in the presence of TMZ. A. GS7-2 and GS12 cells were subjected to 20 uM TMZ treatment in 1% oxygen or 21% oxygen over 7 days with and without SMG1 knockdown and cell viability measured by prestoblue. B. MGG8 and GS6-22 cells that were less sensitive to SMG1 knockdown alone, were subjected to TMZ treatment with or without SMG1 knockdown, and assayed for growth by prestoblue after 7 days. *, **, and *** denote p values <0.5, 0.01 and 0.005 respectively with respect to control, student's two-tailed t-test, bars SD.

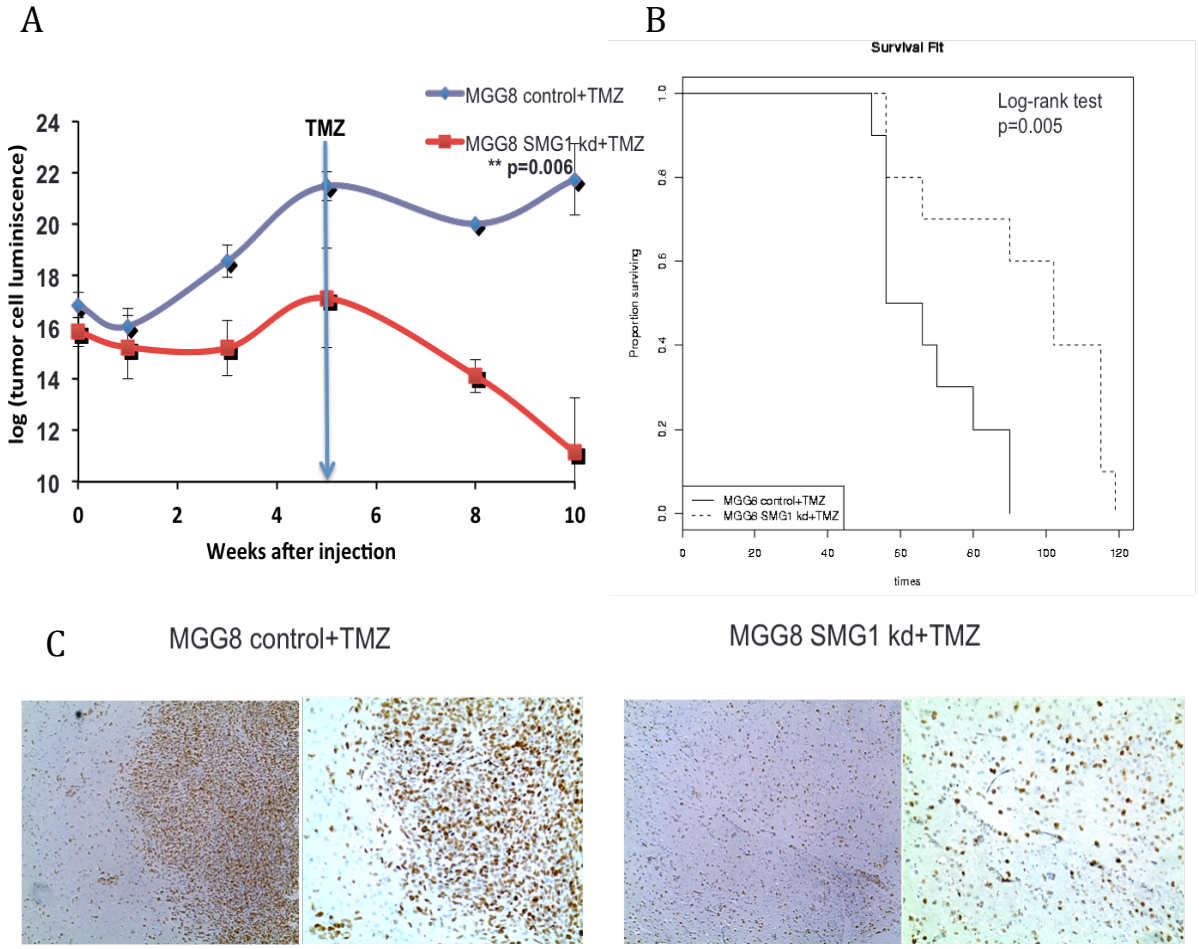

Fig 4.3. SMG1 knockdown and TMZ treatment significantly improves prognosis in mouse xenografts. Control or shSMG1 infected MGG8 luciferase expressing cells were injected intracranially in mice and subjected to 50 mg/kg TMZ treatment after 5 weeks. A. In vivo growth of control vs shSMG1 infected MGG8 cells were measured using bioluminescence IVIS imaging over 10 weeks or until the mice died, p-value = 0.006. B. Kaplan Meier survival curve shows significant survival benefit when SMG1 is knocked down in conjunction with TMZ, as compared to TMZ alone. C. H&E and Ki67 stained brain slices of mice injected with shSMG1 or control vector infected MGG8 cells, p = 0.05.

hypoxia and TMZ-induced stress. The Cell Collective is an online open source collaborative modeling platform (Helikar et al. 2013), and was used to model the dynamic regulatory interactions of SMG1 signaling in GBM stem cells. The Cell Collective implements a boolean logic network (petrinets) with modifications for temporal and concentration dependent events to simulate biological signaling networks (Helikar et al. 2013). Petrinets are simple logic gate driven models that have been used successfully to model signal transduction networks (Sackmann et al. 2006).

Experimental results and data from the literature were integrated to evaluate DNA damage response elements, nonsense mediated mRNA decay elements and hypoxia inducible elements as regulatory variables in the model, as listed in **tablesS4.1-4.3**. The Cell Collective platform enables virtual in-silico experiments to simulate the activation or inhibition of many nodes in these complex interactive pathways and allows us to make systematic predictions about the behaviors of key components upon change of conditions such as inhibition of SMG1 or hypoxia or TMZ treatment (**Fig 4.4A**). The Cell Collective model offers an added advantage over strictly Boolean modeling to allow for real-time concentration dependent simulations of SMG1 signaling in the virtual cell. The model simulations can depict changes in various regulatory nodes to predict key mechanisms behind GS7-2 cell growth inhibition, when SMG1 is inhibited under conditions of hypoxia or TMZ (**Fig 4.4B)**. The simulation found that cell growth was directly influenced by cell cycle S phase continuation, apoptosis and autophagy nodes.

A

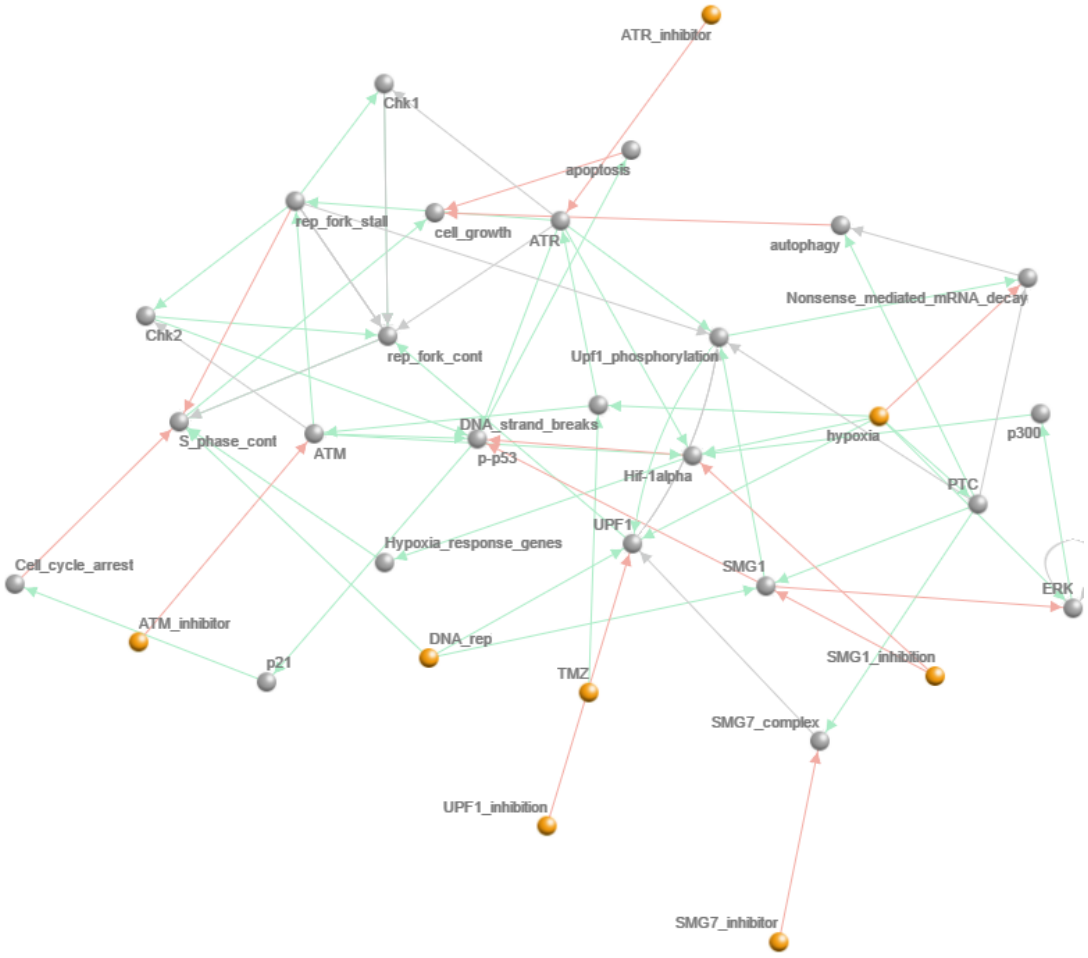
ATR_inhibitor
Chk1
apoptosis
rep_fork_stall
cell_growth
ATR
autophagy
Nonsense_mediated_mRNA_decay
Chk2
rep_fork_cont
Upf1_phosphorylation
DNA_strand_breaks
S_phase_cont
ATM
p-p53
hypoxia
p300
Hif-1alpha
PTC
UPF1
Hypoxia_response_genes
Cell_cycle_arrest
SMG1
ERK
ATM_inhibitor
DNA_rep
SMG1_inhibition
p21
TMZ
SMG7_complex
UPF1_inhibition
SMG7_inhibitor

B

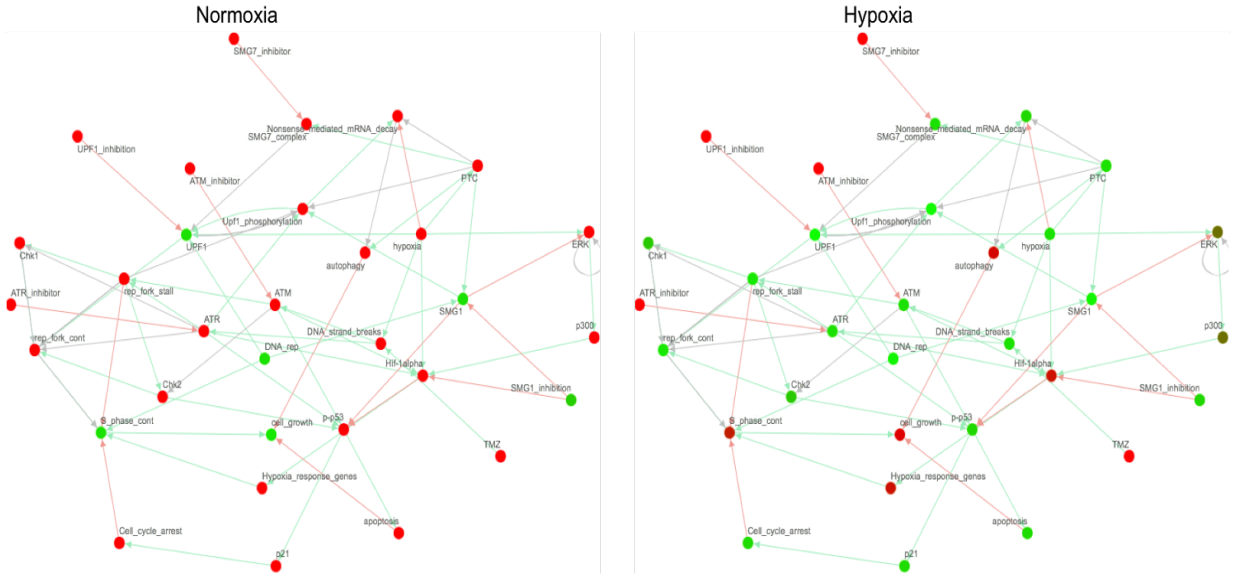
Normoxia
Hypoxia

Fig 4.4. Cell Collective generated simulation of SMG1 kinase network under hypoxia or TMZ.A. Our model consists of about 25 signaling nodes. Yellow nodes are the external nodes of the simulation that can be manipulated, while grey nodes are the internal components of the model. Green arrow indicates positive regulation, while red arrow indicates negative regulation between the nodes. B. Cell Collective modeling was used to simulate GS7-2 cell growth when SMG1 is knocked down under normoxia or hypoxia. Green nodes indicate activation, while red indicates inhibition.

Role of SMG1 in the DNA damage response (DDR) pathway

Given the combinatorial effect of targeting SMG1 with the DNA-damaging drug, TMZ, we investigated if SMG1 knockdown leads to a defect in the DDR pathway. The model predicted that either hypoxia or TMZ treatment results in cellular DNA damage (Hammond et al. 2002; Ito et al. 2013), and then activation of ATM and ATR repair proteins, which stall the replication fork and activate checkpoint proteins, Chk1 and Chk2 (Matsuoka et al. 2000; Gibson et al. 2005). Meanwhile, ATR or SMG1 phosphorylates and activates Upf1, which is also involved in DNA repair (Azzalin and Lingner 2006). Upon efficient repair of the DNA breaks, the replication fork continues and cells proceed through the cell cycle. The model predicted that loss of SMG1 can lead to a block in cell cycle progression through its effect on the p53-p21 axis and/or replication fork continuation by the repair proteins (**Fig 4.5A**). However, we found experimentally that SMG1 knockdown upregulates phospho-p53 (Ser 15), total p53 and p21 protein level in our GSC lines under hypoxia, which is indicative of the DNA damage response (**Fig 4.5B**). This finding contradicts earlier results in U2OS cells, where SMG1 knockdown was shown to deplete p53 phosphorylation under oxidative stress (Brumbaugh et al. 2004). Thus, in vitro testing of the model here elucidated a unique response in GSC and enabled us to refine the model pertinent to our system. Contrary to the literature, p53-p21 activation in this case did not upregulate apoptosis markers, such as cleaved caspase or cleaved PARP (Schuler et al. 2000; Kumari et al, 1998). The activation of cell cycle checkpoint proteins, Chk1 and Chk2 kinases, was then tested experimentally. SMG1 knockdown led to higher phosphorylation of Chk2 relative to control (**Fig 4.5B**), which could be explain the lower Ki67 staining population when SMG1 is knocked down (**Fig**

A

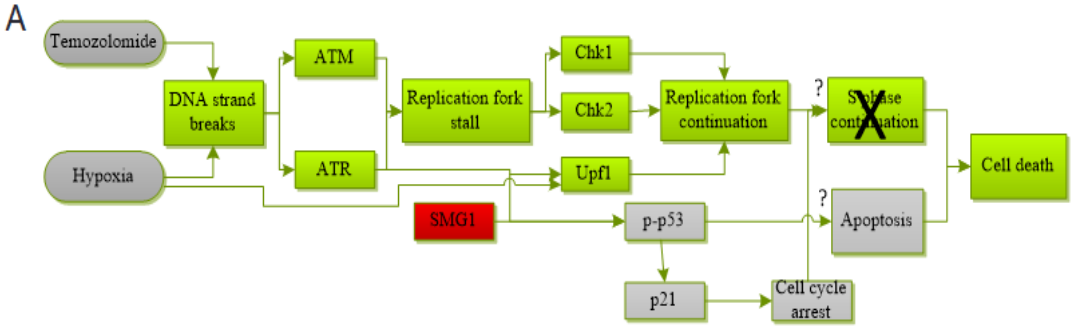

B

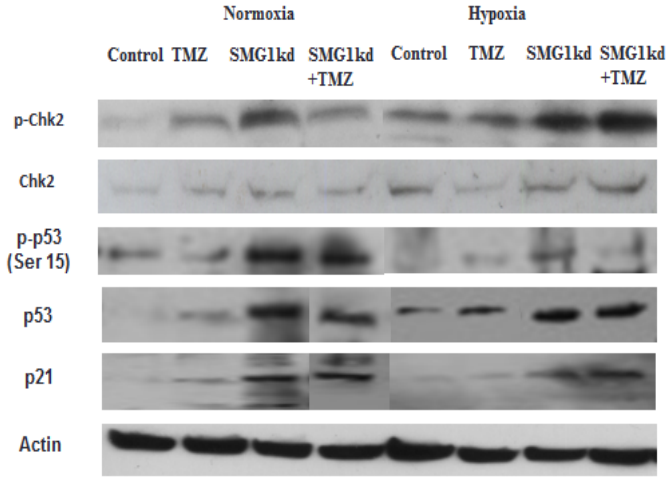

C

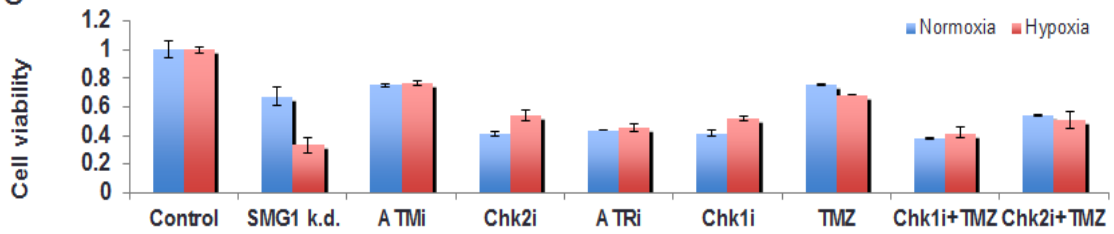

D

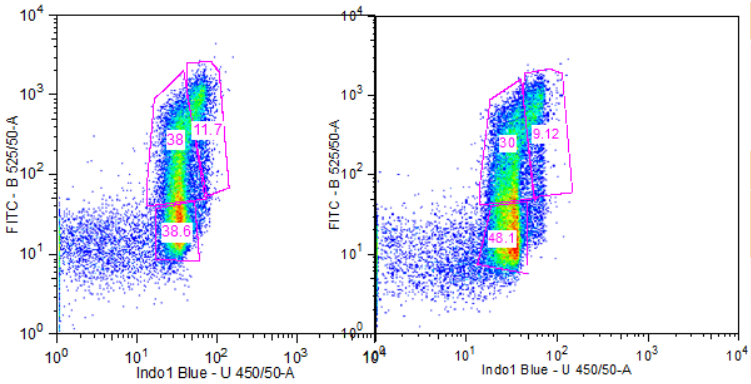

# Cells		
Total	50000	50000
Live subset	31501	31999
% of live subset		
Population subset	7-2 Control	7-2 SMG1 k.d.
G0	38.6	48.1
G1	38	30
S/G2/M	11.7	9.12

Fig 4.5. Role of the DNA damage response pathway in SMG1 loss mediated GBM stem cell growth inhibition under hypoxia or TMZ treatment.A. Cell collective model predicts that hypoxia or TMZ increases the frequency of DNA damage. Loss of inhibits checkpoint protein mediated repair pathway, leading to block in cell cycle and death. B. GS7-2 cells were subjected to doxycycline inducible knockdown of SMG1 alone or with TMZ under normoxia or hypoxia and assayed for p-p53 (Ser 15), p53, p21, p-Chk2 (Thr 68) and Chk2. C. GS7-2 cells were subjected to SMG1 knockdown or inhibitors for ATM, Chk2, ATR, Chk1 alone or with TMZ and assayed for growth under normoxia or hypoxia after 7 days. D. Control or SMG1 knockdown GS7-2 cells were stained for FITC-Ki67 and PI and flow cytometry was used for cell cycle G0, G1 or S/G2/M phase analysis.

4.5D). However, we found experimentally that there was no preferential activation of these DNA damage response proteins in the presence of TMZ or hypoxia alone (**Fig 4.5B**). Finally, we tested experimentally whether inhibiting cell cycle checkpoint signaling proteins phenocopies SMG1 knockdown in sensitizing GS7-2 cells to hypoxia or TMZ. Inhibition of the ATR kinase, but not the ATM kinase, resulted in GS7-2 cell growth inhibition (**Fig S4.5C**), whereas both Chk1 and Chk2 inhibitors led to GS7-2 growth inhibition (**S4.5C**). However, growth inhibition by Chk1 and Chk2 inhibitors was not enhanced by hypoxia or TMZ treatment. These results suggest that preferential growth inhibitory effect by SMG1 kinase loss was not due to its role in the DDR pathway.

Role of SMG1 in Nonsense Mediated Decay pathway

Since the classical role of SMG1 in the NMD pathway has previously been implicated in tumorigenesis (Isken and Maquat 2008), we subsequently tested an alternative model-generated hypothesis that SMG1 knockdown inhibits GS7-2 cell growth under hypoxia or TMZ due to its role in the NMD pathway. The model predicted that hypoxia or TMZ increases the frequency of premature termination codons (PTC), which can no longer be removed by the nonsense mediated mRNA decay (NMD) pathway when SMG1 is knocked down. Hence, autophagy is upregulated leading to cell death (**Fig 4.6A**). We tested the frequency of PTC in these cells by transfecting β-globin (*Gl*) mRNA that was either nonsense-free (Norm) or engineered to express a PTC (Ter) (Zhang et al., 1998a). In line with the model prediction, hypoxia or TMZ led to higher levels of expression of PTC containing beta globin, which was further enhanced upon

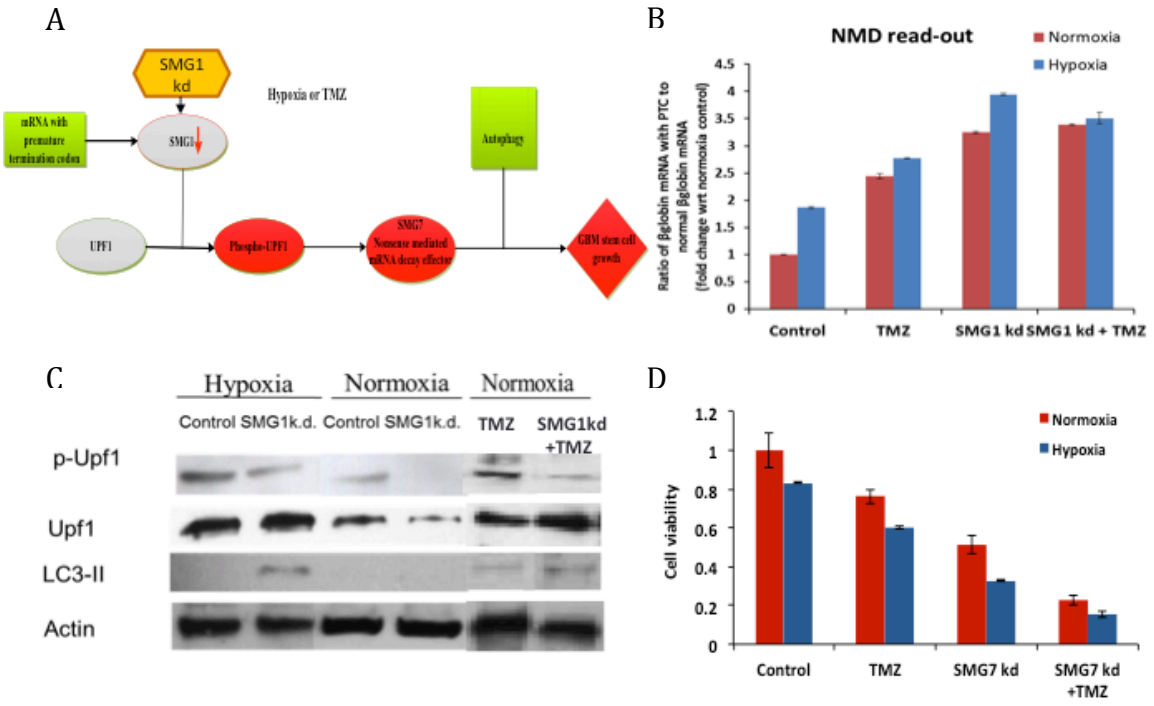

Fig 4.6. Loss of SMG1 inhibits cell growth under hypoxia due to a defect in NMD pathway. A. The model predicts that hypoxia increases the frequency of premature termination codons (PTC), which can no longer be efficiently removed by NMD pathway when SMG1 is knocked down. Hence autophagy is upregulated leading to cell death. B. SMG1 knockdown interferes with nonsense mediated decay of transfected β globin with PTC. C. GS7-2 cells were subjected to doxycycline inducible SMG1 knockdown for 7 days and assayed for its downstream p-Upf1, Upf1 or the autophagy marker, LC3-II, under hypoxia or normoxia, with or without TMZ treatment. D. Knockdown of the downstream NMD effector, SMG7, shows an additive growth inhibition in GS7-2 cells upon TMZ treatment, both under normoxia and hypoxia.

SMG1 knockdown (**Fig 4.6B**). Interestingly, the hypoxia sensitive growth inhibitory effect of SMG1 knockdown correlated with the induction of Upf1 in GS7-2 cells under hypoxia (**Fig 4.6C**). As predicted by our model, indeed, the autophagy marker LC3-IIA was also upregulated specifically under hypoxia (**Fig 4.6C**). In order to test whether the Upf1 induction or autophagy response caused cell growth inhibition, we tested if we could rescue GS7-2 cell growth with siUpf1 or siLC3-IIA (**Fig S4.3A, B**). However,

inhibition of either Upf1 or autophagy induction was not able to rescue GS7-2 growth, suggesting that neither of these mechanisms were responsible for the growth defect caused by SMG1 inhibition. Further, SMG1 knockdown was shown to reduce the protein levels of p-Upf1 as well as SMG7 (**Fig 4.6C, S4.3C**), both of which play important roles in the NMD pathway. We then tested the role of the downstream NMD effector, SMG7, in regulating GBM stem cell growth. SMG7 inhibition phenocopied SMG1 inhibition and resulted in preferential growth inhibition of GS7-2 cells under hypoxia or TMZ (**Fig 4.6D**). Thus, depletion of SMG7 kinase could explain the mechanism by which SMG1 kinase inhibition sensitized GBM stem cell growth to hypoxia and TMZ. These results show that the NMD pathway mediates the preferential growth inhibitory effects of SMG1 in the presence of hypoxia and TMZ, but the exact mechanism of cell death remains elusive.

Discussion

SMG1 was found as a cell line specific and hypoxia-sensitive hit from a pilot RNAi kinome screen of GS7-2 cells. Previously, SMG1 has been shown to play different roles in different tumor types. Consistent with our findings in GBM, downregulation of SMG1 made HPV-positive head and neck squamous cancer cells more sensitive to radiation therapy (Gubanova et al. 2012). A kinome siRNA screen in multiple myeloma cells also identified SMG1 as a common hit in multiple cell lines (Tiedemann et al. 2010). SMG1 gene is amplified in about 15% of metastatic breast cancer samples and alterations in the SMG1 gene correlated with lower patient survival (TCGA datatset, www.cbioportal.org), thereby implicating its role as a potential target oncogene. In

contrast, SMG1 has been reported to exhibit tumor suppressor effects in other cancer cells, like U2OS and HCT116 cells (Gubanova et al. 2013). We confirmed that SMG1 inhibition led to enhanced GBM stem cell growth inhibition under hypoxia using multiple shRNA and CRISPR constructs. Inhibition of GBM cells in hypoxic environments is important for the effective remission of refractory GBM tumors (Soeda et al. 2009). In addition, our data suggests that SMG1 holds significant therapeutic potential since it shows additive growth inhibitory effects in multiple GSC lines in the presence of TMZ and synergistic effects in vivo.

Given that SMG1 has been found to be both oncogenic and anti-oncogenic, it is clear that the overall function of SMG1 depends on its cellular context. Therefore, we used Cell Collective computational modeling system to investigate which molecular mechanisms might be responsible for making GSC lines susceptible to SMG1 inhibition under hypoxia or TMZ-induced stress. The model predictions were tested to evaluate the contribution of the DNA damage response pathway and Nonsense mediated mRNA decay pathway in SMG1 mediated growth inhibition. While SMG1 inhibition showed GBM stem cell specific effects in upregulating DNA damage response pathway components, including p21 and Chk2, these effects did not explain the enhanced growth inhibition by SMG1 loss under hypoxia or TMZ. The model was refined based on our experimental results, which sometimes contradicted results from the literature from other non-GBM cell lines. The model generated an alternative hypothesis, which was verified experimentally to show that SMG1 functions in nonsense mediated mRNA decay to inhibit GBM stem cell growth and survival. This study shows the importance of integrating experimental approaches with computational approaches to generate a

hypothetical model and verify it experimentally to uncover a mechanism of action, relevant to a given biological context.

Since SMG1 functions to degrade aberrant mRNAs containing PTCs, it was no surprise that SMG1 knockdown led to higher levels of PTC containing β-globin. Importantly, we also found a higher incidence of PTC containing β-globin in the presence of hypoxia or DNA damage induced by TMZ treatment in GBM cells. Aberrant mRNA with PTC occur as a result of genomic frameshift or nonsense mutations caused by alternative splicing, which frequently occur in cancer cells (Wang et al. 2011) and could be exacerbated in the presence of cellular stress (Popp and Maquat 2014; Wang et al. 2015), such as hypoxia or DNA-damage induced by TMZ. We, hereby, provide evidence for the first time that support previous suggestions that hypoxia/TMZ potentially inhibits NMD in GBM stem cells. Additionally, experimental depletion of SMG1 was shown to further interfere with the NMD pathway by depleting p-Upf1 and SMG7 proteins, resulting in higher levels of PTC containing β-globin mRNA. Importantly, inhibiting the NMD pathway through SMG7 inhibition phenocopies the effect of SMG1 inhibition in sensitizing GSC to hypoxia and TMZ. These findings suggest that SMG1 primarily acts through its role in the NMD pathway in GBM stem cells. Consistent with the role of NMD in our cells, an earlier RNAi screen found that loss of PHF5A inhibited GSCs through a similar mechanism. PHF5A is a splicing factor, which when mutated was shown to generate more PTCs and thereby induce nonsense mediated decay of many essential growth regulatory proteins (Hubert et al. 2013). In addition, protein complexes involved in NMD, UPF1, SMG7 and SMG8, were identified as core essential genes found from screens in GBM and some other cancers (Vogelstein et al. 2013). This is

further evidence of the critical role of this fundamental NMD process in impacting GBM tumorigenesis through a broad range of target genes.

Since our model predicted that inhibition of NMD activates autophagy consistent with the results of other studies (Wengrod et al. 2013a), we tested and found activated autophagic marker, LC3A, when SMG1 is knocked down under hypoxia or TMZ. However, we could not rescue cell growth by knocking down the autophagy effector gene ATG7 (Vuppalapati et al. 2015), indicating that it is not solely responsible for GSC growth inhibition. Although autophagy is generally a mechanism for cancer cell survival under certain contexts, including hypoxia (Chang et al. 2012; Qiang et al. 2013; Marino et al. 2012; Gong et al. 2012; Cicchini et al. 2015), Wengrod et al have reported that simultaneous inhibition of NMD and autophagy leads to synergistic cell death (Wengrod et al. 2013a). However, our results suggest that autophagy does not play a key role in SMG1 mediated blockade of GBM stem cell proliferation. Future studies will address the mechanism of SMG1 mediated GSC growth inhibition.

Ultimately we would like to construct enhanced computer simulations of the key molecular and genetic nodes in GBM in order to identify which tumors that will likely be responsive to anti-SMG1 therapy. This will eventually help in making informed therapeutic predictions of whether targeting SMG1 will be effective in a given patient. This study is a step towards devising much needed personalized therapy for treating GBMs.

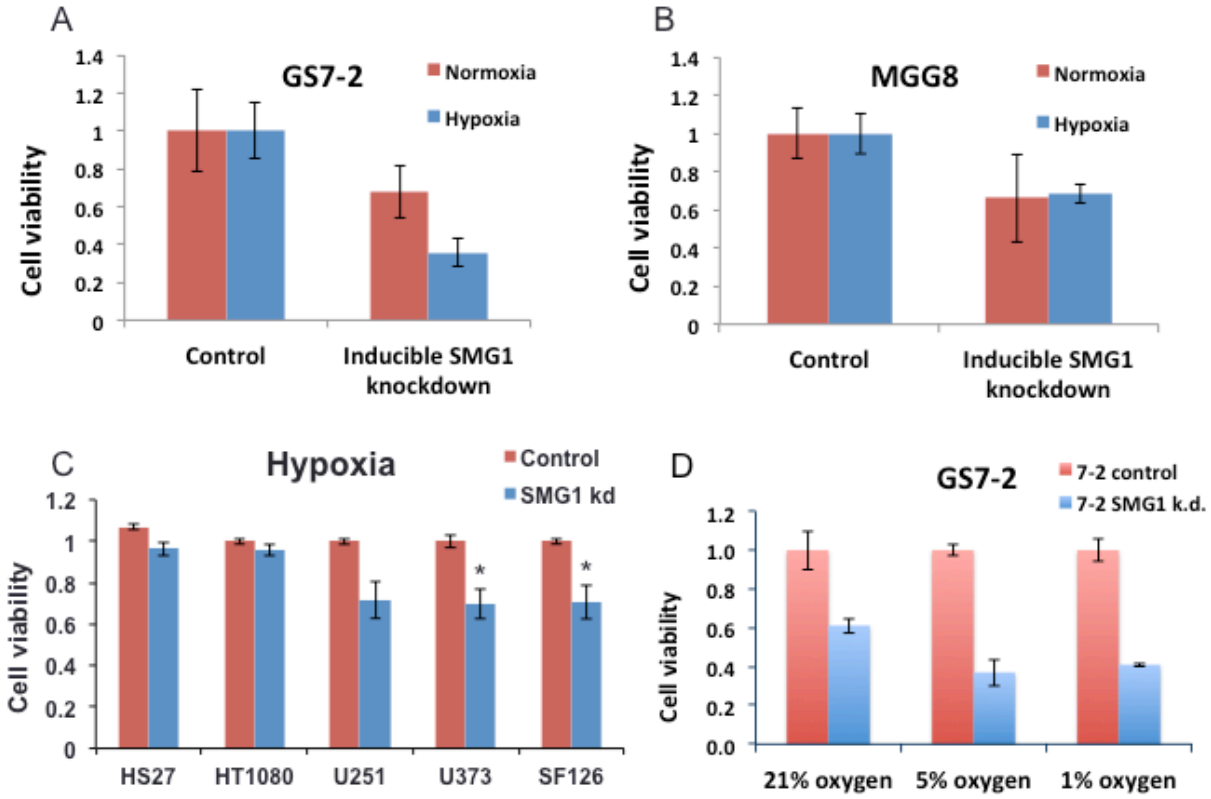

Fig S4.1. SMG1 knockdown has a cell-line and hypoxia sensitive growth inhibitory effect. A. GS7-2 and B. MGG8 cells were stably infected with doxycycline inducible shRNA hairpin for SMG1 and assayed for growth in 1% oxygen or 21% oxygen, with or without doxycycline treatment over 7 days. C. SMG1 knockdown does not inhibit growth of normal fibroblast, HT1080, or serum glioma lines, U251, U373 or SF126. * denotes p value less than 0.05. Student's two-tailed t-test; bars S.D. D. SMG1 knockdown leads to preferential growth inhibition under 5% oxygen as well as 1% oxygen.

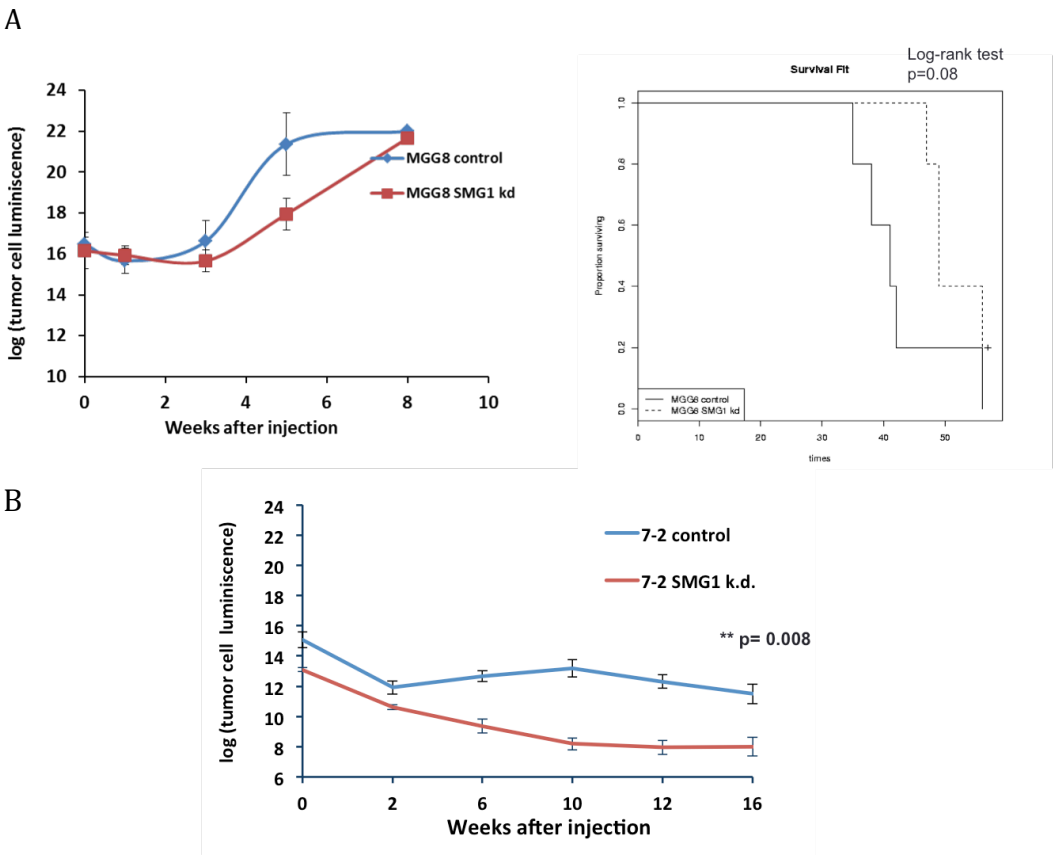

Fig S4.2. SMG1 knockdown alone does not significantly improve prognosis in GSC mouse xenografts. A. Control or shSMG1 infected MGG8 luciferase expressing were monitored in mice using bioluminescence IVIS imaging over 10 weeks or until the mice died. Kaplan Meier survival curve shows minimal improvement in survival benefit when SMG1 is knocked down, as compared to control, p=0.08. B. In-vivo growth rate of SMG1 knocked-down GS7-2 luciferase tumor cells is significantly lower than control, as monitored by bioluminescent IVIS imaging in mice over 16 weeks, p=0.008.

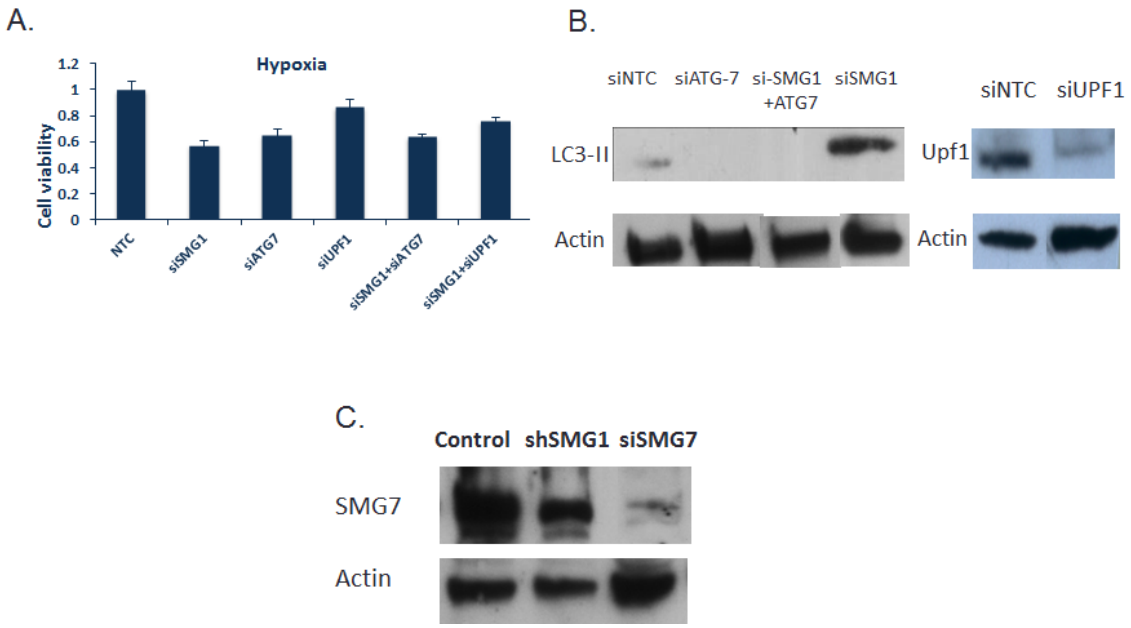

Fig S4.3. Role of NMD and autophagy in SMG1 mediated GSC growth inhibition. A. Upf1 or ATG7 knockdown does not rescue GS7-2 growth inhibition under hypoxia. B. siUpf1 and siATG7 depletes Upf1 and LC3-II proteins respectively. C. SMG7 protein level is reduced upon knockdown of SMG1 and gets depleted upon SMG7 knockdown.

DNA damage response elements	Positive regulators	Conditions for positive regulation	Negative regulators	Conditions for negative regulation	Reference
DNA strand breaks	Hypoxia, TMZ				(Hammond et al. 2002);(Ito et al. 2013).
ATM	DNA strand breaks		ATM inhibitor		(Gewandter et al. 2011)
ATR	DNA strand breaks		ATR inhibitor		(Fallone et al. 2013)
Rep fork stall	ATM, ATR				
Chk1	rep fork stall	if ATR active	Chk1 inhibitor		(Matsuoka et al. 2000)
Chk2	rep fork stall	if ATM active	Chk2 inhibitor		(Gibson et al. 2005)
UPF1	DNA replication,	When SMG7 is	UPF1 inhibition		Fig 4.6, (Popp and

	Hypoxia, UPF1 phosphorylation	active			Maquat 2014)
UPF1 phosphorylation	ATR, SMG1	When UPF1 is active			(Azzalin and Lingner 2006); (Popp and Maquat 2014)
p-p53	ATM, ATR, Chk2		SMG1, Hif-1 alpha		(Matsuoka et al. 2000); (Lee et al. 2012) Fig 4.5
Apoptosis	p-p53				(Schuler et al. 2000; Kumari et al, 1998)
Replication fork continuation	Chk1 Chk2 Upf1	When rep fork stall is active When Chk1			(Smith et al. 2010).; (Azzalin and Lingner

		and rep fork stall is active When ATR and rep fork stall is active			2006)
p21	p-p53				(Matsuoka et al. 2000), fig 4.5B.
Cell cycle arrest	p21				(Matsuoka et al. 2000)
S phase continuation	DNA replication, Hypoxia response genes, replication fork continuation		Cell cycle arrest, Replication fork stall	When replication fork continuation is inactive	(de Oliveira et al. 2009)

Cell_growth	S_phase_cont		Apoptosis, autophagy		(Villalonga-Planells et al. 2011);(Wengrod et al. 2013a)

Table S4.1.DDR pathway regulators. The nodes involved in DDR pathway with their positive and negative regulatory relationships and sources are listed.

Nonsense mediated decay elements	Positive regulators	Conditions for positive regulation	Negative regulators	Reference
PTC	Hypoxia, TMZ			
SMG1	DNA replication, PTC		SMG1 inhibition	(Gewandter et al. 2011)
UPF1	DNA replication, Hypoxia, UPF1 phosphorylation	When SMG7 is active	UPF1 inhibition	Fig 4.6, (Popp and Maquat 2014)

UPF1 phosphorylation	ATR, SMG1	When UPF1 is active		(Azzalin and Lingner 2006); (Popp and Maquat 2014)
SMG7	PTC	SMG7 inhibitor	SMG7 kd	(Popp and Maquat 2014); Fig 4.6
Nonsense mediated mRNA decay	Upf1 phosphorylation	When PTC is active	Hypoxia	(Popp and Maquat 2014); Fig 4.6
mRNA_degrade	NMD_path			Fig 4.6
Autophagy	PTC	When nonsense mediated mRNA decay is inactive		(Wengrod et al. 2013a); Fig 4.6
Cell_growth	S_phase_cont		Apoptosis,	(Villalonga-

			autophagy	Planells et al. 2011, Wengrod et al. 2013a)

Table S4.2.NMD pathway regulators. The nodes involved in NMD pathway are listed with their positive and negative regulatory relationships and sources are listed.

Hypoxia inducible elements	Positive regulators	Conditions for positive regulation	Negative regulators	Conditions for negative regulation	Reference
Hif-1 alpha	ATM, ATR, hypoxia, p300		SMG1 inhibition (dominant)		(Fallone et al. 2013); (Chen et al. 2009)
p300	ERK				(Chen et al. 2009)
ERK	Hypoxia		SMG1	When ERK is active	(Chen et al. 2009)
Hypoxia response genes	HIF-1 alpha				(Chen et al. 2009)

S phase continuation	DNA replication, Hypoxia response genes, replication fork continuation		Cell cycle arrest, Replication fork stall	When replication fork continuation is inactive	(de Oliveira et al. 2009)
Cell_growth	S_phase_cont		Apoptosis, autophagy		(Villalonga-Planells et al. 2011); (Wengrod et al. 2013a)

Table S4.3.Hypoxia inducible pathway regulators. The nodes involved in hypoxia inducible pathway are listed with their positive and negative regulatory relationships and sources are listed.

Chapter 5

Discussion

5.1. Regulation of the JMJD3 (KDM6B) histone demethylase in glioblastoma stem cells by STAT3

We have shown that STAT3 is required for GBM stem cell growth, neurosphere formation and stem cell marker expression. Transient STAT3 inhibition for as little as 4 hours has an irreversible inhibitory effect on neurosphere formation, suggesting an epigenetic mechanism of action. Consistent with this, we found that STAT3 represses the H3K27 demethylase JMJD3. JMJD3 expression decreases neurosphere formation and proliferation, whereas JMJD3 knockdown rescues this sphere formation phenotype. STAT3 regulates multipotency of GSC by repressing neuronal differentiation specific genes like MYT1, FGF21 and GDF15. In summary, I have found that STAT3 is a critical regulator of GBM-SC multipotency, and that targeting STAT3 signaling pathway may be therapeutic in glioblastoma. STAT3 does this by inducing histone demethylase expression, which are instrumental in controlling the balance between GSC self-renewal and differentiation by regulating H3K27 trimethylation.

Based on the observation that STAT3 inhibition has a rapid and irreversible effect on GSC growth, we hypothesized that STAT3 exerts an epigenetic effect that can change the chromatin at multiple promoters in a stable fashion. We investigated histone demethylases as potential STAT3 target genes since they play an important role in normal as well as oncogenic growth and differentiation. Polycomb-mediated repression often maintains multipotency of normal neural stem cells and GSC by regulating tissue-specific gene expression. We focused on the H3K27me3/2 demethylase JMJD3 due to a rapid upregulation of JMJD3 mRNA and protein levels upon STAT3 inhibition. JMJD3 is also upregulated during GBM-SC differentiation, implying that repressive H3K27me3

marks must be removed before transcription of differentiation genes can be activated. We have found that STAT3 interacts directly with the JMJD3 promoter, suggesting that JMJD3 is a direct STAT3 target gene. JMJD3 has been identified as a STAT3 occupied gene in ES cells, which is consistent with our results (Kidder et al. 2008). While STAT3 is best known as a transcriptional activator, we showed that it represses JMJD3. A few earlier studies have also provided evidence that STAT3 acts as a repressor of the cell cycle regulator p21, for example (Fukada et al. 1998; Rokavec et al. 2014). ChIP-ChIP and microarray studies suggest that STAT3 represses genes in multiple cell types (Dauer et al. 2005; Kidder et al. 2008). Our findings suggest recruitment or stabilization of the NCoR repressor complex at the JMJD3 promoter, as a likely mechanism of repression. Previous studies in murine neural stem cells indicated that JMJD3 is repressed by the NCoR and SMRT nuclear co-repressors for the retinoic acid (RA) receptor (Jepsen et al. 2007). In fact, deletion of SMRT/NCoR or exogenous RA relieves this repression. RA as well as JMJD3 can induce neural differentiation of ES or neural stem cells (Okada et al. 2004; Jepsen et al. 2007). We also found that RA can induce JMJD3 expression in GSC, which is consistent with the involvement of the SMRT/RAR complex in JMJD3 repression in our cells. In addition, it was recently shown that inhibiting JMJD3 delayed RA-induced differentiation of human embryonal carcinoma cell line (Kang et al. 2015). While Ene et al (2012) have found evidence that DNA methylation can also contribute to JMJD3 repression, the sites of that STAT3 binds to appear to be distinct from the regions of DNA methylation (Ene et al. 2012). Preliminary methylation-specific PCR (MS-PCR) did not show differences in DNA methylation at JMJD3 when STAT3 was inhibited.

However, given recent evidence that STAT3 can control DNA methylation (Lee et al. 2012), this mechanism of regulation merits further investigation.

This thesis adds to the repertoire of studies showing a complex context-dependent function of aberrant H3K27 trimethylation in several cancers (Ntziachristos et al., 2014; Yamaguchi and Hung, 2014). While induction and maintenance of H3K27me3 mark is pro-oncogenic in medulloblastoma and adult glioblastomas (Zhang et al. 2015; Suvà et al. 2009; Kim et al. 2013; Robinson et al. 2012), global loss of H3K27 methylation is oncogenic in pediatric gliomas (Bender et al., 2013; Venneti et al., 2013). Deep sequencing efforts revealed somatic mutations in H3F3A (affecting lysine (K27) or glycine (G34) residue) in 30% pediatric GBMs and 70% pediatric diffuse intrinsic pontine gliomas, which are associated with poor clinical outcome (Wu et al. 2012; Sturm et al. 2012). Both these gain-of-function histone H3.3 mutations were shown to reprogram the epigenomic and genomic landscape to drive gliomagenesis. While H3.3G34 mutants altered H3K36me3 binding (Bjerke et al. 2013), H3.3K27 mutants are dominant negative inhibitors of PRC2 that result in global reduction in repressive H3K27me3 (Lewis et al. 2013; Venneti et al. 2013; Bender et al. 2013). Restoration of H3K27me3 levels in H3.3K27 mutant pediatric glioma lines by a JMJD3 inhibitor, GSKJ4, significantly reduced their growth and tumorigenicity (Hashizume et al. 2014). However, H3K27 mutations are rare in other forms of cancer, including adult GBMs, thereby suggesting a highly context specific tumorigenic role for loss of H3K27 trimethylation.

Mutation independent anomalies in epigenetic modifiers were also tumorigenic in adult GBM. EZH2 overexpression is necessary for the self-renewal of GSC (Suva et al.,

2009), while inactivating mutations in the H3K27 demethylase UTX (KDM6A) has a tumor-suppressor effect in adult GBM (van Haaften et al., 2009). Studies have shown the role of EZH2 in maintaining growth and tumorigenesis of GSC by regulating c-myc (Suvà et al. 2009), cell cycle genes (Zhang et al. 2015) and other neural developmental genes (K. Zhang et al. 2015; Suvà et al. 2009; Kim et al. 2013; Robinson et al. 2012). In addition, EZH2 is co-regulated in a positive feedback loop with β-catenin/TCF4 or STAT3 pathway, which can transform GSC into a more aggressive mesenchymal phenotype (J. Zhang et al. 2015). Along similar lines, Kim et al. had found that EZH2 mediated methylation of STAT3 led to enhanced STAT3 phosphorylation and activity, thereby promoting GSC tumorigenicity (Kim et al. 2013). Concurrently, we hereby show that STAT3 negatively regulates the histone H3K27 demethylase, JMJD3 expression, and thereby maintains GSC growth and self-renewal. Another recent finding from Ene et al. (2012) in adult GBM stem cells supported our findings, showing induction of histone H3K27 demethylase JMJD3 and concomitant reduction in H3K27me3 during GSC differentiation. In fact, JMJD3 overexpression remarkably reduced self-renewal and tumorigenicity of GSC (Ene et al. 2012). In another study, GSC differentiation corresponded to lower levels of mixed lineage leukemia-5 (MLL5) and higher levels of H3K4me3 and H3.3 variant associated with transcriptionally active regions (Gallo et al. 2015). While STAT3 inhibition did not change global H3K27me3 levels and MLL5 gene expression in our GSC lines, these results warrant investigation of H3K4me3 or H3.3 variant in our cells to negate the possibility of cell-line specific effects. Gallo et al. (2015) found that MLL5 upregulation tended to co-occur with upregulation of JMJD3 and UTX. These investigators also found that GSK-J4 mediated inhibition of JMJD3 and UTX was

shown to reduce the self-renewal of GSC. This was in the opposite direction to our study and Ene et al. (2011) study, whereby overexpression of JMJD3 reduced self-renewal of stem-like neurospheres isolated from adult GBM. However, GSK-J4 has nonspecific inhibitory effects on other Jumanji domain family members (Heinemann et al. 2014), which complicate interpretation of the results observed by Gallo et al. (2015). In the future, levels of other Jumanji family members and related epigenetic and transcriptional changes need to be assessed to resolve such context-dependent anomalous histone H3 mediated effects. The differences observed may be simply due to differences in the cell lines studied. Expression of the dominant negative histone H3.3K27 mutation in adult GBM-SC may shed light on the effect of H3K27me3 in the context of adult GSC lines.

Future directions:

We and others have reported aberrant activation of STAT3 in GBM (Konnikova et al. 2005; Sherry et al. 2009) that was subsequently suggested to be one of the master regulators that drive aggressive mesenchymal transformation in GBM (Carro et al. 2010; Zhang et al. 2013). Given the role of STAT3 in GBM stem cells, it will be intriguing to assess whether STAT3 activation status can be used prognostically to distinguish GBM tumors that generate stem-like neurospheres in culture and be associated with poor patient outcomes. Our data that transient STAT3 inhibition for as little as 4 hours irreversibly depletes neurosphere formation capacity of GSC strengthens the argument that STAT3 inhibition could be effective therapeutically.

Induction of a long-term, irreversible loss of neurosphere formation and GBM stem cell phenotype suggests an epigenetic mechanism of action by STAT3. This is consistent with studies in breast cancer that provided evidence for stable transformation of MCF10A breast cells by STAT3 target genes (Iliopoulos et al. 2010). Tamoxifen treatment activates STAT3 in MCF10A cells, which then regulates the expression of microRNAs, miR-21 and miR-181-B, to induce stable transformation of the cells. This transformed state persists beyond the expression of the microRNAs, suggesting an epigenetic mechanism of action. We have found that maintenance of CSC phenotype by STAT3 is at least partially mediated by JMJD3 repression, as knockdown of JMJD3 in STAT3 inhibited cells rescues the sphere inhibition phenotype in a dose dependent manner. Thus, JMJD3 induction following STAT3 inhibition has the capacity to regulate target genes to reprogram GSC chromatin. These findings are consistent with the findings that STAT3 is essential to maintain ES cell pluripotency and promote iPS cell reprogramming by its regulation of the reprogramming transcription factors c-myc, Klf-4, Oct4 and Nanog, among others (Ko et al. 2006; Yang et al. 2010; Tang et al. 2012). There is also evidence that STAT3 can regulate other epigenetic modifiers, like JMJD1a and Eed in murine ES cells (Ura et al. 2008; Ko et al. 2006).

In order to confirm that JMJD3 upregulation leads to the demethylation of specific target gene promoters, we performed chromatin immunoprecipitation (ChIP) using an antibody to H3K27me3. Myt1 was one of the first human polycomb targets to be described, with a known role in neural differentiation, so it is a plausible JMJD3 target in GSC (Romm et al. 2005; Sarma et al. 2008). We found a consistent decrease in H3K37me3 at the Myt1 promoter correlating with JMJD3 expression upon STAT3

inhibition, however no upregulation in gene expression was observed by STAT3 inhibition alone. We showed that Myt1 gene induction requires additional transcription factor activated by BMP4 such as SMAD2. This is likely to be a widely applicable mechanism whereby JMJD3 causes histone demethylation of its target genes to remove repression and presumably open up the chromatin, but does not necessarily lead to gene activation. As in the case of Myt1, it is likely that additional transcriptional activators like SMAD2 are needed to induce expression of the JMJD3 target genes. In fact, genome wide ChIP experiments have shown that BMP4 activated SMADs are often associated with H3K27me3 marked genes in murine ES cells (Fei et al, 2010). This is analogous to the regulation of the GFAP promoter during neural development, in which both demethylation of the STAT3 binding site and the activation of STAT3 are necessary to activate gene expression (Takizawa et al. 2001). An immediate question is to confirm a similar mechanism in other transcription factor target genes from the ChIP-sequencing and microarray data, which lost H3K27me3 mark but did not get expressed upon STAT3 inhibition.

In order to identify differentiation specific genes induced upon the loss of GSC self-renewal following STAT3 inhibition, genome-wide ChIP-sequencing was combined with microarray analysis to identify neural lineage genes that underwent H3K27 demethylation as well as those that were induced upon STAT3 inhibition. Neural genes, FGF21 and GDF15, were confirmed to lose H3K27me3 mark as well as get induced upon STAT3 inhibition. Experimentally, we could ask whether upregulation of JMJD3 under conditions that favor the differentiation of neurons, astrocytes, or both, has an effect on the expression of Myt1, FGF21 and GDF15. In the future, there is need for validation of

plausible target genes involved in cell cycle, therapy resistance and immune response that exhibited gain of repressive H3K27me3 and are likely mediators of STAT3 in maintaining GSC tumorigenicity or mesenchymal transformation.

JMJD3 expression is not sufficient to completely recapitulate the effects of STAT3 inhibition in inducing differentiation specific genes, such as Myt1 or Beta-III-tubulin, suggesting that other direct STAT3 regulated genes also play a role maintaining GBM stem cells. In fact, STAT3 can also influence other epigenetic regulators, in addition to JMJD3. There is evidence that pluripotency and neural developmental genes are regulated by both JMJD3/UTX demethylase dependent as well as independent manner (Kang et al. 2015). A systematic analysis of the possible epigenetic alterations, such as histone H3 acetylation, H3K4 methylation, H3K9 methylation, and their regulators will help to identify other possible epigenetic mechanisms involved.

We showed that STAT3 also regulates JMJD3 in non-transformed neural stem cells, thereby implying a conserved mechanism of regulation in normal neural and glioblastoma stem cells. This is consistent with the role of STAT3 in maintaining self-renewal in normal stem cell types, including murine and human embryonic stem cells (Niwa et al. 1998) and induced pluripotent cells (iPS) (Tang et al. 2012). This may also explain why knockout of STAT3 is embryonic lethal (Takeda et al. 1997). While this could complicate therapeutic targeting of GBM stem cells without affecting normal neural stem cells, it provides further evidence of a widespread developmentally critical mechanism for maintaining self-renewal in both cancer stem cells and tissue stem cells in this case. Constitutive activation or deletion of STAT3 in the neural stem cell compartment of transgenic glioma mice model, like Mut7 model (Chen et al., 2012), will

help to answer if STAT3 activation is required or sufficient for transformation of neural stem cells. It has not been studied whether STAT3 inhibition has a differential effect on the quiescent stem cell population as opposed to the rapidly dividing progenitor stem cell population.

Consistent with our findings that STAT3 inhibition upregulates JMJD3 to inhibit GSC self-renewal, Ene et al. (2012) showed the therapeutic efficacy of JMJD3 overexpression in inhibiting tumorigenicity of GSC (Ene et al. 2012). Based on our results, it would also be interesting to use an inducible overexpression system to determine whether turning on JMJD3 expression in an established tumor can cause an inhibition or reduction in tumor size, or whether it would render the tumor more sensitive to chemotherapy and radiation. It would also be interesting to compare STAT3 inhibition in vivo in tumors initiated by control and shJMJD3 infected cells. If JMJD3 is necessary for the effects of STAT3 inhibition on tumorigenesis, then we would expect that JMJD3 knockdown would abrogate any improvement we may see with STAT3 inhibition.

While this work focused on the mechanism behind a sustained inhibition of GSC neurosphere formation upon transient STAT3 inhibition, our lab has previously demonstrated the in vivo therapeutic role of targeting STAT3 to block tumor initiation and maintenance. Our in vitro results are consistent with the findings of Wang et al, showing a significant increase in survival when Stat3 signaling was inhibited by anti IL-6 treatment in GSC xenograft tumors (Wang et al. 2009). Consistent with our findings that STAT3 is required to maintain GSC self-renewal in vitro (Sherry et al. 2009), it was recently shown that activation of STAT3 signaling by bone marrow X-linked (BMX)

kinase (Guryanova et al. 2011) or FoxM1 transcription factor (Gong et al. 2015) was required for GSC self-renewal and tumorigenesis (Guryanova et al. 2011). Interestingly, the expression of BMX and its effect on STAT3 activation is specific to GSC, but not the neural progenitor cells or bulk tumor cells, thus making it a selective target upstream of STAT3.

However, it may be possible to limit toxicity of STAT3 targeted therapy by using fewer doses of the inhibitor. We found that transient STAT3 inhibition to permanently arrest the growth of GSC, which has the potential to produce a significant clinical benefit with very few doses of a STAT3 inhibitor. Intracerebral delivery techniques to limit STAT3 inhibitor concentration to the area surrounding the tumor could also limit potential neural stem cell toxicity. Additionally, tumor hypoxia can increase STAT3 activation, which may enhance the effectiveness of STAT3 targeted therapy (Kang et al. 2010). Others have recently reported that STAT3 inhibition in GBM-SC may enhance the anti-tumor immune response (Wei et al. 2010). Conditioned media from GSC inhibited T cell proliferation and cytokine release, and inhibition of STAT3 in the GSC by RNAi diminished this effect (Wei et al. 2010). Thus, inhibiting STAT3 may have the added benefit of increasing the anti-tumor immune response, in addition to its anti-proliferative effect on GBM stem cells. STAT3 inhibition might be more effective in combination with chemotherapy to target the rapidly dividing bulk tumor cells as has been shown in other tumor types..

While STAT3 inhibition prolongs the survival of mice in a wide variety of tumor models, it and other SH2 domain-containing molecules are generally considered to be difficult targets for drug design and do not currently have a clinically tolerable inhibitor

available. Therefore, other members in the lab are working on inhibitors of JAK kinases which are required to activate STAT3 in GBM.. Several JAK inhibitors such as Ruxolitnib (JAK1/2) and Tofacitnib (JAK3) are FDA approved for treating myeloproliferative disorders and rheumatoid arthritis respectively and are fairly well tolerated in patients. Jak2 inhibitors, AZD 1480 and WP-1066, were shown to inhibit STAT3 activity and show favorable response in GBM mice model (Iwamaru et al. 2007; McFarland et al. 2011). However, it is not currently clear that which of the JAK kinases is actually crucial due to the non-specificity of the drugs used in these reports.

Conclusion

We have found that STAT3 regulates proliferation and multipotency of these cells by repression of the histone demethylase JMJD3. Our results suggest that inhibiting STAT3 removes repressive H3K27me3 mark from neural differentiation genes and makes their chromatin accessible to induction by additional transcription factors. We propose that targeting the STAT3 pathway inhibits the growth and self-renewal of GBM stem cells by driving them towards a neural differentiation phenotype. This work adds to the growing body of evidence that STAT3 signaling is important in a variety of human cancers.. It demonstrates a link between STAT3 signaling and aberrant regulation of H3K27 methylation, which is a developmentally critical epigenetic mechanism of cell fate regulation in both normal and tumor stem cells.

5.2. RNAi kinome targets in GBM stem cells

In order to identify additional druggable targets in GSC, an unbiased functional screen was conducted to identify kinases required for growth and survival of multiple

GSC lines. Kinases are very druggable targets and kinase inhibitors were the first successful targeted drugs to be approved for cancer therapy. Some examples are imatinib mesylate (Gleevec™) for treating BCR-Abl in chronic myelogenous leukemia (CML) and gastric stromal tumors and erlotinib for targeting EGFR in metastatic non-small cell lung cancer**.** Therefore, our screen focused on identifying kinases essential for GBM growth and survival since they are important mediators of many signaling pathways and are readily amenable to drug inhibition, thereby making them ideal candidates for developing cancer therapeutics (Knight et al. 2010). Growth inhibition was determined by arrayed lentiviral shRNA screening in order to provide increased sensitivity and direct identification of shRNAs for follow-up without the need for postscreen deconvolution (Moffat et al. 2006). A stringent hit selection method based on median average deviation (MAD) analysis was used to minimize the effect of outliers on hit selection under both normoxic and hypoxic conditions (Chung et al, 2008). An additional stringency measure of at least 50% growth inhibition relative to control was applied to select hits that result in biologically meaningful phenotypes as well as statistically significant hits. Strong oxygen condition sensitive hits were selected by requiring a > 2 z* score distance between inhibition under normoxia and hypoxia for the same shRNA. Although these criteria minimized false positive hits, it is possible to miss some true positive hits due to the stringent selection criteria or inefficient knockdown of the kinases by the shRNA hairpins. This might be the reason that the SMG1 kinase was not identified as a hit in the full kinome screen, but was identified from a pilot screen to be a hypoxia sensitive hit in GS7-2 cells using a different assay method that was noisier than the modified prestoblue assay used for the full kinome screen.

Overall, our screen identified some genes consistent with previous studies as well as some novel hits for GBM stem cells. A number of genes, ERBB3, CDK6, KDR, PLK1 and CHK1 previously known to be involved in gliomagenesis were identified as common hits to all 3 GBM-SC screened through our unbiased screening approach. , This demonstrated the fidelity of our screen findings as well as commonality of some tumor cell kinase addictions in GBM-SC.. Some of the kinase hits identified in our screen, such as PLK1, AURKA, AURKB, CDK6, RPS6KA4, PRKAA1 and PRKDC, are members of the core essential or lethal human genes analyzed from previous loss-of-function screens in CRISPR screens of multiple tumor cell lines (Hart et al. 2015; Hart et al. 2014). These core essential genes are enriched for fundamental DNA replication, transcription, translation and protein degradation processes. Notably, SMG1 was found to be required in subset of our GBM stem cell lines likely due to its role in the nonsense mediated mRNA decay (NMD) - a process that also found in some core lethal genes. Thus, other proteins that take part in NMD, including UPF1, SMG7 and SMG8 were also identified as core essential genes found from screens in GBM as well as other cancers (Hart et al. 2015). A kinome siRNA screen in multiple myeloma cells also identified SMG1 as a common hit in multiple cell lines (Tiedemann et al. 2010). This is further evidence of the critical role of protein complexes involved in NMD and is consistent with our findings in GSC. However, not all the core essential kinase genes were identified as hits in our screen due to possibly due to inefficient knockdown or activation of redundant pathways in our cells.

The hits from our functional screen overlapped with the core pathways enriched in GBM (Cerami et al. 2010). A number of our hits, including EGFR, ERBB3, AKT1,

KDR, PDPK1, PKN1, MAP4K2 and MAP3K12 genes affect RTK/Ras/PI3K pathway. Another fraction of our hits, such as CHEK1, CDK6, PLK1, AURKB and AURKA genes, affect cell cycle control mediated by p53/Rb signaling. It should be noted that we found multiple hits from a given pathway in the same cell-line, indicating that a particular cell line is more susceptible to that signaling node. Some examples of potentially redundant hits are AURKA and AURKB, CDK4 and CDK6 in GS11-1; SIK1 and SIK2, PTK2 and PTK7 in GS6-22; RPS6KA3 and RPS6KA4, PLK1 and PLK4 in GS7-2. Interestingly, a global analysis of driver genes previously identified in most forms of cancer were found to affect a limited number of pathways that can be organized into three core cellular processes that are responsible for a selective growth advantage (**Fig 5.1**) (Vogelstein et al. 2013). A large number of the kinase targets identified from our screen belong to cell cycle/apoptosis and PI3K pathways and collectively affect cell survival. Some of our kinase hits, MAP3K12, STK39, CHEK1 and VRK2 affect the MAPK stress and DNA damage control pathways which are expected to contribute to genome maintenance. Some of our other hits also affected STAT (PIM1, BMX, TYK2), chromatin modification (MAP3K12, BRD2, CDKL5, VRK1), transcriptional regulation (UHMK1, BMP2K) and Notch and Hedgehog (BRD2, CSNK1A1, YES1) pathways that potentially affect GBM stem cell fate. However, enrichment of angiogenic pathways, including VEGF or HGF pathway, have not been identified as driver gene mutations in previous studies of GBM, but are implicated in GBM stem cells (Milkiewicz et al. 2006). Although mutations in the VEGF or HGF receptor might not be common in tumor cells, microenvironment cues like hypoxia can lead to aberrant downstream VEGF pathway activation (Glück et al. 2015; Kaur et al. 2005). Consistent with this, our

functional kinome screen conducted under hypoxia identified hits like KDR or MET, which affect angiogenesis, one of the key factors driving tumor progression. Although our screen used in vitro GSC neurospheres which did not necessarily model angiogenesis in the absence of a matrix or endothelial cell coculture, hypoxia has been previously shown to promote endothelial transdifferentiation of GSC and this may explain why they scored in our screen (Soda et al. 2011; Wang et al. 2010; Ricci-Vitiani et al. 2010).

Fig 5.1: Cancer cell signaling pathways and the cellular processes they regulate. All of cancer driver genes can be classified into one or more of 12 pathways as stated in the middle ring that confer a selective growth advantage (Vogelstein et al. 2013). These pathways can be subdivided into three core cellular processes depicted in the outer ring.

In addition to the hits identified from previous related screens or studies, our screen came up with several novel hits, including YES1, DDR1, CDKL5, PKN1 and TXK common to all 3 GSC lines. However, 75% of our hits were unique to a given cell line, demonstrating significant heterogeneity between the 3 GBM stem cell lines screened. This narrow spectrum of commonality in kinase dependency is in line with genetic heterogeneity observed in GBM tumors and there is also likely to be even greater epigenetic diversity (Ramkissoon et al. 2015). Importantly, 10 to 30% of the hits in each cell line varied under different oxygen levels, which directly demonstrated microenvironmental context dependent heterogeneity in the tumor cell response. None of the hypoxia sensitive hits were common between any 2 GSC lines screened. This raises the question of whether developing hypoxia sensitive inhibitors for a narrow spectrum of GBM patients will be commercially viable. The heterogeneity of the GSC lines and/or the low number of condition sensitive hits might explain this lack of common hypoxia sensitive hits. However, this result suggests that there might not be a common hypoxia resistance mechanism of GSC.

An important distinction of our study is that it is the first GBM RNAi screen conducted under hypoxia. This is therapeutically important since current treatment is believed to fail in part due to the inability to target resistant GBM stem cells which can survive tumor hypoxia and regenerate the tumor mass (Li et al. 2009; Heddleston et al. 2009; Méndez et al. 2010; Bar et al. 2010). Interestingly, our screen generated a number of potentially HIF independent hypoxia resistance mechanisms which might be critical in our GSC lines given the constitutive expression of HIF-1A and HIF-2A in some of our cells. The MAPK/ERK pathway genes, including stress kinases MAP3K12, MAP4K2

and STK39; and focal adhesion kinases, PTK2 and ROCK2, showed the strongest hypoxia sensitivity. Mitogen-associated protein kinases (MAPKs) constitute a HIF-independent alternative route for cell survival under hypoxia by eliciting stress response genes in both cancer cells (Blanco et al. 2007; Laderoute et al. 1999) and neurons (Park and Rongo 2016). MAPK/ERK is the most significantly enriched pathway in glioma (Ceccarelli et al. 2016) and may be a susceptible node that can be targeted in refractory GBM stem cells under hypoxia. Our screen also identified the well-known angiogenic response genes, KDR/VEGF-R2 and MET as hypoxia sensitive hits, presumably because hypoxia has been shown to push GSC towards endothelial lineage and increased stemness (Soda et al. 2011; Bar et al. 2010). Our findings also show that CDC2L1 and BMX kinases, which were previously implicated in multiple myeloma and GBM respectively (Guryanova et al. 2011; Tiedemann et al. 2010), are required in our cells only under normoxic conditions. Thus, drugs that target these kinases might fail to inhibit the stem cells in hypoxic areas of the tumor.

The results presented in this thesis confirm that SMG1 kinase is a cell-line specific and hypoxia enriched hit. 15% of metastatic breast cancer lines show SMG1 gene amplification, implicating its broad role as an oncogene (cbioportal.com). Of the 7 GSC lines tested, SMG1 showed significant hypoxia sensitive growth inhibition in only 2 GSC. More GSC lines will be screened in future to identify cell lines that are inhibited by SMG1 inhibition. Genetic characterization of the cell lines differentially responsive to SMG1 inhibition under hypoxia will be helpful to identify specific lines sensitive to anti-SMG1 therapy. Interestingly, we showed that SMG1 inhibition sensitizes all of the GSC lines tested to the current standard of care, temozolomide (TMZ). Identifying targets for

combination therapy with TMZ is a widely explored avenue to enhance its therapeutic window (Prados et al. 2009; Ramirez et al. 2015; Nadkarni et al. 2012) and motivates the development of SMG1 specific inhibitors to test its efficacy in the clinic (Gopalsamy et al. 2012). I investigated the mechanism behind enhanced growth inhibition by SMG1 under hypoxia or TMZ combinatorial therapy, using computational modeling of context-dependent SMG1 signaling network. My findings showed that the classical nonsense mediated mRNA decay process is an important target for GBM stem cell resistance to cellular stress, including hypoxia as well as DNA damage induced by TMZ.

We hereby report the first such screen done in GBM stem cells under hypoxia to study survival mechanisms of GBM stem cells under limiting oxygen conditions. The kinase dependencies identified in this GSC screen constitute important therapeutic targets for the development of kinase inhibitors. A previous siRNA kinome screen identified key kinases of the MAPK pathway, ERK1 and MAPK3K1, as positive regulators of HIF-1 activity in HELA cells when exposed to hypoxia overnight (Chen et al. 2009). This raises the possibility that the loss of MAPK pathway kinases, identified as hypoxia sensitive hits from our screen, could inhibit GSC growth under hypoxia by restricting HIF-induced tumorigenic response. Intriguingly, an arrayed RNAi kinome screen performed in a colon cancer line identified GAK and IRAK4 kinases as novel HIF independent kinases responsible for cell survival under anoxic stress. Despite differences in cancer type and oxygen levels screened (0.1% vs 1%), some of the candidate anoxia kinases, MAP3K12, MET, PIM1 and SMG1, were also hypoxia sensitive in our GBM stem cells (Pan et al. 2013).

A limited number of high throughput RNAi screens have been recently performed to identify novel targets in glioma. A pooled shRNA kinase screen identified mitotic spindle factors, Bub1B and BugZ, as differentially essential for growth of GSC as compared to normal NSC (Toledo et al. 2014; Ding et al. 2013). Of the 48 kinase genes found to be differentially inhibitory in GSC in this screen, 8 of the kinase hits from all the 3 lines were common with our kinase hits in GSC. These include AURKB, PLK1, PTK2, ROR2, EPHA2, KDR and VRK2, and are therapeutically preferential targets since they were not observed to be inhibitory to normal neural stem cells (Ding et al. 2013). In addition, three of our common hits, CHEK1, PLK1 and AURKB, were part of a larger GBM-specific mitotic subnetwork constructed from TCGA samples (Ding et al. 2013). Another shRNA kinome wide screen identified the TRRAP adapter protein as an inducer of differentiation of GSC that reduced their tumorigenicity (Wurdak et al. 2010). TRRAP or Transformation/Transcription Domain-Associated Protein is a PIKK family protein, but not an active kinase, and is a relevant target in GBM through chromatin-related processes and cell cycle control. Although transcriptional regulation and cell cycle control processes were enriched from our hits, shRNA for the TRRAP gene was not included in our library. However, some of the other kinases identified by Wurdak et al. (2010) as differentiation inducing in GSC, such as NEK7, STK39, PRKACB and FLT, were identified as growth inhibitory kinases in our screen. Another study by Cheng et al. (2015) that combined transcriptomic expression analysis with kinome wide shRNA screening of mesenchymal and proneural GSC identified the receptor tyrosine kinase AXL as a differentially expressed target for reducing self-renewal and tumorigenicity of mesenchymal GSC, but was not identified as a hit in our screens (Cheng et al. 2015).

While sub-classification of our GSC lines is not known currently, some of our kinase hits, MET, ERBB3 and TGFBR2 were found to be highly expressed in mesenchymal GSC line 83 as compared to the proneural GSC line 528 used in this study. Two of our hits common to all the GSC lines screened, PKN1 and PLK1, were also previously identified in a RNAi screen in multiple myeloma (Tiedemann et al. 2010).

Some small molecule kinase inhibitor screens in glioma also identified hits in common with our screen. While CHK1 inhibition alone was lethal in the GSC lines we screened, small molecule inhibitors targeting CHK1 and PDK1 simultaneously showed a synergistic effect in GSC (Signore et al. 2014), while PLK1 was identified as a target in another chemical screen in GSC (Danovi et al. 2013). Such small molecule inhibitor screens are instrumental in identifying combination therapies for overcoming resistance to kinase inhibition. Future studies will aim to integrate findings from our RNAi kinome screening with kinase inhibitor library screening and gene expression profiles and genomic data to be able to predict the kinase dependency in specific cancer cells.

Future Directions

Overall, our unbiased screen identified kinases that can potentially be targeted to curb this extremely aggressive and refractory disease. Kinase targets that are effective in multiple GSC lines under both normoxic and hypoxic conditions need to be carefully validated. This is especially important to overcome inherent limitations of RNAi screen associated with variations in shRNA knockdown efficiencies and off-target effects. While Yes1 has been successfully validated to be a true hit in all 3 cell lines under both normoxia and hypoxia; the other novel hits common to all 3 cell lines, CDKL5, DDR1,

PKN1 and TXK need systematic follow-up. Cell cycle dependent kinase like-5 (CDKL5) is an especially interesting hit due to its potential role in regulating cell cycle arrest and promoting neuronal development (La Montanara et al. 2015; Valli et al. 2012; Leoncini et al. 2015). Moreover, CDKL5 mutations have been detected in primary gastric cancers and gastric cancer lines (Zang et al. 2011) and its role as a tumor-associated antigen makes it a target for immunotherapy in T-cell leukemia (Kawahara et al. 2007).

Finally, kinome screening should be performed in normal neural stem cell lines to attempt to identify therapeutic targets which can impair GBM stem cell growth without any effect on normal stem cells. It will also be interesting to assess differences in kinase dependencies between GBM stem cell lines and differentiated serum GBM lines. Therapeutic relevance of kinase dependency in GSC can be further verified by assessing their activation state in primary patient tumors. This is especially important for kinases, like SMG1, which are not found to be overexpressed or mutated in TCGA glioblastoma database, but might be activated due to enhanced DNA damage or nonsense codons in tumor cells.

Parallel screening of our GSC lines under normoxia and hypoxia puts us in a unique position to investigate novel resistance mechanisms of GSC under hypoxia and to identify targets that effectively inhibit these cells under hypoxia. It would be interesting to follow up unique hypoxia resistance mechanisms of the GSC lines screened by correlating specific genetic profiles of each line with its specific hypoxia or normoxia sensitive hits. Another future experiment would be to validate normoxia enriched hits, such as CDC2L1 or BMX, and investigate the mechanisms by which the drugs targeting these kinases might not function effectively under tumor hypoxic conditions. STK39 is

part of the stress response pathway and has been validated as a hypoxia sensitive hit in GS6-22 cells, warranting a thorough investigation of its underlying mechanism of action. Computational simulation of the various interacting signaling nodes that a kinase is involved in will help pave the way for such mechanistic studies. Importantly, we have pioneered integrating experimental approaches with a computational approach to generate hypotheses and then test them in the lab. We have used this approach to refine/train the computational model to represent the relevant mechanism of action of the kinase hit, SMG1, in the context of GBM stem cells. In the future, our Cell Collective model of SMG1 signaling could be expanded to include other mechanisms regulated by SMG1, including telomere maintenance and Staufen-1 mediated mRNA decay mechanisms (Chawla and Azzalin 2008; Cho et al. 2013). The contribution of two other PI3K family proteins that might play a redundant role as SMG1 in DNA damage, ATM and ATR, were also investigated. In the future, possible redundancies of DNA-PK or the mTOR family of proteins with SMG1 should be investigated. One of the challenges in identifying a critical kinase node is the activation of compensatory redundant pathways (Sun and Bernards 2014). Although STAT3 was the top pathway affected by our kinase hits, redundancy of upstream kinases might explain why only one the 4 JAK kinases scored as a hit in only one of the lines screened.

One of our immediate future plans is to perform RNA-sequencing analysis of the GSC tumor lines, GS6-22, GS7-2 and GS11-1, to correlate unique kinase dependencies in these cells to their gene expression and mutation profile. Detailed genotypic information of the cell lines may allow us to identify which tumor subtypes respond to cell line specific hits, like SMG1. For instance, the high throughput Oncomap platform has been

used to profile GBM tumors for actionable mutations in multiple oncogenes and tumor suppressors simultaneously and come up with customized therapy tailored for that tumor (Ramkissoon et al. 2015). Ultimately, many more GSC lines will need to be characterized to determine whether there are statistically significant correlations between kinase dependencies and GBM subtypes and genotypes.

In addition, epigenetic alterations in GBM stem cells have not been extensively studied. It will be informative to analyse specific changes in chromatin structure, histone modifications and DNA methylation that accompany a specific kinase dependency profile in each tumor line. Such systematic multiparametric analyses of each GSC line may allow us to associate essential kinases identified from the screen with specific gene mutations and expression, chromatin modifications, protein expression or metabolic changes. Information about the genetic diversity of GBM stem cell lines will be ultimately used to design customized therapies by targeting a specific combination of kinases unique to individual patient tumors based on their genetic, epigenetic, proteomic and metabolomic profiles. A future goal will be to build computer simulations to predict which tumors will be likely to respond to which specific kinase(s) inhibition, based on their molecular profile.

Although it is known that microenvironmental factors contribute to oncogenesis, context dependent changes in GBM tumor cells have not been well characterized. In particular, not much is known about genetic or epigenetic changes induced in GSC by hypoxia. Hypoxic cells have been reported to display a decrease in activating histone acetylation and a resultant global gene repression (Ramachandran et al. 2015). H3K9 hypoacetylation or HDAC1 upregulation under hypoxia led to reduced levels of tumor

suppressors, p53, BRCA1 and RAD51 and VHL, which translated to increased expression of HIF1 and VEGF. Additionally, hypoxia induced promoter hypermethylation and repressed the HIF target BNIP3 in pancreatic, colorectal and gastric cancer, thereby deregulating hypoxia-induced cell death (Ramachandran et al. 2015). In GBM, hypoxia was shown to regulate GSC self-renewal and tumorigenicity by inducing histone methyltransferase mixed-lineage leukemia 1 (MLL1) expression resulting in de-repression of HIF2alpha and its target genes (Heddleston et al. 2012). While our screen results have identified kinase vulnerabilities in GBM stem cells under hypoxia, further studies are needed to systematically identify and establish causality of epigenetic changes driving tumor cell adaptation to hypoxia. This can be accomplished by performing genome wide ChIP-sequencing and DNA pyrosequencing analysis to compare histone and DNA methylation changes in GSC between normoxia and hypoxia. These results can then be combined with multiparametric analysis to identify which of these epigenetic changes result in gene expression and protein changes. This will help to identify critical epigenetic regulators that play a functional role in GSC growth and survival under hypoxia. Such studies can even be done in combination with drug or radiation treatment to elucidate mechanisms of therapy resistance in GBM stem cells, which is prevalent under hypoxic conditions.

Inhibition of an essential kinases can create selective pressure for tumorigenic cells to acquire resistance to therapy. Resistance to kinase inhibitors can occur by mutation of the target kinase, disruption of negative regulatory mechanisms and activation of its downstream signaling or redundant pathways (Gross et al. 2015). EGFR inhibitors, erlotinib and gefitinib, failed in the clinic for GBM patients, in part due to

PI3K mediated resistance (Prados et al. 2009). In order to overcome resistance, combination therapies targeting multiple kinases in redundant signaling pathways or combination of kinase inhibitor with cytotoxic chemotherapy drugs need to be explored. As proof of principle, I showed that SMG1 kinase inhibition shows enhanced growth inhibition in the presence of TMZ treatment. RNAi kinome screening can be done in combination with chemotherapeutic drugs, like TMZ, to identify synergistic effects of kinase inhibition with drug treatment on a large scale. In addition, forward genetic screens like ours can be refined to determine synthetic lethality of gene pairs from our screen. Two genes are synthetically lethal if loss of function mutation of either alone does not compromise cell viability but mutating both leads to death (Bommi-Reddy et al. 2008). This can be tested by knocking down gene pairs by a combination of shRNAs in each well or screening specific knock-out cell lines. A systems approach is therefore needed to prioritize kinase target combinations and identify synthetic lethality type interactions for each tumor.

Chemical inhibitor screens can also help identify combinations of kinase co-dependency and synthetic lethality for essential kinases (Szwajda et al. 2015). Therefore, I have also been involved in a complementary kinase inhibitor screening approach using a GSK library to identify inhibitors and thereby kinases essential for the growth of our GBM stem cell lines. Although most of these inhibitors have multiple kinase targets that make it difficult to identify a specific kinase(s) addiction, preliminary analysis shows both common as well as unique hits from the two screening approaches. Future studies will aim to integrate high-throughput drug screening data,

comprehensive kinase inhibition data with mutation and gene expression profiles to predict kinase dependency in GSC.

To determine a more comprehensive list of other targets in GSC, other members of the lab have also performed genome wide pooled shRNA screens with a different shRNA library and confirmed SGK1 as a kinase hit common to both the pooled approach and arrayed approach. The major drawbacks for RNAi screens are false-positive hits due to off-target effects and false-negative hits due to inefficient knockdown by shRNA hairpins. The more recent clustered, regularly interspaced, short palindromic repeats (CRISPR) technology enable knockout screens in mammalian cells may be more sensitive than shRNA screens and has fewer off-target effects (Koike-Yusa et al. 2014). However, both CRISPR and RNAi screens yield false negative results, due to the lack of a high throughput method to confirm efficient knockdown of the target genes in the screening plates. Efforts are underway to screen the GSC with a inducible CRISPR knock-out library to identify additional genes whose complete deletion might affect gliomagenesis. As in the case of SMG1 gene knock-out, CRISPR technology can knockdown gene expression almost entirely and therefore cause a more drastic loss-of-function growth phenotype. This contrasts with the typically incomplete gene knockdown by shRNA that might have residual function and therefore show a weaker phenotype. (However, it should be noted that not all CRISPR guides result in complete elimination of gene expression of the target gene due to variable deletions and targeting efficiency). In the future, CRISPR mediated SMG1 knock-out mouse model or a transgenic heterozygous SMG1 deletion mouse model should be used to confirm the anti-

tumorigenic effects of the kinase. In conclusion, each screening technology has the potential to generate a unique set of hits, which can serve as novel candidate target genes.

Conclusion

RNAi screening in GSC yielded a number of genes known to be involved in gliomagenesis as well as novel hits, of which YES1 kinase has been validated to be inhibitory under both conditions in multiple GSC lines. Notably, 75% of the kinase hits were cell-line specific, thereby demonstrating the need for personalized therapy. In addition, 30% of kinase vulnerabilities were shown to vary according to microenvironmental oxygen conditions and potentially influence treatment efficacy. While the hypoxic hits can reveal critical hypoxia resistance mechanisms for GSC survival, targeting the normoxic specific hits might not be effective for targeting cells in the hypoxic regions of the tumor. A cell-line specific hypoxia sensitive hit, SMG1 kinase was validated and nonsense mediated mRNA decay was found to be an important oncogenic mechanism in GSC under cellular stress induced by hypoxia or TMZ. Thus, SMG1 and other kinases identified here are potentially important targets for the development of kinase inhibitors for treating GBM.

Bibliography

Abdouh, M., Facchino, S., Chatoo, W., Balasingam, V., Ferreira, J., and Bernier, G. (2009). BMI1 sustains human glioblastoma multiforme stem cell renewal. J Neurosci *29*, 8884-8896.

Adli, M., and Bernstein, B.E. (2011). Whole-genome chromatin profiling from limited numbers of cells using nano-ChIP-seq. Nature protocols *6*, 1656-1668.

Agger, K., Cloos, P.A., Christensen, J., Pasini, D., Rose, S., Rappsilber, J., Issaeva, I., Canaani, E., Salcini, A.E., and Helin, K. (2007). UTX and JMJD3 are histone H3K27 demethylases involved in HOX gene regulation and development. Nature *449*, 731-734.

Agger, K., Cloos, P.A., Rudkjaer, L., Williams, K., Andersen, G., Christensen, J. and Helin, K. 2009. The H3K27me3 demethylase JMJD3 contributes to the activation of the INK4A-ARF locus in response to oncogene- and stress-induced senescence. *Genes Dev* 23(10), pp. 1171–1176.

Agherbi, H., Gaussmann-Wenger, A., Verthuy, C., Chasson, L., Serrano, M., and Djabali, M. (2009). Polycomb mediated epigenetic silencing and replication timing at the INK4a/ARF locus during senescence. PLoS One *4*, e5622.

Ailles, L.E. and Weissman, I.L. 2007. Cancer stem cells in solid tumors. *Curr Opin Biotechnol* 18(5), pp. 460–466.

Akizu, N., Estarás, C., Guerrero, L., Martí, E. and Martínez-Balbás, M.A. 2010. H3K27me3 regulates BMP activity in developing spinal cord. *Development (Cambridge, England)*.

Asano, H., Aonuma, M., Sanosaka, T., Kohyama, J., Namihira, M., and Nakashima, K. (2009). Astrocyte differentiation of neural precursor cells is enhanced by retinoic acid through a change in epigenetic modification. Stem Cells *27*, 2744-2752.

Azzalin, C.M. and Lingner, J. 2006. The human RNA surveillance factor UPF1 is required for S phase progression and genome stability. *Curr Biol* 16(4), pp. 433–439.http://f1000.com/work/bibliography/1154918

Bagci-Onder, T., Wakimoto, H., Anderegg, M., Cameron, C. and Shah, K. 2011. A dual PI3K/mTOR inhibitor, PI-103, cooperates with stem cell-delivered TRAIL in experimental glioma models. *Cancer Res* 71(1), pp. 154–163.http://f1000.com/work/bibliography/530845

Bao, S., Wu, Q., McLendon, R.E., Hao, Y., Shi, Q., Hjelmeland, A.B., Dewhirst, M.W., Bigner, D.D. and Rich, J.N. 2006. Glioma stem cells promote radioresistance by preferential activation of the DNA damage response. *Nature* 444(7120), pp. 756–760.

Bao, S., Wu, Q., Sathornsumetee, S., Hao, Y., Li, Z., Hjelmeland, A.B., Shi, Q., McLendon, R.E., Bigner, D.D. and Rich, J.N. 2006. Stem cell-like glioma cells promote tumor angiogenesis through vascular endothelial growth factor. *Cancer Res* 66(16), pp. 7843–7848.

Bao, S., Wu, Q., Sathornsumetee, S., Hao, Y., Li, Z., Hjelmeland, A.B., Shi, Q., McLendon, R.E., Bigner, D.D. and Rich, J.N. 2006. Stem cell-like glioma cells promote tumor angiogenesis through vascular endothelial growth factor. *Cancer Res* 66(16), pp. 7843–7848.http://f1000.com/work/bibliography/531019

Bar EE, Lin A, Mahairaki V, Matsui W, Eberhart CG. Hypoxia increases the expression of stem-cell markers and promotes clonogenicity in glioblastoma neurospheres. Am J Pathol. 2010 Sep;177(3):1491–1502.

Barradas, M., Anderton, E., Acosta, J.C., Li, S., Banito, A., Rodriguez-Niedenführ, M., Maertens, G., Banck, M., Zhou, M.M., Walsh, M.J., Peters, G. and Gil, J. 2009. Histone demethylase JMJD3 contributes to epigenetic control of INK4a/ARF by oncogenic RAS. *Genes Dev* 23(10), pp. 1177–1182.

Bartkova, J., Hamerlik, P., Stockhausen, M.-T., Ehrmann, J., Hlobilkova, A., Laursen, H., Kalita, O., Kolar, Z., Poulsen, H.S., Broholm, H., Lukas, J. and Bartek, J. 2010. Replication stress and oxidative damage contribute to aberrant constitutive activation of DNA damage signalling in human gliomas. *Oncogene* 29(36), pp. 5095–5102.

Beier, D., Hau, P., Proescholdt, M., Lohmeier, A., Wischhusen, J., Oefner, P.J., Aigner, L., Brawanski, A., Bogdahn, U. and Beier, C.P. 2007. CD133(+) and CD133(-) glioblastoma-derived cancer stem cells show differential growth characteristics and molecular profiles. *Cancer Res* 67(9), pp. 4010–4015.

Beier, D., Schulz, J.B. and Beier, C.P. 2011. Chemoresistance of glioblastoma cancer stem cells--much more complex than expected. *Mol Cancer* 10, p. 128.http://f1000.com/work/bibliography/58821

Belgrader P, Maquat LE. Nonsense but not missense mutations can decrease the abundance of nuclear mRNA for the mouse major urinary protein, while both types of mutations can facilitate exon skipping. Mol Cell Biol. 1994 Sep;14(9):6326–6336.

Bender, S., Tang, Y., Lindroth, A.M., Hovestadt, V., Jones, D.T., Kool, M., Zapatka, M., Northcott, P.A., Sturm, D., Wang, W*., et al.* (2013). Reduced H3K27me3 and DNA hypomethylation are major drivers of gene expression in K27M mutant pediatric high-grade gliomas. Cancer Cell *24*, 660-672.

Bergers, G. and Benjamin, L.E. 2003. Tumorigenesis and the angiogenic switch. *Nat Rev Cancer* 3(6), pp. 401–410.http://f1000.com/work/bibliography/661817

Bhat, K.P., Balasubramaniyan, V., Vaillant, B., Ezhilarasan, R., Hummelink, K., Hollingsworth, F., Wani, K., Heathcock, L., James, J.D., Goodman, L.D., Conroy, S., Long, L., Lelic, N., Wang, S., Gumin, J., Raj, D., Kodama, Y., Raghunathan, A., Olar, A., Joshi, K., Pelloski, C.E., Heimberger, A., Kim, S.H., Cahill, D.P., Rao, G., Den Dunnen, W.F., Boddeke, H.W., Phillips, H.S., Nakano, I., Lang, F.F., Colman, H., Sulman, E.P. and Aldape, K. 2013. Mesenchymal differentiation mediated by NF-κB promotes radiation resistance in glioblastoma. *Cancer Cell* 24(3), pp. 331–346.

Bhinder, B. and Djaballah, H. 2013. Systematic analysis of RNAi reports identifies

dismal commonality at gene-level and reveals an unprecedented enrichment in pooled shRNA screens. *Comb Chem High Throughput Screen* 16(9), pp. 665–681.

Bibliography

Bjerke, L., Mackay, A., Nandhabalan, M., Burford, A., Jury, A., Popov, S., Bax, D.A., Carvalho, D., Taylor, K.R., Vinci, M., Bajrami, I., McGonnell, I.M., Lord, C.J., Reis, R.M., Hargrave, D., Ashworth, A., Workman, P. and Jones, C. 2013. Histone H3.3. mutations drive pediatric glioblastoma through upregulation of MYCN. *Cancer Discov* 3(5), pp. 512–519.http://f1000.com/work/bibliography/77412

Blanco, S., Santos, C. and Lazo, P.A. 2007. Vaccinia-related kinase 2 modulates the stress response to hypoxia mediated by TAK1. *Mol Cell Biol* 27(20), pp. 7273–7283.

Bol, D., and Ebner, R. (2006). Gene expression profiling in the discovery, optimization and development of novel drugs: one universal screening platform. Pharmacogenomics *7*, 227–235Anon p53, the Cellular Gatekeeper Review for Growth and Division.

Bommi-Reddy, A., Almeciga, I., Sawyer, J., Geisen, C., Li, W., Harlow, E., Kaelin, W.G. and Grueneberg, D.A. 2008. Kinase requirements in human cells: III. Altered kinase requirements in VHL-/- cancer cells detected in a pilot synthetic lethal screen. *Proc Natl Acad Sci U S A* 105(43), pp. 16484–16489.http://f1000.com/work/bibliography/59131

Bonni, A., Sun, Y., Nadal-Vicens, M., Bhatt, A., Frank, D.A., Rozovsky, I., Stahl, N., Yancopoulos, G.D., and Greenberg, M.E. (1997). Regulation of gliogenesis in the central nervous system by the JAK-STAT signaling pathway. Science *278*, 477-483.

Bracken, A.P., and Helin, K. (2009). Polycomb group proteins: navigators of lineage pathways led astray in cancer. Nature reviews *9*, 773-784.

Bromberg, J., and Darnell, J.E., Jr. (2000). The role of STATs in transcriptional control and their impact on cellular function. Oncogene *19*, 2468-2473.

Bromberg, J.F., Horvath, C.M., Besser, D., Lathem, W.W. and Darnell, J.E. 1998. Stat3 activation is required for cellular transformation by v-src. *Mol Cell Biol* 18(5), pp. 2553–2558.http://f1000.com/work/bibliography/320553

Bromberg, J.F., Horvath, C.M., Besser, D., Lathem, W.W., and Darnell, J.E. (1998). Stat3 activation is required for cellular transformation by v-src. Mol Cell Biol *18*, 2553–2558.

Brumbaugh KM, Otterness DM, Geisen C, Oliveira V, Brognard J, Li X, et al. The mRNA surveillance protein hSMG-1 functions in genotoxic stress response pathways in mammalian cells. Mol Cell. 2004 Jun 4;14(5):585–598.

Burgold, T., Spreafico, F., De Santa, F., Totaro, M.G., Prosperini, E., Natoli, G. and Testa, G. 2008. The histone H3 lysine 27-specific demethylase Jmjd3 is required for neural commitment. *PLoS ONE* 3(8), p. e3034.

Burroughs, S.K., Kaluz, S., Wang, D., Wang, K., Van Meir, E.G. and Wang, B. 2013.

Hypoxia inducible factor pathway inhibitors as anticancer therapeutics. *Future Med Chem* 5(5), pp. 553–572.

Cancer Genome Atlas Research Network 2008. Comprehensive genomic characterization defines human glioblastoma genes and core pathways. *Nature* 455(7216), pp. 1061–1068.

Cancer Genome Atlas Research Network, Brat, D.J., Verhaak, R.G., Aldape, K.D., Yung, W.K., et al. 2015. Comprehensive, Integrative Genomic Analysis of Diffuse Lower-Grade Gliomas. *N Engl J Med* 372(26), pp. 2481–2498.

Carrillo-Garcia, C., Prochnow, S., Simeonova, I.K., Strelau, J., Holzl-Wenig, G., Mandl, C., Unsicker, K., von Bohlen Und Halbach, O., and Ciccolini, F. (2014). Growth/differentiation factor 15 promotes EGFR signalling, and regulates proliferation and migration in the hippocampus of neonatal and young adult mice. Development *141*, 773-783.

Carro, M.S., Lim, W.K., Alvarez, M.J., Bollo, R.J., Zhao, X., Snyder, E.Y., Sulman, E.P., Anne, S.L., Doetsch, F., Colman, H., Lasorella, A., Aldape, K., Califano, A. and Iavarone, A. 2010. The transcriptional network for mesenchymal transformation of brain tumours. *Nature* 463(7279), pp. 318–325.http://f1000.com/work/bibliography/57472

Ceccarelli, M., Barthel, F.P., Malta, T.M., Sabedot, T.S., Salama, S.R., Murray, B.A., Morozova, O., Newton, Y., Radenbaugh, A., Pagnotta, S.M., Anjum, S., Wang, J., Manyam, G., Zoppoli, P., Ling, S., Rao, A.A., Grifford, M., Cherniack, A.D., Zhang, H., Poisson, L. and Verhaak, R.G.W. 2016. Molecular Profiling Reveals Biologically Discrete Subsets and Pathways of Progression in Diffuse Glioma. *Cell* 164(3), pp. 550–563.

Cerami, E., Demir, E., Schultz, N., Taylor, B.S. and Sander, C. 2010. Automated network analysis identifies core pathways in glioblastoma. *PLoS ONE* 5(2), p. e8918.http://f1000.com/work/bibliography/58866

Cerami, E., Gao, J., Dogrusoz, U., Gross, B.E., Sumer, S.O., Aksoy, B.A., Jacobsen, A., Byrne, C.J., Heuer, M.L., Larsson, E., Antipin, Y., Reva, B., Goldberg, A.P., Sander, C. and Schultz, N. 2012. The cBio cancer genomics portal: an open platform for exploring multidimensional cancer genomics data. *Cancer Discov* 2(5), pp. 401–404.

Chan, K.S., Sano, S., Kiguchi, K., Anders, J., Komazawa, N., Takeda, J., and DiGiovanni, J. (2004). Disruption of Stat3 reveals a critical role in both the initiation and the promotion stages of epithelial carcinogenesis. J Clin Invest *114*, 720–728.

Chang Y, Yan W, He X, Zhang L, Li C, Huang H, et al. miR-375 inhibits autophagy and reduces viability of hepatocellular carcinoma cells under hypoxic conditions. Gastroenterology. 2012 Jul;143(1):177–87.e8.

Chang, C.J. and Hung, M.C. 2012. The role of EZH2 in tumour progression. *Br J Cancer* 106(2), pp. 243–247.

Chang, Y., Yan, W., He, X., Zhang, L., Li, C., Huang, H., Nace, G., Geller, D.A., Lin, J. and Tsung, A. 2012. miR-375 inhibits autophagy and reduces viability of hepatocellular carcinoma cells under hypoxic conditions. *Gastroenterology* 143(1), pp. 177–87.e8.http://f1000.com/work/bibliography/1191429

Chawla, R. and Azzalin, C.M. 2008. The telomeric transcriptome and SMG proteins at the crossroads. *Cytogenet Genome Res* 122(3-4), pp. 194–201.http://f1000.com/work/bibliography/1262940

Chen, J., Li, Y., Yu, T.S., McKay, R.M., Burns, D.K., Kernie, S.G. and Parada, L.F. 2012. A restricted cell population propagates glioblastoma growth after chemotherapy. *Nature* 488(7412), pp. 522–526.

Chen, R.-Q., Yang, Q.-K., Chen, Y.-L., Oliveira, V.A., Dalton, W.S., Fearns, C. and Lee, J.-D. 2009. Kinome siRNA screen identifies SMG-1 as a negative regulator of hypoxia-inducible factor-1alpha in hypoxia. *J Biol Chem* 284(25), pp. 16752–16758.http://f1000.com/work/bibliography/58426

Chen, S., Ma, J., Wu, F., Xiong, L.J., Ma, H., Xu, W., Lv, R., Li, X., Villen, J., Gygi, S.P., *et al.* (2012). The histone H3 Lys 27 demethylase JMJD3 regulates gene expression by impacting transcriptional elongation. Genes & development *26*, 1364-1375.

Cheng, P.-Y., Lin, Y.-P., Chen, Y.-L., Lee, Y.-C., Tai, C.-C., Wang, Y.-T., Chen, Y.-J., Kao, C.-F. and Yu, J. 2011. Interplay between SIN3A and STAT3 mediates chromatin conformational changes and GFAP expression during cellular differentiation. *PLoS ONE* 6(7), p. e22018.http://f1000.com/work/bibliography/58031

Cheng, P., Phillips, E., Kim, S.-H., Taylor, D., Hielscher, T., Puccio, L., Hjelmeland, A.B., Lichter, P., Nakano, I. and Goidts, V. 2015. Kinome-wide shRNA screen identifies the receptor tyrosine kinase AXL as a key regulator for mesenchymal glioblastoma stem-like cells. *Stem Cell Reports* 4(5), pp. 899–913.

Cheng, P., Phillips, E., Kim, S.-H., Taylor, D., Hielscher, T., Puccio, L., Hjelmeland, A.B., Lichter, P., Nakano, I. and Goidts, V. 2015. Kinome-wide shRNA screen identifies the receptor tyrosine kinase AXL as a key regulator for mesenchymal glioblastoma stem-like cells. *Stem Cell Reports* 4(5), pp. 899–913.http://f1000.com/work/bibliography/804236

Chi, J.-T., Wang, Z., Nuyten, D.S.A., Rodriguez, E.H., Schaner, M.E., Salim, A., Wang, Y., Kristensen, G.B., Helland, A., Børresen-Dale, A.-L., Giaccia, A., Longaker, M.T., Hastie, T., Yang, G.P., van de Vijver, M.J. and Brown, P.O. 2006. Gene expression programs in response to hypoxia: cell type specificity and prognostic significance in human cancers. *PLoS Med* 3(3), p. e47.http://f1000.com/work/bibliography/58647

Chi, Y., Huang, S., Peng, H., Liu, M., Zhao, J., Shao, Z. and Wu, J. 2015. Critical role of CDK11(p58) in human breast cancer growth and angiogenesis. *BMC Cancer* 15, p. 701.

Chi, Y., Huang, S., Wang, Lei, Zhou, R., Wang, Lisha, Xiao, X., Li, D., Cai, Y.,

Zhou, X. and Wu, J. 2014. CDK11p58 inhibits ERα-positive breast cancer invasion by targeting integrin β3 via the repression of ERα signaling. *BMC Cancer* 14, p. 577.

Cho, H., Han, S., Park, O.H. and Kim, Y.K. 2013. SMG1 regulates adipogenesis via targeting of staufen1-mediated mRNA decay. *Biochim Biophys Acta* 1829(12), pp. 1276–1287.http://f1000.com/work/bibliography/1262943

Chow, C.R., Ebine, K., Knab, L.M., Bentrem, D.J., Kumar, K. and Munshi, H.G. 2016. Cancer Cell Invasion in Three-dimensional Collagen Is Regulated Differentially by Gα13 Protein and Discoidin Domain Receptor 1-Par3 Protein Signaling. *J Biol Chem* 291(4), pp. 1605–1618.

Christophersen, N.S. and Helin, K. 2010. Epigenetic control of embryonic stem cell fate. *J Exp Med* 207(11), pp. 2287–2295.

Chung, N., Zhang, X.D., Kreamer, A., Locco, L., Kuan, P.-F., Bartz, S., Linsley, P.S., Ferrer, M. and Strulovici, B. 2008. Median absolute deviation to improve hit selection for genome-scale RNAi screens. *J Biomol Screen* 13(2), pp. 149–158.

Cicchini M, Karantza V, Xia B. Molecular pathways: autophagy in cancer--a matter of timing and context. Clin Cancer Res. 2015 Feb 1;21(3):498–504.

Ciriello, G., Cerami, E., Sander, C. and Schultz, N. 2012. Mutual exclusivity analysis identifies oncogenic network modules. *Genome Res* 22(2), pp. 398–406.

Clark, P.A., Iida, M., Treisman, D.M., Kalluri, H., Ezhilan, S., Zorniak, M., Wheeler, D.L. and Kuo, J.S. 2012. Activation of multiple ERBB family receptors mediates glioblastoma cancer stem-like cell resistance to EGFR-targeted inhibition. *Neoplasia* 14(5), pp. 420–428.

Classen, A.-K., Bunker, B.D., Harvey, K.F., Vaccari, T. and Bilder, D. 2009. A tumor suppressor activity of Drosophila Polycomb genes mediated by JAK-STAT signaling. *Nat Genet* 41(10), pp. 1150–1155.http://f1000.com/work/bibliography/664790

Clement, V., Sanchez, P., de Tribolet, N., Radovanovic, I. and Ruiz i Altaba, A. 2007. HEDGEHOG-GLI1 signaling regulates human glioma growth, cancer stem cell self-renewal, and tumorigenicity. *Curr Biol* 17(2), pp. 165–172.

Costello, J.F., Berger, M.S., Huang, H.S. and Cavenee, W.K. 1996. Silencing of p16/CDKN2 expression in human gliomas by methylation and chromatin condensation. *Cancer Res* 56(10), pp. 2405–2410.http://f1000.com/work/bibliography/1261271

Creighton, C.J., Li, X., Landis, M., Dixon, J.M., Neumeister, V.M., Sjolund, A., Rimm, D.L., Wong, H., Rodriguez, A., Herschkowitz, J.I., et al. (2009). Residual breast cancers after conventional therapy display mesenchymal as well as tumor-initiating features. Proc Natl Acad Sci U S A *106*, 13820–13825.

Dancey, J., and Sausville, E.A. (2003). Issues and progress with protein kinase inhibitors for cancer treatment. Nat Rev Drug Discov *2*, 296–313.

Danovi, D., Folarin, A., Gogolok, S., Ender, C., Elbatsh, A.M.O., Engström, P.G., Stricker, S.H., Gagrica, S., Georgian, A., Yu, D., U, K.P., Harvey, K.J., Ferretti, P., Paddison, P.J., Preston, J.E., Abbott, N.J., Bertone, P., Smith, A. and Pollard, S.M. 2013. A high-content small molecule screen identifies sensitivity of glioblastoma stem cells to inhibition of polo-like kinase 1. *PLoS ONE* 8(10), p. e77053.

Darnell, J.E. (2005). Validating Stat3 in cancer therapy. Nat Med *11*, 595-596.

Dauer, D.J., Ferraro, B., Song, L., Yu, B., Mora, L., Buettner, R., Enkemann, S., Jove, R. and Haura, E.B. 2005. Stat3 regulates genes common to both wound healing and cancer. *Oncogene* 24(21), pp. 3397–3408.http://f1000.com/work/bibliography/57477

Dave, B.J., Pickering, D.L., Hess, M.M., Weisenburger, D.D., Armitage, J.O. and Sanger, W.G. 1999. Deletion of cell division cycle 2-like 1 gene locus on 1p36 in non-Hodgkin lymphoma. *Cancer Genet Cytogenet* 108(2), pp. 120–126.

De Oliveira, P.E.Q., Zhang, L., Wang, Z. and Lazo, J.S. 2009. Hypoxia-mediated regulation of Cdc25A phosphatase by p21 and miR-21. *Cell Cycle* 8(19), pp. 3157–3164.http://f1000.com/work/bibliography/1283540

De Santa, F., Totaro, M., Prosperini, E., Notarbartolo, S., Testa, G., and Natoli, G. (2007). The histone H3 lysine-27 demethylase Jmjd3 links inflammation to inhibition of polycomb-mediated gene silencing. Cell *130*, 1083-1094.

Di Croce, L. and Helin, K. 2013. Transcriptional regulation by Polycomb group proteins. *Nat Struct Mol Biol* 20(10), pp. 1147–1155.

Dick, J.E. 2008. Stem cell concepts renew cancer research. *Blood* 112(13), pp. 4793–4807.

Dick, J.E. 2009. Looking ahead in cancer stem cell research. *Nat Biotechnol* 27(1), pp. 44–46.

Ding, Y., Hubert, C.G., Herman, J., Corrin, P., Toledo, C.M., Skutt-Kakaria, K., Vazquez, J., Basom, R., Zhang, B., Risler, J.K., Pollard, S.M., Nam, D.-H., Delrow, J.J., Zhu, J., Lee, J., DeLuca, J., Olson, J.M. and Paddison, P.J. 2013. Cancer-Specific requirement for BUB1B/BUBR1 in human brain tumor isolates and genetically transformed cells. *Cancer Discov* 3(2), pp. 198–211.

Dirks, P.B. 2010. Brain tumor stem cells: the cancer stem cell hypothesis writ large. *Mol Oncol* 4(5), pp. 420–430.

Dolecek, T.A., Propp, J.M., Stroup, N.E. and Kruchko, C. 2012. CBTRUS statistical report: primary brain and central nervous system tumors diagnosed in the United States in 2005-2009. *Neuro Oncol* 14 Suppl 5, pp. v1–49.

Ene, C.I., Edwards, L., Riddick, G., Baysan, M., Woolard, K., Kotliarova, S., Lai, C., Belova, G., Cam, M., Walling, J., Zhou, M., Stevenson, H., Kim, H.S., Killian, K., Veenstra, T., Bailey, R., Song, H., Zhang, W. and Fine, H.A. 2012. Histone demethylase Jumonji D3 (JMJD3) as a tumor suppressor by regulating p53 protein

nuclear stabilization. *PLoS ONE* 7(12), p. e51407.http://f1000.com/work/bibliography/58357

Estarás, C., Akizu, N., García, A., Beltrán, S., de la Cruz, X. and Martínez-Balbás, M.A. 2012. Genome-wide analysis reveals that Smad3 and JMJD3 HDM co-activate the neural developmental program. *Development* 139(15), pp. 2681–2691.

Fallone, F., Britton, S., Nieto, L., Salles, B. and Muller, C. 2013. ATR controls cellular adaptation to hypoxia through positive regulation of hypoxia-inducible factor 1 (HIF-1) expression. *Oncogene* 32(37), pp. 4387–4396.http://f1000.com/work/bibliography/1283542

Fan, X., Khaki, L., Zhu, T.S., Soules, M.E., Talsma, C.E., Gul, N., Koh, C., Zhang, J., Li, Y.M., Maciaczyk, J., Nikkhah, G., Dimeco, F., Piccirillo, S., Vescovi, A.L. and Eberhart, C.G. 2010. NOTCH pathway blockade depletes CD133-positive glioblastoma cells and inhibits growth of tumor neurospheres and xenografts. *Stem Cells* 28(1), pp. 5–16.

Fanelli, M., Caprodossi, S., Ricci-Vitiani, L., Porcellini, A., Tomassoni-Ardori, F., Amatori, S., Andreoni, F., Magnani, M., De Maria, R., Santoni, A., Minucci, S. and Pelicci, P.G. 2008. Loss of pericentromeric DNA methylation pattern in human glioblastoma is associated with altered DNA methyltransferases expression and involves the stem cell compartment. *Oncogene* 27(3), pp. 358–365.http://f1000.com/work/bibliography/1261279

Fei, T., Xia, K., Li, Z., Zhou, B., Zhu, S., Chen, H., Zhang, J., Chen, Z., Xiao, H., Han, J.-D.J., et al. (2010). Genome-wide mapping of SMAD target genes reveals the role of BMP signaling in embryonic stem cell fate determination. Genome Res *20*, 36–44.

Francis, J.M., Zhang, C.-Z., Maire, C.L., Jung, J., Manzo, V.E., Adalsteinsson, V.A., Homer, H., Haidar, S., Blumenstiel, B., Pedamallu, C.S., Ligon, A.H., Love, J.C., Meyerson, M. and Ligon, K.L. 2014. EGFR variant heterogeneity in glioblastoma resolved through single-nucleus sequencing. *Cancer Discov* 4(8), pp. 956–971.http://f1000.com/work/bibliography/808852

Franovic, A., Holterman, C.E., Payette, J. and Lee, S. 2009. Human cancers converge at the HIF-2alpha oncogenic axis. *Proc Natl Acad Sci U S A* 106(50), pp. 21306–21311.http://f1000.com/work/bibliography/58112

Frias, M.A., Thoreen, C.C., Jaffe, J.D., Schroder, W., Sculley, T., Carr, S.A., and Sabatini, D.M. (2006). mSin1 is necessary for Akt/PKB phosphorylation, and its isoforms define three distinct mTORC2s. Curr Biol *16*, 1865-1870.

Fu, X.Y., Schindler, C., Improta, T., Aebersold, R. and Darnell, J.E. 1992. The proteins of ISGF-3, the interferon alpha-induced transcriptional activator, define a gene family involved in signal transduction. *Proc Natl Acad Sci U S A* 89(16), pp. 7840–7843.http://f1000.com/work/bibliography/1156577

Fukada, T., Ohtani, T., Yoshida, Y., Shirogane, T., Nishida, K., Nakajima, K., Hibi, M. and Hirano, T. 1998. STAT3 orchestrates contradictory signals in cytokine-induced G1 to S cell-cycle transition. *EMBO J* 17(22), pp. 6670–6677.http://f1000.com/work/bibliography/1169316

Gallo, M., Coutinho, F.J., Vanner, R.J., Gayden, T., Mack, S.C., Murison, A., Remke, M., Li, R., Takayama, N., Desai, K., Lee, L., Lan, X., Park, N.I., Barsyte-Lovejoy, D., Smil, D., Sturm, D., Kushida, M.M., Head, R., Cusimano, M.D., Bernstein, M. and Dirks, P.B. 2015. MLL5 Orchestrates a Cancer Self-Renewal State by Repressing the Histone Variant H3.3 and Globally Reorganizing Chromatin. *Cancer Cell* 28(6), pp. 715–729.http://f1000.com/work/bibliography/1080719

Gao, J., Aksoy, B.A., Dogrusoz, U., Dresdner, G., Gross, B., Sumer, S.O., Sun, Y., Jacobsen, A., Sinha, R., Larsson, E., Cerami, E., Sander, C. and Schultz, N. 2013. Integrative analysis of complex cancer genomics and clinical profiles using the cBioPortal. *Sci Signal* 6(269), p. pl1.

Gaspar, N., Marshall, L., Perryman, L., Bax, D.A., Little, S.E., Viana-Pereira, M., Sharp, S.Y., Vassal, G., Pearson, A.D., Reis, R.M., Hargrave, D., Workman, P. and Jones, C. 2010. MGMT-independent temozolomide resistance in pediatric glioblastoma cells associated with a PI3-kinase-mediated HOX/stem cell gene signature. *Cancer Res* 70(22), pp. 9243–9252.

Geng, L., Donnelly, E., McMahon, G., Lin, P.C., Sierra-Rivera, E., Oshinka, H. and Hallahan, D.E. 2001. Inhibition of vascular endothelial growth factor receptor signaling leads to reversal of tumor resistance to radiotherapy. *Cancer Res* 61(6), pp. 2413–2419.

Gewandter, J.S., Bambara, R.A. and O'Reilly, M.A. 2011. The RNA surveillance protein SMG1 activates p53 in response to DNA double-strand breaks but not exogenously oxidized mRNA. *Cell Cycle* 10(15), pp. 2561–2567.http://f1000.com/work/bibliography/58654

Gibson, S.L., Bindra, R.S. and Glazer, P.M. 2005. Hypoxia-induced phosphorylation of Chk2 in an ataxia telangiectasia mutated-dependent manner. *Cancer Res* 65(23), pp. 10734–10741.http://f1000.com/work/bibliography/1276907

Gilbertson, R.J. and Rich, J.N. 2007. Making a tumour's bed: glioblastoma stem cells and the vascular niche. *Nat Rev Cancer* 7(10), pp. 733–736.http://f1000.com/work/bibliography/530135

Glück, A.A., Aebersold, D.M., Zimmer, Y. and Medová, M. 2015. Interplay between receptor tyrosine kinases and hypoxia signaling in cancer. *Int J Biochem Cell Biol* 62, pp. 101–114.http://f1000.com/work/bibliography/1173576

Gong C, Song E, Codogno P, Mehrpour M. The roles of BECN1 and autophagy in cancer are context dependent. Autophagy. 2012 Dec 1;8(12):1853–1855.

Gong, A.-H., Wei, P., Zhang, S., Yao, J., Yuan, Y., Zhou, A.-D., Lang, F.F., Heimberger, A.B., Rao, G. and Huang, S. 2015. FoxM1 Drives a Feed-Forward STAT3-Activation Signaling Loop That Promotes the Self-Renewal and

Tumorigenicity of Glioblastoma Stem-like Cells. *Cancer Res* 75(11), pp. 2337–2348.http://f1000.com/work/bibliography/809426

Gong, C., Song, E., Codogno, P. and Mehrpour, M. 2012. The roles of BECN1 and autophagy in cancer are context dependent. *Autophagy* 8(12), pp. 1853–1855.http://f1000.com/work/bibliography/1191433

Gopalsamy, A., Bennett, E.M., Shi, M., Zhang, W.-G., Bard, J. and Yu, K. 2012. Identification of pyrimidine derivatives as hSMG-1 inhibitors. *Bioorg Med Chem Lett* 22(21), pp. 6636–6641.http://f1000.com/work/bibliography/1283710

Gordan, J.D., Bertout, J.A., Hu, C.-J., Diehl, J.A. and Simon, M.C. 2007. HIF-2alpha promotes hypoxic cell proliferation by enhancing c-myc transcriptional activity. *Cancer Cell* 11(4), pp. 335–347.http://f1000.com/work/bibliography/58142

Gross, S., Rahal, R., Stransky, N., Lengauer, C. and Hoeflich, K.P. 2015. Targeting cancer with kinase inhibitors. *J Clin Invest* 125(5), pp. 1780–1789.http://f1000.com/work/bibliography/552446

Gu, F., Hata, R., Ma, Y.-J., Tanaka, J., Mitsuda, N., Kumon, Y., Hanakawa, Y., Hashimoto, K., Nakajima, K. and Sakanaka, M. 2005. Suppression of Stat3 promotes neurogenesis in cultured neural stem cells. *J Neurosci Res* 81(2), pp. 163–171.http://f1000.com/work/bibliography/1156613

Gubanova E, Brown B, Ivanov SV, Helleday T, Mills GB, Yarbrough WG, et al. Downregulation of SMG-1 in HPV-positive head and neck squamous cell carcinoma due to promoter hypermethylation correlates with improved survival. Clin Cancer Res. 2012 Mar 1;18(5):1257–1267.

Gubanova E, Issaeva N, Gokturk C, Djureinovic T, Helleday T. SMG-1 suppresses CDK2 and tumor growth by regulating both the p53 and Cdc25A signaling pathways. Cell Cycle. 2013 Oct 4;12(24).

Gubanova, E., Brown, B., Ivanov, S.V., Helleday, T., Mills, G.B., Yarbrough, W.G. and Issaeva, N. 2012. Downregulation of SMG-1 in HPV-positive head and neck squamous cell carcinoma due to promoter hypermethylation correlates with improved survival. *Clin Cancer Res* 18(5), pp. 1257–1267.http://f1000.com/work/bibliography/1139770

Gubanova, E., Issaeva, N., Gokturk, C., Djureinovic, T. and Helleday, T. 2013. SMG-1 suppresses CDK2 and tumor growth by regulating both the p53 and Cdc25A signaling pathways. *Cell Cycle* 12(24), pp. 3770–3780.http://f1000.com/work/bibliography/1139755

Guryanova, O.A., Wu, Q., Cheng, L., Lathia, J.D., Huang, Z., Yang, J., MacSwords, J., Eyler, C.E., McLendon, R.E., Heddleston, J.M., Shou, W., Hambardzumyan, D., Lee, J., Hjelmeland, A.B., Sloan, A.E., Bredel, M., Stark, G.R., Rich, J.N. and Bao, S. 2011. Nonreceptor tyrosine kinase BMX maintains self-renewal and tumorigenic potential of glioblastoma stem cells by activating STAT3. *Cancer Cell* 19(4), pp. 498–511.

Hammond, E.M., Denko, N.C., Dorie, M.J., Abraham, R.T. and Giaccia, A.J. 2002. Hypoxia links ATR and p53 through replication arrest. *Mol Cell Biol* 22(6), pp. 1834–1843.http://f1000.com/work/bibliography/1280295

Han, X., Zhang, W., Yang, X., Wheeler, C.G., Langford, C.P., Wu, L., Filippova, N., Friedman, G.K., Ding, Q., Fathallah-Shaykh, H.M., Gillespie, G.Y. and Nabors, L.B. 2014. The role of Src family kinases in growth and migration of glioma stem cells. *Int J Oncol* 45(1), pp. 302–310.

Haring, M., Offermann, S., Danker, T., Horst, I., Peterhansel, C., and Stam, M. (2007). Chromatin immunoprecipitation: optimization, quantitative analysis and data normalization. Plant methods *3*, 11.

Hart, T., Brown, K.R., Sircoulomb, F., Rottapel, R. and Moffat, J. 2014. Measuring error rates in genomic perturbation screens: gold standards for human functional genomics. *Mol Syst Biol* 10, p. 733.

Hart, T., Chandrashekhar, M., Aregger, M., Steinhart, Z., Brown, K.R., MacLeod, G., Mis, M., Zimmermann, M., Fradet-Turcotte, A., Sun, S., Mero, P., Dirks, P., Sidhu, S., Roth, F.P., Rissland, O.S., Durocher, D., Angers, S. and Moffat, J. 2015. High-Resolution CRISPR Screens Reveal Fitness Genes and Genotype-Specific Cancer Liabilities. *Cell* 163(6), pp. 1515–1526.

Hashizume, R., Andor, N., Ihara, Y., Lerner, R., Gan, H., Chen, X., Fang, D., Huang, X., Tom, M.W., Ngo, V., Solomon, D., Mueller, S., Paris, P.L., Zhang, Z., Petritsch, C., Gupta, N., Waldman, T.A. and James, C.D. 2014. Pharmacologic inhibition of histone demethylation as a therapy for pediatric brainstem glioma. *Nat Med* 20(12), pp. 1394–1396.http://f1000.com/work/bibliography/59085

Haskell, H., Natarajan, M., Hecker, T.P., Ding, Q., Stewart, J., Grammer, J.R., and Gladson, C.L. (2003). Focal adhesion kinase is expressed in the angiogenic blood vessels of malignant astrocytic tumors in vivo and promotes capillary tube formation of brain microvascular endothelial cells. Clin Cancer Res *9*, 2157–2165.

Hayes, T.E., Kitchen, A.M. and Cochran, B.H. 1987. Inducible binding of a factor to the c-fos regulatory region. *Proc Natl Acad Sci U S A* 84(5), pp. 1272–1276.http://f1000.com/work/bibliography/1155098

Hebenstreit, D., Gu, M., Haider, S., Turner, D.J., Lio, P., and Teichmann, S.A. (2011). EpiChIP: gene-by-gene quantification of epigenetic modification levels. Nucleic Acids Res *39*, e27.

Heddleston, J.M., Li, Z., McLendon, R.E., Hjelmeland, A.B. and Rich, J.N. 2009. The hypoxic microenvironment maintains glioblastoma stem cells and promotes reprogramming towards a cancer stem cell phenotype. *Cell Cycle* 8(20), pp. 3274–3284.http://f1000.com/work/bibliography/57549

Heddleston, J.M., Wu, Q., Rivera, M., Minhas, S., Lathia, J.D., Sloan, A.E., Iliopoulos, O., Hjelmeland, A.B. and Rich, J.N. 2012. Hypoxia-induced mixed-lineage leukemia 1 regulates glioma stem cell tumorigenic potential. *Cell Death Differ* 19(3), pp. 428–439.http://f1000.com/work/bibliography/57703

Hedvat, M., Huszar, D., Herrmann, A., Gozgit, J.M., Schroeder, A., Sheehy, A., Buettner, R., Proia, D., Kowolik, C.M., Xin, H., Armstrong, B., Bebernitz, G., Weng, S., Wang, L., Ye, M., McEachern, K., Chen, H., Morosini, D., Bell, K., Alimzhanov, M., Ioannidis, S., McCoon, P., Cao, Z.A., Yu, H., Jove, R. and Zinda, M. 2009. The JAK2 inhibitor AZD1480 potently blocks Stat3 signaling and oncogenesis in solid tumors. *Cancer Cell* 16(6), pp. 487–497.

Hegi, M.E., Diserens, A.-C., Gorlia, T., Hamou, M.-F., de Tribolet, N., Weller, M., Kros, J.M., Hainfellner, J.A., Mason, W., Mariani, L., Bromberg, J.E.C., Hau, P., Mirimanoff, R.O., Cairncross, J.G., Janzer, R.C. and Stupp, R. 2005. MGMT gene silencing and benefit from temozolomide in glioblastoma. *N Engl J Med* 352(10), pp. 997–1003.http://f1000.com/work/bibliography/58989

Hegi, M.E., Liu, L., Herman, J.G., Stupp, R., Wick, W., Weller, M., Mehta, M.P. and Gilbert, M.R. 2008. Correlation of O6-methylguanine methyltransferase (MGMT) promoter methylation with clinical outcomes in glioblastoma and clinical strategies to modulate MGMT activity. *J Clin Oncol* 26(25), pp. 4189–4199.

Heinemann, B., Nielsen, J.M., Hudlebusch, H.R., Lees, M.J., Larsen, D.V., Boesen, T., Labelle, M., Gerlach, L.-O., Birk, P. and Helin, K. 2014. Inhibition of demethylases by GSK-J1/J4. *Nature* 514(7520), pp. E1–E2.http://f1000.com/work/bibliography/58947

Helikar T, Kowal B, McClenathan S, Bruckner M, Rowley T, Madrahimov A, et al. The Cell Collective: toward an open and collaborative approach to systems biology. BMC Syst Biol. 2012 Aug 7;6:96.

Helikar, T., Kowal, B. and Rogers, J.A. 2013. A cell simulator platform: the cell collective. *Clin Pharmacol Ther* 93(5), pp. 393–395.http://f1000.com/work/bibliography/58955

Helikar, T., Kowal, B., McClenathan, S., Bruckner, M., Rowley, T., Madrahimov, A., Wicks, B., Shrestha, M., Limbu, K. and Rogers, J.A. 2012. The Cell Collective: toward an open and collaborative approach to systems biology. *BMC Syst Biol* 6, p. 96.http://f1000.com/work/bibliography/58658

Hino, R., Uozaki, H., Murakami, N., Ushiku, T., Shinozaki, A., Ishikawa, S., Morikawa, T., Nakaya, T., Sakatani, T., Takada, K., et al. (2009). Activation of DNA methyltransferase 1 by EBV latent membrane protein 2A leads to promoter hypermethylation of PTEN gene in gastric carcinoma. Cancer Res *69*, 2766–2774.

Huang, D.A.W., Sherman, B.T., and Lempicki, R.A. (2009). Systematic and integrative analysis of large gene lists using DAVID bioinformatics resources. Nat Protoc *4*, 44–57.

Huang, X., Hu, J., Li, Y., Zhuyun Yang, Z., Zhu, H., Zhou, L., Ma, K., Schachner, M., Xiao, Z., and Li, Y. (2013). The cell adhesion molecule L1 regulates the expression of FGF21 and enhances neurite outgrowth. Brain Res *1530*, 13-21.

Hubert, C.G., Bradley, R.K., Ding, Y., Toledo, C.M., Herman, J., Skutt-Kakaria, K., Girard, E.J., Davison, J., Berndt, J., Corrin, P., Hardcastle, J., Basom, R., Delrow, J.J.,

Webb, T., Pollard, S.M., Lee, J., Olson, J.M. and Paddison, P.J. 2013. Genome-wide RNAi screens in human brain tumor isolates reveal a novel viability requirement for PHF5A. *Genes Dev* 27(9), pp. 1032–1045.http://f1000.com/work/bibliography/58465

Hulsen, T., de Vlieg, J. and Alkema, W. 2008. BioVenn - a web application for the comparison and visualization of biological lists using area-proportional Venn diagrams. *BMC Genomics* 9, p. 488.

Hwang, J., Sato, H., Tang, Y., Matsuda, D. and Maquat, L.E. 2010. UPF1 association with the cap-binding protein, CBP80, promotes nonsense-mediated mRNA decay at two distinct steps. *Mol Cell* 39(3), pp. 396–409.http://f1000.com/work/bibliography/1242875

Ignatova, T.N., Kukekov, V.G., Laywell, E.D., Suslov, O.N., Vrionis, F.D. and Steindler, D.A. 2002. Human cortical glial tumors contain neural stem-like cells expressing astroglial and neuronal markers in vitro. *Glia* 39(3), pp. 193–206.

Ikushima, H., Todo, T., Ino, Y., Takahashi, M., Miyazawa, K. and Miyazono, K. 2009. Autocrine TGF-beta signaling maintains tumorigenicity of glioma-initiating cells through Sry-related HMG-box factors. *Cell Stem Cell* 5(5), pp. 504–514.

Iliopoulos, D., Hirsch, H.A., and Struhl, K. (2009). An epigenetic switch involving NF-kappaB, Lin28, Let-7 MicroRNA, and IL6 links inflammation to cell transformation. Cell *139*, 693-706.

Iliopoulos, D., Jaeger, S.A., Hirsch, H.A., Bulyk, M.L. and Struhl, K. 2010. STAT3 activation of miR-21 and miR-181b-1 via PTEN and CYLD are part of the epigenetic switch linking inflammation to cancer. *Mol Cell* 39(4), pp. 493–506.http://f1000.com/work/bibliography/57851

Iliopoulos, D., Jaeger, S.A., Hirsch, H.A., Bulyk, M.L. and Struhl, K. 2010. STAT3 activation of miR-21 and miR-181b-1 via PTEN and CYLD are part of the epigenetic switch linking inflammation to cancer. *Mol Cell* 39(4), pp. 493–506.http://f1000.com/work/bibliography/57851

Inda, M.M., Bonavia, R. and Seoane, J. 2014. Glioblastoma multiforme: a look inside its heterogeneous nature. *Cancers (Basel)* 6(1), pp. 226–239.

Ishigaki, Y., Li, X., Serin, G. and Maquat, L.E. 2001. Evidence for a pioneer round of mRNA translation: mRNAs subject to nonsense-mediated decay in mammalian cells are bound by CBP80 and CBP20. *Cell* 106(5), pp. 607–617.http://f1000.com/work/bibliography/1242876

Isken O, Maquat LE. The multiple lives of NMD factors: balancing roles in gene and genome regulation. Nat Rev Genet. 2008 Sep;9(9):699–712.

Ito, M., Ohba, S., Gaensler, K., Ronen, S.M., Mukherjee, J. and Pieper, R.O. 2013. Early Chk1 phosphorylation is driven by temozolomide-induced, DNA double strand break- and mismatch repair-independent DNA damage. *PLoS ONE* 8(5), p. e62351.http://f1000.com/work/bibliography/47258

Ivanchuk, S.M., Mondal, S., Dirks, P.B., and Rutka, J.T. (2001). The INK4A/ARF locus: role in cell cycle control and apoptosis and implications for glioma growth. J Neurooncol *51*, 219-229.

Iwamaru, A., Szymanski, S., Iwado, E., Aoki, H., Yokoyama, T., Fokt, I., Hess, K., Conrad, C., Madden, T., Sawaya, R., Kondo, S., Priebe, W. and Kondo, Y. 2007. A novel inhibitor of the STAT3 pathway induces apoptosis in malignant glioma cells both in vitro and in vivo. *Oncogene* 26(17), pp. 2435–2444.http://f1000.com/work/bibliography/1154896

Jain, R.K. (2005). Normalization of tumor vasculature: an emerging concept in antiangiogenic therapy. Science *307*, 58–62.

Jepsen, K., Solum, D., Zhou, T., McEvilly, R.J., Kim, H.-J., Glass, C.K., Hermanson, O. and Rosenfeld, M.G. 2007. SMRT-mediated repression of an H3K27 demethylase in progression from neural stem cell to neuron. *Nature* 450(7168), pp. 415–419.http://f1000.com/work/bibliography/58460

Johnstone, R.W. 2002. Histone-deacetylase inhibitors: novel drugs for the treatment of cancer. *Nat Rev Drug Discov* 1(4), pp. 287–299.

Joo, K.M., Jin, J., Kim, E., Ho Kim, K., Kim, Y., Gu Kang, B., Kang, Y.-J., Lathia, J.D., Cheong, K.H., Song, P.H., Kim, H., Seol, H.J., Kong, D.-S., Lee, J.-I., Rich, J.N., Lee, J. and Nam, D.-H. 2012. MET signaling regulates glioblastoma stem cells. *Cancer Res* 72(15), pp. 3828–3838.

Joshi, K., Banasavadi-Siddegowda, Y., Mo, X., Kim, S.H., Mao, P., Kig, C., Nardini, D., Sobol, R.W., Chow, L.M., Kornblum, H.I., Waclaw, R., Beullens, M. and Nakano, I. 2013. MELK-dependent FOXM1 phosphorylation is essential for proliferation of glioma stem cells. *Stem Cells* 31(6), pp. 1051–1063.

Kang, S.-H., Yu, M.O., Park, K.-J., Chi, S.-G., Park, D.-H. and Chung, Y.-G. 2010. Activated STAT3 regulates hypoxia-induced angiogenesis and cell migration in human glioblastoma. *Neurosurgery* 67(5), pp. 1386–95; discussion 1395.http://f1000.com/work/bibliography/1276845

Kang, S.C., Kim, S.K., Chai, J.C., Kim, S.H., Won, K.-J., Lee, Y.S., Jung, K.H. and Chai, Y.G. 2015. Transcriptomic Profiling and H3K27me3 Distribution Reveal Both Demethylase-Dependent and Independent Regulation of Developmental Gene Transcription in Cell Differentiation. *PLoS ONE* 10(8), p. e0135276.http://f1000.com/work/bibliography/1278201

Karolchik, D., Hinrichs, A.S., and Kent, W.J. (2009). The UCSC Genome Browser. Current protocols in bioinformatics / editoral board, Andreas D Baxevanis [et al] *Chapter 1*, Unit1 4.

Kaur, B., Khwaja, F.W., Severson, E.A., Matheny, S.L., Brat, D.J. and Van Meir, E.G. 2005. Hypoxia and the hypoxia-inducible-factor pathway in glioma growth and angiogenesis. *Neuro Oncol* 7(2), pp. 134–153.

Kawahara, M., Hori, T., Matsubara, Y., Okawa, K. and Uchiyama, T. 2007. Cyclin-

dependent kinaselike 5 is a novel target of immunotherapy in adult T-cell leukemia. *J Immunother* 30(5), pp. 499–505.

Kidder, B.L., Yang, J. and Palmer, S. 2008. Stat3 and c-Myc genome-wide promoter occupancy in embryonic stem cells. *PLoS ONE* 3(12), p. e3932.http://f1000.com/work/bibliography/57506

Kim, C.K., Nguyen, T.L.X., Joo, K.M., Nam, D.-H., Park, J., Lee, K.-H., Cho, S.-W. and Ahn, J.-Y. 2010. Negative regulation of p53 by the long isoform of ErbB3 binding protein Ebp1 in brain tumors. *Cancer Res* 70(23), pp. 9730–9741.

Kim, E., Kim, M., Woo, D.-H., Shin, Y., Shin, J., Chang, N., Oh, Y.T., Kim, H., Rheey, J., Nakano, I., Lee, C., Joo, K.M., Rich, J.N., Nam, D.-H. and Lee, J. 2013. Phosphorylation of EZH2 activates STAT3 signaling via STAT3 methylation and promotes tumorigenicity of glioblastoma stem-like cells. *Cancer Cell* 23(6), pp. 839–852.http://f1000.com/work/bibliography/58486

Kim, J.E., Patel, M., Ruzevick, J., Jackson, C.M. and Lim, M. 2014. STAT3 Activation in Glioblastoma: Biochemical and Therapeutic Implications. *Cancers (Basel)* 6(1), pp. 376–395.http://f1000.com/work/bibliography/1156600

Kim, J.E., Patel, M., Ruzevick, J., Jackson, C.M., and Lim, M. (2014). STAT3 Activation in Glioblastoma: Biochemical and Therapeutic Implications. Cancers (Basel) *6*, 376–395.

Kirmizis, A., Bartley, S.M., Kuzmichev, A., Margueron, R., Reinberg, D., Green, R., and Farnham, P.J. (2004). Silencing of human polycomb target genes is associated with methylation of histone H3 Lys 27. Genes Dev *18*, 1592-1605.

Knight, Z.A., Lin, H. and Shokat, K.M. 2010. Targeting the cancer kinome through polypharmacology. *Nat Rev Cancer* 10(2), pp. 130–137.

Ko, S.Y., Kang, H.Y., Lee, H.S., Han, S.Y. and Hong, S.H. 2006. Identification of Jmjd1a as a STAT3 downstream gene in mES cells. *Cell Struct Funct* 31(2), pp. 53–62.http://f1000.com/work/bibliography/1158315

Koh, M., Woo, Y., Valiathan, R.R., Jung, H.Y., Park, S.Y., Kim, Y.N., Kim, H.-R.C., Fridman, R. and Moon, A. 2015. Discoidin domain receptor 1 is a novel transcriptional target of ZEB1 in breast epithelial cells undergoing H-Ras-induced epithelial to mesenchymal transition. *Int J Cancer* 136(6), pp. E508–E520.

Koike-Yusa, H., Li, Y., Tan, E.-P., Velasco-Herrera, M.D.C. and Yusa, K. 2014. Genome-wide recessive genetic screening in mammalian cells with a lentiviral CRISPR-guide RNA library. *Nat Biotechnol* 32(3), pp. 267–273.http://f1000.com/work/bibliography/44642

Konnikova, L., Kotecki, M., Kruger, M.M. and Cochran, B.H. 2003. Knockdown of STAT3 expression by RNAi induces apoptosis in astrocytoma cells. *BMC Cancer* 3, p. 23.

Konnikova, L., Simeone, M.C., Kruger, M.M., Kotecki, M. and Cochran, B.H. 2005. Signal transducer and activator of transcription 3 (STAT3) regulates human

telomerase reverse transcriptase (hTERT) expression in human cancer and primary cells. *Cancer Res* 65(15), pp. 6516–6520.http://f1000.com/work/bibliography/1156602

Kroon, P., Berry, P.A., Stower, M.J., Rodrigues, G., Mann, V.M., Simms, M., Bhasin, D., Chettiar, S., Li, C., Li, P.K., Maitland, N.J. and Collins, A.T. 2013. JAK-STAT blockade inhibits tumor initiation and clonogenic recovery of prostate cancer stem-like cells. *Cancer Res* 73(16), pp. 5288–5298.

Kruczyk, M., Przanowski, P., Dabrowski, M., Swiatek-Machado, K., Mieczkowski, J., Wallerman, O., Ronowicz, A., Piotrowski, A., Wadelius, C., Kaminska, B., et al. (2014). Integration of genome-wide of Stat3 binding and epigenetic modification mapping with transcriptome reveals novel Stat3 target genes in glioma cells. Biochim Biophys Acta *1839*, 1341–1350.

Kumari, S.R., Mendoza-Alvarez, H., and Alvarez-Gonzalez, R. (1998). Functional interactions of p53 with poly(ADP-ribose) polymerase (PARP) during apoptosis following DNA damage: covalent poly(ADP-ribosyl)ation of p53 by exogenous PARP and noncovalent binding of p53 to the M(r) 85,000 proteolytic fragment. Cancer Res *58*, 5075–5078.

Kunz, M. and Ibrahim, S.M. 2003. Molecular responses to hypoxia in tumor cells. *Molecular Cancer*. Available at: https://molecular-cancer.biomedcentral.com/articles/10.1186/1476-4598-2-23.

Kurosaki T, Li W, Hoque M, Popp MW, Ermolenko DN, Tian B, et al. A post-translational regulatory switch on UPF1 controls targeted mRNA degradation. Genes Dev. 2014 Sep 1;28(17):1900–1916.

Kuzmichev, A., Nishioka, K., Erdjument-Bromage, H., Tempst, P., and Reinberg, D. (2002). Histone methyltransferase activity associated with a human multiprotein complex containing the Enhancer of Zeste protein. Genes & development *16*, 2893-2905.

La Montanara, P., Rusconi, L., Locarno, A., Forti, L., Barbiero, I., Tramarin, M., Chandola, C., Kilstrup-Nielsen, C. and Landsberger, N. 2015. Synaptic synthesis, dephosphorylation, and degradation: a novel paradigm for an activity-dependent neuronal control of CDKL5. *J Biol Chem* 290(7), pp. 4512–4527.http://f1000.com/work/bibliography/1259269

Laderoute, K.R., Amin, K., Calaoagan, J.M., Knapp, M., Le, T., Orduna, J., Foretz, M., and Viollet, B. (2006). 5'-AMP-activated protein kinase (AMPK) is induced by low-oxygen and glucose deprivation conditions found in solid-tumor microenvironments. Mol Cell Biol *26*, 5336–5347.

Laderoute, K.R., Mendonca, H.L., Calaoagan, J.M., Knapp, A.M., Giaccia, A.J. and Stork, P.J. 1999. Mitogen-activated protein kinase phosphatase-1 (MKP-1) expression is induced by low oxygen conditions found in solid tumor microenvironments. A candidate MKP for the inactivation of hypoxia-inducible stress-activated protein kinase/c-Jun N-terminal protein kinase activity. *J Biol Chem* 274(18), pp. 12890–

12897.

Laks, D.R., Masterman-Smith, M., Visnyei, K., Angenieux, B., Orozco, N.M., Foran, I., Yong, W.H., Vinters, H.V., Liau, L.M., Lazareff, J.A., Mischel, P.S., Cloughesy, T.F., Horvath, S. and Kornblum, H.I. 2009. Neurosphere formation is an independent predictor of clinical outcome in malignant glioma. *Stem Cells* 27(4), pp. 980–987.

Lall N, Henley-Smith CJ, De Canha MN, Oosthuizen CB, Berrington D. Viability Reagent, PrestoBlue, in Comparison with Other Available Reagents, Utilized in Cytotoxicity and Antimicrobial Assays. Int J Microbiol. 2013 Apr 4;2013:420601.

Lamalice, L., Le Boeuf, F. and Huot, J. 2007. Endothelial cell migration during angiogenesis. *Circ Res* 100(6), pp. 782–794.

Lan, F., Bayliss, P.E., Rinn, J.L., Whetstine, J.R., Wang, J.K., Chen, S., Iwase, S., Alpatov, R., Issaeva, I., Canaani, E., Roberts, T.M., Chang, H.Y. and Shi, Y. 2007. A histone H3 lysine 27 demethylase regulates animal posterior development. *Nature* 449(7163), pp. 689–694.http://f1000.com/work/bibliography/43806

Lathia, J.D., Heddleston, J.M., Venere, M. and Rich, J.N. 2011. Deadly teamwork: neural cancer stem cells and the tumor microenvironment. *Cell Stem Cell* 8(5), pp. 482–485.http://f1000.com/work/bibliography/57794

Lathia, J.D., Hitomi, M., Gallagher, J., Gadani, S.P., Adkins, J., Vasanji, A., Liu, L., Eyler, C.E., Heddleston, J.M., Wu, Q., et al. (2011). Distribution of CD133 reveals glioma stem cells self-renew through symmetric and asymmetric cell divisions. Cell Death Dis *2*, e200.

Lathia, J.D., Heddleston, J.M., Venere, M., and Rich, J.N. (2011). Deadly teamwork: neural cancer stem cells and the tumor microenvironment. Cell Stem Cell *8*, 482–485.

Lathia, J.D., Mack, S.C., Mulkearns-Hubert, E.E., Valentim, C.L. and Rich, J.N. 2015. Cancer stem cells in glioblastoma. *Genes Dev* 29(12), pp. 1203–1217.

Lee, C., Fotovati, A., Triscott, J., Chen, J., Venugopal, C., Singhal, A., Dunham, C., Kerr, J.M., Verreault, M., Yip, S., Wakimoto, H., Jones, C., Jayanthan, A., Narendran, A., Singh, S.K. and Dunn, S.E. 2012. Polo-like kinase 1 inhibition kills glioblastoma multiforme brain tumor cells in part through loss of SOX2 and delays tumor progression in mice. *Stem Cells* 30(6), pp. 1064–1075.

Lee, H., Zhang, P., Herrmann, A., Yang, C., Xin, H., Wang, Z., Hoon, D.S.B., Forman, S.J., Jove, R., Riggs, A.D. and Yu, H. 2012. Acetylated STAT3 is crucial for methylation of tumor-suppressor gene promoters and inhibition by resveratrol results in demethylation. *Proc Natl Acad Sci U S A* 109(20), pp. 7765–7769.http://f1000.com/work/bibliography/58071

Lee, J.-H., Jin, Y., He, G., Zeng, S.X., Wang, Y.V., Wahl, G.M. and Lu, H. 2012. Hypoxia activates tumor suppressor p53 by inducing ATR-Chk1 kinase cascade-mediated phosphorylation and consequent 14-3-3γ inactivation of MDMX protein. *J*

Biol Chem 287(25), pp. 20898–20903.http://f1000.com/work/bibliography/1281845

Lee, J.-K., Chang, N., Yoon, Y., Yang, H., Cho, H., Kim, E., Shin, Y., Kang, W., Oh, Y.T., Mun, G.I., Joo, K.M., Nam, D.-H. and Lee, J. 2016. USP1 targeting impedes GBM growth by inhibiting stem cell maintenance and radioresistance. *Neuro Oncol* 18(1), pp. 37–47.

Lee, J., Kim, E., Ryu, S.-W., Choi, C. and Choi, K. 2016. Combined inhibition of vascular endothelial growth factor receptor signaling with temozolomide enhances cytotoxicity against human glioblastoma cells via downregulation of Neuropilin-1. *J Neurooncol*.

Lee, J., Kotliarova, S., Kotliarov, Y., Li, A., Su, Q., Donin, N.M., Pastorino, S., Purow, B.W., Christopher, N., Zhang, W., Park, J.K. and Fine, H.A. 2006. Tumor stem cells derived from glioblastomas cultured in bFGF and EGF more closely mirror the phenotype and genotype of primary tumors than do serum-cultured cell lines. *Cancer Cell* 9(5), pp. 391–403.http://f1000.com/work/bibliography/57796

Lee, J., Son, M.J., Woolard, K., Donin, N.M., Li, A., Cheng, C.H., Kotliarova, S., Kotliarov, Y., Walling, J., Ahn, S., Kim, M., Totonchy, M., Cusack, T., Ene, C., Ma, H., Su, Q., Zenklusen, J.C., Zhang, W., Maric, D. and Fine, H.A. 2008. Epigenetic-mediated dysfunction of the bone morphogenetic protein pathway inhibits differentiation of glioblastoma-initiating cells. *Cancer Cell* 13(1), pp. 69–80.

Lee, S.H., Krisanapun, C., and Baek, S.J. (2010). NSAID-activated gene-1 as a molecular target for capsaicin-induced apoptosis through a novel molecular mechanism involving GSK3beta, C/EBPbeta and ATF3. Carcinogenesis *31*, 719-728.

Leoncini, S., De Felice, C., Signorini, C., Zollo, G., Cortelazzo, A., Durand, T., Galano, J.-M., Guerranti, R., Rossi, M., Ciccoli, L. and Hayek, J. 2015. Cytokine Dysregulation in MECP2- and CDKL5-Related Rett Syndrome: Relationships with Aberrant Redox Homeostasis, Inflammation, and ω-3 PUFAs. *Oxid Med Cell Longev* 2015, p. 421624.

Levy, D.E., Kessler, D.S., Pine, R., Reich, N. and Darnell, J.E. 1988. Interferon-induced nuclear factors that bind a shared promoter element correlate with positive and negative transcriptional control. *Genes Dev* 2(4), pp. 383–393.http://f1000.com/work/bibliography/1156575

Lewis, P.W., Müller, M.M., Koletsky, M.S., Cordero, F., Lin, S., Banaszynski, L.A., Garcia, B.A., Muir, T.W., Becher, O.J. and Allis, C.D. 2013. Inhibition of PRC2 activity by a gain-of-function H3 mutation found in pediatric glioblastoma. *Science* 340(6134), pp. 857–861.http://f1000.com/work/bibliography/46426

Li, G.H., Wei, H., Lv, S.Q., Ji, H., and Wang, D.L. (2010). Knockdown of STAT3 expression by RNAi suppresses growth and induces apoptosis and differentiation in glioblastoma stem cells. Int J Oncol *37*, 103-110.

Li, J.-L., Sainson, R.C.A., Oon, C.E., Turley, H., Leek, R., Sheldon, H., Bridges, E., Shi, W., Snell, C., Bowden, E.T., et al. (2011). DLL4-Notch signaling mediates tumor

resistance to anti-VEGF therapy in vivo. Cancer Res *71*, 6073–6083.

Li, L., He, L., Zhao, J.-L., Xiao, J., Liu, M., Li, X. and Tang, H. 2015. MiR-17-5p up-regulates YES1 to modulate the cell cycle progression and apoptosis in ovarian cancer cell lines. *J Cell Biochem* 116(6), pp. 1050–1059.

Li, Z., Bao, S., Wu, Q., Wang, H., Eyler, C., Sathornsumetee, S., Shi, Q., Cao, Y., Lathia, J., McLendon, R.E., Hjelmeland, A.B. and Rich, J.N. 2009. Hypoxia-inducible factors regulate tumorigenic capacity of glioma stem cells. *Cancer Cell* 15(6), pp. 501–513.http://f1000.com/work/bibliography/57537

Liu, Y. and Gray, N.S. 2006. Rational design of inhibitors that bind to inactive kinase conformations. *Nat Chem Biol* 2(7), pp. 358–364.http://f1000.com/work/bibliography/1295997

Livak, K.J., and Schmittgen, T.D. (2001). Analysis of relative gene expression data using real-time quantitative PCR and the 2(-Delta Delta C(T)) Method. Methods (San Diego, Calif *25*, 402-408.

Lou, C.H., Shao, A., Shum, E.Y., Espinoza, J.L., Huang, L., Karam, R. and Wilkinson, M.F. 2014. Posttranscriptional control of the stem cell and neurogenic programs by the nonsense-mediated RNA decay pathway. *Cell Rep* 6(4), pp. 748–764.http://f1000.com/work/bibliography/1125251

Lovén, J., Hoke, H.A., Lin, C.Y., Lau, A., Orlando, D.A., Vakoc, C.R., Bradner, J.E., Lee, T.I. and Young, R.A. 2013. Selective inhibition of tumor oncogenes by disruption of super-enhancers. *Cell* 153(2), pp. 320–334.

Lu, K.V., Chang, J.P., Parachoniak, C.A., Pandika, M.M., Aghi, M.K., Meyronet, D., Isachenko, N., Fouse, S.D., Phillips, J.J., Cheresh, D.A., Park, M. and Bergers, G. 2012. VEGF inhibits tumor cell invasion and mesenchymal transition through a MET/VEGFR2 complex. *Cancer Cell* 22(1), pp. 21–35.

Luo, B., Cheung, H.W., Subramanian, A., Sharifnia, T., Okamoto, M., Yang, X., Hinkle, G., Boehm, J.S., Beroukhim, R., Weir, B.A., Mermel, C., Barbie, D.A., Awad, T., Zhou, X., Nguyen, T., Piqani, B., Li, C., Golub, T.R., Meyerson, M., Hacohen, N. and Root, D.E. 2008. Highly parallel identification of essential genes in cancer cells. *Proc Natl Acad Sci U S A* 105(51), pp. 20380–20385.

Lykke-Andersen, S. and Jensen, T.H. 2015. Nonsense-mediated mRNA decay: an intricate machinery that shapes transcriptomes. *Nat Rev Mol Cell Biol* 16(11), pp. 665–677.http://f1000.com/work/bibliography/1125118

Mack, G.S. (2010). To selectivity and beyond. Nat Biotechnol *28*, 1259–1266.

Maher, E.A., Furnari, F.B., Bachoo, R.M., Rowitch, D.H., Louis, D.N., Cavenee, W.K. and DePinho, R.A. 2001. Malignant glioma: genetics and biology of a grave matter. *Genes Dev* 15(11), pp. 1311–1333.

Mao, P., Joshi, K., Li, J., Kim, S.H., Li, P., Santana-Santos, L., Luthra, S., Chandran, U.R., Benos, P.V., Smith, L., Wang, M., Hu, B., Cheng, S.Y., Sobol, R.W. and Nakano, I. 2013. Mesenchymal glioma stem cells are maintained by activated

glycolytic metabolism involving aldehyde dehydrogenase 1A3. *Proc Natl Acad Sci U S A* 110(21), pp. 8644–8649.

Marei, H.E., Althani, A., Afifi, N., Michetti, F., Pescatori, M., Pallini, R., Casalbore, P., Cenciarelli, C., Schwartz, P., and Ahmed, A.E. (2011). Gene expression profiling of embryonic human neural stem cells and dopaminergic neurons from adult human substantia nigra. PLoS One *6*, e28420.

Marino ML, Pellegrini P, Di Lernia G, Djavaheri-Mergny M, Brnjic S, Zhang X, et al. Autophagy is a protective mechanism for human melanoma cells under acidic stress. J Biol Chem. 2012 Aug 31;287(36):30664–30676.

Marotta, L.L., Almendro, V., Marusyk, A., Shipitsin, M., Schemme, J., Walker, S.R., Bloushtain-Qimron, N., Kim, J.J., Choudhury, S.A., Maruyama, R., Wu, Z., Gönen, M., Mulvey, L.A., Bessarabova, M.O., Huh, S.J., Silver, S.J., Kim, S.Y., Park, S.Y., Lee, H.E., Anderson, K.S., Richardson, A.L., Nikolskaya, T., Nikolsky, Y., Liu, X.S., Root, D.E., Hahn, W.C., Frank, D.A. and Polyak, K. 2011. The JAK2/STAT3 signaling pathway is required for growth of $CD44^{+}CD24^{-}$ stem cell-like breast cancer cells in human tumors. *J Clin Invest* 121(7), pp. 2723–2735.

Martinez-Ledesma, E., de Groot, J.F. and Verhaak, R.G. 2015. Seek and destroy: relating cancer drivers to therapies. *Cancer Cell* 27(3), pp. 319–321.

Matsuoka, S., Rotman, G., Ogawa, A., Shiloh, Y., Tamai, K. and Elledge, S.J. 2000. Ataxia telangiectasia-mutated phosphorylates Chk2 in vivo and in vitro. *Proc Natl Acad Sci U S A* 97(19), pp. 10389–10394.http://f1000.com/work/bibliography/1276905

Maze, I., Feng, J., Wilkinson, M.B., Sun, H., Shen, L., and Nestler, E.J. (2011). Cocaine dynamically regulates heterochromatin and repetitive element unsilencing in nucleus accumbens. Proc Natl Acad Sci U S A *108*, 3035-3040.

McFarland, B.C., Ma, J.-Y., Langford, C.P., Gillespie, G.Y., Yu, H., Zheng, Y., Nozell, S.E., Huszar, D. and Benveniste, E.N. 2011. Therapeutic potential of AZD1480 for the treatment of human glioblastoma. *Mol Cancer Ther* 10(12), pp. 2384–2393.http://f1000.com/work/bibliography/58670

McIlwain DR, Pan Q, Reilly PT, Elia AJ, McCracken S, Wakeham AC, et al. Smg1 is required for embryogenesis and regulates diverse genes via alternative splicing coupled to nonsense-mediated mRNA decay. Proc Natl Acad Sci U S A. 2010 Jul 6;107(27):12186–12191.

Mellinghoff, I.K., Schultz, N., Mischel, P.S. and Cloughesy, T.F. 2012. Will kinase inhibitors make it as glioblastoma drugs? *Curr Top Microbiol Immunol* 355, pp. 135–169.

Méndez, O., Zavadil, J., Esencay, M., Lukyanov, Y., Santovasi, D., Wang, S.-C., Newcomb, E.W. and Zagzag, D. 2010. Knock down of HIF-1alpha in glioma cells reduces migration in vitro and invasion in vivo and impairs their ability to form tumor spheres. *Mol Cancer* 9, p. 133.http://f1000.com/work/bibliography/57558

Miklossy, G., Hilliard, T.S. and Turkson, J. 2013. Therapeutic modulators of STAT signalling for human diseases. *Nat Rev Drug Discov* 12(8), pp. 611–629.http://f1000.com/work/bibliography/805634

Milkiewicz, M., Ispanovic, E., Doyle, J.L. and Haas, T.L. 2006. Regulators of angiogenesis and strategies for their therapeutic manipulation. *Int J Biochem Cell Biol* 38(3), pp. 333–357.http://f1000.com/work/bibliography/1173575

Moffat, J., Grueneberg, D.A., Yang, X., Kim, S.Y., Kloepfer, A.M., Hinkle, G., Piqani, B., Eisenhaure, T.M., Luo, B., Grenier, J.K., Carpenter, A.E., Foo, S.Y., Stewart, S.A., Stockwell, B.R., Hacohen, N., Hahn, W.C., Lander, E.S., Sabatini, D.M. and Root, D.E. 2006. A lentiviral RNAi library for human and mouse genes applied to an arrayed viral high-content screen. *Cell* 124(6), pp. 1283–1298.

Momota H, Nerio E, Holland EC. Perifosine inhibits multiple signaling pathways in glial progenitors and cooperates with temozolomide to arrest cell proliferation in gliomas in vivo. Cancer Research. 2005 August 15;65(16):7429-35.

Moreno, M., Fernández, V., Monllau, J.M., Borrell, V., Lerin, C. and de la Iglesia, N. 2015. Transcriptional Profiling of Hypoxic Neural Stem Cells Identifies Calcineurin-NFATc4 Signaling as a Major Regulator of Neural Stem Cell Biology. *Stem Cell Reports* 5(2), pp. 157–165.http://f1000.com/work/bibliography/629908

Morrison, S.J. and Spradling, A.C. 2008. Stem cells and niches: mechanisms that promote stem cell maintenance throughout life. *Cell* 132(4), pp. 598–611.http://f1000.com/work/bibliography/65456

Murat, A., Migliavacca, E., Gorlia, T., Lambiv, W.L., Shay, T., Hamou, M.F., de Tribolet, N., Regli, L., Wick, W., Kouwenhoven, M.C., Hainfellner, J.A., Heppner, F.L., Dietrich, P.Y., Zimmer, Y., Cairncross, J.G., Janzer, R.C., Domany, E., Delorenzi, M., Stupp, R. and Hegi, M.E. 2008. Stem cell-related "self-renewal" signature and high epidermal growth factor receptor expression associated with resistance to concomitant chemoradiotherapy in glioblastoma. *J Clin Oncol* 26(18), pp. 3015–3024.

Nadkarni, A., Shrivastav, M., Mladek, A.C., Schwingler, P.M., Grogan, P.T., Chen, J. and Sarkaria, J.N. 2012. ATM inhibitor KU-55933 increases the TMZ responsiveness of only inherently TMZ sensitive GBM cells. *J Neurooncol* 110(3), pp. 349–357.

Natsume, A., Ito, M., Katsushima, K., Ohka, F., Hatanaka, A., Shinjo, K., Sato, S., Takahashi, S., Ishikawa, Y., Takeuchi, I., Shimogawa, H., Uesugi, M., Okano, H., Kim, S.U., Wakabayashi, T., Issa, J.P., Sekido, Y. and Kondo, Y. 2013. Chromatin regulator PRC2 is a key regulator of epigenetic plasticity in glioblastoma. *Cancer Res* 73(14), pp. 4559–4570.

Niwa, H., Burdon, T., Chambers, I. and Smith, A. 1998. Self-renewal of pluripotent embryonic stem cells is mediated via activation of STAT3. *Genes Dev* 12(13), pp. 2048–2060.http://f1000.com/work/bibliography/65578

Niyazi, M., Harter, P.N., Hattingen, E., Rottler, M., von Baumgarten, L., Proescholdt, M., Belka, C., Lauber, K. and Mittelbronn, M. 2015. Bevacizumab and radiotherapy for the treatment of glioblastoma: brothers in arms or unholy alliance? *Oncotarget*.

Noushmehr, H., Weisenberger, D.J., Diefes, K., Phillips, H.S., Pujara, K., Berman, B.P., Pan, F., Pelloski, C.E., Sulman, E.P., Bhat, K.P., Verhaak, R.G., Hoadley, K.A., Hayes, D.N., Perou, C.M., Schmidt, H.K., Ding, L., Wilson, R.K., Van Den Berg, D., Shen, H., Bengtsson, H., Neuvial, P., Cope, L.M., Buckley, J., Herman, J.G., Baylin, S.B., Laird, P.W., Aldape, K. and Cancer Genome Atlas Research Network 2010. Identification of a CpG island methylator phenotype that defines a distinct subgroup of glioma. *Cancer Cell* 17(5), pp. 510–522.

Ntziachristos, P., Tsirigos, A., Welstead, G.G., Trimarchi, T., Bakogianni, S., Xu, L., Loizou, E., Holmfeldt, L., Strikoudis, A., King, B.*, et al.* (2014). Contrasting roles of histone 3 lysine 27 demethylases in acute lymphoblastic leukaemia. Nature *514*, 513-517.

Okada, Y., Shimazaki, T., Sobue, G. and Okano, H. 2004. Retinoic-acid-concentration-dependent acquisition of neural cell identity during in vitro differentiation of mouse embryonic stem cells. *Dev Biol* 275(1), pp. 124–142.http://f1000.com/work/bibliography/1276829

Omuro, A. and DeAngelis, L.M. 2013. Glioblastoma and other malignant gliomas: a clinical review. *JAMA* 310(17), pp. 1842–1850.

Ory, D.S., Neugeboren, B.A., and Mulligan, R.C. (1996). A stable human-derived packaging cell line for production of high titer retrovirus/vesicular stomatitis virus G pseudotypes. Proc Natl Acad Sci U S A *93*, 11400-11406.

Pan, J., Zhang, J., Hill, A., Lapan, P., Berasi, S., Bates, B., Miller, C. and Haney, S. 2013. A kinome-wide siRNA screen identifies multiple roles for protein kinases in hypoxic stress adaptation, including roles for IRAK4 and GAK in protection against apoptosis in VHL-/- renal carcinoma cells, despite activation of the NF-κB pathway. *J Biomol Screen* 18(7), pp. 782–796.http://f1000.com/work/bibliography/58558

Pardal, R., Clarke, M.F. and Morrison, S.J. 2003. Applying the principles of stem-cell biology to cancer. *Nat Rev Cancer* 3(12), pp. 895–902.

Park, E.C. and Rongo, C. 2016. The p38 MAP kinase pathway modulates the hypoxia response and glutamate receptor trafficking in aging neurons. *elife* 5.

Parsons, D.W., Jones, S., Zhang, X., Lin, J.C., Leary, R.J., Angenendt, P., Mankoo, P., Carter, H., Siu, I.M., Gallia, G.L., Olivi, A., McLendon, R., Rasheed, B.A., Keir, S., Nikolskaya, T., Nikolsky, Y., Busam, D.A., Tekleab, H., Diaz, L.A., Hartigan, J., Smith, D.R., Strausberg, R.L., Marie, S.K., Shinjo, S.M., Yan, H., Riggins, G.J., Bigner, D.D., Karchin, R., Papadopoulos, N., Parmigiani, G., Vogelstein, B., Velculescu, V.E. and Kinzler, K.W. 2008. An integrated genomic analysis of human glioblastoma multiforme. *Science* 321(5897), pp. 1807–1812.

Patel, A.P., Tirosh, I., Trombetta, J.J., Shalek, A.K., Gillespie, S.M., Wakimoto, H., Cahill, D.P., Nahed, B.V., Curry, W.T., Martuza, R.L., Louis, D.N., Rozenblatt-

Rosen, O., Suvà, M.L., Regev, A. and Bernstein, B.E. 2014. Single-cell RNA-seq highlights intratumoral heterogeneity in primary glioblastoma. *Science* 344(6190), pp. 1396–1401.

Pattabiraman, D.R. and Weinberg, R.A. 2014. Tackling the cancer stem cells - what challenges do they pose? *Nat Rev Drug Discov* 13(7), pp. 497–512.

Peñuelas, S., Anido, J., Prieto-Sánchez, R.M., Folch, G., Barba, I., Cuartas, I., García-Dorado, D., Poca, M.A., Sahuquillo, J., Baselga, J. and Seoane, J. 2009. TGF-beta increases glioma-initiating cell self-renewal through the induction of LIF in human glioblastoma. *Cancer Cell* 15(4), pp. 315–327.

Pezuk, J A, Brassesco, M.S., Morales, A.G., de Oliveira, J.C., de Paula Queiroz, R.G., Machado, H.R., Carlotti, C.G., Neder, L., Scrideli, C.A. and Tone, L.G. 2013. Polo-like kinase 1 inhibition causes decreased proliferation by cell cycle arrest, leading to cell death in glioblastoma. *Cancer Gene Ther* 20(9), pp. 499–506.

Pezuk, Julia Alejandra, Brassesco, M.S., Morales, A.G., de Oliveira, J.C., de Oliveira, H.F., Scrideli, C.A. and Tone, L.G. 2013. Inhibition of polo-like kinase 1 induces cell cycle arrest and sensitizes glioblastoma cells to ionizing radiation. *Cancer Biother Radiopharm* 28(7), pp. 516–522.

Piccirillo, S.G., Reynolds, B.A., Zanetti, N., Lamorte, G., Binda, E., Broggi, G., Brem, H., Olivi, A., Dimeco, F., and Vescovi, A.L. (2006). Bone morphogenetic proteins inhibit the tumorigenic potential of human brain tumour-initiating cells. Nature *444*, 761-765.

Pollard, S.M., Yoshikawa, K., Clarke, I.D., Danovi, D., Stricker, S., Russell, R., Bayani, J., Head, R., Lee, M., Bernstein, M., et al. (2009). Glioma stem cell lines expanded in adherent culture have tumor-specific phenotypes and are suitable for chemical and genetic screens. Cell Stem Cell *4*, 568–580.

Popp MW, Maquat LE. The dharma of nonsense-mediated mRNA decay in mammalian cells. Mol Cells. 2014 Jan 27;37(1):1–8.

Prados, M.D., Chang, S.M., Butowski, N., DeBoer, R., Parvataneni, R., Carliner, H., Kabuubi, P., Ayers-Ringler, J., Rabbitt, J., Page, M., Fedoroff, A., Sneed, P.K., Berger, M.S., McDermott, M.W., Parsa, A.T., Vandenberg, S., James, C.D., Lamborn, K.R., Stokoe, D. and Haas-Kogan, D.A. 2009. Phase II study of erlotinib plus temozolomide during and after radiation therapy in patients with newly diagnosed glioblastoma multiforme or gliosarcoma. *J Clin Oncol* 27(4), pp. 579–584.http://f1000.com/work/bibliography/1012203

Pulak, R. and Anderson, P. 1993. mRNA surveillance by the Caenorhabditis elegans smg genes. *Genes Dev* 7(10), pp. 1885–1897.http://f1000.com/work/bibliography/1281903

Qiang L, Wu C, Ming M, Viollet B, He YY. Autophagy controls p38 activation to promote cell survival under genotoxic stress. J Biol Chem. 2013 Jan 18;288(3):1603–1611.

Quintana, E., Shackleton, M., Sabel, M.S., Fullen, D.R., Johnson, T.M. and Morrison, S.J. 2008. Efficient tumour formation by single human melanoma cells. *Nature* 456(7222), pp. 593–598.

Quiros, S., Roos, W.P. and Kaina, B. 2011. Rad51 and BRCA2--New molecular targets for sensitizing glioma cells to alkylating anticancer drugs. *PLoS ONE* 6(11), p. e27183.http://f1000.com/work/bibliography/1281912

Rahaman, S.O., Harbor, P.C., Chernova, O., Barnett, G.H., Vogelbaum, M.A. and Haque, S.J. 2002. Inhibition of constitutively active Stat3 suppresses proliferation and induces apoptosis in glioblastoma multiforme cells. *Oncogene* 21(55), pp. 8404–8413.

Rajan, P. (2011). STATus and Context within the Mammalian Nervous System. Mol Med *17*, 965–973.

Rajan, P., and McKay, R.D. (1998). Multiple routes to astrocytic differentiation in the CNS. J Neurosci *18*, 3620-3629.

Ramachandran, S., Ient, J., Göttgens, E.-L., Krieg, A.J. and Hammond, E.M. 2015. Epigenetic Therapy for Solid Tumors: Highlighting the Impact of Tumor Hypoxia. *Genes (Basel)* 6(4), pp. 935–956.http://f1000.com/work/bibliography/1149461

Ramirez, Y.P., Mladek, A.C., Phillips, R.M., Gynther, M., Rautio, J., Ross, A.H., Wheelhouse, R.T. and Sakaria, J.N. 2015. Evaluation of novel imidazotetrazine analogues designed to overcome temozolomide resistance and glioblastoma regrowth. *Mol Cancer Ther* 14(1), pp. 111–119.

Ramkissoon, S.H., Bi, W.L., Schumacher, S.E., Ramkissoon, L.A., Haidar, S., Knoff, D., Dubuc, A., Brown, L., Burns, M., Cryan, J.B., Abedalthagafi, M., Kang, Y.J., Schultz, N., Reardon, D.A., Lee, E.Q., Rinne, M.L., Norden, A.D., Nayak, L., Ruland, S., Doherty, L.M. and Ligon, K.L. 2015. Clinical implementation of integrated whole-genome copy number and mutation profiling for glioblastoma. *Neuro Oncol* 17(10), pp. 1344–1355.http://f1000.com/work/bibliography/771652

Rebhan, M., Chalifa-Caspi, V., Prilusky, J. and Lancet, D. 1998. GeneCards: a novel functional genomics compendium with automated data mining and query reformulation support. *Bioinformatics* 14(8), pp. 656–664.

Reithmeier, T., Graf, E., Piroth, T., Trippel, M., Pinsker, M.O. and Nikkhah, G. 2010. BCNU for recurrent glioblastoma multiforme: efficacy, toxicity and prognostic factors. *BMC Cancer* 10, p. 30.

Reynolds, A. and Weiss. Generation of Neurons and Astrocytes from Isolated Cells of the Adult Mammalian Central Nervous System.

Reynolds, B.A. and Vescovi, A.L. 2009. Brain Cancer Stem Cells: Think Twice before Going Flat. *Cell Stem Cell* 5(5), pp. 466–467.

Rheinbay, E., Suvà, M.L., Gillespie, S.M., Wakimoto, H., Patel, A.P., Shahid, M., Oksuz, O., Rabkin, S.D., Martuza, R.L., Rivera, M.N., Louis, D.N., Kasif, S., Chi,

A.S. and Bernstein, B.E. 2013. An aberrant transcription factor network essential for Wnt signaling and stem cell maintenance in glioblastoma. *Cell Rep* 3(5), pp. 1567–1579.

Ricci-Vitiani, L., Pallini, R., Biffoni, M., Todaro, M., Invernici, G., Cenci, T., Maira, G., Parati, E.A., Stassi, G., Larocca, L.M. and De Maria, R. 2010. Tumour vascularization via endothelial differentiation of glioblastoma stem-like cells. *Nature* 468(7325), pp. 824–828.

Rich, J.N. and Bigner, D.D. 2004. Development of novel targeted therapies in the treatment of malignant glioma. *Nat Rev Drug Discov* 3(5), pp. 430–446.

Roadmap Epigenomics Consortium, Kundaje, A., Meuleman, W., Ernst, J., Bilenky, M., Yen, A., Heravi-Moussavi, A., Kheradpour, P., Zhang, Z., Wang, J., Ziller, M.J., Amin, V., Whitaker, J.W., Schultz, M.D., Ward, L.D., Sarkar, A., Quon, G., Sandstrom, R.S., Eaton, M.L., Wu, Y.-C. and Kellis, M. 2015. Integrative analysis of 111 reference human epigenomes. *Nature* 518(7539), pp. 317–330.http://f1000.com/work/bibliography/48808

Robinson, G., Parker, M., Kranenburg, T.A., Lu, C., Chen, X., Ding, L., Phoenix, T.N., Hedlund, E., Wei, L., Zhu, X., Chalhoub, N., Baker, S.J., Huether, R., Kriwacki, R., Curley, N., Thiruvenkatam, R., Wang, J., Wu, G., Rusch, M., Hong, X. and Gilbertson, R.J. 2012. Novel mutations target distinct subgroups of medulloblastoma. *Nature* 488(7409), pp. 43–48.http://f1000.com/work/bibliography/58927

Rokavec, M., Öner, M.G., Li, H., Jackstadt, R., Jiang, L., Lodygin, D., Kaller, M., Horst, D., Ziegler, P.K., Schwitalla, S., Slotta-Huspenina, J., Bader, F.G., Greten, F.R. and Hermeking, H. 2014. IL-6R/STAT3/miR-34a feedback loop promotes EMT-mediated colorectal cancer invasion and metastasis. *J Clin Invest* 124(4), pp. 1853–1867.http://f1000.com/work/bibliography/93341

Romm, E., Nielsen, J.A., Kim, J.G. and Hudson, L.D. 2005. Myt1 family recruits histone deacetylase to regulate neural transcription. *J Neurochem* 93(6), pp. 1444–1453.http://f1000.com/work/bibliography/1169323

Rosenbluh, J., Nijhawan, D., Cox, A.G., Li, X., Neal, J.T., Schafer, E.J., Zack, T.I., Wang, X., Tsherniak, A., Schinzel, A.C., Shao, D.D., Schumacher, S.E., Weir, B.A., Vazquez, F., Cowley, G.S., Root, D.E., Mesirov, J.P., Beroukhim, R., Kuo, C.J., Goessling, W. and Hahn, W.C. 2012. β-Catenin-driven cancers require a YAP1 transcriptional complex for survival and tumorigenesis. *Cell* 151(7), pp. 1457–1473.

Ruano, Y., Mollejo, M., Ribalta, T., Fiaño, C., Camacho, F.I., Gómez, E., de Lope, A.R., Hernández-Moneo, J.-L., Martínez, P. and Meléndez, B. 2006. Identification of novel candidate target genes in amplicons of Glioblastoma multiforme tumors detected by expression and CGH microarray profiling. *Mol Cancer* 5, p. 39.

Sackmann A, Heiner M, Koch I. Application of Petri net based analysis techniques to signal transduction pathways. BMC Bioinformatics. 2006 Nov 2;7:482.

Sarma, K., Margueron, R., Ivanov, A., Pirrotta, V. and Reinberg, D. 2008. Ezh2 requires PHF1 to efficiently catalyze H3 lysine 27 trimethylation in vivo. *Mol Cell Biol* 28(8), pp. 2718–2731.http://f1000.com/work/bibliography/93348

Sato, A., Sekine, M., Virgona, N., Ota, M. and Yano, T. 2012. Yes is a central mediator of cell growth in malignant mesothelioma cells. *Oncol Rep* 28(5), pp. 1889–1893.

Schneider, H., Schwartzberg, P.L. and Rudd, C.E. 1998. Resting lymphocyte kinase (Rlk/Txk) phosphorylates the YVKM motif and regulates PI 3-kinase binding to T-cell antigen CTLA-4. *Biochem Biophys Res Commun* 252(1), pp. 14–19.

Schuler, M., Bossy-Wetzel, E., Goldstein, J.C., Fitzgerald, P. and Green, D.R. 2000. p53 induces apoptosis by caspase activation through mitochondrial cytochrome c release. *J Biol Chem* 275(10), pp. 7337–7342.http://f1000.com/work/bibliography/1258554

Schwartzentruber, J., Korshunov, A., Liu, X.-Y., Jones, D.T.W., Pfaff, E., Jacob, K., Sturm, D., Fontebasso, A.M., Quang, D.-A.K., Tönjes, M., Hovestadt, V., Albrecht, S., Kool, M., Nantel, A., Konermann, C., Lindroth, A., Jäger, N., Rausch, T., Ryzhova, M., Korbel, J.O. and Jabado, N. 2012. Driver mutations in histone H3.3 and chromatin remodelling genes in paediatric glioblastoma. *Nature* 482(7384), pp. 226–231.http://f1000.com/work/bibliography/57952

Seidel, S., Garvalov, B.K., Wirta, V., von Stechow, L., Schänzer, A., Meletis, K., Wolter, M., Sommerlad, D., Henze, A.-T., Nistér, M., Reifenberger, G., Lundeberg, J., Frisén, J. and Acker, T. 2010. A hypoxic niche regulates glioblastoma stem cells through hypoxia inducible factor 2 alpha. *Brain* 133(Pt 4), pp. 983–995.http://f1000.com/work/bibliography/57821

Sen, G.L., Webster, D.E., Barragan, D.I., Chang, H.Y., and Khavari, P.A. (2008). Control of differentiation in a self-renewing mammalian tissue by the histone demethylase JMJD3. Genes & development *22*, 1865-1870.

Sherry, M.M., Reeves, A., Wu, J.K. and Cochran, B.H. 2009. STAT3 is required for proliferation and maintenance of multipotency in glioblastoma stem cells. *Stem Cells* 27(10), pp. 2383–2392.http://f1000.com/work/bibliography/57460

Shimizu, S., Kadowaki, M., Yoshioka, H., Kambe, A., Watanabe, T., Kinyamu, H.K., and Eling, T.E. (2013). Proteasome inhibitor MG132 induces NAG-1/GDF15 expression through the p38 MAPK pathway in glioblastoma cells. Biochem Biophys Res Commun *430*, 1277-1282.

Shojaei, F., Lee, J.H., Simmons, B.H., Wong, A., Esparza, C.O., Plumlee, P.A., Feng, J., Stewart, A.E., Hu-Lowe, D.D. and Christensen, J.G. 2010. HGF/c-Met acts as an alternative angiogenic pathway in sunitinib-resistant tumors. *Cancer Res* 70(24), pp. 10090–10100.

Siddiquee, K., Zhang, S., Guida, W.C., Blaskovich, M.A., Greedy, B., Lawrence, H.R., Yip, M.L., Jove, R., McLaughlin, M.M., Lawrence, N.J., *et al.* (2007). Selective

chemical probe inhibitor of Stat3, identified through structure-based virtual screening, induces antitumor activity. Proc Natl Acad Sci U S A *104*, 7391-7396.

Signore, M., Pelacchi, F., di Martino, S., Runci, D., Biffoni, M., Giannetti, S., Morgante, L., De Majo, M., Petricoin, E.F., Stancato, L., Larocca, L.M., De Maria, R., Pallini, R. and Ricci-Vitiani, L. 2014. Combined PDK1 and CHK1 inhibition is required to kill glioblastoma stem-like cells in vitro and in vivo. *Cell Death Dis* 5, p. e1223.

Singh, S.K., Hawkins, C., Clarke, I.D., Squire, J.A., Bayani, J., Hide, T., Henkelman, R.M., Cusimano, M.D. and Dirks, P.B. 2004. Identification of human brain tumour initiating cells. *Nature* 432(7015), pp. 396–401.

Sithanandam, G. and Anderson, L.M. 2008. The ERBB3 receptor in cancer and cancer gene therapy. *Cancer Gene Ther* 15(7), pp. 413–448.

Smith, J., Tho, L.M., Xu, N. and Gillespie, D.A. 2010. The ATM-Chk2 and ATR-Chk1 pathways in DNA damage signaling and cancer. *Adv Cancer Res* 108, pp. 73–112.http://f1000.com/work/bibliography/120045

Soda, Y., Marumoto, T., Friedmann-Morvinski, D., Soda, M., Liu, F., Michiue, H., Pastorino, S., Yang, M., Hoffman, R.M., Kesari, S. and Verma, I.M. 2011. Transdifferentiation of glioblastoma cells into vascular endothelial cells. *Proc Natl Acad Sci U S A* 108(11), pp. 4274–4280.

Soeda, A., Park, M., Lee, D., Mintz, A., Androutsellis-Theotokis, A., McKay, R.D., Engh, J., Iwama, T., Kunisada, T., Kassam, A.B., et al. (2009). Hypoxia promotes expansion of the CD133-positive glioma stem cells through activation of HIF-1alpha. Oncogene *28*, 3949–3959.

Soler, M., Mancini, F., Meca-Cortés, O., Sánchez-Cid, L., Rubio, N., López-Fernández, S., Lozano, J.J., Blanco, J., Fernández, P.L. and Thomson, T.M. 2009. HER3 is required for the maintenance of neuregulin-dependent and -independent attributes of malignant progression in prostate cancer cells. *Int J Cancer* 125(11), pp. 2565–2575.

Son, M.J., Woolard, K., Nam, D.H., Lee, J. and Fine, H.A. 2009. SSEA-1 is an enrichment marker for tumor-initiating cells in human glioblastoma. *Cell Stem Cell* 4(5), pp. 440–452.

Song, H., Wang, R., Wang, S., and Lin, J. (2005). A low-molecular-weight compound discovered through virtual database screening inhibits Stat3 function in breast cancer cells. Proc Natl Acad Sci U S A *102*, 4700-4705.

Song, M.R., and Ghosh, A. (2004). FGF2-induced chromatin remodeling regulates CNTF-mediated gene expression and astrocyte differentiation. Nat Neurosci *7*, 229-235.

Stechishin, O.D., Luchman, H.A., Ruan, Y., Blough, M.D., Nguyen, S.A., Kelly, J.J., Cairncross, J.G. and Weiss, S. 2013. On-target JAK2/STAT3 inhibition slows disease

progression in orthotopic xenografts of human glioblastoma brain tumor stem cells. *Neuro Oncol* 15(2), pp. 198–207.

Stupp, R., Mason, W.P., van den Bent, M.J., Weller, M., Fisher, B., Taphoorn, M.J., Belanger, K., Brandes, A.A., Marosi, C., Bogdahn, U., Curschmann, J., Janzer, R.C., Ludwin, S.K., Gorlia, T., Allgeier, A., Lacombe, D., Cairncross, J.G., Eisenhauer, E., Mirimanoff, R.O., European Organisation for Research and Treatment of Cancer Brain Tumor and Radiotherapy Groups and National Cancer Institute of Canada Clinical Trials Group 2005. Radiotherapy plus concomitant and adjuvant temozolomide for glioblastoma. *N Engl J Med* 352(10), pp. 987–996.

Sturm, D., Witt, H., Hovestadt, V., Khuong-Quang, D.-A., Jones, D.T.W., Konermann, C., Pfaff, E., Tönjes, M., Sill, M., Bender, S., Kool, M., Zapatka, M., Becker, N., Zucknick, M., Hielscher, T., Liu, X.-Y., Fontebasso, A.M., Ryzhova, M., Albrecht, S., Jacob, K. and Pfister, S.M. 2012. Hotspot mutations in H3F3A and IDH1 define distinct epigenetic and biological subgroups of glioblastoma. *Cancer Cell* 22(4), pp. 425–437.http://f1000.com/work/bibliography/58673

Sun, C. and Bernards, R. 2014. Feedback and redundancy in receptor tyrosine kinase signaling: relevance to cancer therapies. *Trends Biochem Sci* 39(10), pp. 465–474.http://f1000.com/work/bibliography/1296256

Suvà, M.-L., Riggi, N., Janiszewska, M., Radovanovic, I., Provero, P., Stehle, J.-C., Baumer, K., Le Bitoux, M.-A., Marino, D., Cironi, L., Marquez, V.E., Clément, V. and Stamenkovic, I. 2009. EZH2 is essential for glioblastoma cancer stem cell maintenance. *Cancer Res* 69(24), pp. 9211–9218.http://f1000.com/work/bibliography/57430

Szwajda, A., Gautam, P., Karhinen, L., Jha, S.K., Saarela, J., Shakyawar, S., Turunen, L., Yadav, B., Tang, J., Wennerberg, K. and Aittokallio, T. 2015. Systematic Mapping of Kinase Addiction Combinations in Breast Cancer Cells by Integrating Drug Sensitivity and Selectivity Profiles. *Chem Biol* 22(8), pp. 1144–1155.http://f1000.com/work/bibliography/648075

Takeda, K., Noguchi, K., Shi, W., Tanaka, T., Matsumoto, M., Yoshida, N., Kishimoto, T. and Akira, S. 1997. Targeted disruption of the mouse Stat3 gene leads to early embryonic lethality. *Proc Natl Acad Sci U S A* 94(8), pp. 3801–3804.http://f1000.com/work/bibliography/318682

Takizawa, T., Nakashima, K., Namihira, M., Ochiai, W., Uemura, A., Yanagisawa, M., Fujita, N., Nakao, M. and Taga, T. 2001. DNA methylation is a critical cell-intrinsic determinant of astrocyte differentiation in the fetal brain. *Dev Cell* 1(6), pp. 749–758.http://f1000.com/work/bibliography/443408

Tang, Y., Dai, Y., Grant, S. and Dent, P. 2012. Enhancing CHK1 inhibitor lethality in glioblastoma. *Cancer Biol Ther* 13(6), pp. 379–388.

Tang, Y., Luo, Y., Jiang, Z., Ma, Y., Lin, C.-J., Kim, C., Carter, M.G., Amano, T., Park, J., Kish, S. and Tian, X.C. 2012. Jak/Stat3 signaling promotes somatic cell

reprogramming by epigenetic regulation. *Stem Cells* 30(12), pp. 2645–2656.http://f1000.com/work/bibliography/989196

Tang, Y., Luo, Y., Jiang, Z., Ma, Y., Lin, C.-J., Kim, C., Carter, M.G., Amano, T., Park, J., Kish, S., et al. (2012). Jak/Stat3 signaling promotes somatic cell reprogramming by epigenetic regulation. Stem Cells *30*, 2645–2656.http://f1000.com/work/bibliography/989196

Taylor, J.W., Dietrich, J., Gerstner, E.R., Norden, A.D., Rinne, M.L., Cahill, D.P., Stemmer-Rachamimov, A., Wen, P.Y., Betensky, R.A., Giorgio, D.H., Snodgrass, K., Randall, A.E., Batchelor, T.T. and Chi, A.S. 2015. Phase 2 study of bosutinib, a Src inhibitor, in adults with recurrent glioblastoma. *J Neurooncol* 121(3), pp. 557–563.

Tiedemann, R.E., Zhu, Y.X., Schmidt, J., Yin, H., Shi, C.-X., Que, Q., Basu, G., Azorsa, D., Perkins, L.M., Braggio, E., Fonseca, R., Bergsagel, P.L., Mousses, S. and Stewart, A.K. 2010. Kinome-wide RNAi studies in human multiple myeloma identify vulnerable kinase targets, including a lymphoid-restricted kinase, GRK6. *Blood* 115(8), pp. 1594–1604.

Toledo, C.M., Herman, J.A., Olsen, J.B., Ding, Y., Corrin, P., Girard, E.J., Olson, J.M., Emili, A., DeLuca, J.G. and Paddison, P.J. 2014. BuGZ is required for Bub3 stability, Bub1 kinetochore function, and chromosome alignment. *Dev Cell* 28(3), pp. 282–294.http://f1000.com/work/bibliography/1197629

Tsai, M.C., Manor, O., Wan, Y., Mosammaparast, N., Wang, J.K., Lan, F., Shi, Y., Segal, E. and Chang, H.Y. 2010. Long noncoding RNA as modular scaffold of histone modification complexes. *Science* 329(5992), pp. 689–693.

Turkson, J., Bowman, T., Garcia, R., Caldenhoven, E., De Groot, R.P. and Jove, R. 1998. Stat3 activation by Src induces specific gene regulation and is required for cell transformation. *Mol Cell Biol* 18(5), pp. 2545–2552.

Ura, H., Usuda, M., Kinoshita, K., Sun, C., Mori, K., Akagi, T., Matsuda, T., Koide, H. and Yokota, T. 2008. STAT3 and Oct-3/4 control histone modification through induction of Eed in embryonic stem cells. *J Biol Chem* 283(15), pp. 9713–9723.http://f1000.com/work/bibliography/1158305

Urayama, S., Semi, K., Sanosaka, T., Hori, Y., Namihira, M., Kohyama, J., Takizawa, T., and Nakashima, K. (2013). Chromatin Accessibility at a STAT3 Target Site Is Altered Prior to Astrocyte Differentiation. Cell Struct Funct *38*, 55-66.

Valli, E., Trazzi, S., Fuchs, C., Erriquez, D., Bartesaghi, R., Perini, G. and Ciani, E. 2012. CDKL5, a novel MYCN-repressed gene, blocks cell cycle and promotes differentiation of neuronal cells. *Biochim Biophys Acta* 1819(11-12), pp. 1173–1185.http://f1000.com/work/bibliography/1259280

van Haaften, G., Dalgliesh, G.L., Davies, H., Chen, L., Bignell, G., Greenman, C., Edkins, S., Hardy, C., O'Meara, S., Teague, J.*, et al.* (2009). Somatic mutations of the histone H3K27 demethylase gene UTX in human cancer. Nature genetics *41*, 521-523.

Vanner, R.J., Remke, M., Gallo, M., Selvadurai, H.J., Coutinho, F., Lee, L., Kushida, M., Head, R., Morrissy, S., Zhu, X., Aviv, T., Voisin, V., Clarke, I.D., Li, Y., Mungall, A.J., Moore, R.A., Ma, Y., Jones, S.J., Marra, M.A., Malkin, D., Northcott, P.A., Kool, M., Pfister, S.M., Bader, G., Hochedlinger, K., Korshunov, A., Taylor, M.D. and Dirks, P.B. 2014. Quiescent sox2(+) cells drive hierarchical growth and relapse in sonic hedgehog subgroup medulloblastoma. *Cancer Cell* 26(1), pp. 33–47.

Venneti, S., Garimella, M.T., Sullivan, L.M., Martinez, D., Huse, J.T., Heguy, A., Santi, M., Thompson, C.B. and Judkins, A.R. 2013. Evaluation of histone 3 lysine 27 trimethylation (H3K27me3) and enhancer of Zest 2 (EZH2) in pediatric glial and glioneuronal tumors shows decreased H3K27me3 in H3F3A K27M mutant glioblastomas. *Brain Pathol* 23(5), pp. 558–564.http://f1000.com/work/bibliography/58459

Verhaak, R.G., Hoadley, K.A., Purdom, E., Wang, V., Qi, Y., Wilkerson, M.D., Miller, C.R., Ding, L., Golub, T., Mesirov, J.P., Alexe, G., Lawrence, M., O'Kelly, M., Tamayo, P., Weir, B.A., Gabriel, S., Winckler, W., Gupta, S., Jakkula, L., Feiler, H.S., Hodgson, J.G., James, C.D., Sarkaria, J.N., Brennan, C., Kahn, A., Spellman, P.T., Wilson, R.K., Speed, T.P., Gray, J.W., Meyerson, M., Getz, G., Perou, C.M., Hayes, D.N. and Cancer Genome Atlas Research Network 2010. Integrated genomic analysis identifies clinically relevant subtypes of glioblastoma characterized by abnormalities in PDGFRA, IDH1, EGFR, and NF1. *Cancer Cell* 17(1), pp. 98–110.

Vescovi, A.L., Galli, R., and Reynolds, B.A. (2006). Brain tumour stem cells. Nat Rev Cancer *6*, 425-436.

Villalonga-Planells, R., Coll-Mulet, L., Martínez-Soler, F., Castaño, E., Acebes, J.-J., Giménez-Bonafé, P., Gil, J. and Tortosa, A. 2011. Activation of p53 by nutlin-3a induces apoptosis and cellular senescence in human glioblastoma multiforme. *PLoS ONE* 6(4), p. e18588.

Viré, E., Brenner, C., Deplus, R., Blanchon, L., Fraga, M., Didelot, C., Morey, L., Van Eynde, A., Bernard, D., Vanderwinden, J.M., Bollen, M., Esteller, M., Di Croce, L., de Launoit, Y. and Fuks, F. 2006. The Polycomb group protein EZH2 directly controls DNA methylation. *Nature* 439(7078), pp. 871–874.

Vogelstein, B., Papadopoulos, N., Velculescu, V.E., Zhou, S., Diaz, L.A. and Kinzler, K.W. 2013. Cancer genome landscapes. *Science* 339(6127), pp. 1546–1558.

Vuppalapati, K.K., Bouderlique, T., Newton, P.T., Kaminskyy, V.O., Wehtje, H., Ohlsson, C., Zhivotovsky, B. and Chagin, A.S. 2015. Targeted Deletion of Autophagy Genes Atg5 or Atg7 in the Chondrocytes Promotes Caspase-Dependent Cell Death and Leads to Mild Growth Retardation. *J Bone Miner Res* 30(12), pp. 2249–2261.

Wakimoto, H., Mohapatra, G., Kanai, R., Curry, W.T., Yip, S., Nitta, M., Patel, A.P., Barnard, Z.R., Stemmer-Rachamimov, A.O., Louis, D.N., Martuza, R.L. and Rabkin, S.D. 2012. Maintenance of primary tumor phenotype and genotype in glioblastoma stem cells. *Neuro Oncol* 14(2), pp. 132–144.

Wang, D., Zavadil, J., Martin, L., Parisi, F., Friedman, E., Levy, D., Harding, H., Ron, D. and Gardner, L.B. 2011. Inhibition of nonsense-mediated RNA decay by the tumor microenvironment promotes tumorigenesis. *Mol Cell Biol* 31(17), pp. 3670–3680.

Wang, H., Lathia, J.D., Wu, Q., Wang, J., Li, Z., Heddleston, J.M., Eyler, C.E., Elderbroom, J., Gallagher, J., Schuschu, J., MacSwords, J., Cao, Y., McLendon, R.E., Wang, X.-F., Hjelmeland, A.B. and Rich, J.N. 2009. Targeting interleukin 6 signaling suppresses glioma stem cell survival and tumor growth. *Stem Cells* 27(10), pp. 2393–2404.http://f1000.com/work/bibliography/59046

Wang, L., Yu, Y., Chow, D.-C., Yan, F., Hsu, C.-C., Stossi, F., Mancini, M.A., Palzkill, T., Liao, L., Zhou, S., Xu, J., Lonard, D.M. and O'Malley, B.W. 2015. Characterization of a Steroid Receptor Coactivator Small Molecule Stimulator that Overstimulates Cancer Cells and Leads to Cell Stress and Death. *Cancer Cell* 28(2), pp. 240–252.

Wang, R., Chadalavada, K., Wilshire, J., Kowalik, U., Hovinga, K.E., Geber, A., Fligelman, B., Leversha, M., Brennan, C. and Tabar, V. 2010. Glioblastoma stem-like cells give rise to tumour endothelium. *Nature* 468(7325), pp. 829–833.

Wei, J., Barr, J., Kong, L.-Y., Wang, Y., Wu, A., Sharma, A.K., Gumin, J., Henry, V., Colman, H., Priebe, W., Sawaya, R., Lang, F.F. and Heimberger, A.B. 2010. Glioblastoma cancer-initiating cells inhibit T-cell proliferation and effector responses by the signal transducers and activators of transcription 3 pathway. *Mol Cancer Ther* 9(1), pp. 67–78.

Wen, P.Y., Chang, S.M., Lamborn, K.R., Kuhn, J.G., Norden, A.D., Cloughesy, T.F., Robins, H.I., Lieberman, F.S., Gilbert, M.R., Mehta, M.P., Drappatz, J., Groves, M.D., Santagata, S., Ligon, A.H., Yung, W.K.A., Wright, J.J., Dancey, J., Aldape, K.D., Prados, M.D. and Ligon, K.L. 2014. Phase I/II study of erlotinib and temsirolimus for patients with recurrent malignant gliomas: North American Brain Tumor Consortium trial 04-02. *Neuro Oncol* 16(4), pp. 567–578.

Wengrod, J., Martin, L., Wang, D., Frischmeyer-Guerrerio, P., Dietz, H.C. and Gardner, L.B. 2013a. Inhibition of nonsense-mediated RNA decay activates autophagy. *Mol Cell Biol* 33(11), pp. 2128–2135.

White, P.S., Maris, J.M., Beltinger, C., Sulman, E., Marshall, H.N., Fujimori, M., Kaufman, B.A., Biegel, J.A., Allen, C., Hilliard, C., et al. (1995). A region of consistent deletion in neuroblastoma maps within human chromosome 1p36.2-36.3. Proc Natl Acad Sci U S A *92*, 5520–5524.

Wiedemeyer, W.R., Dunn, I.F., Quayle, S.N., Zhang, J., Chheda, M.G., Dunn, G.P., Zhuang, L., Rosenbluh, J., Chen, S., Xiao, Y., Shapiro, G.I., Hahn, W.C. and Chin, L. 2010. Pattern of retinoblastoma pathway inactivation dictates response to CDK4/6 inhibition in GBM. *Proc Natl Acad Sci U S A* 107(25), pp. 11501–11506.

Wiencke, J.K., Zheng, S., Jelluma, N., Tihan, T., Vandenberg, S., Tamgüney, T., Baumber, R., Parsons, R., Lamborn, K.R., Berger, M.S., Wrensch, M.R., Haas-

Kogan, D.A. and Stokoe, D. 2007. Methylation of the PTEN promoter defines low-grade gliomas and secondary glioblastoma. *Neuro Oncol* 9(3), pp. 271–279.

Wilson, W.R. and Hay, M.P. 2011. Targeting hypoxia in cancer therapy. *Nat Rev Cancer* 11(6), pp. 393–410.

Woolard, K., and Fine, H.A. (2009). Glioma stem cells: better flat than round. Cell Stem Cell *4*, 466–467.

Wu, G., Broniscer, A., McEachron, T.A., Lu, C., Paugh, B.S., Becksfort, J., Qu, C., Ding, L., Huether, R., Parker, M., Zhang, Junyuan, Gajjar, A., Dyer, M.A., Mullighan, C.G., Gilbertson, R.J., Mardis, E.R., Wilson, R.K., Downing, J.R., Ellison, D.W., Zhang, Jinghui and St. Jude Children's Research Hospital–Washington University Pediatric Cancer Genome Project 2012. Somatic histone H3 alterations in pediatric diffuse intrinsic pontine gliomas and non-brainstem glioblastomas. *Nat Genet* 44(3), pp. 251–253.

Wu, G., Broniscer, A., McEachron, T.A., Lu, C., Paugh, B.S., Becksfort, J., Qu, C., Ding, L., Huether, R., Parker, M.*, et al.* (2012). Somatic histone H3 alterations in pediatric diffuse intrinsic pontine gliomas and non-brainstem glioblastomas. Nature genetics *44*, 251-253.

Wurdak, H., Zhu, S., Romero, A., Lorger, M., Watson, J., Chiang, C.-Y., Zhang, J., Natu, V.S., Lairson, L.L., Walker, J.R., Trussell, C.M., Harsh, G.R., Vogel, H., Felding-Habermann, B., Orth, A.P., Miraglia, L.J., Rines, D.R., Skirboll, S.L. and Schultz, P.G. 2010. An RNAi screen identifies TRRAP as a regulator of brain tumor-initiating cell differentiation. *Cell Stem Cell* 6(1), pp. 37–47.

Wurmser, A.E., Nakashima, K., Summers, R.G., Toni, N., D'Amour, K.A., Lie, D.C., and Gage, F.H. (2004). Cell fusion-independent differentiation of neural stem cells to the endothelial lineage. Nature *430*, 350–356.

Xiang, Y., Zhu, Z., Han, G., Lin, H., Xu, L., and Chen, C.D. (2007). JMJD3 is a histone H3K27 demethylase. Cell research *17*, 850-857.

Yamaguchi, H., and Hung, M.-C. (2014). Regulation and Role of EZH2 in Cancer. Cancer research and treatment : official journal of Korean Cancer Association *46*, 209-222.

Yan, Y., Shin, S., Jha, B.S., Liu, Q., Sheng, J., Li, F., Zhan, M., Davis, J., Bharti, K., Zeng, X.*, et al.* (2013). Efficient and rapid derivation of primitive neural stem cells and generation of brain subtype neurons from human pluripotent stem cells. Stem Cells Transl Med *2*, 862-870.

Yang, J., van Oosten, A.L., Theunissen, T.W., Guo, G., Silva, J.C.R. and Smith, A. 2010. Stat3 activation is limiting for reprogramming to ground state pluripotency. *Cell Stem Cell* 7(3), pp. 319–328.

Yang, L., Lian, X., Cowen, A., Xu, H., Du, H., and Yan, C. (2004). Synergy between signal transducer and activator of transcription 3 and retinoic acid receptor-alpha in

regulation of the surfactant protein B gene in the lung. Mol Endocrinol *18*, 1520-1532.

Yao, X., Ping, Y., Liu, Y., Chen, K., Yoshimura, T., Liu, M., Gong, W., Chen, C., Niu, Q., Guo, D., Zhang, X., Wang, J.M. and Bian, X. 2013. Vascular endothelial growth factor receptor 2 (VEGFR-2) plays a key role in vasculogenic mimicry formation, neovascularization and tumor initiation by Glioma stem-like cells. *PLoS ONE* 8(3), p. e57188.

Yoshimatsu, T., Kawaguchi, D., Oishi, K., Takeda, K., Akira, S., Masuyama, N., and Gotoh, Y. (2006). Non-cell-autonomous action of STAT3 in maintenance of neural precursor cells in the mouse neocortex. Development *133*, 2553–2563.

Yu, H., and Jove, R. (2004). The STATs of cancer--new molecular targets come of age. Nature reviews *4*, 97-105.

Zang, Z.J., Ong, C.K., Cutcutache, I., Yu, W., Zhang, S.L., Huang, D., Ler, L.D., Dykema, K., Gan, A., Tao, J., Lim, S., Liu, Y., Futreal, P.A., Grabsch, H., Furge, K.A., Goh, L.K., Rozen, S., Teh, B.T. and Tan, P. 2011. Genetic and structural variation in the gastric cancer kinome revealed through targeted deep sequencing. *Cancer Res* 71(1), pp. 29–39.

Zhang J, Sun X, Qian Y, Maquat LE. Intron function in the nonsense-mediated decay of beta-globin mRNA: indications that pre-mRNA splicing in the nucleus can influence mRNA translation in the cytoplasm. RNA. 1998 Jul;4(7):801–815.

Zhang, J.-X., Zhang, J., Yan, W., Wang, Y.-Y., Han, L., Yue, X., Liu, N., You, Y.-P., Jiang, T., Pu, P.-Y. and Kang, C.-S. 2013. Unique genome-wide map of TCF4 and STAT3 targets using ChIP-seq reveals their association with new molecular subtypes of glioblastoma. *Neuro Oncol* 15(3), pp. 279–289.

Zhang, J., Chen, L., Han, L., Shi, Z., Zhang, J., Pu, P., and Kang, C. (2015). EZH2 is a negative prognostic factor and exhibits pro-oncogenic activity in glioblastoma. Cancer Lett *356*, 929-936.

Zhang, K., Sun, X., Zhou, X., Han, L., Chen, L., Shi, Z., Zhang, A., Ye, M., Wang, Q., Liu, C., Wei, J., Ren, Y., Yang, J., Zhang, J., Pu, P., Li, M. and Kang, C. 2015. Long non-coding RNA HOTAIR promotes glioblastoma cell cycle progression in an EZH2 dependent manner. *Oncotarget* 6(1), pp. 537–546.

Zhang, Q., Wang, H.Y., Marzec, M., Raghunath, P.N., Nagasawa, T. and Wasik, M.A. 2005. STAT3- and DNA methyltransferase 1-mediated epigenetic silencing of SHP-1 tyrosine phosphatase tumor suppressor gene in malignant T lymphocytes. *Proc Natl Acad Sci U S A* 102(19), pp. 6948–6953.

Zhang, X.D. 2011. Illustration of SSMD, z score, SSMD*, z* score, and t statistic for hit selection in RNAi high-throughput screens. *J Biomol Screen* 16(7), pp. 775–785.

Zhang, X.D., Yang, X.C., Chung, N., Gates, A., Stec, E., Kunapuli, P., Holder, D.J., Ferrer, M., and Espeseth, A.S. (2006). Robust statistical methods for hit selection in RNA interference high-throughput screening experiments. Pharmacogenomics *7*,

299–309.

Zhu, T.S., Costello, M.A., Talsma, C.E., Flack, C.G., Crowley, J.G., Hamm, L.L., He, X., Hervey-Jumper, S.L., Heth, J.A., Muraszko, K.M., et al. (2011). Endothelial cells create a stem cell niche in glioblastoma by providing NOTCH ligands that nurture self-renewal of cancer stem-like cells. Cancer Res *71*, 6061–6072.

Zhu, Y., Guignard, F., Zhao, D., Liu, L., Burns, D.K., Mason, R.P., Messing, A., and Parada, L.F. (2005). Early inactivation of p53 tumor suppressor gene cooperating with NF1 loss induces malignant astrocytoma. Cancer Cell *8*, 119–130.